UNIVERSIDADE ESTADUAL DE CAMPINAS
INSTITUTO DE QUÍMICA

MAÍRA FASCIOTTI PINTO LIMA

USO DA ESPECTROMETRIA DE MASSAS PARA A CARACTERIZAÇÃO DE PRODUTOS LIGADOS À BIODIVERSIDADE, QUÍMICA VERDE E SUSTENTABILIDADE

CAMPINAS
2018

MAÍRA FASCIOTTI PINTO LIMA

USO DA ESPECTROMETRIA DE MASSAS PARA A CARACTERIZAÇÃO DE PRODUTOS LIGADOS À BIODIVERSIDADE, QUÍMICA VERDE E SUSTENTABILIDADE

Tese de Doutorado apresentada ao Instituto de Química da Universidade Estadual de Campinas como parte dos requisitos exigidos para a obtenção do título de Doutora em Ciências

Orientador: Prof. Dr. Marcos Nogueira Eberlin
Coorientadora: Profa. Dra. Alessandra Sussulini

O arquivo digital corresponde à versão final da Tese defendida pela aluna Maíra Fasciotti Pinto Lima e orientada pelo prof. Dr. Marcos Nogueira Eberlin.

CAMPINAS
2018

Agência(s) de fomento e nº(s) de processo(s): Não se aplica.
ORCID: https://orcid.org/0000-0002-6358-6067

Ficha catalográfica
Universidade Estadual de Campinas
Biblioteca do Instituto de Química
Camila Barleta Fullin - CRB 8462

L628u

Lima, Maíra Fasciotti Pinto, 1987-
Uso da espectrometria de massas para a caracterização de produtos ligados à biodiversidade, química verde e sustentabilidade / Maíra Fasciotti Pinto Lima. – Campinas, SP : [s.n.], 2018.

Orientador: Marcos Nogueira Eberlin.
Coorientador: Alessandra Sussulini.
Tese (doutorado) – Universidade Estadual de Campinas, Instituto de Química.

1. Espectrometria de massas. 2. Mogno - Amazônia. 3. Biocombustíveis. 4. Óleo amazônico. I. Eberlin, Marcos Nogueira, 1959-. II. Sussulini, Alessandra, 1981-. III. Universidade Estadual de Campinas. Instituto de Química. IV. Título.

Informações para Biblioteca Digital

Título em outro idioma: Use of mass spectrometry for the characterization of products linked to biodiversity, green chemistry and sustainability
Palavras-chave em inglês:
Mass spectrometry
Mahogany - Amazônia
Biofuels
Amazonian oil
Área de concentração: Química Analítica
Titulação: Doutora em Ciências
Banca examinadora:
Marcos Nogueira Eberlin [Orientador]
Leandro Wang Hantao
Rodinei Augusti
Heliara Dalva Lopes Nascimento
Annibal Duarte Pereira Netto
Data de defesa: 06-12-2018
Programa de Pós-Graduação: Química

BANCA EXAMINADORA

Prof. Dr. Marcos Nogueira Eberlin (Orientador)

Prof. Dr. Annibal Duarte Pereira Netto (UFF/Niterói)

Prof. Dr. Rodinei Augusti (UFMG/Belo Horizonte)

Profa. Dra. Heliara Dalva Lopes Nascimento (CPTI)

Prof. Dr. Leandro Wang Hantao (IQ-UNICAMP)

A Ata da defesa assinada pelos membros da Comissão Examinadora, consta no SIGA/Sistema de Fluxo de Dissertação/Tese e na Secretaria do Programa da Unidade.

Este exemplar corresponde à redação final da Tese de Doutorado defendida pelo(a) aluno(a) **MAÍRA FASCIOTTI PINTO LIMA,** aprovada pela Comissão Julgadora em 06 de dezembro de 2018.

"So crucify the ego, before it's far too late
To leave behind this place so negative and blind and cynical...
And you will come to find that we are all ONE MIND,
capable of all that's imagined and all conceivable.

Just let the light touch you,
And let the words spill through,
And let them pass right through,
Bringing out our hope and reason...
Before WE PINE AWAY."

Reflection- Tool

AGRADECIMENTOS

Em primeiro lugar, agradeço a **Deus** por ter me proporcionado o privilégio de poder realizar esta tese;

Agradeço imensamente a minha mãe, **Ednéa**, por nunca ter poupado esforços para me ver feliz e realizada, sempre me amparando em todos os momentos com muito amor e carinho, e por ter sido um exemplo de pessoa e de profissional, que certamente me guiou até aqui e me guiará adiante. Devo TUDO a você;

Agradeço ao meu pai, **Marco Antonio**, que, embora não mais presente entre nós, deixou as melhores lembranças sobre o que é caráter e sobre batalhar arduamente e honestamente em busca de seus objetivos;

Agradeço a **Jolie**, por todo amor e carinho dedicado em absolutamente todos os momentos;

Agradeço ao meu orientador, professor **Marcos Eberlin** pelas oportunidades e conhecimento que compartilhou comigo nesses últimos nove anos, e também à minha coorientadora, professora **Alessandra Sussulini**, por toda ajuda na reta final;

Agradeço a todos os meus **amigos do Laboratório ThoMSon** por terem sido "meus braços direitos" em Campinas durante os anos do meu doutorado. Um agradecimento especial para Dena e Heliara por terem "me adotado" enquanto cursava as disciplinas presenciais na Unicamp;

Agradeço às meus colaboradores da **Waters Brasil**, por terem me aberto as portas do laboratório de demonstrações para que eu pudesse realizar alguns dos experimentos desta tese, e pela a ajuda com problemas técnicos em momentos de contingenciamento de verba; e também ao **CENPES/PETROBRAS** pela parceria na área de espectrometria de massas de razão isotópica;

Agradeço aos meus **colegas do INMETRO**, em especial a Thays V. C. Monteiro, por toda sua dedicação aos nossos trabalhos, e por ter sido também meu braço direito ao longo dos últimos cinco anos;

Agradeço à **FINEP** e à **FAPERJ** pelos recursos financeiros fundamentais para a elaboração desta tese;

Agradeço ao Instituto Nacional de Tecnologia, à EMBRAPA solos, à EMBRAPA Amazônia Oriental e à empresa Amazon Oil pelo fornecimento das amostras exploradas nesta tese;

Por fim, agradeço à **banca examinadora**, pela disposição em contribuir para o melhoramento deste trabalho.

RESUMO

Atualmente, uma das demandas mais urgentes é a busca pela sustentabilidade dos processos químicos e para a preservação da biodiversidade através da exploração sustentável dos recursos naturais do planeta. Sendo assim, esta tese demonstrou a aplicação de diversas modalidades de espectrometria de massas para a caracterização de matérias primas ligadas à biodiversidade brasileira e para a prospecção e certificação de combustíveis feitos de fontes renováveis.

No primeiro artigo, foi demonstrado que um método quimiotaxonômico baseado na análise de possíveis marcadores fitoquímicos distintos é capaz de caracterizar e diferenciar amostras de madeira de mogno nativo da Amazônica e de mogno Africano que vem sendo utilizado para reflorestamento de áreas desmatadas. Para isso, utilizou-se uma metodologia simples e rápida através da análise direta por espectrometria de massas e ionização por *electrospray* (ESI-MS) de um extrato metanólico obtido de um pedaço de madeira.

O segundo artigo descreveu uma metodologia para determinar com exatidão os valores de $\delta^{13}C$ em ésteres metílicos de ácidos graxos (FAMEs) da *Jatropha curcas* (pinhão manso), através da técnica de cromatografia gasosa acoplada à espectrometria de massas de razão isotópica (GC-IRMS). O valor médio de $\delta^{13}C$ determinado para os FAMEs de 9 amostras diferentes de *J. curcas* foi $\delta^{13}C_{VPDB}$ = –29,51 ± 1,03 mUr, enquanto o valor obtido com a técnica de referência, (EA-IRMS) foi de –28,97 ± 0,43 mUr, que é uma assinatura típica de plantas C3.

Já no terceiro artigo foram demonstradas estratégias para caracterizar extratos de microalgas utilizando a mobilidade iônica acoplada à espectrometria de massas (TWIM-MS). Primeiramente, os extratos foram analisados por infusão direta na fonte ESI. A segunda estratégia foi a análise de metabolômica e lipidômica *untargeted* por cromatografia líquida de ultra-eficiência (UPLC) acoplada a TWIM por análise independente de dados (DIA) - $HDMS^E$. Dezesseis biomassas de microalgas foram avaliadas por ambos os métodos. A DI-ESI-TWIM-MS pôde separar diferentes classes de metabólitos, tornando a tipificação de microalgas mais evidente. Já a análise por UPLC-$HDMS^E$, identificou 1251 diferentes metabólitos, detalhando quimicamente os perfis lipídicos desses extratos de biomassa de microalga.

Por fim, o quarto e último artigo desta tese se tratou de um compêndio sobre a composição de óleos de espécies nativas da Amazônia. Foram descritos os perfis de FAMEs e dos TAGs intactos de dezesseis espécies oleaginosas da Amazônia. Os TAGs foram caracterizados de forma detalhada através de seus espectros de MS/MS. Todas as amostras amazônicas foram comparadas a óleos comerciais como soja, milho, coco e azeite, e seus espectros de massas foram avaliados estatisticamente por meio de análise de componentes principais (PCA). Os resultados mostraram a formação de três grupos principais: manteigas, óleos com alto teor de ácido oleico e óleos com alto teor de ácido linoleico, além de algumas manteigas diferenciadas, como bacuri e cupuaçu, com composições mais próximas dos óleos do que a de outras manteigas.

Através das diferentes aplicações apresentadas nesta tese, almeja-se contribuir com ferramentas analíticas para a proteção de espécies nativas brasileiras, bem como auxiliar nas pesquisas para o uso adequado dos seus recursos naturais do planeta.

ABSTRACT

One of the most urgent demands in the world nowadays is the search for sustainability of the chemical processes and for the exploitation of natural resources of the planet. Thus, this thesis aimed to demonstrate the application of several mass spectrometry (MS) modalities for the characterization of raw materials from Brazilian biodiversity, as well as for prospecting and certification of biofuels made from renewable sources.

In the first article, it is demonstrated that a wood chemotaxonomic method based on distinct profiles of phytochemical markers is able to characterize both the Amazonian native and foreign mahogany species. This challenging task has been performed via a simple, fast and unambiguous methodology using direct electrospray ionization mass spectrometry (ESI-MS) analysis of a simple methanolic extract of a tiny wood chip.

The second article described a methodology to accurately determine the $\delta^{13}C$ values in *Jatropha curcas* FAMEs. The determined $\delta^{13}C$ average value for the FAMEs of 9 different samples of *J. curcas* was $\delta^{13}C_{VPDB} = -29.51 \pm 1.03$ mUr, while the bulk value obtained with EA-IRMS was -28.97 ± 0.43 mUr, a typical signature of C3-plants. This work also demonstrates that major quality procedures must indeed be applied for accurate determinations of isotopic values, especially in GC analysis, following the identical treatment principle.

In the third article, were reported strategies to characterize microalgae extracts via traveling wave ion mobility – mass spectrometry (TWIM-MS). First, we analyzed microalgae extracts by direct infusion to an electrospray ion source (ESI) with no previous chromatographic separation (DI-ESI-TWIM-MS). Second, we screened metabolites and lipids in the extracts via an untargeted high throughput method by ultra-performance liquid chromatography (UPLC) coupled to TWIM using data independent analysis (DIA) – MSE (UPLC-HDMS^E). Sixteen different microalgae biomasses were evaluated by both approaches. DI-ESI-TWIM-MS was able, via distinct drift times, to set apart different classes of metabolites, making microalgae typification more evident. UPLC-HDMS^E, identified 1251 different metabolites,

The fourth and last article in this thesis was about a compendium on Amazonian oils composition, in which a detailed fatty acids and intact TAGs of sixteen different oleaginous Amazonian species was reported, The TAGs were characterized by their MS/MS spectrum resulting in a detailed study about TAGs composition in these samples. All the Amazonian samples were compared to trivial oils such as soybean, corn, coconut and olive oil, and their mass spectra were statistically evaluated using principal component analysis (PCA). The results showed a formation of three main groups: butters, high oleic acid oils and high linoleic acids oils, plus some disconnected butters such as bacuri and cupuaçu with compositions closer to oils than to other butters. composition, and additionally, encourage the sustainable production and appropriate use of Amazon forest resources.

From the applications presented in this thesis, we are expecting to contribute with analytical tools for the protection of Brazilian native species, as well as to help the researches that leads to the proper use of planet's natural resources.

LISTA DE ABREVIATURAS

% -	Porcento
$[M + H]^+$ -	Molécula protonada
$[M+Na]^+$ -	Molécula sodiada
‰ -	permil
$Å^2$ -	Ângstron ao quadrado
APCI -	*Asmospheric Pressure Chemical Ionization*
APPI -	*Atmospheric Pressure Photo Ionization*
ASAP -	*Atmospheric Pressure Solids Analisys Probe*
CCS -	*Collision Cross Section*
CERFLOR	Certificação florestal
CI -	*Chemical ionization*
CID -	*Collision Induced Dissotiation*
CITES	*Convention on International Trade in Endangered Species*
cm -	Centímetros
cm^3 -	Centímetros cúbicos
Da -	Dalton
DART	*Direct analysis in real time*
DESI -	*Desorption electrospray ionization*
DFT -	*Density Functional Theory*
DIA -	*Data independent analysis*
dt -	*Drift time*
E -	Campo elétrico
EA	*Elemental analysis ou elemental analyzer*
EASI	Easy ambient sonic-spray ionization
EI -	*Electron ionization*
EPA	*Environmental Protection Agency*
ESI -	*Electrospray*
ESI(-) -	*Electrospray negativo*
ESI(+) -	*Electospray positivo*
ESI-MS	*Mass Spectrometry Electrospray Ionization*
EUA -	*United States of America*

eV -	*Eletronvolts*
FAB -	*Fast atom bombardment*
FAME -	*Fatty acid methyl ester*
FT ICR -	*Fourier Transform Ion Cyclotron Ressonance*
FT ICR-MS -	*Fourier Transform Ion Cyclotron Ressonance Mass Spectrometry*
G1 -	Synapt G1
G2 -	Synapt G2
GC-MS -	*Gas Chromatography Mass Spectrometry*
GHG -	*Green house gases*
HD -	*High definition*
HDMS -	*High Definition Mass Spectrometry*
HMDB	*Human metabolome data base*
HPLC -	*High Performance Liquid Chromatography*
IAEA -	International Atomic Energy Agency
IBAMA -	Instituto Brasileiro do Meio Ambiente e dos Recursos Naturais Renováveis
ICP -	*Inductively coupled plasma*
IM -	*Ion Mobility*
IM-MS -	*Ion Mobility Mass Spectrometry*
IMS -	*Ion Mobility Spectrometry*
INMETRO -	Instituto nacional de Metrologia, Qualidade e Tecnologia
IRMS -	Isotope Ratio Mass Spectrometry
K -	Mobilidade Iônica
KDa -	quilo Dalton
kV -	quilo Volts
L / h -	Litro por hora
LC -	*Liquid chromatography*
LDI -	*Laser Dessorption Ionization*
LIPID MAPS -	Banco de dados para lipidômica
LIT-FT ICR -	*Linear ion trap - Fourier-transform ion cyclotron resonance*
m -	Massa
m/m -	massa sobre massa ou razão mássica
m/s -	Metros por segundo

m/z -	Razão massa sobre carga
MA -	Mogno Africano
MALDI -	*Matrix Assisted Laser Dessorption Ionization*
MB -	Mogno Brasilero
mbar -	milibar
MCP -	*Microchannel plate detector*
MCR -	Modelo de Cargas Residuais
MDI -	Modelo da Dissociação de Íons
MDIC -	Ministério da Indústria, Comércio Exterior e Serviços
mg -	miligramas
min -	minuto
mL -	mililitros
mL/min -	mililitros por minuto
MR -	Material de referência
MRC -	Material de referência certificado
MS -	*Mass Spectrometry*
ms -	milisegundos
MS/MS -	*Tandem Mass Spectrometry*
mUr -	miliurey
NALDI -	*Nanoassisted laser desorption-ionization*
NBS-22 -	Material de refência certificado da série National Bureau of Standards, número 22
NIST -	National Institute of Standards and Technology
ºC -	Graus Celsius
ºC / min -	Graus Celsius por minuto
ONU -	Organização das Nações Unidas
PCA -	*Principal component analysis*
PDB -	Pee Dee Belemnite
ppb -	partes por bilhão
ppm -	partes por milhão
ppt -	partes por trilhão
Q -	Quadrupolo
q -	Carga

QIT-orbitrap - *Quadrupole - ion trap - orbitrap*

QqLIT - *Quadrupole-Linear ion Trap*

QqQ - Triplo quadrupolo

QTOF - *Quadrupole-Time of Flight*

RF - Radio frequência

SIMS - *Secondary ion mass spectrometry*

T - Temperatura

TAGs - Triacilgliceróis

TOF - *Time of Flight*

TOF/TOF - *Time of Flight* em modo tandem

T-wave - *Traveling Wave*

TWIM - Traveling wave ion mobility

TWIM - *Traveling Wave Ion Mobility*

TWIM-MS - *Traveling Wave Ion Mobility Mass Spectrometry*

UK - *United Kingdom*

UPLC - *Ultra Performance Liquid Chromatography*

V - Volts

v/v - Volume por volume

VPDB - Viena Pee Dee Belemnite

μ - Mass reduzida do íon e do gás

μL - Microlitro

v - Velocidade de Fluxo

Ω - Seção de choque

ÍNDICE

CAPÍTULO 1. INTRODUÇÃO

1.1. Problemática e conceitos

Desde meados do século XVIII, com a primeira revolução industrial, o homem vem alterando sua forma de extrair recursos do planeta Terra ao longo do tempo. Inicialmente, empregava-se um meio de produção fundamentalmente artesanal, em que o próprio ser humano era a principal ferramenta de produção das manufaturas da época.[1] Esse processo foi drasticamente alterado com a introdução de maquinários alimentados principalmente com energia derivada de combustíveis fósseis, como o carvão, [2,3] principalmente para as indústrias têxteis e metalúrgicas, que estavam em pleno desenvolvimento na época. [4] Já ao final do século XIX, o mundo experimentou a segunda revolução industrial, em que um rápido desenvolvimento tecnológico fez com que ocorresse a maioria dos avanços industriais que permitiram a comercialização de bens de consumo de diversos setores, que movimentam a base da sociedade atual. Sendo assim, ocorreu a solidificação de indústrias como a automotiva e de motores, dos meios de comunicação, dos materiais derivados do petróleo, da indústria farmacêutica, computacional, ou seja, de praticamente toda base industrial e tecnológica do nosso século, sendo a revolução mais significativa que já houve até hoje. [5]

Entretanto, a exploração completamente desordenada dos recursos naturais do planeta Terra nos últimos 300 anos obviamente teve impactos que hoje ameaçam a existência dos seres vivos das próximas gerações. A quantidade de resíduo oriundo de todos os avanços industriais dos últimos séculos foi durante muito tempo negligenciado e hoje é um dos maiores desafios globais,[6,7] afinal como diz a ideia oriunda dos estudos de A. L. Lavoisier:

---

[1] J. de Vries, The Industrial Revolution and the Industrious Revolution. *The Journal of Economic History*, **1994**, 54, 249.
[2] J. Fahrenkamp-Uppenbrink, The heroes of the Industrial Revolution. *Science*, **2015**, 150.
[3] C. A. Berg, Process Innovation and Changes in Industrial Energy Use. *Science,* **1978**, 608.
[4] M. Fores, The myth of a british industrial revolution. *History*, **1981**, 66, 181.
[5] A. Spilhaus, The Next Industrial Revolution, *Science,* **1970**, 167(3926), 1673.
[6] M. El-Fadel, A. N. Findikakis, J. O. Leckie, Environmental Impacts of Solid Waste Landfilling. *Journal of Environmental Management*, **1997**, 50, 1.
[7] B. H. Robinson, E-waste: An assessment of global production and environmental impacts, *Science of The Total Environment*, **2009**, 408 (2), 183.

"Nada se perde, nada se cria, tudo se transforma".

Ou seja, os resíduos industriais continuarão "a existir" no planeta enquanto um melhor destino não seja dado a eles, tendo em vista o fato de que o processo natural de degradação é por vezes muito mais lento do que o da geração de novos resíduos. Além disso, todos esses avanços foram conseguidos à custa da exploração energética e material do petróleo, que é uma fonte não renovável (pelo menos não a "curto" prazo) e altamente poluidora. Atualmente, sabe-se que a poluição causou danos praticamente irreversíveis ao meio ambiente. [8] O aumento antropogênico da emissão dos *Green House Gases* (GHG) [9] oriunda da exploração do petróleo e da destruição de florestas é hoje uma preocupação mundial que demanda uma força tarefa de todas as nações, com o objetivo de frear as mudanças climáticas, principalmente um fenômeno de aquecimento global. [10] A industrialização rápida também causou danos em outras esferas, como solos e as águas, impactando de múltiplas formas a qualidade de vida dos seres vivos e a preservação da biodiversidade. Sabe-se que, atualmente, devido à exploração descontrolada dos recursos naturais, a biodiversidade, tanto marinha, quanto terrestre, encontra-se ameaçada, sendo que muitas espécies (animais e vegetais) já foram extintas ou estão em processo de extinção.

Em pleno século XXI, embora de forma tardia, a sociedade e a comunidade científico-industrial já visualizaram que as formas de interação com o meio ambiente e de exploração dos recursos naturais do planeta precisam ser alterados. Em plena Era da terceira revolução industrial, em que hoje tem-se uma indústria química extremamente refinada e tecnológica, depara-se, também, com uma nova revolução que é oriunda dos incríveis avanços da ciência.[11] Basicamente, espera-se que essa atual revolução venha tratar dos impactos gerados por suas antecessoras.

Com a mudança de mentalidade frente aos graves problemas ambientais do planeta e a aceitação de que algo precisava ser feito para mitigar tamanhos danos, desenvolveram-se os conceitos de "química verde" e "sustentabilidade", que

[8] E. H. Allison, H. R. Bassett. Climate change in the oceans: Human impacts and responses. *Science*, **2015**, 13, 778.
[9] *Green house gases* abrangem CO_2, N_2O, CH_4 e gases fluorados.
[10] S. H. Schneider. The Greenhouse Effect: Science and Policy. *Science*, **1989**, 243 (4892), 771.
[11] P.H. Abelson. A Third Technological Revolution. *Science*, **1998**, 279(5359), 2019a.

basicamente incentivam um olhar mais atento aos impactos que os processos industriais causam à natureza.

O primeiro princípio da Conferência das Nações Unidas sobre Meio Ambiente e Desenvolvimento,[12] que se reuniu no Rio de Janeiro, de 3 a 14 de junho de 1992, diz que:

> *"Os seres humanos estão no centro das preocupações com o desenvolvimento sustentável. Têm direito a uma vida saudável e produtiva, em harmonia com a natureza."*

Sendo assim, o papel da química para se alcançar esse objetivo é inquestionável. Somente nos Estados Unidos, segundo dados da Agência de Proteção Ambiental (EPA), somente em 1991 aproximadamente 278 milhões de toneladas de resíduos tóxicos foram gerados, não somente pelas indústrias químicas, mas elas foram sim as principais responsáveis.[13] Como resultado, grandes corporações como a Dow Chemical e a DuPont, começaram a dedicar seus esforços para obedecer a regulamentações ambientais cada vez mais restritivas, lançando mão, então, das práticas de química verde. Este termo, que foi criado pelo químico Paul Anastas na década de 1990, visa basicamente o desenvolvimento e a implementação de produtos e processos químicos para reduzir ou eliminar, tanto a utilização, quanto a geração de substâncias nocivas à saúde humana e ao ambiente, tendo 12 princípios básicos,[14] resumidos a seguir: 1) Prevenção; 2) Economia de átomos para que as reações orgânicas e metodologias sintéticas sejam desenhadas de forma a maximizar a incorporação de todos os materiais de partida no produto final; 3) Síntese de produtos menos perigosos e tóxicos; 4) Desenho de produtos seguros, que realizem a função desejada e não sejam tóxicos; 5) Solventes e reagentes auxiliares mais seguros ou inócuos; 6) Busca pela eficiência de energia; 7) Uso de fontes renováveis de matéria-prima; 8) Evitar a formação de derivados em processos de derivatização e/ou utilização de grupos protetores em síntese; 9) Catalisadores mais seletivos quanto possível; 10) Desenho de produtos para a degradação e geração de produtos inócuos;

---

[12] Rio Declaration on Environment and Development, disponível em: http://www.onu.org.br/rio20/img/2012/01/rio92.pdf (acessado em 27/09/2018)
[13] K. Sanders. It's not easy being green. *Nature*, **2011**, 469, 18.
[14] P. T. Anastas, J. C. Warner, Green Chemistry: Theory and Practice, *Oxford University Press*: New York, **1998**, 30.

11) Análise em tempo real para a prevenção da poluição; 12) Química intrinsecamente segura para a prevenção de acidentes.

Na prática esses conceitos de química verde revolucionaram a maneira de se planejar novos projetos e pesquisas na área de química e impactaram suas subáreas nas mais diversas aplicações.

Já o termo “sustentabilidade” tem sua definição direta um pouco mais complexa. A EPA coloca que a sustentabilidade tem como princípio básico que tudo o que precisamos para nossa sobrevivência e bem-estar depende, direta ou indiretamente, do nosso ambiente natural.[15] Perseguir a sustentabilidade é criar e manter as condições sob as quais os seres humanos e a natureza podem existir em harmonia para apoiar o desenvolvimento das gerações atuais e futuras. Outra definição também amplamente citada vem da Comissão Mundial sobre Meio Ambiente e Desenvolvimento da ONU: “desenvolvimento sustentável é um desenvolvimento que atende às necessidades do presente sem comprometer a capacidade das gerações futuras de atender suas próprias necessidades”.[16] Na prática, o conceito de sustentabilidade se refere ao uso dos recursos naturais do planeta sem o comprometer as gerações futuras, ou seja, elas também têm que ser capazes de atender suas próprias necessidades e se desenvolver com qualidade de vida. As práticas sustentáveis têm que incentivar a saúde ecológica, humana e econômica, partindo do princípio de que os recursos do planeta são finitos e devem ser usados de maneira sábia e conservadora, visando prioridades e avaliando as consequências de longo prazo das formas como os recursos são usados.

A combinação de toda a filosofia que carrega esses termos definidos anteriormente fez com que, atualmente, exista uma demanda mundial para a criação de uma indústria que invista na manufatura de produtos advindos de fontes renováveis, que ajudem na preservação da biodiversidade e feitos de forma sustentável, colocando em prática os preceitos da química verde.

O Brasil é um dos maiores produtores de matéria prima e insumos para diversas áreas e mercados de consumo mundiais. Isto se deve à sua grande área territorial e ao clima extremamente favorável à agricultura, e ao fato de que o Brasil abriga uma

[15] Disponível em: https://www.epa.gov/sustainability/learn-about-sustainability#what (acessado em 27/09/2018).
[16] Disponível em: http://www.un-documents.net/ocf-02.htm (acessado em 27/09/2018).

das biodiversidades mais ricas do mundo.[17] Entretanto, o desenvolvimento de novos produtos derivados de fontes renováveis requer algo que vai além do desenvolvimento de protocolos de processos de obtenção de produtos de maior valor agregado: requer a garantia da qualidade, comprovação de eficácia, e a certeza de que eles são realmente obtidos de fontes renováveis, através da certificação de sua origem (matéria prima e origem geográfica), e da verificação de que são oriundos de processos sustentáveis.[18,19,20]

Quando se fala em matérias primas, ou seja, materiais disponíveis na natureza em suas formas brutas, ou já semimanufaturados, sabe-se que elas podem apresentar composição química extremamente complexa, contendo compostos orgânicos e inorgânicos de diversas classes químicas. Caracterizar a composição dessas matérias primas é uma etapa fundamental para garantir o seu melhor aproveitamento, ou seja, quais seriam os destinos em que se poderia obter seus maiores benefícios ou desempenhos em diversos setores que poderiam ser empregados, seja para a área de alimentos, biocombustíveis, indústria de cosméticos, farmacêutica, etc. Em contrapartida, a exploração de recursos naturais deve ser feita de forma controlada e sustentável, a fim de evitar danos ao meio ambiente e aos ecossistemas, tal como a extinção de determinada espécie na natureza ou a alteração da fauna e da flora local.

1.2. Fundamentos da espectrometria de massas e sua contribuição para o tema

Dentro do contexto descrito acima sobre a análise química de misturas complexas, a técnica de espectrometria de massas (*Mass Spectrometry – MS*) é, atualmente, uma das técnicas de análise mais versáteis disponíveis na área da química analítica. Não é uma tarefa fácil imaginar uma molécula orgânica, inorgânica ou organometálica, que não possa ser analisada por alguma das muitas modalidades

[17] M. Tabarelli, L. P. Pinto, J. M. Silva, M. Hirota, L. Bedê, , Challenges and Opportunities for Biodiversity Conservation in the Brazilian Atlantic Forest, *Conservation Biology*, **2005**, 19, 695.
[18] W. A. Bizzo, Lenco, P.C. ; D. J. Carvalho, J. P. Soto Veiga, The generation of residual biomass during the production of bio-ethanol from sugarcane, its characterization and its use in energy production. *Renewable & Sustainable Energy Reviews*, **2014**, 29, 589 – 603.
[19] M. Foston, A. J. Ragauskas. Biomass Characterization: Recent Progress in Understanding Biomass Recalcitrance. *Industrial Biotechnology*, **2012**, 8, 191 – 208.
[20] C. A. G. Quispe, C. J. R. Coronado, J. A.Carvalho Jr., Glycerol: Production, consumption, prices, characterization and new trends in combustion. *Renewable & Sustainable Energy Reviews*, **2013**, 27, 475 - 493.

de MS atualmente disponíveis comercialmente. No campo da MS de moléculas orgânicas, consegue-se analisar desde a molécula de metano [21] até uma proteína complexa na ordem de quilo Dalton (kDa).[22] Entre estes extremos, há um universo de moléculas que podem ser identificadas, elucidadas e quantificadas utilizando a técnica de MS adequada para cada caso.

De maneira muito geral, espectrômetros de massas são instrumentos analíticos que detectam moléculas ionizadas, presentes ou transferidas para a fase gasosa, com base em suas razões massa sobre carga (*m/z*), medindo-se suas abundâncias através do registro de um sinal eletrônico em um detector. [23] Com essa finalidade, a técnica é utilizada em uma vasta gama de aplicações, como: na determinação muito precisa da massa atômica e molecular, na medida da abundância de isótopos, na determinação das concentrações de substâncias em níveis de partes por bilhão ou trilhão – ppb ou ppt – em amostras, auxiliando na caracterização de compostos presentes em matrizes complexas, assim como na elucidação da estrutura de compostos químicos mesmo que estes se apresentem em misturas com outras várias substâncias. [24]

Com o desenvolvimento tecnológico contínuo dentro da análise instrumental, a MS despontou como uma das técnicas mais poderosas existentes atualmente na química, sendo este fato um consenso dentro da comunidade científica de química analítica mundial. A razão desta popularização da técnica se deve à enorme multidisciplinaridade que é inerente à técnica de MS. Em todos os campos da ciência, encontram-se aplicações pertinentes utilizando a MS como ferramenta: de experimentos fundamentais sobre a físico-química de íons em fase gasosa ou condensada, [25] a estudos clínicos e diagnósticos em medicina avançada. [26] Este grande aumento nas possibilidades de aplicação que a técnica teve nos últimos 50 anos, deu-se graças ao desenvolvimento de tecnologias para a construção de novas

---

[21] L. G. Smith, Ionization and Dissociation of Polyatomic Molecules by Electron Impact. I. Methane, *Phys. Rev.*, **1937**, 51, p. 263

[22] J. B. Fenn, M. Mann, C. K. Meng, S. F. Wong, C. M. Whitehouse, Electrospray ionization for mass spectrometry of large biomolecules, *Science*, **1989**, 64.

[23] A. El-Aneed, A. Cohen, J. Banoub, Mass Spectrometry, Review of the Basics: Electrospray, MALDI, and Commonly Used Mass Analyzers. *Applied Spectroscopy Reviews*, **2009**, 44 (3)

[24] H. H. Maurer, Multi-analyte procedures for screening for and quantification of drugs in blood, plasma, or serum by liquid chromatography-single stage or tandem mass spectrometry (LC-MS or LC-MS/MS) relevant to clinical and forensic toxicology, *Clinical Biochemistry*, **2005**, 38 (4), 310 – 318.

[25] A. Mota, et al. Structural Organization and Supramolecular Interactions of the Task-specific Ionic Liquid 1-Methyl-3-Carboxymethylimidazolium Chloride: Solid, Solution and Gas Phase Structures, *Journal of Physical Chemistry C*, **2014**, 118, 1789.

[26] J. Zhang, et al. Nondestructive tissue analysis for ex vivo and in vivo cancer diagnosis using a handheld mass spectrometry system, *Science translational medicine*, **2017**.

fontes de ionização, permitindo a ionização e consequente análise de substâncias de grande variabilidade química presentes em amostras de qualquer estado físico, seja ele gasoso, líquido ou sólido. [27] Além disso, novas tecnologias também foram desenvolvidas e implementadas nos analisadores de massas, que contribuíram da mesma forma para o aumento da versatilidade da técnica, [28] conferindo maior resolução, seletividade e detectabilidade nas análises. Atualmente é possível realizar a identificação ou quantificação de diversas moléculas de forma simultânea em amostras complexas, tal como o petróleo bruto ou milhares de proteínas e metabólitos em amostras biológicas. [29,30] A **Figura 1** mostra um esquema geral de um espectrômetro de massas, assim como a grande variedade de combinação entre fontes de ionização, analisadores de massas e acoplamentos com outras técnicas analíticas.

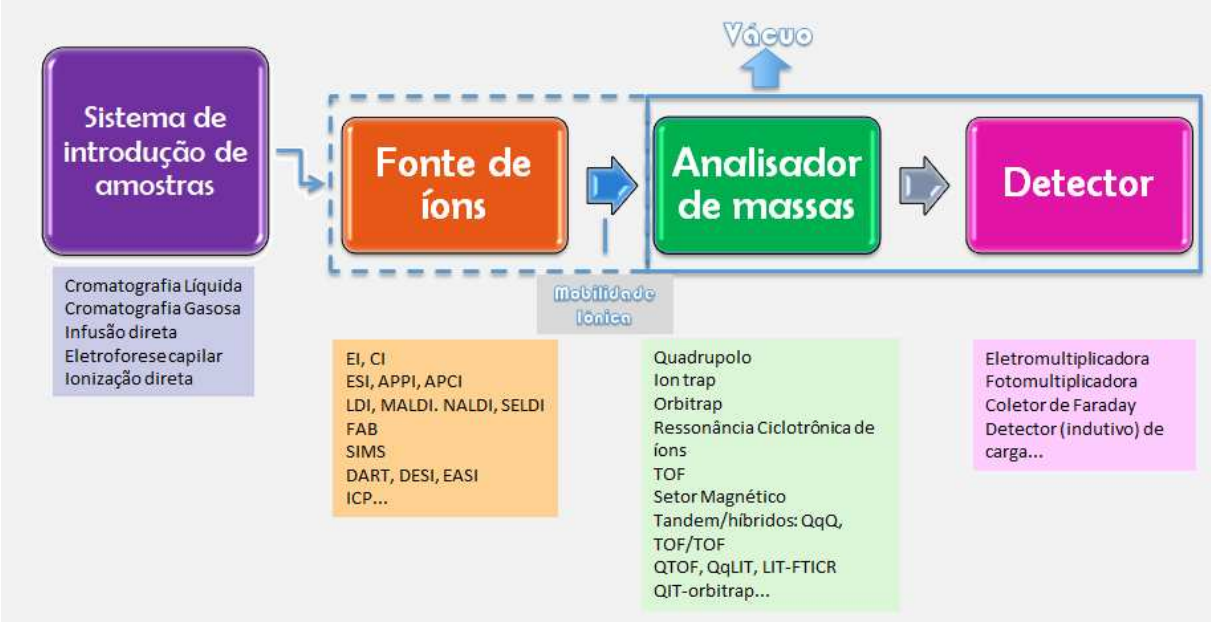

Figura 1. Esquema geral de um espectrômetro de massas e seus possíveis constituintes.

[27] A. Venter, M. Nefliu, R. G. Cooks, Ambient desorption ionization mass spectrometry, TrAC *Trends in Analytical Chemistry*, **2008**, 27 (4), 284.
[28] A. G. Marshall, "Milestones in Fourier Transform Ion Cyclotron Resonance Mass Spectrometry Technique Development," *Int. J. Mass Spectrom.*, **2000**, 200, 331.
[29] A. G. Marshall, R. P. Rodgers, Petroleomics: The Next Grand Challenge for Chemical Analysis, *Acc. Chem. Res.*, **2004**, 37 (1), 53.
[30] R. Aebersold, M. Mann, Mass spectrometry-based proteomics, *Nature*, **2003**, 422, 198.

1.3. Técnicas de espectrometria de massas utilizadas nesta tese

Como exposto, uma das demandas mais urgentes do mundo hoje é a busca por sustentabilidade dos processos químicos e da exploração de recursos naturais do planeta. Sendo assim, esta tese demonstrou a aplicação de diversas modalidades de MS para a caracterização de matérias primas ligadas à biodiversidade brasileira (madeiras e óleos nativos provenientes da Amazônia), bem como para a prospecção e certificação de combustíveis feitos de fontes renováveis (oleaginosas e microalgas). Desta forma, espera-se contribuir para a proteção de espécies nativas brasileiras, bem como garantir o uso adequado dos seus recursos naturais do planeta. A seguir, serão apresentados os fundamentos básicos das principais técnicas de espectrometria de massas aplicadas nos diferentes temas abordados nesta tese.

1.3.1. Espectrometria de massas com analisador híbrido quadrupolo-tempo de voo e fonte de íons e*lectrospray* (ESI-QTOF)

O espectrômetro de massas com analisador híbrido quadrupolo e tempo de voo (*quadrupole – time of flight* - QTOF) pode ser descrito de maneira mais simples como um triplo quadrupolo que teve o seu último quadrupolo substituído por um analisador do tipo TOF, [31] tendo basicamente os seguintes componentes:

- uma fonte de ionização (por exemplo: *electrospray*, ionização química a pressão atmosférica (APCI), fotoionização a pressão atmosférica (APPI), MALDI, ionização ambiente, etc).
- um analisador quadrupolo (Q);
- uma cela de colisão, geralmente hexapolar;
- um analisador tempo de voo (TOF) de aceleração ortogonal;
- um detector (por exemplo, *microchannel plate* - MCP).

[31] I. V. Chernushevich, A. V. Loboda, B. A. Thomson, An introduction to quadrupole–time-of-flight mass spectrometry, *Journal of mass spectrometry*, **2001**, 36, 849.

De acordo com a **Figura 2**, os íons gerados na fonte são transferidos para o analisador quadrupolo via lentes RF. Após a saída do quadrupolo os íons são transferidos através da cela de colisão e chegam ao segundo analisador, TOF, onde o feixe de íons é acelerado pelo *Pusher*, passando pelo *Reflectron* e chegando ao detector (MCP) com diferentes velocidades.

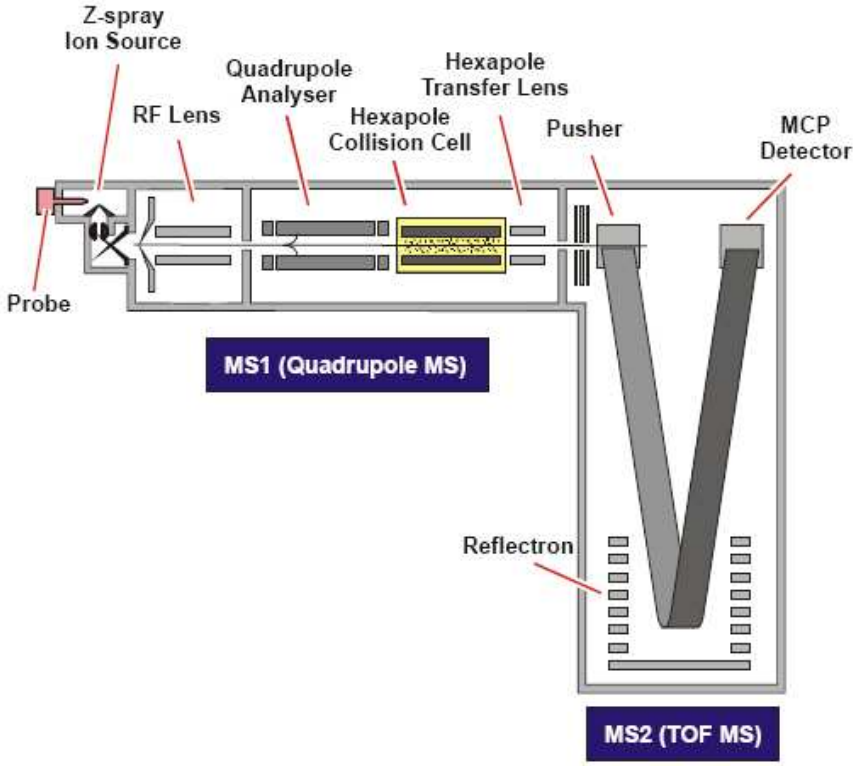

Figura 2. Esquema do espectrômetro de massas QTOF. (Fonte: QTOF User's Guide, Micromass, UK)

O QTOF pode operar tanto em modo MS, quanto em modo *tandem* ou MS/MS. Em modo MS, o primeiro quadrupolo (Q1) atua basicamente como um componente de transmissão de íons, enquanto o analisador TOF é utilizado para gerar o espectro. Resumidamente, o TOF separa íons, após sofrerem uma aceleração inicial feita por um campo elétrico, de acordo com suas velocidades ao percorrerem uma região livre de campo elétrico chamada de *drift tube*, em que os íons de *m/z* mais alta demoram mais tempo para alcançar o detector. Em modo MS/MS, o Q1 seleciona o íon precursor de interesse, que é, então acelerado com uma energia que varia geralmente entre 10 e 200 eV antes de entrar na cela de colisão, onde sofre dissociação induzida por colisão (*collision induced dissociation* - CID) ao colidir com as moléculas neutras

do gás de colisão, geralmente argônio ou nitrogênio. [32] O resultado são espectros contendo íons fragmentos, além dos íon precursor remanescente, ambos medidos com alta resolução e exatidão de *m/z*. Atualmente, espectrômetros de massas do tipo QTOF podem alcançar até 50.000 de resolução e erro de *m/z* inferior a 1 ppm,[33] podendo ser utilizado tanto em estudos qualitativos, quanto para a quantificação de substâncias em nível traço. [34, 35]

Nesta tese, a principal fonte de íons utilizada foi a ESI, em que a ionização é realizada à pressão atmosférica e que produz íons em fase gasosa a partir de uma solução de amostra inserida através de um capilar, ao qual uma tensão elétrica elevada (cerca de 2 a 4 kV) é aplicada. A ESI é uma técnica que produz moléculas ionizadas por protonação, desprotonação ou formação de adutos com cátions ou ânions, a partir de uma solução líquida da amostra, seguida da transferência para a fase gasosa. Esse processo pode ser dividido em três etapas principais: a nebulização da solução da amostra em gotículas carregadas decorrentes da aplicação direta de voltagem no capilar, a liberação dos íons a partir das gotículas e o transporte dos íons da região de pressão atmosférica da fonte para a região de alto vácuo do analisador de massas.

Essa técnica de ionização tem basicamente dois fundamentos principais, que descrevem os mecanismos de liberação dos íons a partir das gotículas carregadas: o modelo de cargas residuais (MCR) e o modelo da dessorção dos íons (MDI). [36] O MCR sugere que as gotículas carregadas saem da ponta do capilar através de spray de formato cônico chamado de cone de Taylor. Com o auxílio de um fluxo de gás aquecido (N_2), as gotículas carregadas com várias unidades de carga sofrem um processo de evaporação do solvente. A redução no tamanho e o consequente aumento da densidade de carga torna a repulsão entre as cargas maior que a tensão superficial da microgotícula resultante. Isto faz com que as gotículas se colapsem a

---

[32] H. R. Morris, et al. High Sensitivity Collisionally-activated Decomposition Tandem Mass Spectrometry on a Novel Quadrupole/Orthogonal-acceleration Time-of-flight Mass Spectrometer, Rapid Commun. Mass Spectrom., **1996**, 10, 889.

[33] W. Abushareeda, et al. Comparison of Gas Chromatography Quadrupole Time-Of-Flight and Quadrupole Orbitrap Mass Spectrometry in Anti-doping Analysis: I. Detection of Anabolic-androgenic Steroids. Rapid Commun Mass Spectrom. **2018**, in press.

[34] H. Jin, et al. Trace analysis of tetracycline antibiotics in human urine using UPLC–QToF mass spectrometry, Microchemical Journal, **2010**, 94, 139.

[35] A. Lesur, B. Domon, Advances in high-resolution accurate mass spectrometry application to targeted proteomics. Proteomics, **2015**, 15, 880.

[36] L. Konermann, E. Ahadi, A. D. Rodriguez, S. Vahidi, Unraveling the Mechanism of Electrospray Ionization, *Analytical Chemistry*, **2013**, 85 (1), 2.

gotículas ainda menores e o mesmo processo pode ser repetido até que o solvente seja evaporado por completo, restando apenas os íons da amostra.

Já o MDI, propõe que o aumento da densidade superficial de carga devido à evaporação do solvente cria um campo superficial que supera as forças de solvatação dos íons antes de exceder a tensão superficial do solvente, causando a ejeção do íon antes da explosão coulômbica. Estes mecanismos favorecem a formação de íons multiplamente carregados, característica que pode ser utilizada para a análise de macromoléculas. Em um característico espectro de ESI, os íons podem se apresentar mono ou multicarregados.

Espectrômetros de massas do tipo ESI-QTOF são atualmente um dos mais populares em laboratórios que utilizam a técnica de MS. Sua habilidade de identificar e caracterizar compostos desconhecidos em amostras devido à alta resolução e exatidão, tanto para MS quanto para MS/MS, além de permitir a quantificação, o tornou esse arranjo instrumental a principal técnica de escolha principalmente para o estudo de amostras complexas, sendo principalmente utilizado para estudos de proteômica, [37] lipidômica e metabolômica, principalmente para análises do tipo *untargeted,* [38] ou seja, em que não define anteriormente o conjunto de substâncias a serem identificadas ou quantificadas, mas fornece resposta analítica (detecção, caracterização e/ou quantificação) para um amplo conjunto de analitos presentes nas amostras analisadas.

1.3.2. Espectrometria de massas de razão isotópica

A espectrometria de massas de razão isotópica (*isotope ratio mass spectrometry* - IRMS) é uma modalidade de espectrometria de massas que mede pequenas diferenças na abundância de isótopos estáveis em amostras ou em moléculas específicas. [39] Os avanços das últimas décadas sofridos na instrumentação de IRMS tornaram-na uma técnica analítica cada vez mais utilizada para estudo de

[37] A. Lesur, S. Gallien, B. Domon, Hyphenation of fast liquid chromatography with high-resolution mass spectrometry for quantitative proteomics analyses, TrAC Trends in Analytical Chemistry, **2016**, 84, 144.
[38] Tomas Cajka, O. Fiehn, Toward Merging Untargeted and Targeted Methods in Mass Spectrometry-Based Metabolomics and Lipidomics, *Analytical Chemistry*, **2016**, 88 (1), 524.
[39] W. A. Brand, High precision Isotope Ratio Monitoring Techniques in Mass Spectrometry. *Journal of mass spectrometry*, **1996**, 31, 225.

diferentes tipos de amostras e campos de aplicação. [40] Quando a concentração em si de uma molécula específica (ou um grupo delas) não é um parâmetro capaz de diferenciar amostras de acordo com alguma característica específica, pode-se determinar a sua composição isotópica, procurando variações que possam estar relacionadas a certos processos, como o metabolismo, origem geográfica, matéria-prima e muitos outros. Essas pequenas diferenças nas concentrações de isótopos em um sistema ocorrem devido ao fenômeno de fracionamento isotópico. [41]

O espectrômetro de massas de razão isotópica foi inicialmente desenvolvido por Nier em 1940, [42,43] com a função de medir, de forma exata, determinadas massas sequencialmente na amostra e na referência. [44] De maneira geral, nestes equipamentos as amostras a serem analisadas são inseridas por meio de um sistema de introdução de amostra na fonte de ionização, onde são ionizadas em uma fonte de ionização por elétrons (*electron ionization* – EI) e aceleradas a vários kV (quilovolts). [45] Ao passar pelo campo magnético os íons separados são detectados por coletores de íons do tipo Faraday, os quais são posicionados ao longo do plano focal do instrumento de IRMS. Diferentes técnicas de introdução de amostras e interfaces são usadas para introdução de amostra no equipamento de IRMS, como o analisador elementar (*elemental analyzer* – EA), a cromatografia gasosa (*gas chromatography* – GC) e o cromatografia líquida (*liquid chromatograpy* – LC). [46,47] Nesta tese, foram utilizados apenas os sistemas de EA-IRMS e GC-IRMS.

Com relação à técnica de GC-IRMS, os compostos são separados por cromatografia gasosa e sofrem combustão de maneira a transformar estes compostos em gases (CO_2, N_2, e potencialmente, outros gases estáveis), para que suas razões isotópicas sejam analisadas separadamente, o que permite, então, a determinação da razão isotópica de compostos orgânicos específicos presentes amostras, que estejam

---

[40] J. Vogl, Advances in Isotope Ratio Mass Spectrometry and Required Isotope Reference Materials. *Mass Spectrom (Tokyo)*, **2013**, 2, S0020.
[41] J. Kubásek, O,Urban, J. Santrucek. C4 plants use fluctuating light less efficiently than do C3 plants: a study of growth, photosynthesis and carbon isotope discrimination. *Physiologia Plantarum*, **2013**, *149*, 528.
[42] A. O. Nier, Mass and relatives abundances of isotopes. *Ann. Rev. Nucl. Sci*. **1952**, 1, 137.
[43] J. R. De Bièvre, P. de Laeter, H. S. Peiser, Isotope mass spectrometry in metrology. *Mass Spectrometry Reviews*, 11, **1992**, 193.
[44] D. E. Matthews, J. M. Hayes, Isotope-ratio monitoring gas chromatography mass spectrometry. *Analytical Chemistry*, **1978**, 50, 1465.
[45] W. Meier-Augenstein, Applied gas chromatography coupled to isotope ratio mass spectrometry, *Journal of Chromatography*, **1999**, 842, 351.
[46] Z. Muccio, G. P. Jackson, Isotope ratio mass spectrometry, *Analyst*, **2009**, 134, 213.
[47] A. L. Sessions, Isotope-ratio detection for gas chromatography – Review. *Journal of Separation Science*, **2006**, 29, 1946.

cromatograficamente resolvidos, obedecendo ao requisito da volatilidade e estabilidade térmica. Já o EA-IRMS, mede a razão isotópica global para um dado elemento na amostra, que pode estar no estado sólido e ser não-volátil.

Para a determinação da razão isotópica de carbono, ou seja, a razão $^{13}C/^{12}C$ em amostras, os gases resultantes da combustão passam por um forno de redução que tem a função de transformar compostos nitrogenados do tipo N_xO_y para N_2, evitando a interferência de moléculas isobáricas ao CO_2 nos coletores de Faraday. Em seguida, o CO_2 obtido para cada componente da amostra entra na fonte de íons onde é submetido a uma ionização por um feixe de elétrons. Após a formação dos íons de carga positiva, os mesmos são extraídos da câmera de ionização e acelerados por uma voltagem de aceleração. Em seguida, são separados em um analisador de massas do tipo setor magnético de baixa resolução. A razão $^{13}C/^{12}C$ será calculada através das massas *m/z* 44 ($^{12}CO_2$), *m/z* 45 ($^{13}CO_2$ e $^{12}C^{17}O^{16}O$) e *m/z* 46 ($^{12}C^{18}O^{16}O$), que serão detectados pelos coletores de Faraday, sendo que os respectivos sinais são amplificados e registrados na forma de um pico cromatográfico. Esta razão é comparada a um CO_2 de referência de valor $\delta^{13}C$ conhecido e rastreável para, então, ser determinada a composição isotópica de cada componente da amostra. Os esquemas dos equipamentos de IRMS mais comuns estão apresentados na **Figura 3**.

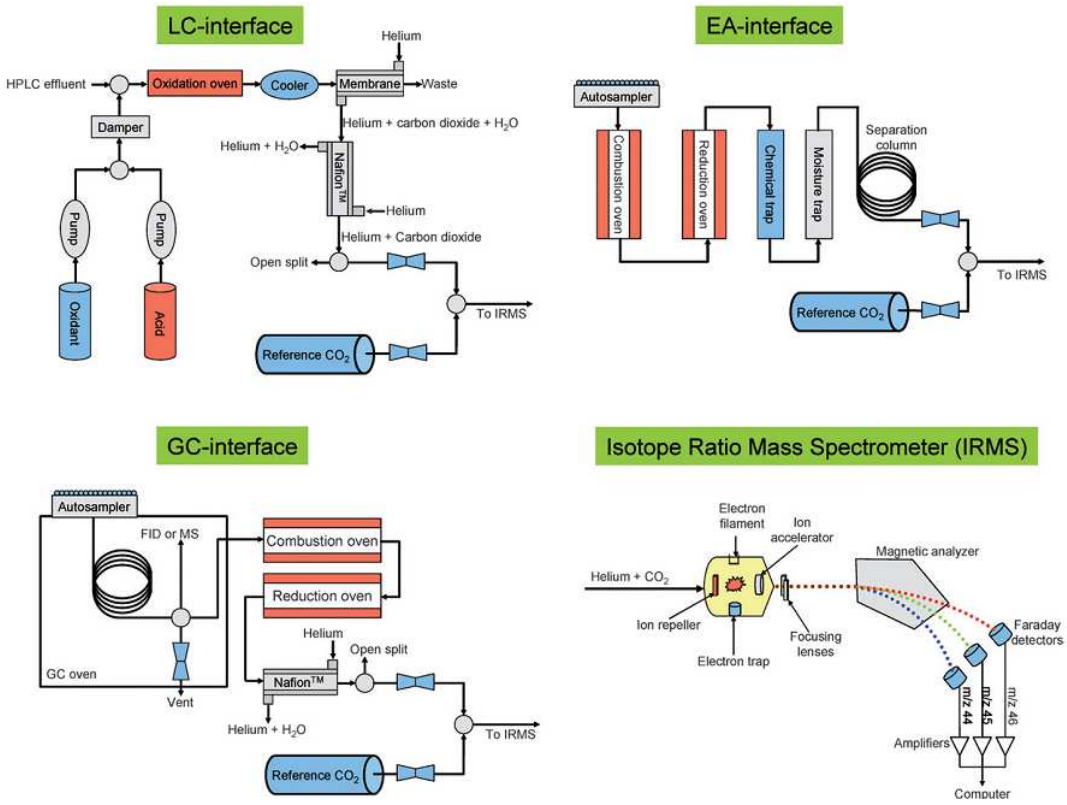

Figura 3. Esquema do espectrômetro de massas de razão isotópica (IRMS) acoplado aos principais sistemas de introdução de amostras: cromatografia líquida (LC – *liquid chromatography*), cromatografia gasosa (GC – *gas chromatography*) e analisador elementar (EA – *elemental analyzer*). (Reproduzido com autorização da Royal Society of Chemistry. Fonte: Analyst, 2009, 134, 213–222)

Como descrito anteriormente, na técnica de IRMS as amostras (ou compostos específicos) são convertidas em um gás através de processos de oxidação e/ou redução e comparado a um gás de referência cujo valor isotópico atribuído por meios de padrões e rastreável a escala internacional. Para isso, os materiais de referência certificados (MRC) são utilizados para atribuir um valor isotópico ao gás de referência, assim como para normalizar os valores isotópicos brutos determinados nas amostras, seja através de curvas de calibração, ou normalização do tipo *single* ou *two-point*. [48]

[48] A) W. A. Brand, T. B. Coplen, J. Vogl, M. Rosner, T. Prohaska. Assessment of international reference materials for isotope-ratio analysis (IUPAC Technical Report). *Pure and Applied Chemistry,* **2014**, 86, 425. B) L. Ke, Z. Lin, Z. Guoxing. Study of normalization method of isotopic compositions to isotope reference scales. *Journal of Chemical and Pharmaceutical Research* , **2014**, 6, 1. C) H. Kipphardt, S. Valkiers, P. D. P. Taylor, P. De Biévre. "Calibration" in isotopic measurements. *International Journal of Mass Spectrometry*, **2000**, 198, 71.
D) J. F. Carter, B. Fry. Ensuring the reliability of stable isotope ratio data—beyond the principle of identical treatment, *Anal Bioanal Chem.* **2013**, 405, 2799. E) D. Paul, G. Skrzypek, I. Fórizs. Normalization of measured stable isotopic compositions to isotope reference scales – a review. *Rapid Commun. Mass Spectrom.* **2007**, 21, 3006 F) R. A. Werner, W. A. Brand. Referencing strategies and techniques in stable isotope ratio analysis, *Rapid Commun. Mass Spectrom.* **2014**, 28, 1674.

Como os MRC aceitos internacionalmente para medições isotópicas são sólidos não voláteis ou materiais viscosos, eles são exclusivamente compatíveis com analisadores elementares, o que dificulta a garantia da rastreabilidade metrológica para metodologias cromatográficas. Neste caso, os métodos de normalização dos dados brutos são altamente recomendados, utilizando padrões secundários de trabalho com propriedades físicas e químicas semelhantes aos analitos de interesse, mesma faixa de valores isotópicos, devidamente determinados e rastreáveis de acordo com a escala internacional. [49]

As razões isotópicas mais comumente determinadas para moléculas orgânicas são $^{13}C/^{12}C$, $^{2}H/^{1}H$, $^{15}N/^{14}N$, $^{18}O/^{16}O$ e $^{34}S/^{32}S$. [50] Elas são expressas usando a notação δ (delta) que relaciona as concentrações do isótopo menos abundante do elemento em relação a concentração do mais abundante. A maneira pela qual, geralmente, o valor de uma medida isotópica é expresso em relação a um padrão internacional e de composição isotópica conhecida é através da notação δ, dada pela Equação 1:

$$\delta^{13}\mathrm{C}\ (‰) = \delta^{13/12}\mathrm{C} = [\frac{R_{amostra}}{R_{padrão}} - 1] * 1000$$

Equação 1

Onde: $R_{amostra}$ é a razão isotópica $^{13}C/^{12}C$ da amostra e $R_{padrão}$ é a razão $^{13}C/^{12}C$ isotópica do padrão.

A variável $R_{padrão}$ é geralmente a razão isotópica de um gás de referência, injetado no equipamento de IRMS juntamente com a amostra, cujo valor é determinado através da utilização de materiais de referências certificados para valores isotópicos, e

[49] L. A. Neves, et al. The influence of different referencing methods on the accuracy of $\delta^{13}C$ value measurement of ethanol fuel by gas chromatography combustion/isotope ratio mass spectrometry, *Rapid Commun. Mass Spectrom*. **2015**, 29, 1938.

[50] A) Simon J. Prosser, Charles M. Scrimgeour, High-Precision Determination of $^{2}H/^{1}H$ in H_2 and H_2O by Continuous-Flow Isotope Ratio Mass Spectrometry. *Anal. Chem*., **1995**, 67 (13), 1992; B) M. H. Engel, V. Andrusevich, S. A. Macko, M. E. Uhle, Stable Nitrogen Isotope Analysis of Amino Acid Enantiomers by Gas Chromatography/Combustion/Isotope Ratio Mass Spectrometry, *Anal. Chem*., **1997**, 69 (5), 926; C) D. A. Merritt, J. M. Hayes, D. J. Des Marais, Carbon isotopic analysis of atmospheric methane by isotope-ratio-monitoring gas chromatography-mass spectrometry, *Journal of Geophysical Research: Atmospheres*, **1995**, 100, 1317; D) J. Koziet, Isotope ratio mass spectrometric method for the on-line determination of oxygen-18 in organic matter, *Journal of Mass Spectrometry*, **1997**, 32, 103; E) N. V. Grassineau , D. P. Mattey, D. Lowry. Sulfur Isotope Analysis of Sulfide and Sulfate Minerals by Continuous Flow-Isotope Ratio Mass Spectrometry, *Anal. Chem*., **2001**, 73 (2), 220.

medidos com relação a uma escala internacional. Para medidas de $\delta^{13}C$, por exemplo, todas as medidas isotópicas são feitas com relação à escala VPDB (Viena Pee Dee Belemnite)[51], que é o ponto zero (*"zero point"*) internacional para a medida de $\delta^{13}C$. [52] Como essas diferenças são geralmente mínimas, as notações δ são expressas em permil (‰) ou mili Urey (mUr).

A IRMS é uma técnica que tem sido cada vez mais aplicada a diferentes tipos de estudos, como por exemplo, para a determinação da origem (exógena ou endógena) de substâncias proibidas na área de dopagem no esporte; [53] para a determinação da fonte de matéria prima para a produção fermentativa do etanol; [54] para a determinação da origem do petróleo (lacustre ou marinho); [55] para a investigação da adulteração de alimentos e bebidas, [56] entre muitos outros. É uma técnica bastante poderosa em termos de resposta analítica, que fornece resultados adicionais a estudos em que apenas a identificação ou quantificação de um analito (ou um grupo deles) não fornece evidências suficientes para a elaboração de uma conclusão irrefutável.

1.3.3. Mobilidade iônica acoplada à espectrometria de massas

Quando acoplada à MS, a mobilidade iônica (*ion mobility* – IM) se torna uma ferramenta analítica importante para a investigação estrutural de compostos orgânicos e para a caracterização de amostras complexas. O acoplamento da IM com a MS é geralmente referido como IM-MS. Enquanto a MS mede primariamente a *m/z* dos íons, a IM adiciona uma nova dimensão aos dados fornecendo para cada valor de *m/z* um

---

[51] O padrão universal utilizado como *zero point* (valor de δ = 0 ‰) para a composição isotópica de carbono é o PDB (Pee Dee Belemnite), que consiste em um fóssil composto de carbonato de cálcio marinho de uma belemnite do período Cretácio (*Belemnitella americana*) da formação Pee Dee, da Carolina do Sul, nos Estados Unidos. Esse padrão de referência internacional, o PDB, esgotou-se e foi substituído pelo Vienna Pee Dee Belemnite (VPDB), um padrão secundário, para a determinação da razão isotópica $^{13}C/^{12}C$. Por razões práticas, é mais conveniente adotar um padrão de trabalho no laboratório, calibrando o gás de referência segundo este padrão de valor certificado, realizando a rastreabilidade à escala internacional, ou seja, ao VPBD.

[52] A. Schimmelmann, et al., Organic Reference Materials for Hydrogen, Carbon, and Nitrogen Stable Isotope-Ratio Measurements: Caffeines, n-Alkanes, Fatty Acid Methyl Esters, Glycines, l-Valines, Polyethylenes, and Oils, *Analytical Chemistry*, **2016**, 88 (8), 4294.

[53] A. Casilli, et al. Optimization of an online heart-cutting multidimensional gas chromatography clean-up step for isotopic ratio mass spectrometry and simultaneous quadrupole mass spectrometry measurements of endogenous anabolic steroid in urine. *Drug Test. Analysis*, **2016**, 8, 1204.

[54] L. A. Neves, et al., The carbon isotopic ($^{13}C/^{12}C$) signature of sugarcane bioethanol: certifying the major source of renewable fuel from Brazil, *Analytical Methods*, **2015**, 7, 4780.

[55] A. Wilhelms, S.R. Larter, K. Hall, A comparative study of the stable carbon isotopic composition of crude oil alkanes and associated crude oil asphaltene pyrolysate alkanes, *Organic Geochemistry*, 21, **1994**, 751.

[56] K. A. van Leeuwen, P. D. Prenzler, D. Ryan, F. Camin, Gas Chromatography-Combustion-Isotope Ratio Mass Spectrometry for Traceability and Authenticity in Foods and Beverages. *Comprehensive Reviews in Food Science and Food Safety*, **2014**, 13, 814.

espectro de *drift time*, que é tempo que o íon demora em atravessar a cela de mobilidade e alcançar o analisador de massas. Semelhantemente ao espectrômetro de massas QTOF (Fig. 2), o equipamento de IM-MS também apresenta a mesma configuração, porém tem uma cela de mobilidade iônica entre a fonte de íons e o analisador por tempo de voo. [57]

A técnica baseia-se no princípio de que a velocidade com que diferentes íons atravessam um gás neutro sob a influência de um campo elétrico fraco é dependente de sua mobilidade iônica, que por sua vez depende de parâmetros como pressão e a natureza química do gás de mobilidade, temperatura do sistema, carga, massa, seção de choque do íon e da interação química do íon do analito e o gás de mobilidade. [58] Todos estes parâmetros juntos farão com que diferentes íons atravessem a cela de mobilidade com diferentes velocidades, podendo ser separados antes de atingir o analisador por tempo de voo, como representado na **Figura 4**. O espectro de massas da técnica têm três dimensões: um eixo de intensidade, outro de *m/z* e o terceiro com o *drift time* associado a cada íon do espectro de MS.

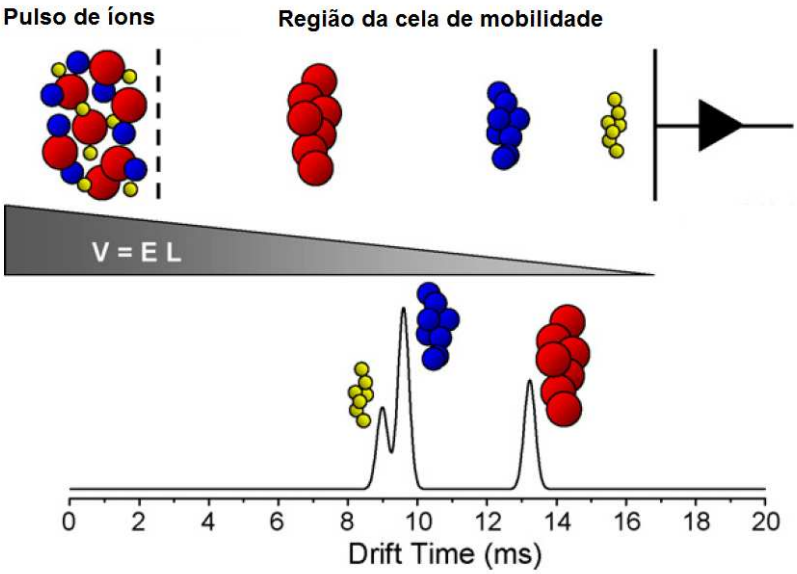

Figura 4. Esquema demonstrando o princípio básico da separação por mobilidade iônica, em que íons com diferentes estruturas tridimensionais irão atravessar a cela de mobilidade com diferentes tempos (*drift times*).

[57] C. Wu, W. F. Siems, G. R. Asbury, H. H. Hill Electrospray Ionization High-Resolution Ion Mobility Spectrometry–Mass Spectrometry, *Analytical Chemistry*, **1998**, 70 (23), 4929.
[58] A. B. Kanu, P. Dwivedi, M. Tam, L. Matz, H. H. Hill Jr, Ion mobility-mass spectrometry, *Journal of Mass Spectrometry,* **2008,** 43, 1.

Em termos matemáticos, a mobilidade iônica (K) é característica para cada íon e depende de diversos fatores como a carga do íon (q), a densidade molar do gás de mobilidade (N), a massa reduzida do ion e do gás (μ), da temperatura absoluta (T) e da seção de choque do íon (Ω) e são relacionados matematicamente através da equação de Mason-Schamp [59] (equação 2):

$$K = \frac{3}{16} \times \frac{q}{N} \times \left(\frac{1}{\mu} \times \frac{2\pi}{kT} \right)^{\frac{1}{2}} \times \frac{1}{\Omega}$$

Equação 2

Esta equação mostra que a mobilidade de um íon é inversamente proporcional à raiz quadrada da massa reduzida e também inversamente proporcional à seção de choque do íon. Entretanto, esta equação não leva em consideração as interações entre o íon e o gás de mobilidade do tipo íon-dipolo/dipolo induzido, sendo basicamente válida apenas quando hélio (gás "clássico" de mobilidade) é utilizado como gás de mobilidade, quando estas interações podem ser desconsideradas, já que o hélio é um gás que pode ser considerado pouco ou não polarizável. Entretanto, estudos mostram que a utilização de gases mais polarizáveis pode melhorar a separação por mobilidade. [60] Em um conjunto de experimentos em que todos os parâmetros do gás permaneçam constantes (temperatura, pressão e a natureza do gás), pode-se considerar que a mobilidade iônica (K) fica então dependente somente da seção de choque e da *m/z* dos íons, de acordo com a relação apresentada na equação 3:

$$K^{-1} \alpha \left(\frac{m}{q} \right) \Omega$$

Equação 3

Da relação acima, obtém-se o aspecto mais interessante da técnica de IM-MS: a capacidade de separação de íons de mesma *m/z*, porém com distintas conformações espaciais em fase gasosa. Os íons com menor Ω e, portanto com maior mobilidade, irão atravessar a cela de mobilidade com maior rapidez e alcançarão o

[59] A. Ahmed, et al. Application of the Mason–Schamp Equation and Ion Mobility Mass Spectrometry To Identify Structurally Related Compounds in Crude Oil, *Analytical Chemistry*, **2011**, 83 (1), 77.
[60] G. R. Asbury, H. H. Hill Jr., Using Different Drift Gases To Change Separation Factors (α) in Ion Mobility Spectrometry, *Analytical Chem*istry, **2000**, 72, 580.

detector mais rapidamente. O conjunto de íons que foram separados ao longo da travessia da cela de mobilidade chega ao analisador de massas em tempos diferentes resultando em um pico no espectro de mobilidade para cada íon. O tempo que um íon demora a atravessar a cela de mobilidade é chamado de *drift time* (dt) e geralmente é medido em milisegundos.

Basicamente, um equipamento de IM-MS deve conter 5 principais componentes: um sistema de introdução de amostra, a fonte de íons, a cela de mobilidade, o analisador de massas e o detector de íons. A amostra pode ser introduzida em um instrumento de IM-MS praticamente em todos os estados: sólido, líquido e vapor. Todas as fontes utilizadas em MS são compatíveis com equipamentos de IM-MS. [61]

Os equipamentos clássicos de mobilidade iônica utilizam um campo elétrico uniforme e estático para conduzir os íons através do gás na cela de mobilidade iônica. Esses equipamentos apresentam baixa sensibilidade devido ao longo tempo que os íons levam para atravessar o equipamento e a difusão da nuvem iônica durante a separação. Um dos grandes avanços sofridos pela técnica de IM-MS foi alcançada através da utilização de um gradiente de voltagem ao invés de uma voltagem fixa na espectrometria de mobilidade iônica. Foi quando em 2004, desenvolveu-se a técnica denominada de Traveling Wave Ion Mobility Mass Spectrometry (TWIM-MS), [62] instrumentalmente comercializada pela Waters Corporation (Manchester, UK), equipamento batizado comercialmente de *Synapt HDMS*. Nesta modalidade, os íons são acumulados e periodicamente liberados na cela de mobilidade, onde serão separados de acordo com suas mobilidades sobre a ação de pulsos periódicos transientes de voltagens que são aplicados nos eletrodos que constituem a cela de mobilidade, controlados através de RF (rádio frequência).[63]

Em seguida, a Waters comercializou versões aprimoradas deste equipamento: o Synapt G2, com maior poder de resolução tanto de *m/z*, tanto quanto de mobilidade iônica; o G2S, que oferece maior sensibilidade; e por último o G2-S*i,* que permite também a determinação experimental do valor da seção de choque (Ω) através da

[61] S. D. Pringle, et al. An investigation of the mobility separation of some peptide and protein ions using a new hybrid quadrupole/travelling wave IMS/oa-ToF instrument *Int. J. Mass Spectrom.* **2007**, 261, 1.
[62] K. Giles, S. D. Pringle, K. R. Worthington, D. Little, J. L.Wildgoose, R. H. Bateman. Applications of a travelling wave-based radio-frequency-only stacked ring ion guide, *Rapid Commun. Mass Spectrom.* **2004**, 18, 2401.
[63] A. A. Shvartsburg, R. D. Smith, Fundamentals of Traveling Wave Ion Mobility Spectrometry, *Analytical Chemistry.* **2008,** 80*,* 9689.

calibração da cela de mobilidade iônica através da utilização de padrões cujos valores de Ω para os íons seja conhecido. [64] A determinação da seção de choque de um íon é mais um parâmetro de confirmação da identidade química de um analito, visto que atualmente existem bancos de dados com valores de Ω para diversas classes de substâncias, [65] determinados tanto experimentamente, quanto através de cálculos teóricos computacionais. [66] Muitos outros fabricantes atualmente também comercializam equipamentos de IM-MS, que diferem basicamente na configuração da cela de mobilidade, ou seja, em seu tamanho, na forma como o campo elétrico é aplicado, e na magnitude da pressão do gás de mobilidade. [67]

O esquema do equipamento de TWIM-MS é apresentado na **Figura 5**. O analisador de massas desse equipamento também é do tipo QTOF. Um dos aspectos fundamentais deste equipamento é a região de mobilidade iônica, que compreende três "guias de íons" (*ion guides*), que juntos são denominados de *TriWave*:

- O *Trap* acumula os íons e os libera em "pacotes" para a cela de mobilidade;
- Na cela de mobilidade ocorre a separação de íons com diferentes mobilidades iônicas, através da interação dos íons com o gás de mobilidade que preenche a cela, sob a influência de um campo elétrico oscilante;
- O *Transfer* tem a função de conduzir os íons separados na cela de mobilidade para o analisador de massa (TOF).

[64] S. D. P. Smith et al. Deciphering drift time measurements from travelling wave ion mobility spectrometry-mass spectrometry studies. *European Journal of Mass Spectrometry*, **2009**, *15*, 113.
[65] Z. Zhou, J. Tu, X. Xin, X. Shen, Z.-J. Zhu, LipidCCS: Prediction of Collision Cross-Section Values for Lipids with High Precision to Support Ion Mobility-Mass Spectrometry based Lipidomics, *Analytical Chemistry*, **2017**, 89, 9559.
[66] A. Marchand, S. Livet, F. Rosu, V. Gabelica, Drift Tube Ion Mobility: How to Reconstruct Collision Cross Section Distributions from Arrival Time Distributions?, *Analytical Chemistry*, 2017, 89 (23), 12674.
[67] R. Cumeras, E. Figueras, C. E. Davis, J. I. Baumbach, I. Gràcia, Review on Ion Mobility Spectrometry. Part 1: current instrumentation, *Analyst*, **2015**, 140, 1376.

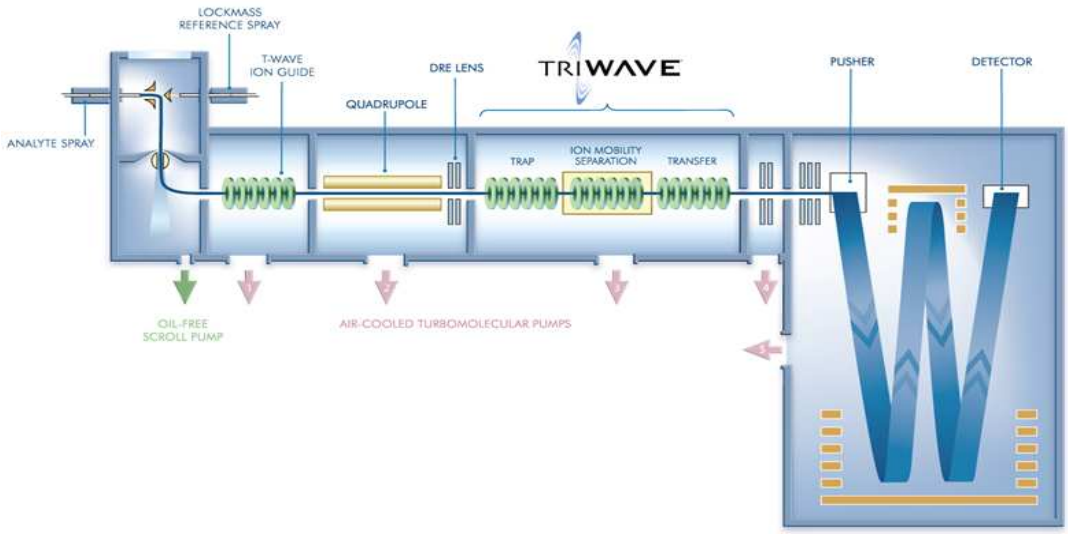

Figura 5. Esquema do equipamento de TWIM-MS Synapt HDMS (Waters Corporation, Manchester, UK).

A IM-MS está cada vez mais sendo aplicada com diversas finalidades, como a diferenciação de isômeros, [68] para a caracterização de misturas complexas como polímeros e petróleo, [69] e também para estudos de proteômica, [70] metabolômica [71] e lipidômica, [72] pois a adição de mais um parâmetro físico-químico aos dados de MS ajuda na identificação de analitos desconhecidos.

[68] P. M. Lalli et al. Baseline resolution of isomers by traveling wave ion mobility mass spectrometry: investigating the effects of polarizable drift gases and ionic charge distribution. *Journal of Mass Spectrometry*, **2013**, *48*, 989.
[69] A) M. Fasciotti et al. Petroleomics by Traveling Wave Ion Mobility–Mass Spectrometry Using CO_2 as a Drift Gas, *Energy & Fuels*, **2013**, 27 (12), 7277; B) J. M. Santos et al. Petroleomics by ion mobility mass spectrometry: resolution and characterization of contaminants and additives in crude oils and petrofuels, *Analytical Methods*, **2015**, 7, 4450.
[70] G.H.M.F. Souza, P.C. Guest, D. Martins-de-Souza, LC-MS(E), Multiplex MS/MS, Ion Mobility, and Label-Free Quantitation in Clinical Proteomics. *Methods in Molecular Biology*, **2017**, 1546, 57.
[71] M. McCullagh, D. Douce, E. Van Hoeck, S. Goscinny, Exploring the Complexity of Steviol Glycosides Analysis Using Ion Mobility Mass Spectrometry, *Analytical Chemistry*, **2018**, 90(7), 4585.
[72] G. Paglia, G. Astarita, Metabolomics and lipidomics using traveling-wave ion mobility mass spectrometry. *Nature Protocols*, **2017**, 12, 797.

CAPÍTULO 2. ARTIGOS PUBLICADOS OU EM FASE DE PUBLICAÇÃO

Nos tópicos a seguir, serão apresentados os artigos publicados, assim como os manuscritos em fase de elaboração para publicação, que foram resultantes das pesquisas desenvolvidas no contexto desta tese de doutorado.

2.1. Wood Chemotaxonomy via ESI-MS profiles of phytochemical markers: The challenging case of African versus Brazilian Mahogany woods

Publicado originalmente em: *Analytical Methods*, 2015, 7, 8847-8980. O artigo também foi capa externa da revista.

Volume 7 | Number 20 | 21 October 2015 | Pages 8487–8980

Analytical Methods

www.rsc.org/methods

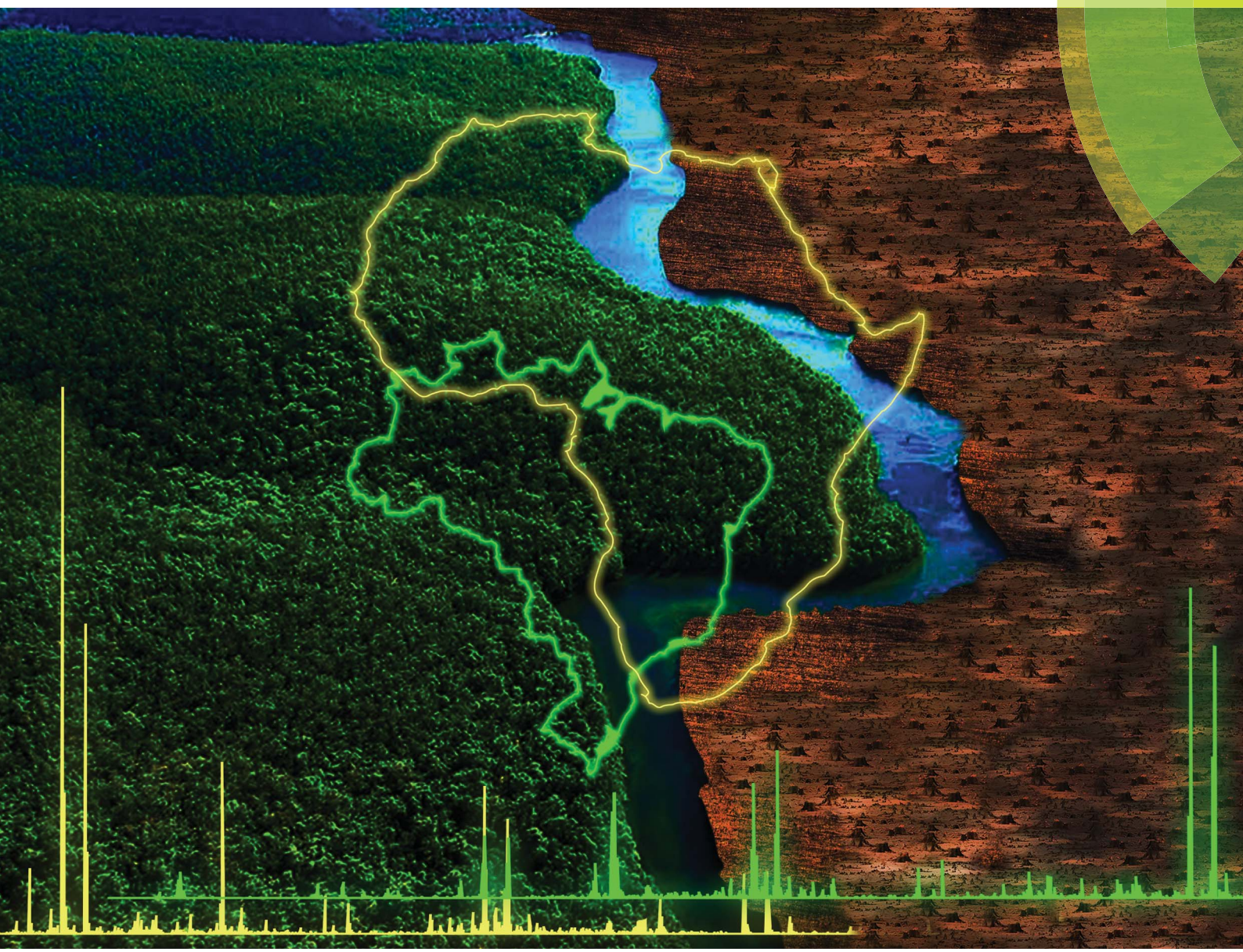

ISSN 1759-9660

ROYAL SOCIETY OF CHEMISTRY

PAPER

Maíra Fasciotti *et al.*

Wood chemotaxonomy *via* ESI-MS profiles of phytochemical markers: the challenging case of African *versus* Brazilian mahogany woods

Analytical Methods

PAPER

Cite this: *Anal. Methods*, 2015, 7, 8576

Wood chemotaxonomy *via* ESI-MS profiles of phytochemical markers: the challenging case of African *versus* Brazilian mahogany woods

Maíra Fasciotti,*[ab] Rosana M. Alberici,[ab] Elaine C. Cabral,[bc] Valnei S. Cunha,[a] Paulo R. M. Silva,[a] Romeu J. Daroda[a] and Marcos N. Eberlin*[b]

Received 3rd July 2015
Accepted 14th August 2015

DOI: 10.1039/c5ay01725d

www.rsc.org/methods

The harvesting of Brazilian mahogany (*Swietenia macrophylla*) is a main cause of the Brazilian Amazon deforestation and has been therefore prohibited. African mahogany (*Khaya ivorensis*) was then introduced for Amazon reforestation and the commercialization of such wood is legal, thus creating a challenging problem for wood certification. Herein we report that a wood chemotaxonomic method based on distinct profiles of phytochemical markers is able to promptly characterize both the native and foreign mahogany species. This challenging task has been performed *via* a simple, fast and unambiguous methodology using direct electrospray ionization mass spectrometry (ESI-MS) analysis of a simple methanolic extract of a tiny wood chip. Typical limonoids such as khivorin, khayanolide A and mexicanolide for African mahogany and phragmalin-type limonoids for the native Brazilian species, as well as distinct polyphenols such as catechin derivatives and cinchonain, form the characteristic phytochemical marker pools for both species. This rapid methodology could therefore be used to monitor legal and illegal mahogany tree harvesting, and hence to control Amazon deforestation. It could also be applied to create a wood certification program for African and Brazilian mahogany trees, as well as for wood certification in general.

Introduction

Mahogany (*Swietenia macrophylla*) – also known as "green gold" – is probably one of the most precious wood species from the Brazilian Amazon. Due to the superior aesthetics, physical characteristics and ease of woodworking, mahogany has been used to produce noble and luxurious furniture items.[1] During the 1990's, millions of cubic meters of native mahogany were removed from the Amazon forest,[2] and this devastation is listed among the main causes of the dramatic Brazilian Amazon deforestation. Consequently, mahogany was included in 2002 in Appendix II of the Convention on International Trade in Endangered Species (CITES), which established strict regulations for international trade of an endangered species.[3] Due to its endangered status and importance in the global market, mahogany is the focus of many efforts towards its conservation, harvesting and regeneration.[4]

In 2003, the Brazilian government prohibited the harvesting of native mahogany trees.[5] Even though several legal actions are in place to counter illegal logging and the subsequent trade, there is however a lack of effective mechanisms to identify the origin of timber and wood products. To solve this problem, the Brazilian forest certification program (Cerflor) was established in 2002, and has been developed by the National Institute of Metrology, Quality and Technology (INMETRO).[6]

Khaya ivorensis, which occurs on the West Coast of Africa from Sierra Leone to Cabinda, is also a famous African mahogany species. Due to its high-quality timber and its high resistance to the drill pointer (*Hypsiphyla grandella*), the major pest of Brazilian mahogany (*S. macrophylla*), African mahogany has been increasingly used for Amazon reforestation. This tree species was found to grow about 30% faster than Brazilian mahogany. Currently, it is estimated that there are over one million African mahogany trees planted in Brazil and investments to encourage this culture are increasing.[7]

Brazilian and African mahogany species belong to the same Meliaceae family and *Swietenioideae* subfamily differing only in genus but most importantly in their pools of phytomarkers. African mahogany belongs to the *Khaya* genus whereas Brazilian mahogany belongs to the *Swietenia* genus.[8] The Meliaceae family is characterized by the presence of limonoids with a large range of biological activities.[9–11] The *Khaya* genus is closely related to the *Swietenia* genus, but is known to exhibit unique

[a]*National Institute of Metrology, Quality and Technology-INMETRO, Division of Chemical Metrology, 25250-020, Duque de Caxias, RJ, Brazil. E-mail: mfasciotti@inmetro.gov.br*

[b]*ThoMSon Mass Spectrometry Laboratory, Institute of Chemistry, University of Campinas-UNICAMP, 13083-970, Campinas, SP, Brazil. E-mail: eberlin@iqm.unicamp.br*

[c]*Chemical, Biological and Agricultural Pluridisciplinary Research Center (CPQBA), Chemistry of Natural Products Division, University of Campinas – Unicamp, CEP 13081-970, Campinas, São Paulo, Brazil*

phytochemical markers. For instance, several limonoid classes, such as khivorins, angolensates, mexicanolides and fissinolides, have been isolated from different parts of *K. ivorensis*,[12–14] whereas *S. macrophylla* shows mainly phragamalin-class limonoids.[15–18] The configuration at C-6 of mexicanolides, phragmalins and khayanolides from *Khaya* is also of the 6*S* configuration whereas those from *Swietenia* species are 6*R*. These metabolic differences indicate that their chemotaxonomic differentiation is feasible.

Direct infusion mass spectrometry (MS) using electrospray ionization (ESI-MS) has been widely applied for rapid, direct and effective fingerprint characterization of complex mixtures including extracts of natural products.[19–24] Recently, both ESI-MS and[25] Venturi easy ambient sonic-spray ionization MS (V-EASI-MS)[26] fingerprinting have been applied to characterize typical phytochemical markers[17,18] which were found to be unique to Brazilian mahogany and absent in other typical species of very similar morphology but quite contrasting Brazilian wood families.[27] Herein, direct ESI-MS fingerprinting of a methanolic extract obtained from a tiny wood chip in which pools of phytochemical markers are detected was performed. This is a very challenging task to promptly and effectively differentiate woods from Brazilian and African mahogany trees that belongs to different species but to the same tree family.

Experimental

Wood samples

Samples of certified African mahogany (*K. ivorensis*) were donated by the Brazilian Agricultural Research Corporation (EMBRAPA – Oriental Amazon). African mahogany was raised in the city of Belem, in Pará State in Brazil; wood pieces of certified Brazilian mahogany (*S. macrophylla*) were donated by a local lumberyard. We ensured that no Brazilian mahogany tree was harvested to conduct this work.

Sample preparation

An extract of the wood sample was prepared "*in situ*" before analysis. The most external layers were discarded to avoid the sampling of oxidized compounds or even some possible contamination. For Brazilian mahogany (BM), the samples were randomly collected from wood pieces and mixed just before extraction. For African mahogany (AM), the samples were collected over the whole tree stem cross-section radius, from sampling points spaced by 3 cm from each other (Scheme 1). After collection, the wood samples were cut into small pieces (*ca.* 0.5 mm of diameter) and 10 μL of methanol (HPLC Grade, Tedia, Brazil) was added to each 1 mg of wood precisely weighed. The samples were vortexed for 2 min and then centrifuged for 5 min in a microtube centrifuge. Methanolic extracts were then diluted (1 : 100 v/v) in methanol with 0.1% of ammonium hydroxide for ESI(−)-MS. For ESI(+)-MS, 2 μL of a sodium chloride 0.1 mmol L^{-1} aqueous solution was added to the final solution to favor the formation of sodium adducts.

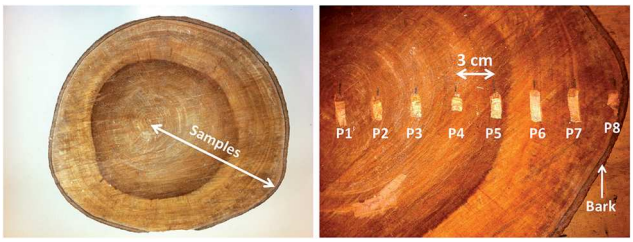

Scheme 1 Sampling scheme for African mahogany wood. The samples were collected in selected parts throughout the whole radius of the tree stem cross-section.

ESI-MS and ESI-MS/MS analysis

ESI-MS and ESI-MS/MS data were acquired in both the negative and positive ion modes using a QTOF (Micromass, Manchester, UK) mass spectrometer. The operation conditions are as follows: 3.0 kV capillary voltage, 100 °C source temperature, desolvation temperature of 100 °C, sampling cone voltage of 30 V and extraction voltage of 3.0 V. The diluted methanolic extract was directly injected into the ESI source by using an automatic injection pump (Harvard Apparatus) with a continuous flow of 10 μL min^{-1}. The full scan ESI-MS spectra were acquired in the range of *m*/*z* 50 to 2000 and the total time for acquisition of each spectrum was set at 2 min, at an acquisition rate of 1 scan per

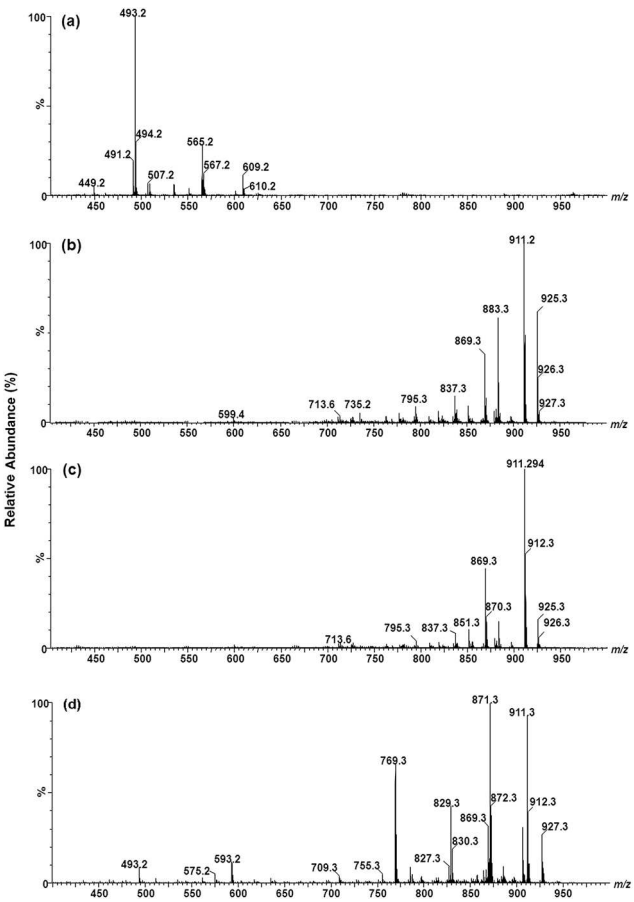

Fig. 1 ESI(+)-MS spectra of the methanolic extracts for (a) AM and (b–d) three BM samples from three different trees.

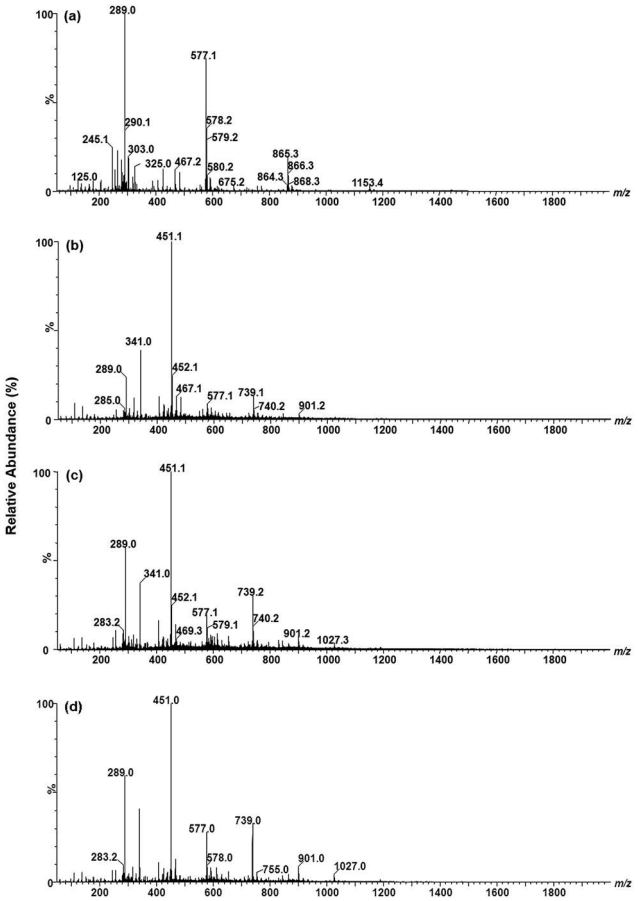

Fig. 2 ESI(−)-MS spectra of the methanolic extracts for (a) AM and (b–d) BM samples from three different trees.

second. The ESI-MS/MS spectra were obtained *via* collision-induced dissociation (CID) and acquired from *m*/*z* 50 to *m*/*z* values slightly above those of the ion under study. Argon was used as collision gas, with collision energies varying from 10 to 40 eV, optimized for each ion. Spectra were processed using the MassLynx 4.0 software (Waters, Manchester, UK). The TOF analyzer was daily calibrated with a 0.1% (v/v) phosphoric acid solution in acetonitrile/water 1 : 1 (v/v). The same solution was used for internal lock-mass calibration in ESI-MS acquisition.

For an unambiguous molecular attribution, FT-ICR-MS analysis was performed in a Thermo Scientific 7.2 T electrospray ionization Fourier transform ion cyclotron resonance mass spectrometer (Thermo Scientific, Bremen, Germany). A scan range of *m*/*z* 200–1000 was used, and 100 microscans were summed in each acquisition. The average resolving power (R_p) was 400 000 at *m*/*z* 400. Time-domain data (ICR signal or transient signal) were acquired for 700 ms and microscans were co-added using Xcalibur version 2.0 (Thermo Scientific).

Results and discussion

ESI-MS QTOF fingerprinting

Woods are mainly composed of cellulose, hemicellulose and lignin[28] and such a composition is known to vary as a function of several parameters such as tree part, geographic origin and environmental conditions.[29] The most detailed identification of trees has been commonly achieved not based on these major constituents but on the analysis of the minor constituents in an approach known as chemotaxonomy.[30,31] Such minor relatively low MW constituents, known as extractives (around 4–10%), can be obtained from the wood sample *via* extraction with water or organic solvents such as methanol.[32,33]

The composition of the methanolic extracts of Brazilian and African mahogany woods was therefore investigated using high resolution ESI-MS. Fig. 1 shows the ESI(+)-QTOF spectra of the methanolic extracts for both African (AM) and Brazilian mahogany (BM). Fig. 1a shows a representative spectrum of an extract obtained from a pool of wood fragments collected from all the sampling points of the AM stem cross-section (Scheme 1), whereas Fig. 1b–d show the spectra of three different BM samples.

Note that the differences between the phytochemical markers detected in the mass spectra for the AM and BM samples are truly remarkable. All the 3 BM samples display a set of very abundant ions in the *m*/*z* 700 to 900 range (Fig. 1b–d), whereas in the AM spectrum (Fig. 1a) no ions of significant abundance are detected in this *m*/*z* range. Both trees belonging to the same family are quite morphologically similar and hence they are hard to distinguish *via* visual inspection, but their different genus strongly impact the chemical profile of secondary metabolites obtained *via* simple and rapid methanolic extraction.

Table 1 Molecular formula and DBE (Double Bond Equivalents) of $[M + Na]^+$ ions attributed to marker phytochemicals *via* ESI(+)-FT-ICR-MS analysis in the methanolic extracts of BM samples

Experimental *m*/*z* by FT-ICR MS	Theoretical *m*/*z*	Error (ppm)	Molecular formula	DBE	Possible components or their isomers	References
735.26195	735.26232	−0.51	$C_{37}H_{44}O_{14}Na$	15.5	(**1**) Swietephragmin J	18
795.28305	795.28345	−0.51	$C_{39}H_{48}O_{16}Na$	15.5	(**2**) Swietenitin D	17
827.30880	827.30967	−1.05	$C_{40}H_{52}O_{17}Na$	14.5	(**3**) Swietenalide D	17
837.29358	837.29358	−0.52	$C_{41}H_{50}O_{17}Na$	16.5	(**4**) Swietenitin C	17
869.31977	869.32023	−0.53	$C_{42}H_{54}O_{18}Na$	15.5	(**5**) 2-Acetoxyswietenalide D	17
883.33544	883.33588	−0.50	$C_{43}H_{56}O_{18}Na$	15.5	(**6**) Swietenitin I	17
885.31429	885.31515	−0.26	$C_{42}H_{54}O_{19}Na$	15.5	(**7**) Swietenitin K	17
911.33047	911.33080	−0.36	$C_{44}H_{56}O_{19}Na$	16.5	(**8**) 2,11-Diacetoxyswietenalide D	17
927.32549	927.32571	−0.24	$C_{44}H_{56}O_{20}Na$	16.5	(**9**) Swietenitin M	17

Table 2 Molecular formula and DBE attributed to marker ions *via* ESI(−)-FT-ICR-MS analysis in the methanolic extracts of BM samples

Experimental *m*/*z* by FTICR MS	Theoretical *m*/*z*	Error (ppm)	Molecular formula	DBE	Possible compound name and isomers	References
289.07110	289.07066	0.82	$C_{15}H_{13}O_6$	9.5	(+)-Catechin/(−)-epicatechin	46
341.06707	341.06612	1.00	$C_{18}H_{13}O_7$	12.5	Cinchonain fragment	—
451.10412	451.10290	1.22	$C_{24}H_{19}O_9$	15.5	Cinchonain IA or IB	47
577.13626	577.13405	1.49	$C_{30}H_{25}O_{12}$	18.5	Procyanidin dimer	46

The phytochemicals present in the methanolic extracts were also investigated *via* ESI(−)-QTOF. As shown in Fig. 2, the spectra of BM and AM samples are quite similar and have a set of common ions such as those of *m*/*z* 289, 577 and 865, but again differentiation is properly attained *via* the presence of a very abundant and unique marker ion of *m*/*z* 451 which unambiguously characterizes the BM samples. This ion is barely detected in the AM extracts.

FT-ICR-MS analysis with molecular formula attribution

The secondary metabolites identified as phytochemical ion markers for both AM and BM samples may belong to several classes of natural products such as flavonoids, terpenes, phenols, alkaloids, sterols, waxes, fats, tannins, sugars, carotenoids, polyphenols, and limonoids.[34,35] These molecules play important roles in the plant metabolism[36] and important phytochemicals have been identified in mahogany trees using different analytical tools.[37] These extractives are complex mixtures of several isobaric species and, of course, isomeric species which cannot be separated by MS. To obtain unambiguous molecular formula for these marker ions *via* accurate (<1 ppm) mass measurements, FT-ICR-MS analysis of the extracts with ultra-high resolution and accuracy was performed (Tables 1–3).

Table 1 summarizes the attributions of the ESI(+)-FT-ICR-MS ions from BM samples. Note that the presence of phragmalin-type limonoids in the BM extracts has been indicated by ESI(+)-MS analysis[27] and by other classical phytochemical approaches.[15,16,18,38]

Via ESI(−)-MS and based on common classes found in wood extracts, we postulate that mainly organic acids and polyphenols are detected,[39] as indeed indicated in Table 2. The major marker ion of *m*/*z* 451, which is unique in the BM extracts, could be attributed to cinchonain IA/IB. Note that this molecule has also been reported in other types of tree woods such as *Phyllocladus trichomanoides*,[40] *Rhizoma Smilacis glabrae*[41] and *Trichilia catigua*,[42] but this is the first report of this biomarker as the main polyphenol in *Swietenia macrophylla*.

Tables 3 and 4 summarize the ion attributions of the AM extract, whereas Fig. 3 shows the chemical structures and numbers (according to Tables 1 and 3) of the most important limonoids identified in both AM and BM extracts.

Note in Table 3 that khayanolide and seneganolide-type limonoids are attributed as the major limonoids detected in the AM sample, a finding that agrees with the known chemotaxonomy of such a genus.[18]

Table 4 also shows polyphenols such as (−)-epicatechin/(+)-catechines as the major constituents attributed in the ESI(−) spectrum of the AM sample. Note that a series of ions were attributed to polymeric epi/catechin detected in their deprotonated forms $[M - H]^-$, *e.g.* as catechin dimers of *m*/*z* 577, trimers of *m*/*z* 865 and tetramers of *m*/*z* 1153, which are known as proanthocyanidins.[43] This same series of polymeric tannins was also identified in the BM samples (Table 2).

ESI-MS/MS

Further information that helps to characterize the key chemotaxonomic marker ions was also obtained *via* ESI-MS/MS

Table 3 Molecular formula of $[M + Na]^+$ ions and DBE attributed to marker phytochemicals *via* ESI(+)-FT-ICR MS analysis in the methanolic extracts of AM samples

Experimental *m*/*z* by FT-ICR-MS	Theoretical *m*/*z*	Error (ppm)	Molecular formula	DBE	Possible compound name and isomers	References
491.20367	491.20402	−0.35	$C_{27}H_{32}O_7Na$	11.5	(**10**) Mexicanolide	13
493.21934	493.21967	−0.33	$C_{27}H_{34}O_7Na$	10.5	(**11**) Methyl angolensate	10 and 14
509.21423	509.21459	−0.36	$C_{27}H_{34}O_8Na$	10.5	(**12**) Methyl 6-hydroxyangolensate	10 and 14
535.22982	535.23024	−0.42	$C_{29}H_{36}O_8Na$	11.5	(**13**) Fissinolide	46
539.18831	539.18877	−0.46	$C_{27}H_{32}O_{10}Na$	11.5	(**14**) 1-*O*-Deacetylkhayanolide E	14
541.20396	541.20442	−0.46	$C_{27}H_{34}O_{10}Na$	10.5	(**15**) Khayalactol	14
551.22492	551.22515	−0.23	$C_{29}H_{36}O_9Na$	11.5	(**16a**) 3-Acetylswietenolide; (**16b**) 2-hydroxyfissinolide or (**16c**) 3-*O*-detigloyl-3-*O*-acetylswietenine	10 and 13
567.25606	567.25645	−0.69	$C_{30}H_{40}O_9Na$	10.5	(**17**) 3-Deacetylkhivorin	10
583.21464	583.21555	−0.59	$C_{29}H_{36}O_{11}Na$	11.5	(**18**) 1-*O*-Acetylkhayanolide B	14
609.26657	609.26702	−0.99	$C_{32}H_{42}O_{10}Na$	6.5	(**19**) Khivorin	13

Table 4 Formula and DBE attributed to marker ions *via* ESI(−)-FT-ICR-MS analysis in the methanolic extracts of AM samples

Experimental *m*/*z* by FT-ICR-MS	Theoretical *m*/*z*	Error (ppm)	Molecular formula	DBE	Possible compound name and isomers	References
289.07162	289.07066	−0.48	$C_{15}H_{13}O_6$	9.5	(+)-Catechin/(−)-epicatechin	48
577.13490	577.13045	−0.43	$C_{30}H_{25}O_{12}$	18.5	Procyanidin dimer	48
865.19826	865.19744	−0.32	$C_{45}H_{37}O_{18}$	27.5	Procyanidin trimer	48
1153.26139	1153.26082	−0.46	$C_{60}H_{49}O_{24}$	36.5	Cinnamtannin A2	46

experiments (Fig. 4). For instance, the ion of *m*/*z* 577 (Fig. 4a) was attributed to $[M - H]^-$ of the procyanidin dimer, fragments as expected mainly to the ion of *m*/*z* 289, *e.g.* to the monomeric epi/catechin. The ion of *m*/*z* 493 (methyl angolensate), which forms the base ion peak of the AM extract in the ESI(+) spectra (Fig. 1a), forms a major fragment ion of *m*/*z* 81 (Fig. 4b), which can be attributed to the pyrylium ion,[44] which together with the ion of *m*/*z* 83, forms a pair of marker fragments for the limonoid class.[45]

The very unique BM anion of *m*/*z* 451 (Fig. 4c) dissociates to a very abundant fragment ion of *m*/*z* 341 likely due to the loss of one catecol moiety from the cinchonain structure. The $[M + Na]^+$ ion of *m*/*z* 911, which is the most abundant ion in the ESI(+)-MS spectra of the BM extract (Fig. 1b–d), dissociates as expected from its proposed structure mostly through the neutral loss of acetic acid (60 Da) to form the fragment ion of *m*/*z* 851 (Fig. 4d).[27]

Spatial distribution of phytochemicals in African mahogany

To investigate whether different parts of a tree would provide different pools of phytochemical markers detected by ESI-MS, the variation of ESI(±)-MS of the methanolic extracts as a function of the stem cross-section of the AM tree was monitored (Fig. 5 and 6). Samples were collected from points separated by 3 cm and numbered from P1 (central point) to P8 (most external

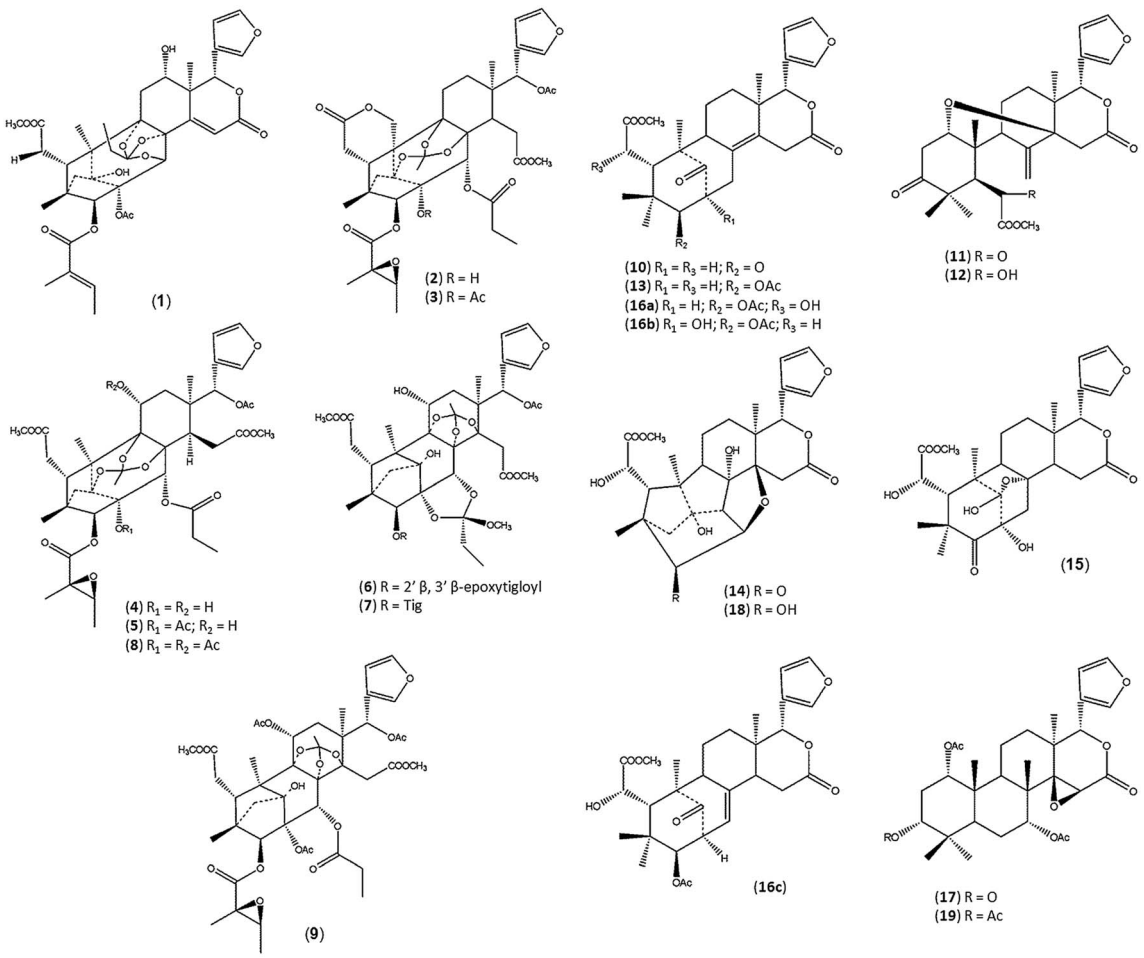

Fig. 3 Chemical structures of the most important limonoids identified in both AM and BM.

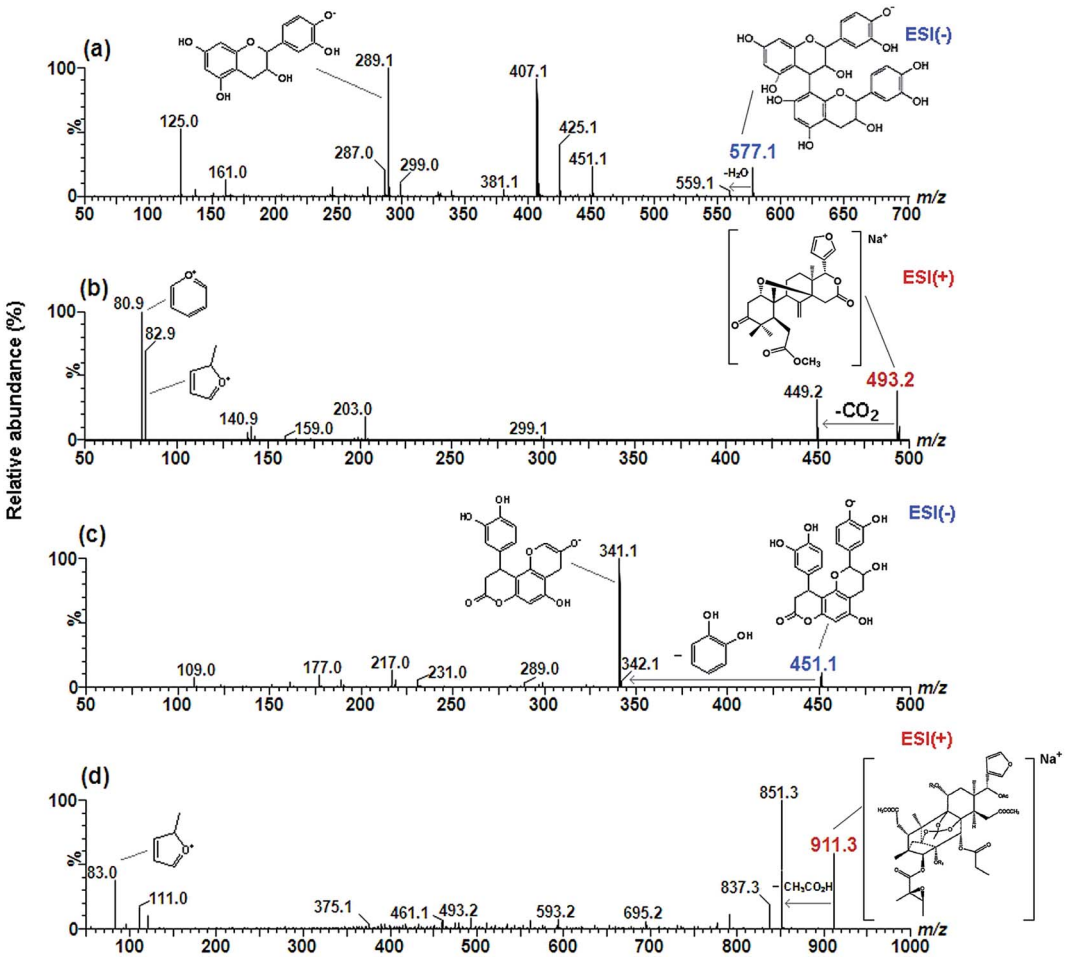

Fig. 4 MS/MS spectra of representative marker ions. (a) ESI(−)-MS/MS of procyanidin dimer (*m*/*z* 577) of AM; (b) ESI(+)-MS/MS of methyl angolensate (*m*/*z* 493) of AM; (c) ESI(−)-MS/MS of cinchonain (*m*/*z* 451) of BM and (d) ESI(+)-MS/MS of 2,11-diacetoxyswietenalide D (*m*/*z* 911) of BM.

point) and bark, as detailed in the Experimental section and Scheme 1. Samples were therefore collected from the major parts of the tree, including the pith (P1), the primary and secondary xylem (P2 to P4), cambium (P5), phloem (P6 and P7), P8 (phloem inner bark) and external bark.

Fig. 5 shows very similar ESI(+)-MS profiles except for P7 (Fig. 5d), with an abundant and unique ion of *m*/*z* 365 and most particularly for the bark (Fig. 5e), with a predominant and unique ion of *m*/*z* 509. Even though the ion of *m*/*z* 365 is the base peak in P7, it cannot be considered a trustable phytochemical marker of AM, because it is not present in all the collected samples throughout the tree radius.

The ESI(−)-MS profiles (Fig. 6) show an interesting trend, that is, the relative abundance of the epi/catechin polymer ions, that is of the dimer (*m*/*z* 577), trimer (*m*/*z* 865) and tetramer (*m*/*z* 1153), increases as a function of tree radius, and this trend can be clearly seen, for instance in Fig. 7, for the ion of *m*/*z* 865. This finding seems to agree with the knowledge that polymerization of tannins increases with tree aging.[46] Another important aspect is again the uniqueness of the bark spectrum (Fig. 6e) similar to what was observed for ESI(+)-MS. Indeed, it has been reported that the amount and variability of secondary metabolites are much higher in the bark.[29] Samples from the bark should therefore be avoided when using phytomarkers of mahogany samples for chemotaxonomy differentiation.

Conclusions

A set of well characterized phytochemical markers that can be used to differentiate both BM and AM were detected by ESI-MS. Although more accurate MS instrumentation was used in this study, the methodology should work as well in simpler mass spectrometers, such as quadrupoles, or even portable mass spectrometers with miniaturized ion traps[49] allowing field screening of illegal tree harvesting.

ESI-MS in both the negative and positive ion modes of a methanolic extract of a tiny piece of wood sample has been therefore demonstrated to provide a rapid and efficient way to differentiate wood. The differentiation of the African and Brazilian mahogany samples has demonstrated that the methodology is selective enough to differentiate woods even when belonging to the same family. The concern that too distinct pools of phytochemical markers would be detected from

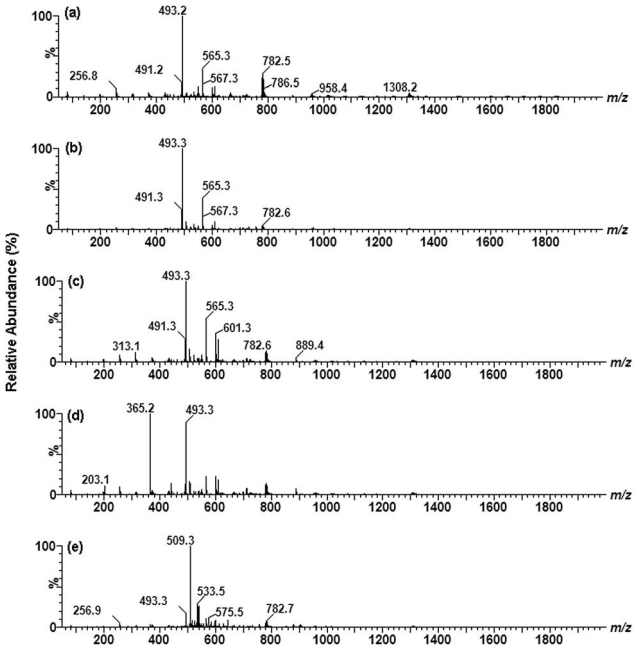

Fig. 5 ESI(+)-MS profiles of methanolic extracts of AM from different sampling points collected across the stem cross-section. (a) P1, (b) P3, (c) P5, (d) P7 and (e) bark.

different parts of the tree has also been eliminated since quite similar characteristic profiles were obtained except from the bark region. We propose that this prompt and unmistakable chemotaxonomic differentiation involving simple and rapid analyses can be useful not only to investigate legal and illegal exploration of mahogany in Brazil, but also could be expanded to other wood chemotaxonomic differentiation cases *via* both laboratory and field analyses.

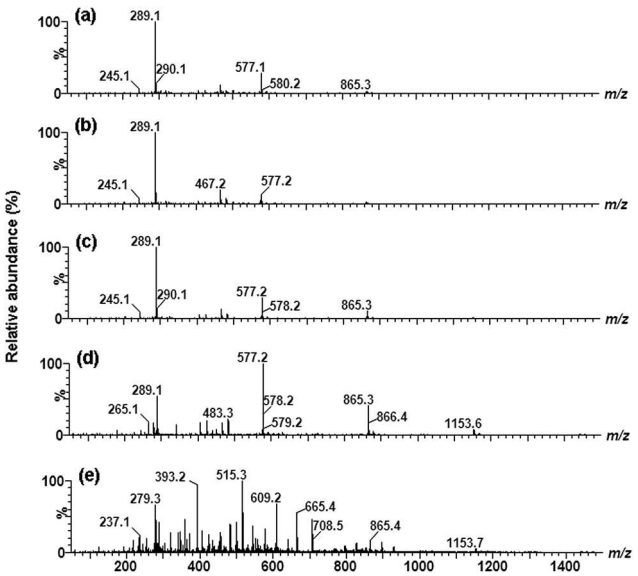

Fig. 6 ESI(−)-MS profiles of methanolic extracts of AM from different sampling points collected across the steam cross-section. (a) P1, (b) P3, (c) P5, (d) P7 and (e) bark.

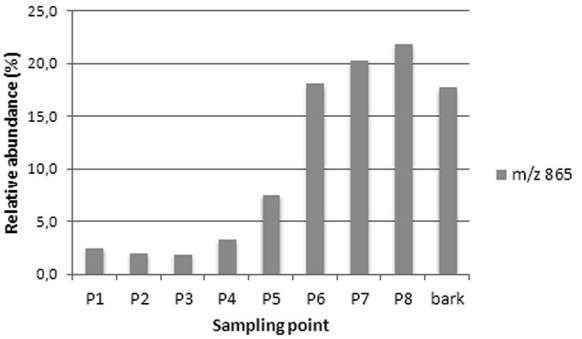

Fig. 7 Relative abundance of a procyanidin trimer as measured by the ion of *m/z* 865 in each sampling point in the African mahogany tree radius.

Acknowledgements

We thank the State of São Paulo Research Foundation (FAPESP), the Brazilian National Council for Scientific and Technological Development (CNPq) and the Financing Agency of Studies and Projects (FINEP) for financial assistance. We gratefully acknowledge Dr José Edmar Urano de Carvalho, Embrapa Oriental – Brazil for donating the African mahogany. We would also like to acknowledge the wood sellers for the donation of certified Brazilian mahogany.

Notes and references

1 J. Grogan, P. Barreto and A. Veríssimo, *Mahogany in the Brazilian Amazon: Ecology and Perspectives on Management*, IMAZON, Belém, 2002.
2 A. Veríssimo, P. Barreto, R. Tarifa and C. Uhl, Extraction of a high-value natural resource in Amazonia: the case of mahogany, *For. Ecol. Manage.*, 1995, **72**, 39.
3 http//www.cites.org/eng/app/appendices, Accessed in April 2013.
4 J. Grogan and M. Schulze, *Environ. Conserv.*, 2008, **35**, 26.
5 http://www.planalto.gov.br/ccivil_03/decreto/2003/D4722.htm, Accessed in April 2013.
6 http://yale.edu/forestcertification/symposium/pdfs/brazil_symposium.pdf, Accessed in September 2014.
7 http://g1.globo.com/economia/agronegocios/noticia/2012/04/mogno-africano-cresce-rapido-e-ganha-espaco-entre-os-agricultores.html, Accessed in September 2014.
8 Q. G. Tan and X. D. Luo, *Chem. Rev.*, 2011, **11**, 7437.
9 S. Z. Moghadamtousi, B. H. Goh, C. K. Chan, T. Shabab and H. A. Kadir, *Molecules*, 2013, **18**, 10465.
10 S. A. M. Abdelgaleil, F. Hashinaga and M. Nakatani, *Pest Manage. Sci.*, 2005, **61**, 186.
11 I. C. Falesi and A. R. C. Baena, *Embrapa Amazônia Oriental, Documentos*, 1999, 4, p. 52.
12 E. K. Adesogan and D. A. H. Taylor, *J. Chem. Soc. C*, 1970, 1710.
13 G. A. Adesida, E. K. Adesogan, D. A. Okorie, D. A. H. Taylor and B. T. Styles, *Phytochemistry*, 1971, **10**, 1845.

14 B. Zhang, S.-P. Yang, S. Yin, C.-R. Zhang, Y. Wu and J.-M. Yue, *Phytochemistry*, 2009, **70**, 1305.
15 M. N. Silva, M. S. P. Arruda, K. C. F. Castro, M. F. Silva, G. F. Fernandes and P. C. Vieira, *J. Nat. Prod.*, 2008, **71**, 1983.
16 J. Chen, S. Huang, C. Liao, D. Wei, P. Sung, T. Wang and M. Cheng, *Food Chem.*, 2010, **120**, 379.
17 B. Lin, C. Zhang, S. Yang, S. Zhang, Y. Wu and J. Yue, *J. Nat. Prod.*, 2009, **72**, 1305.
18 S. Tan, H. Osman, K. Wong and P. Boey, *Food Chem.*, 2009, **115**, 1279.
19 J. B. Fenn, M. Mann, C. K. Meng, S. F. Wong and C. M. Whitehouse, *Science*, 1989, **246**, 64.
20 R. R. Catharino, H. M. S. Milagre, S. Saraiva, C. M. Garcia, U. Schuchardt, R. Augusti, R. A. Cardoso, M. Guimarães, G. F. de Sá, J. M. Rodrigues, V. Souza and M. N. Eberlin, *Energy Fuels*, 2007, **21**, 3698.
21 A. S. Araújo, L. L. Rocha, D. M. Tomazela, A. C. H. F. Sawaya, R. R. Almeida, R. R. Catharino and M. N. Eberlin, *Analyst*, 2005, **130**, 884.
22 R. R. Catharino, R. Haddad, L. G. Cabrini, I. B. S. Cunha, A. C. H. F. Sawaya and M. N. Eberlin, *Anal. Chem.*, 2005, **77**, 7429.
23 A. C. H. F. Sawaya, I. B. S. Cunha, M. C. Marcucci, D. S. Aidar, E. C. A. Silva, C. A. L. Carvalho and M. N. Eberlin, *Apidologie*, 2007, **38**, 93.
24 E. C. Cabral, G. F. Cruz, R. C. Simas, G. B. Sanvido, L. V. Gonçalves, R. V. P. Leal, R. C. F. Silva, J. C. T. Silva, L. E. Barata, V. S. Cunha, L. F. França, R. J. Daroda, G. F. de Sá and M. N. Eberlin, *Anal. Methods*, 2013, **5**, 1385.
25 R. M. Alberici, R. C. Simas, G. S. Sanvido, W. Romão, P. M. Lalli, M. Benassi, I. B. S. Cunha and M. N. Eberlin, *Anal. Bioanal. Chem.*, 2010, **398**, 265.
26 V. G. Santos, T. Regiane, F. F. G. Dias, W. Romão, J. L. P. Jara, C. F. Klitzke, F. Coelho and M. N. Eberlin, *Anal. Chem.*, 2011, **83**, 1375.
27 E. C. Cabral, R. C. Simas, V. G. Santos, C. L. Queiroga, V. S. Cunha, G. F. de Sá, R. J. Daroda and M. N. Eberlin, *J. Mass Spectrom.*, 2012, **47**, 1.
28 R. P. Overend, T. A. Milne and L. Mudge, *Fundamentals of Thermochemical Biomass Conversion Cellulose, Hemicellulose and Extractives*, Elsevier Science Pub. Co. Inc., New York, 1985, pp. 35–60.
29 R. C. Pettersen, *The Chemistry of Solid Wood*, American Chemical Society, 1984, Ch 2, pp. 57–126.
30 R. Hegnauer, *Phytochemistry*, 1986, **25**, 1519.
31 G. Tjitrosoepomo, *Environmentalist*, 1984, **4**, 19–21.
32 W. E. Hillis, *Phytochemistry*, 1972, **11**, 1207.
33 T. P. Schultz and D. D. Nicholas, *Phytochemistry*, 2000, **54**, 47.
34 O. R. Gottlieb, *Phytochemistry*, 1990, **29**, 1715.
35 J. E. Poulton, *The Biochemistry of Plants. Secondary Plant Products*, ed. E. E. Conn, Academic Press, New York, 1981, vol 7, p. 667.
36 R. J. Molyneux, S. T. Lee, D. R. Gardner, K. E. Panter and L. F. James, *Phytochemistry*, 2007, **68**, 2973.
37 H. Zhang, J. Tan, D. van Derveer, X. Wang, M. J. Wargovich and F. Chen, *Phytochemistry*, 2009, **70**, 294.
38 K. Kojima, K. Isaka and Y. Oghiara, *Chem. Pharm. Bull.*, 1998, **46**, 523.
39 A. Crozier, M. N. Clifford and H. Ashihara, *Plant secondary metabolites. Occurrence, structure and Role in Human Diet*, Blackwell Publishing, 2006, pp. 2–19.
40 L. Y. Foo, *Phytochemistry*, 1987, **26**, 2825.
41 S. D. Chen and C. J. Lu, *Molecules*, 2014, **19**, 10427.
42 F. L. Beltrame, E. R. Filho, F. A. P. Barros, D. A. G. Cortez and Q. B. Cass, *J. Chromatogr. A*, 2006, **1119**, 257.
43 M. A. S. Marles, H. Ray and M. Y. Gruber, *Phytochemistry*, 2003, **64**, 367.
44 R. Spilker and H. F. Griitzmacher, *Org. Mass Spectrom.*, 1986, **21**, 459.
45 W. Yang, D. M. Fang, H. P. He, X. J. Hao, Z. J. Wu and G. L. Zhang, *Rapid Commun. Mass Spectrom.*, 2013, **27**, 1203.
46 D. Y. Xie and R. A. Dixon, *Phytochemistry*, 2005, **66**, 2127.
47 S. Falah, T. Suzuki and T. Katayama, *Pak. J. Biol. Sci.*, 2008, **11**, 2007.
48 S. E. Atawodi, J. C. Atawoki and J. Pala, *Electronic Journal of Biology*, 2009, **5**, 80.
49 P. I. Hendricks, J. K. Dalgleish, J. T. Shelley, M. A. Kirleis, M. T. McNicholas, L. Li, T.-C. Chen, C.-H. Chen, J. S. Duncan, F. Boudreau, R. J. Noll, J. P. Denton, T. A. Roach, Z. Ouyang and R. G. Cooks, *Anal. Chem.*, 2014, **86**, 2900.

2.1.1. Autorização para reprodução do artigo

De acordo com o site da revista, autores e coautores não precisam de autorização formal para reproduzir o artigo em tese (informação retirada do site da revista em 19/09/2018 - http://www.rsc.org/journals-books-databases/journal-authors-reviewers/licences-copyright-permissions/)

2.2. Two-point normalization using internal and external standards for a traceable determination of $\delta^{13}C$ values of fatty acid methyl esters by gas chromatography/combustion/isotope ratio mass spectrometry

Publicado originalmente em: *International Journal of Mass Spectrometry*, 2017, 418, 41-50.

International Journal of Mass Spectrometry 418 (2017) 41–50

Contents lists available at ScienceDirect

International Journal of Mass Spectrometry

journal homepage: www.elsevier.com/locate/ijms

Two-point normalization using internal and external standards for a traceable determination of $\delta^{13}C$ values of fatty acid methyl esters by gas chromatography/combustion/isotope ratio mass spectrometry

Maíra Fasciotti [a,b,*], Thays V.C. Monteiro [a], Alexandre A. Ferreira [c], Marcos N. Eberlin [b], Laura A. Neves [a]

[a] National Institute of Metrology, Quality and Technology – INMETRO, Division of Chemical Metrology, 25250-020 Duque de Caxias, RJ, Brazil
[b] ThoMSon Mass Spectrometry Laboratory, Institute of Chemistry, University of Campinas – UNICAMP, 13083-970 Campinas, SP, Brazil
[c] PETROBRAS Research and Development Center – CENPES, Division of Geochemistry, 21941-915, Ilha do Fundão, Rio de Janeiro, RJ, Brazil

ARTICLE INFO

Article history:
Received 31 July 2016
Received in revised form
26 November 2016
Accepted 1 December 2016
Available online 5 December 2016

Keywords:
FAME
Gas chromatography isotope ratio mass spectrometry
Traceability
Normalization methods
Biodiesel
Jatropha curcas

ABSTRACT

Isotope ratio mass spectrometry (IRMS) is a technique that measures subtle differences in the abundances of stable isotopes in samples or specific molecules. One important group of molecules is the fatty acids methyl esters (FAME), due to its importance to areas such as food control, geochemistry and, more recently, bio-based fuels such as biodiesel. The technique of choice for FAME analysis is gas chromatography (GC), but the lack of GC compatible stable isotope certified reference materials may cause inaccuracy in isotopic values determination. In this work, we proposed a simple methodology to accurately determine the $\delta^{13}C$ values in *Jatropha curcas* FAMEs as a test case, by using a two-point normalization using internal and external standards to correct the isotopic fractionation from the transesterification reaction and from the GC/C/IRMS analysis itself. We observed that the transesterification process may lead up to 2 mUr of deviation of $\delta^{13}C$ values for the internal standard (FAME C22:0). After the two point normalization, the determined $\delta^{13}C$ average value for the FAMEs of 9 different samples of *J. curcas* was $\delta^{13}C_{VPDB} = -29.51 \pm 1.03$ mUr, while the bulk value obtained with EA/IRMS was -28.97 ± 0.43 mUr, a typical signature of C3-plants. This work also demonstrates that major quality procedures must indeed be applied for accurate determinations of isotopic values, especially in GC analysis, following the identical treatment principle.

1. Introduction

Isotope ratio mass spectrometry (IRMS) is a modality of mass spectrometry that measures subtle differences in the abundances of stable isotopes in samples or in specific molecules present in natural or synthetic systems [1]. During the last decades, the advances on the correspondent instrumentation made IRMS a widely used analytical technique that can be applied to the study of different types of samples from different fields [2]. When the concentration of a specific molecule (or a group of them) is not a parameter to differentiate samples according to some specific characteristic, one can determine their isotopic composition, looking for variations that can be related to certain processes such as metabolic pathways in plants, geographical origin, raw material, and many others, that leads to slightly different concentrations of isotopes due to the well-known phenomenon of isotopic fractionation [3].

IRMS can be hyphenated to elemental analysis (EA), gas chromatography (GC) and liquid chromatography (LC), being the last two applied to compound-specific isotope analysis (CSIA), whereas EA is used for the determination of bulk isotope ratios [4]. The most commonly measured stable isotopic ratios are $^{13}C/^{12}C$, $^{2}H/^{1}H$, $^{15}N/^{14}N$, $^{18}O/^{16}O$ and $^{34}S/^{32}S$ for organic molecules [5], expressed using δ (delta) notations which relate the concentrations of the less abundant isotope of a certain element to the concentration of the most abundant one [6]. Since these differences are usually minimal, δ notations are expressed in *permil* (‰). However, this unit was recently considered to be deprecated, according to the International System of units (IS) and IUPAC guidelines, and the unit mUr (milli Urey) is being recommended instead [7].

The samples (or specific compounds) are converted into a gas (depending on the element of interest) through oxidation/reducing

* Corresponding author at: Avenida Nossa Senhora das Graças, 50 – Prédio 28, 25250-020 – Xerém, Duque de Caxias, Rio de Janeiro, Brazil.
E-mail address: mfasciotti@inmetro.gov.br (M. Fasciotti).

http://dx.doi.org/10.1016/j.ijms.2016.12.002
1387-3806/

processes in an interface (in the inlets such as elemental analyzer or a gas chromatograph) and compared to a working gas with a known isotopic signature, traceable to an international scale. For that, internationally agreed organic stable isotope reference materials (RM) are implemented to assign a true isotopic value for the working gas, as well as for normalization methods of the raw isotopic values of the samples [8–13]. For example, the stable carbon isotopic composition is expressed relative to *Vienna Pee Dee Belemnite* (VPDB) – the international scale zero point for carbon – on a scale normalized such that the $\delta^{13}C$ values of NBS 19 calcium carbonate and LSVEC lithium carbonate standards are +1.95 mUr and −46.6 mUr, respectively, and both should be cited when one reports an isotopic ratio value. The NBS 22 stable carbon isotopic composition, for example, is expressed and certified as $\delta^{13}C_{VPDB\text{-}LSVEC} = -30.03 \pm 0.06$ mUr. [6,8–13]

Sincemostly internationally agreed RM for stable isotopic measurements are non-volatile solids or viscous materials, they are exclusively compatible with EA inlets, which makes chromatographic methodologies struggle to be traceable to the international scale thereof. In this case, normalization methods of the raw data are strongly recommended, using working standards with similar physical-chemical properties to the analytes of interest, ranging the same isotopic values, properly determined, and traceable to the international scale [14–17]. We have [18] recently showed that the isotopic reference material for working gas calibration and the analytical GC column had a considerable effect on the $\delta^{13}C$ measurements of ethanol samples, leading to inaccurate results, biased of almost 2–3 mUr, when the identical treatment (IT) principle was not followed. Several sources of isotopic fractionation are indeed present in IRMS methodologies, from the sample preparation – especially when derivatization methods are implemented [19] –to the chromatographic process or the sample conversion to a gas in the peripheral interface [20,21].

IRMS are being applied to several areas of remarkable importance, for example to detect the adulteration in food and beverages [22–26]; the origin of alcohols [27,28]; environmental pollutants [29]; forensic analysis [30,31]; doping control [32,33]; fuel contaminants [34]; geographic origin determination of vegetable oils such as olive oils [35,36]; and several others [4]. In all cases, accurate and traceable determination of the isotopic signatures must be performed, in order to ensure reliable conclusions.

Among these applications, one important group of molecules in many analytical areas are the fatty acids methyl esters (FAMEs). FAME analysis by GC/IRMS is among the very first applications of commercially available GC/IRMS, and is being widely applied ever since. The analysis of this class of compounds is usually required in food characterization [37], biological systems [38], environmental spheres such as sediments, [39] and nowadays for biodiesel and other bio-based fuels. The production of FAMEs in samples often requires derivatization through transesterification reaction of the glycerides precursors, that are commonly analyzed by gas chromatography.

The technique of GC/IRMS has been successfully applied, for example, in the analysis of FAMEs from vegetable oils by Woodbury and co-workers [40] and sources of adulteration could be identified. This is possible because the measurement of the carbon isotope ratios (among others) can be related to the oleaginous seed and its geographical origin. For example, corn oil has a C4-plant characteristic $\delta^{13}C$ signature (from −16.36 to −13.71 mUr), while most oleaginous plants have a characteristic C3 biosynthetic pathway, with $\delta^{13}C$ values in the range of −32.39 to −25.28 mUr [36,41,42]. Therefore, the addition of corn oil to other C3-plant vegetable oils can be easily detected. This is an important tool to access the adulteration of more expensive oils, such as olive oil, for instance [43]. Moreover, with the advent of biodiesel as one of the most important biofuels being implemented during the last decades, several oleaginous plants have been in focus of developments and genetic improvements to ensure its biodiesel quality for better engines performances [44]. Based on this, IRMS can be used as well as an important tool to differentiate and determine the isotopic signatures of different sources and raw materials of biodiesel.

Jatropha curcas is one of the most prominent oleaginous for biodiesel production due to its good oxidative stability, low acidity and higher cetane index, as well as good yields in oil production, being very suitable for biodiesel production [45]. Many countries and companies around the world are investing a lot of resources in *J. Curcas* as a potential raw material for biodiesel [46]. Therefore, this work aimed to develop a methodology to determine the $^{13}C/^{12}C$ isotope ratios of *J. curcas* oils of different geographical origins from Brazil, as well as the carbon isotopic composition of the correspondent FAMEs from the biodiesel samples, to report its isotopic $\delta^{13}C$ signature. For that goal, we have investigated the sources of isotope fractionation, from the oil extraction to the GC/C/IRMS analyses, and used both internal and external standards to correct the isotope fractionation that occurs during sample transesterification and chromatographic analysis. With this two-point anchoring data normalization, we can ensure that reliable values of $\delta^{13}C$, traceable to the VPDB-LSVEC, are being reported, allowing us to determine an accurate $\delta^{13}C$ signature for this oleaginous being produced in Brazil.

2. Experimental

2.1. Reagents

The stable isotopic reference material C18:0 methyl ester (stearic acid methyl ester, certified value of $\delta^{13}C_{VPDB} = -23.24 \pm 0.01$ mUr) from Indiana University (Bloomington, IN, USA), was used for CO_2 calibration of the GC/C/IRMS system and for quality control. A certified reference material (CRM 2772, soybean biodiesel), produced by NIST (National Institute of Standards and Technology, USA) and INMETRO (National Institute of Metrology, Quality and Technology, Duque de Caxias, RJ, Brazil) was used to optimize the chromatographic method. The C22:0 methyl ester standard (docosanoic acid methyl ester, Sigma-Aldrich, purity 99%) and C19:0 (nonadecanoic acid methyl ester, Sigma-Aldrich, purity 98% GC) were used as internal and external standards, respectively.

Hexane (Tedia Brazil, HPLC grade, purity 99.9) was used for the Soxhlet extraction of *J. curcas* oil. For the transesterification of *J. curcas* oil, methanol (Tedia Brazil, HPLC grade, purity 99.9), KOH (Sigma-Aldrich) and BF_3-methanol complex (boron trifluoride-methanol, Supelco Inc., Bellafonte, PA, USA) were used (the same flasks for all samples, to ensure the same isotopic composition). Toluene (Tedia Brazil, HPLC grade, purity 99.9) was used to prepare the final solutions for GC/C/IRMS and GC/MS and as cleaning solvent between injections.

2.2. Samples

This work was conducted with six *J. curcas* seed samples (donated by the Brazilian Agricultural Research Corporate – EMBRAPA) from different geographic regions of Brazil. One of these samples has an unknown origin; and three samples of *J. curcas* oil were obtained from São Paulo state (Table 1). The *J. curcas* seeds samples were stored at room temperature and the *J. curcas* oil samples were analyzed without any previous treatment and stored as received at 4 °C.

Extraction of *J. curcas* oil – solvent extraction

Initially, a study was conducted to investigate if the process of *J. curcas* seed oil extraction has any source of contamination. All the extraction apparatus (Soxhlet flask and condenser), acrylic wool

Table 1
Samples of *J. curcas* analyzed in this work and its origin.

Sample Code	Origin (City/State)	*J. curcas* sample
264	Dourados/MS	Seed
201	Lavras/MG	Seed
136	Maranhão	Seed
299	Rio Grande do Sul	Seed
112	Petrolina/PE	Seed
813	Unknown	Seed
100	São Paulo	Oil
101	São Paulo	Oil
102	São Paulo	Oil

Table 2
$\delta^{13}C_{VPDB}$ values of *J. curcas* oil of different geographical origins measured by EA/IRMS.

Sample code	Average $\delta^{13}C_{VPDB}$ (mUr) ± sd[a]
813	−28.70 ± 0.03
100	−28.50 ± 0.05
101	−29.90 ± 0.09
102	−28.57 ± 0.07
201	−29.05 ± 0.02
136	−29.32 ± 0.02
112	−28.89 ± 0.01
299	−28.98 ± 0.02
264	−28.82 ± 0.11
Average	−28.97 ± 0.43

[a] sd: standard deviation, n = 3 replicates.

(brand Vigo AR) and the filter paper were washed for 4 h with hexane to eliminate possible contaminants. Then, they were dried and used as filtering materials during the oil extraction from the seeds. The process was repeated for each sample extraction.

The hexane (blank) of these devices was evaporated in a rotary evaporator to a volume of 1 mL and analyzed by GC/MS and GC/C/IRMS to monitor any possible contamination in the blank of extraction.

The *J. curcas* seeds from different regions were dried for 1 hour at 50°C and mashed in a mill (IKA, A11b, 50/60 Hz, 160 W). Then, approximately 30 g of seeds were placed in Soxhlet extractor packed with the previously cleaned acrylic wool and filtering paper.

For the extraction of *J. curcas* oil, approximately 500 mL of hexane were used as extraction solvent, at a temperature of 70 °C during 3 h in the Soxhelt. The extractions were performed in triplicate simultaneously in three (3) different Soxhlet extractors. After extraction, the hexane was evaporated under a rotatory evaporator, resulting in the pure *J. curcas* oil. Then, the oil was weighted to calculate the yield (in% – w/w) by dividing the obtained oil mass and the initial mass of seed.

2.3. Transesterification reaction

Approximately 0.8 g of each *J. curcas* oil sample was weighed and approximately 50 mg of methyl ester C22:0 and 5.0 mL of KOH in methanol (1 mol/L) were added, in Schott Flasks of borosilicate of 25 mL. The mixture was placed on an ultrasonic bath (ELMASONIC 30 H), at 70 °C for three hours, under a frequency of 80 kHz and 480 W (peak). Then the fatty acids were esterified with 5.0 mL of BF_3-methanol complex and ultrasound for 1 h. The reaction was quenched with 1.0 mL of a saturated NaCl solution and approximately 10 mL of hexane. After separation, the hexane upper phase was transferred to 25 mL bechers. The solvent was completely evaporated at 50 °C, resulting in the mixture of FAMEs.

2.4. Sample preparation

For both GC/MS and GC/C/IRMS analyses, 5 mg of the standard C19:0 and 5 mg of the FAME mixtures (biodiesel) were precisely weighted in the GC vials. Then, approximately 1 mL of toluene was added to the vial, and precisely weighted as well. The mixture was vortexed for aproximately 15 s until complete dissolution, and then the vials were placed on the autosampler of the equipment (either GC/MS or GC/C/IRMS) for the analysis.

2.5. $\delta^{13}C_{VPDB}$ correction for FAME isotopic composition due to carbon incorporation in the transesterification reaction

The isotopic shift due to the introduction of one carbon in the fatty acid chain from the methylation step was corrected by a mass balance, according to the Eq. (1) [47]:

$$\delta^{13}C_{FAME} = \frac{[\delta^{13}C_{FAME\ \ Mesurement} \times (1+n) - \delta^{13}C_{MeOH}]}{n} \quad (1)$$

where $\delta^{13}C_{FAME}$ and $\delta^{13}C_{MeOH}$ are the carbon isotopic compositions of the fatty acid methyl ester and the bulk methanol used in the reaction media for methylation of the fatty acid, respectively. *n* is the number of carbons in the fatty acid methyl ester chain. The carbon isotopic composition of the reaction media was determined by EA/IRMS as $\delta^{13}C_{VPDB}$ = −38.41 mUr.

2.5. Instrumental

The identification and quantification of the methyl esters content produced from the transesterification of the *J. curcas* oils were performed using gas chromatography with mass spectrometer detector (GC/MS – Shimadzu GCMS-QP2010, Tokyo, Japan).

The EA/IRMS analyses of the *J. curcas* oils were performed in a continuous-flow isotope-ratio mass spectrometry using a Delta-Plus XL mass spectrometer coupled to a ConFlo III interface linked to a Flash EA^{TM}1112 elemental analyzer fitted with a 50-position autosampler (all from Thermo Scientific, Bremen, Germany).

The GC/C/IRMS analyses of biodiesel were performed using a Delta V Plus mass spectrometer (Thermo Scientific, Bremen, Germany) with a CG IsoLink combustion reactor (GC Combustion III) (Thermo Scientific, Bremen, Germany) interface coupled to a gas chromatograph (7890A – Agilent Technologies). Samples were introduced using an A7693 autosampler (Agilent Technologies).

3. Methods

Methyl ester content analysis of *J. curcas* oils by GC/MS

The quantification of methyl ester of the *J. curcas* oils was performed and validated according to the standard procedure – EN 14103:2011: Determination of ester and linolenic acid methyl ester contents [48].

The chromatographic separation of methyl ester was performed in a Rtx-Wax column (Varian, 30 m x, 0.25 mm i.d. x 0.32 μm film thickness). 1 μL of sample was injected in splitless mode. The splitless injector temperature was set to 250 °C. The oven temperature program started at 60 °C hold for 2 min, to 200 °C at 10 °C min^{-1}, and to 240 °C at 5 °C min^{-1}, hold for 7 min. Helium was used as the carrier gas at a constant flow rate of 3 mL/min. Samples were analyzed in triplicates.

3.1. CO_2 calibration in EA/IRMS system

The working gas CO_2 was calibrated against the international reference material NBS22 ($\delta^{13}C_{VPDB}$ = −30.031 mUr). Approximately 0.5 mg of the reference material was weighted into tin capsules and placed into the auto-sampler. For the measurements, the oxidation and reduction reactors were set to 900 °C and 680 °C, respectively.

Isotopic Analysis of *J. curcas* oils by EA/IRMS

Approximately 0.5 mg of each *J. curcas* oil sample was weighted into tin capsules and placed into the auto-sampler. For the measurements, the oxidation and reduction reactors were set to 900 °C and 680 °C, respectively.

Data were processed using the instrument manufacturer's proprietary Isodat NT software, version 2.0 (Thermo Scientific, Bremen, Germany). The measured $^{13}C/^{12}C$ isotope ratios were also expressed as $\delta^{13}C$-values (in mUr) relative to the VPDB scale.

3.2. CO_2 calibration in GC/IRMS system

The CO_2 working gas in GC/C/IRMS system was calibrated using the C18:0 ($\delta^{13}C_{VPDB}$ = −23.24 ± 0.01 mUr) from Indiana University (Bloomington, IN, USA). This standard was injected 10 times and the peak corresponding to C18:0 was considered the reference for all analyses. The average of the $\delta^{13}C$ values obtained for CO_2 was used as the reference isotopic value during the analyses of the samples.

3.3. Isotopic $\delta^{13}C$ analysis of methyl esters by GC/C/IRMS

The chromatographic separation of the methyl esters was performed in a DB-23 column (J&W Scientifc, 30 m x, 0.25 mm i.d. x 0.25 μm film thickness). 0.1 μL of sample was injected in a splitless mode. The injector temperature was set to 250 °C. The oven temperature program was as follows: 60 °C to 200 °C at 7 °C min^{-1}, then a 2 °C min^{-1} ramp to 216 °C for 2 min. Helium was used as the carrier gas at a constant flow rate of 1 mL/min. Samples were analyzed in triplicates.

Three Faraday cup detectors monitored simultaneously and continuously the CO_2 signals for the three major ions of *m*/*z* 44, *m*/*z* 45 and *m*/*z* 46. For the methyl esters analysis, five pulses of CO_2 reference gas were admitted into the inlet system for about 30 s with a backflush time of 950 s and a total run time of 1950s. The temperature of the combustion reactor was set to 950 °C during all the analysis.

Data were processed using the instrument manufacturer's proprietary Isodat NT software, version 2.0 (Thermo Scientific, Bremen, Germany). The measured $^{13}C/^{12}C$ isotope ratios were also expressed as $\delta^{13}C$-values (in mUr) relative to the VPDB scale.

3.4. Normalization method (Two-point normalization)

For normalization of the raw $\delta^{13}C$ values, a two-point normalization method was applied using the C22:0 (internal standard) and C19:0 (external standard), according to Eq. (2) [18]:

$$x_{Sample} = \frac{x_2 - x_1}{y_2 - y_1}\left(y_{sample} - y_1\right) + x_1 \quad (2)$$

Where y denotes the instrumental response. The values of the standards are denoted by x_1 and x_2, the respective responses by y_1 and y_2, the response of the sample by y_{sample}, and the normalized value of the sample by x_{sample}.

4. Results and discussion

The first step of this work was the oil extraction optimization, to verify – and minimize – any source of contamination or isotopic fractionation, as both processes can lead to biased isotopic values. As we were using the classic Soxhlet solvent extraction, we have performed several hexane blanks of the system until no peaks were detected by both GC/MS and GC/C/IRMS, before each seed extraction. Moreover, we have observed that regular cellulosic cartridges for Soxhlet extractor leaded to some contaminant peaks at the chromatogram that can co-elute with the FAMEs peaks causing systematic errors of the $\delta^{13}C$ values. For this purpose, we have performed the extraction using regular filtering papers and acrylic wool to involve the powdered seeds during extraction. The extractions were successful, obtaining from 32.1 to 43.7% (w/w) of oil yield for the *J. curcas* seeds (Table S1), which are the expected values for these oleaginous seeds [42].

We have also performed the extraction of the seeds in triplicate, to check if there could be any variation of the $\delta^{13}C$ due to sample inhomogeneity and due to isotopic fractionation during the oil extraction. To evaluate this, we have measured all the three replicates of oil extraction of the sample 813 by EA/IRMS (Table S2). The averages values were completely equivalent, being the standard deviation of the $\delta^{13}C$ values for each replicate of extraction compatible with the standard deviation of the measurement of the

Table 4
Average values for the C22:0, measured between the samples and as an internal standard,and the average values of C19:0 as an external standard.

Standards	Average $\delta^{13}C$ (mUr)
C22:0 between injections	−27.31 ± 0.94 [a]
C22:0 as internal standard	−25.52 ± 0.88 [b]
C22:0 reference value	−27.09 ± 0.06 [c]
C19:0 as external standard	−30.39 ± 0.55 [d]
C19:0 reference value	−30.02 ± 0.0 [e]

[a] C22:0 injected as a standard between each sample, n = 10 replicates.
[b] C22:0 as internal standard of the transesterification reaction, determined at the same chromatographic run of the J. curcas samples, n = 27 replicates.
[c] Reference value provided by EA/IRMS, traceable to VPDB via NBS22 standard, from n = 11 replicates of measurements.
[d] C19:0 as external standard of the GC/C/IRMS analysis, determined at the same chromatographic run of the *J. curcas samples*, n = 27 replicates.
[e] Reference value provided by EA/IRMS, traceable to VPDB via NBS22 standard, from n = 7 replicates of measurements.

Table 3
Reference material and secondary working standards used for working gas calibration and raw data normalization and their reference values determined by EA/IRMS.

Standard	Reference $\delta^{13}C_{VPDB}$ value (mUr)
FAME C18:0 (Indiana University, Bloomington, IN, USA)	− 23.24 ± 0.,01 [a]
FAME C22:0 (internal standard of the transesterification reaction)	− 27.09 ± 0.06 [b]
FAME C19:0 (external standard for the GC/C/IRMS analysis)	−30.02 ± 0.02 [c]

[a] Reference material provided by Indiana University.
[b] Secondary working standard, with the reference value provided by EA/IRMS, traceable to VPDB via NBS22 standard, from n = 11 replicates of measurement.
[c] Secondary working standard, with the reference value provided by EA/IRMS, traceable to VPDB via NBS22 standard, from n = 7 replicates of measurement.

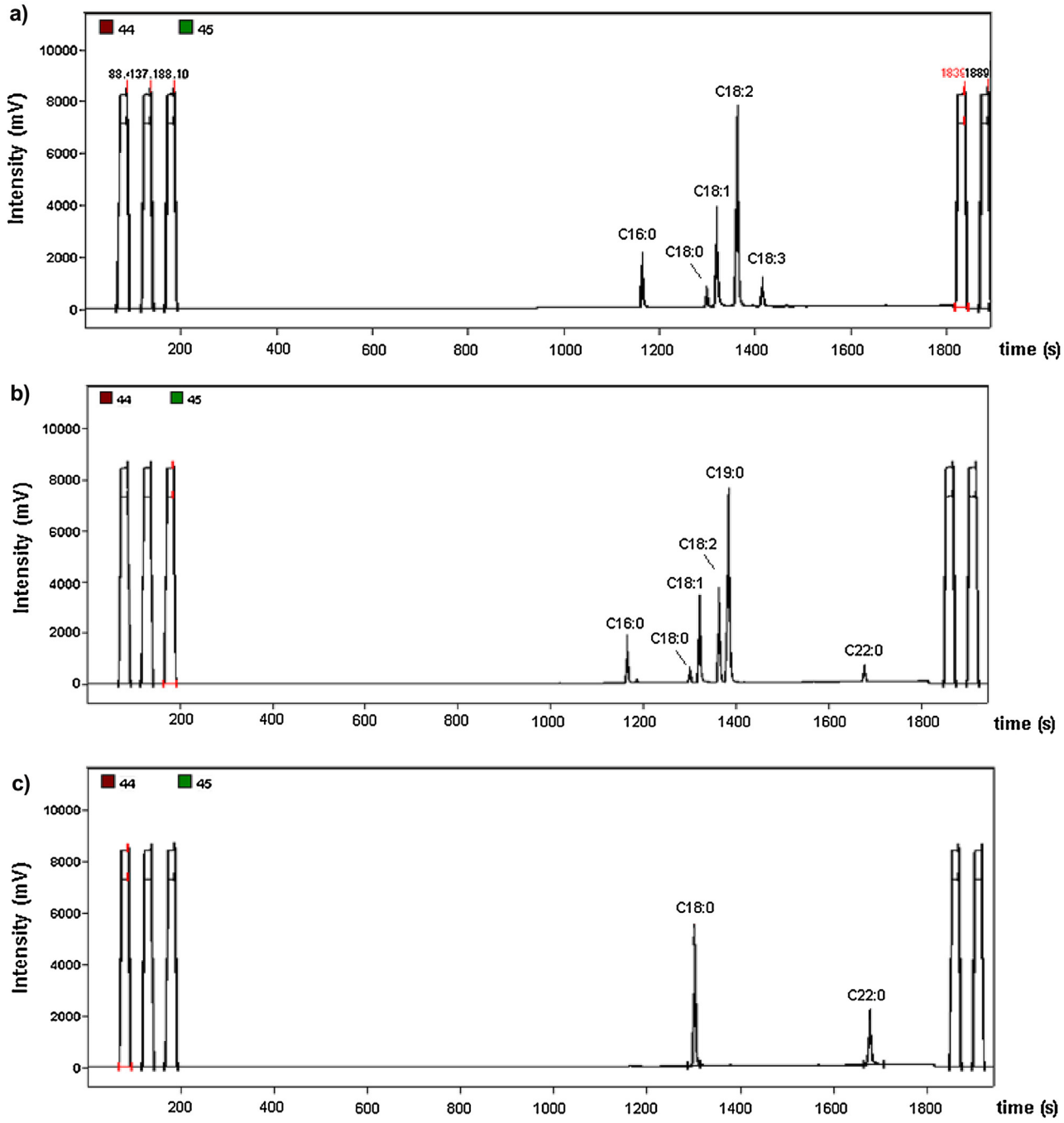

Fig. 1. GC/C/IRMS chromatograms (m/z 44 and 45 ion currents as a function of time) correspondent to the carbon isotopic analysis of a) CRM 2772 (NIST/INMETRO) soybean-based biodiesel; b) representative sample of *J. curcas* FAMEs with C19:0 and C22:0 as external and internal standards; and c) mixture of C18:0 RM and the secondary working standard – C22:0. Three pulses of CO_2 were introduced before the elution of the FAMEs peaks and two pulses after the elution. Reference peaks 2–5 (elution times 138.1, 187.9,1869.5 and 1919.5 s, respectively) were considered to be the reference gases in the software for the calculation of the $\delta^{13}C$ values of all the FAMEs. DB-23 was used as the GC column.

same sample (0.04 *versus* 0.03 mUr). Therefore, the replicates of oil extraction could be merged in only one sample, as no inhomogeneity or any isotopic fractionation was observed in this first step.

The bulk $\delta^{13}C_{VPDB}$ values of *J. curcas* oil of different geographical origins of Brazil were then measured by EA/IRMS, and the results are shown in Table 2. The values were very close to each other for all samples, ranging from −29.90 to −28.50 mUr, with the average value of -28.97 ± 0.43 mUr (n = 9 samples). The results for *J. curcas* $\delta^{13}C_{VPDB}$ isotopic signature were in accordance with the expected values for C3 plants, such as rape seed, palm, soybean and olive oil, and varied from ca. −31 to −29 mUr, as previously reported [39].

The next step consisted in the optimization of the transesterification method of *J. curcas* oil. The methylation method described in this work allowed us to obtain more than 95% of total esters content (Table S3) and all the samples could be derivatized simultaneously in the ultrasonic bath, which is suitable to ensure repeatability conditions during sample derivatization and minimize different magnitudes of isotopic fractionation within the samples. Another important aspect of this sample preparation was the addition of the standard C22:0 at the beginning of the reaction, along with the *J.*

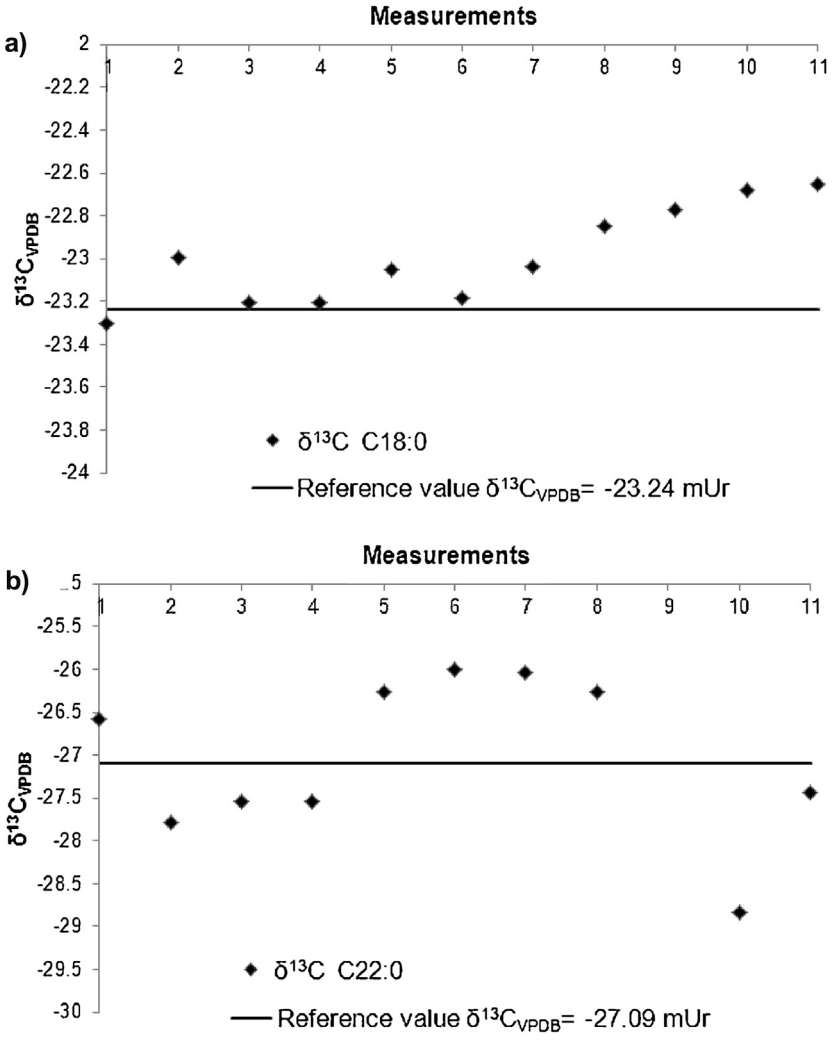

Fig. 2. Control charts of the raw isotopic values $\delta^{13}C$ of a) C18:0 and b) C22:0 injected between samples.

curcas oils and the methanol-BF_3, which means that the standard was submitted to the principal of the identical treatment in the reaction media and can be used to correct any isotopic fractionation that came from this process. Moreover, the FAMEs extraction and purification used here avoids the presence of halogenated compounds (i.e BF_3) in the samples, so it will help to avoid the damage of the combustion reactor, making it last for a longer period.

After the sample transesterification, the standard C19:0 was used as an external standard, to correct instrumental drifts or isotopic fractionation during the course of analysis. Table 3 summarizes all the standards used in this methodology to ensure accuracy and traceability. The stable organic RM FAME C18:0 (Indiana University, Bloomington, IN, USA) was very adequate for working gas calibration, since it is an ester that is present in the samples, and because it has an isotopic value in the range of the expected values of *J. curcas* FAME values. Both C22:0 and C19:0 were used as internal and external standards as described: the first one to correct the sources of deviation that comes from the transesterification; and the other to correct deviations from the GC/C/IRMS analysis itself. Their true values were determined with EA/IRMS, being traceable to the international scale via the primary standard NBS22. Their reference values are also reported in Table 3, and they were used as the "true" values to normalize the raw measured values of *J. curcas* FAMEs by using a two-point normalization method.

Alongside with the normalization approach using two standards, the chromatographic resolution is another very important aspect of the analysis to ensure the accuracy and precision of the results. Normally, columns as CP-WAX are strongly recommended for FAME separation [35,49], but comparing the peak resolutions of GC/MS and GC/C/IRMS techniques, the final peak resolution of GC/C/IRMS tends to be poorer, due to a longitudinal diffusion process at the combustion interface, resulting in broader or tailored chromatographic peaks thereof. Therefore, an improved chromatographic resolution is required, that could be achieved using a GC column with a more polar stationary phase as the DB-23. Previous works report a baseline resolution even for some cis/trans FAMEs isomers in this column [50]. Moreover, the DB-23 column is less susceptible for "bleeding" processes in higher temperatures compared to WAX columns, which can minimize another source of interferences during the FAME elution and, thus, an inaccurate $\delta^{13}C$ determination.

To optimize the chromatographic separation, a certified reference material of soybean-based biodiesel (NIST/INMETRO, CRM 2772) was used to evaluate the peak resolution and its symmetry. A very good GC resolution and peak symmetry was indeed achieved. Fig. 1 shows the GC/C/IRMS analysis of the CRM 2772 (Fig. 1a), a representative sample of *J. curcas* FAMEs showing both peaks of C19:0 and C22:0 (Fig. 1b); and the mixture of C18:0 RM and the secondary working standard – C22:0–injected between each sam-

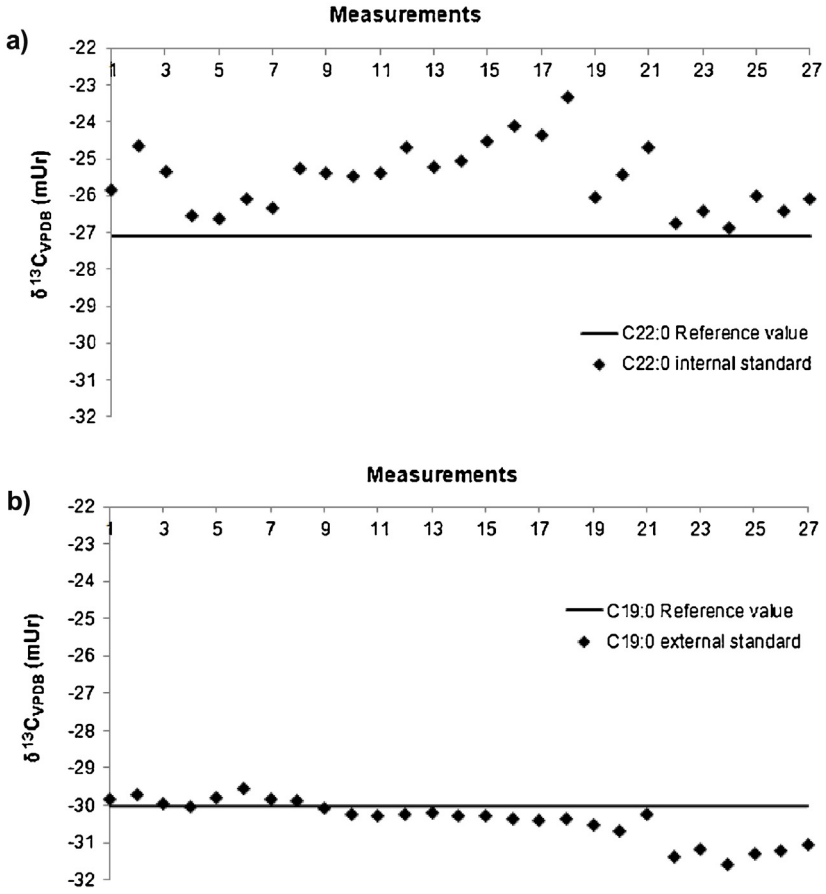

Fig. 3. Control charts of the $\delta^{13}C$ values of a) C19:0 and b) C22:0 determined along with the *J. curcas* FAMEs, showing the drifts in the measurements during the course of the batch analyses.

ple (Fig. 1c), as a control chart to evaluate how the isotopic values were drifting during the batch of analysis.

Fig. 2 shows the control charts of the raw isotopic values of both C18:0 and C22:0 injected between samples to verify the instrumental response of the equipment. Indeed, a considerable deviation from the reference values is observed (higher than the expected standard deviation for a GC/C/IRMS measurement, of ca. ± 0.20 mUr). This behavior points out that the sample raw results, in fact, must be submitted to normalization to ensure accuracy. Another remarkable fact is that these two standards did not present the same behavior: the $\delta^{13}C$ of C18:0 was, in average, positively biased (−22.99 mUr *versus* the reference value of −23.24 mUr) while the C22:0 was negatively biased (−27.31 mUr *versus* the reference value measured by EA/IRMS of −27.09 mUr). Therefore, at least two standards must indeed be implemented for the data normalization to avoid the introduction of systematic errors during the measurements. Note that the data reported in Fig. 2 only represents the deviations in the instrumental response during analysis, so, in fact data normalization is required even in short-term experiments, or in conditions of repeatability.

Comparing the average measured value of the secondary standard C22:0 determined between the injection of the samples and its average value when it was added in the beginning of the derivatization process, a bias of approximately 2 mUr was observed. The average value by GC/C/IRMS between the samples injections was −27.31 mUr, while the value measured when C22:0 was added as internal standards were −25.52 mUr, being the reference value (determined by EA/IRMS) −27.09 mUr, as shown in Table 4. Moreover, evaluating the average value of the C19:0 (−30.39 mUr) used as external standard (added right before the GC/C/IRMS analysis, at the final solution, along with the FAME mixture of *J. curcas* oil) and comparing with the reference value (−30.02 mUr), a smaller deviation was verified. This result points out that the derivatization processes is an important source of isotopic fractionation. The derivatization leaded to a positive bias of approximately 2 mUr, whereas the deviation due to the analyses (comparing GC/C/IRMS and EA/IRMS) was about 0.3 mUr for both C22:0 and C19:0, which is acceptable when comparing these two different techniques.

Even though the standard C22:0 does not "react" together and in the same way compared with sample fatty acids, at some point of the derivatization process an important isotope fractionation plays a role, but the exact step in which it happens still needs to be determined. As the standard C22:0 is not methylated (since it is already an ester), one hypothesis is that the isotopic fractionation occurs during the final liquid–liquid extraction, when slightly different equilibrium rates and solvent partitioning coefficients for molecules containing different abundances of the heavier/lighter isotope may lead to this observed bias of approximately 2 mUr.

Indeed, observing the raw data for both C19:0 and C22:0 during the course of the batch analyses, one can note that all the values of the C22:0 are positively biased (Fig. 3a), while the C19:0 has a different behavior: their values tends to decrease with the analysis (Fig. 3b), thus, short periods of oxidation could be recommended to minimize this effect (especially in more modern systems such as Isolink I or II, as these interfaces can perform a fast oxidation of the combustion reactor in the beginning of each run). But, the most important conclusion about the trends showed in Fig. 3, is that the sample preparation has a more pronounced contribution for the results inaccuracy, leading in systematic errors as observed for C22:0 standard.

Admitting that the *J. curcas* FAMEs are being submitted to the same processes of the standards C19:0 and C22:0, in both steps of derivatization and GC/C/IRMS analysis, and that they are following the identical treatment principle, the measured $\delta^{13}C$ of both standards were used to correct the raw measured $\delta^{13}C$ for all the FAMEs in *J. curcas* samples. Comparing the raw data and the normalized data by using the two-point normalization procedure reported here, showed in Table 5, we observed random deviations between both set of values, sometimes less critical, but in some cases being of almost 1 mUr, which is a lot higher than the technique precision, thus, requiring correction.

The normalized and corrected $\delta^{13}C_{VPDB}$ values (corrected considering the incorporation of one atom of carbon from methanol in the fatty acid chain, as described by mass balance in equation 1) are reported in Table 6. The average isotopic values ranged between −28.29 and −30.82 mUr, being the C18:2 the fatty acid with the lower isotopic value for all samples. The global average isotopic values for all the samples and fatty acid chains was of -29.51 ± 1.03 mUr, which is in accordance to the average value for bulk samples determined by EA/IRMS, -28.97 ± 0.43 mUr, indicating the accuracy of the normalized results.

All the data presented in this work showed that major quality procedures must be used in order to ensure accurate results, even for simpler derivatizations procedures, such as transesterifications, and simple samples like pure vegetable oils. The transesterification reaction is the main source of isotopic fractionation and biased results, followed by the measurement itself. Both effects can be eliminated – or at least minimized – by using proper internal and external standards for raw data normalization, following the identical treatment principle as described in this work.

The use of 2 different standards will correct the 2 major sources of isotopic fractionation: the sample preparation and the instrumental analysis itself. Note that one could use as many standards as wished, depending on how much expensive the analysis could be, or how many standards are available to properly be applied to correct any source of isotopic fractionation. In the case of this work, both standards correct all possible sources of isotopic fractionation. The C22:0 is there since the beginning of sample preparation; and C19:0 is added immediately before injection, so it only suffers the influence of the analysis. Note also that C22:0 is also influenced, of course, by the analysis. Therefore, 2 standards are indeed being used for the correction of instrumental responses, and that it is a good enough approach, considering the benefits.

In fact, the results shown in this work points out that normalization procedures must be implemented, or at least evaluated, to make sure that we are reporting accurate values for GC/C/IRMS, not only for FAMEs, but for every analyte.

5. Conclusion

In this work, we have described a simple methodology for a traceable and accurate determination of $\delta^{13}C_{VPDB}$ values in fatty acid methyl esters, using real samples of *J. curcas* biodiesel as a proof-of-concept for the method.

It was observed that the transesterification method using the classic procedure with methanol-BF_3 under ultrasonic bath causes an isotopic fractionation that results in positively biased values of approximately 2 mUr, observed for the standard C22:0, added in the beginning of the sample preparation and analyzed by GC/C/IRMS. Due to that, the raw results of FAMEs in *J. curcas* samples were normalized using the measured values and the reference values (obtained by EA/IRMS) of both C22:0 and C19:0, which was the internal and external standards, respectively. The first one to correct any isotopic fractionation due to the derivatization process; the last one to correct any random error in the instrumental response

Table 5
Comparison of raw and normalized (two-point normalization) $\delta^{13}C$ values for the *J. curcas* FAMEs.

Samples	813		136		112		100		201		101		102		264		299	
FAME	Raw values	Normalized	Raw values	Normalized	Raw values	Normalized	Raw values	Normalized	Raw values	Normalized	Raw values	Normalized	Raw values	Normalized	Raw values	Normalized	Raw values	Normalized
C16:0	−29.84	−30.03	−29.93	−30.14	−30.03	−30.10	−30.09	−29.92	−30.04	−29.90	−29.95	−29.83	−29.89	−30.14	−30.02	−29.17	−29.60	−29.09
C18:0	−30.14	−30.22	−30.18	−30.35	−30.25	−30.25	−30.28	−30.04	−30.19	−29.98	−30.07	−29.88	−29.98	−30.19	−30.08	−29.21	−29.65	−29.12
C18:1	−28.61	−29.24	−28.92	−29.26	−29.14	−29.48	−29.30	−29.47	−29.41	−29.55	−29.48	−29.61	−29.55	−29.28	−29.41	−28.80	−29.11	−28.80
C18:2	−29.84	−30.03	−29.94	−30.14	−30.04	−30.10	−30.09	−29.93	−30.04	−29.90	−29.95	−29.83	−29.89	−31.08	−30.49	−29.46	−29.97	−29.32

Table 6
Normalized carbon isotope ratios ($\delta^{13}C_{VPDB}$) of individual fatty acids chains of *J. curcas* oil samples.

Fatty acid chain	Normalized $\delta^{13}C_{VPDB}$ (mUr) values[a] *J. curcas* samples									
	813	136	112	100	201	101	102	264	299	Average ± sd
C16:0	−29.50 ± 0.15	−30.33 ± 0.03	−29.44 ± 0.24	−29.10 ± 0.02	−29.29 ± 0.12	−29.63 ± 0.07	−29.63 ± 0.07	−28.57 ± 0.09	−28.72 ± 0.16	−29.36 ± 0.53
C18:0	−29.76 ± 0.30	−30.58 ± 0.41	−29.71 ± 0.28	−29.16 ± 0.27	−29.24 ± 0.25	−29.74 ± 0.12	−29.74 ± 0.41	−29.28 ±0.06	−29.16 ± 0.18	−29.60 ± 0.46
C18:1	−28.73 ± 0.38	−29.00 ± 0.37	−27.99 ± 0.20	−27.95 ± 0.08	−28.25 ± 0.15	−28.77 ± 0.12	−28.77 ± 0.41	−27.29 ± 0.21	−27.85 ± 0.24	−28.29 ± 0.56
C18:2	−29.56 ± 0.22	−30.79 ± 0.91	−31.77 ± 0.18	−30.86 ± 0.30	−30.86 ± 0.17	−30.67 ± 0.05	−30.67 ± 0.67	−30.92 ± 0.02	−31.26 ± 0.20	−30.82 ± 0.58
									Global Average	−29.51 ± 1.03

[a] Corrected with methanol mass balance described in Eq. (1).

of the GC/C/IRMS system. In this way, accurate results could be obtained: the average values of all the fatty acids chains of all the samples was $\delta^{13}C_{VPDB} = -29.51 \pm 1.03$ mUr, while the bulk value obtained with EA/IRMS was −28.97 ± 0.43 mUr, a typical signature of C3-plants.

This work also demonstrates that major quality procedures must indeed be applied for accurate determinations of isotopic values, especially in GC analysis. The lack of proper stable isotope reference materials could be overcome by using secondary working standards with the reference values properly determined by EA/IRMS and traceable to the international scale via internationally agreed reference materials, along with the application of the identical treatment principle.

Acknowledgements

We thank the State of São Paulo Research Foundation (FAPESP), State of Rio de Janeiro Research Foundation (FAPERJ), the Brazilian National Council for Scientific and Technological Development (CNPq) and the Financing Agency of Studies and Projects (FINEP) for financial assistance. We gratefully acknowledge Gabriel Moraes Silva and Clarisse Lacerda Torres for the assistance with EA/IRMS analyses at CENPES/PETROBRAS. We also thank EBRAPA for samples donation and the referees of this work to contribute for its quality improvement.

Appendix A. Supplementary data

Supplementary data associated with this article can be found, in the online version, at http://dx.doi.org/10.1016/j.ijms.2016.12.002.

References

[1] W.A. Brand, High precision isotope ratio monitoring techniques in mass spectrometry, J. Mass Spectrom. 31 (1996) 225–235.
[2] J. Vogl, Advances in isotope ratio mass spectrometry and required isotope reference materials, Mass Spectrom. (Tokyo) 2 (2013) S0020.
[3] J. Kubásek, O. Urban, J. Santrucek, C4 plants use fluctuating light less efficiently than do C3 plants: a study of growth, photosynthesis and carbon isotope discrimination, Physiol. Plant. 149 (2013) 528.
[4] M. Zealand, G.P. Jackson, Isotope ratio mass spectrometry, Analyst 134 (2009) 213.
[5] (a) Simon J. Simon, Charles M. Scrimgeour, High-Precision determination of $^{2}H/^{1}H$ in H_2 and H_2O by continuous-Flow isotope ratio mass spectrometry, Anal. Chem. 67 (13) (1995) 1992–1997.
[6] T.B. Coplen, Guidelines and recommended terms for expression of stable isotope-ratio and gas-ratio measurement results, Rapid Commun. Mass Spectrom. 25 (2011) 2538.
[7] A. Schimmelmann, H. Qi, T.B. Coplen, W.A. Brand, J. Fong, W. Meier-Augenstein, H.F. Kemp, B. Toman, A. Ackermann, S. Assonov, A.T. A.-Bijma, R. Brejcha, Y. Chikaraishi, T. Darwish, M. Elsner, M. Gehre, H. Geilmann, M. Gröning, J.-F. Hélie, S. Herrero-Martín, H.A.J. Meijer, P.E. Sauer, A.L. Sessions, R.A. Werner, Organic reference materials for hydrogen, carbon, and nitrogen stable isotope-ratio measurements: caffeines, *n*-alkanes, fatty acid methyl esters, glycines, *l*-valines, polyethylenes, and oils, Anal. Chem. 88 (8) (2016) 4294–4302.
[8] W.A. Brand, T.B. Coplen, J. Vogl, M. Rosner, T. Prohaska, Assessment of international reference materials for isotope-ratio analysis (IUPAC Technical Report), Pure Appl. Chem. 86 (2014) 425.
[9] L. Ke, Z. Lin, Z. Guoxing, Study of normalization method of isotopic compositions to isotope reference scales, J. Chem. Pharm. Res. 6 (2014) 1.
[10] H. Kipphardt, S. Valkiers, P.D.P. Taylor, P. De Biévre, Calibration in isotopic measurements, Int. J. Mass spectrom. 198 (2000) 71.
[11] J.F. Carter, B. Fry, Ensuring the reliability of stable isotope ratio data—beyond the principle of identical treatment, Anal. Bioanal. Chem. 405 (2013) 2799.
[12] D. Paul, G. Skrzypek, I. Fórizs, Normalization of measured stable isotopic compositions to isotope reference scales – a review, Rapid Commun. Mass Spectrom. 21 (2007) 3006.
[13] R.A. Werner, W.A. Brand, Referencing strategies and techniques in stable isotope ratio analysis, Rapid Commun. Mass Spectrom. 28 (2014) 1674.
[14] W.A. Brand, L. Huang, H. Mukai, A. Chivulescu, J.M. Richter, M. Rothe, How well do we know VPDB? Variability of delta13C and delta18O in CO_2 generated from NBS19-calcite, Rapid Commun. Mass Spectrom. 23 (6) (2009) 915–926.
[15] A. Schimmelmann, M.J. DeNiro, Determination of oxygen stable isotope ratios in organic matter containing carbon, oxygen, hydrogen, and nitrogen, Anal. Chem. 57 (1985) 2644–2646.

[16] T.B. Coplen, Normalization of oxygen and hydrogen isotope data, Chem. Geol. Isotope Geosci. Sect. 72 (4) (1988) 293–297.
[17] T.B. Coplen, Reporting of stable hydrogen, carbon, and oxygen isotopic abundances, Geothermics 24 (5) (1995) 707–712.
[18] L.A. Neves, J.M. Rodrigues, R.J. Daroda, P.R.M. Silva, A.A. Ferreira, Donato A.G. Aranda, M.N. Eberlin, M. Fasciotti, The influence of different referencing methods on the accuracy of $\delta^{13}C$ value measurement of ethanol fuel by gas chromatography combustion/isotope ratio mass spectrometry, Rapid Commun. Mass Spectrom. 29 (2015) 1938–1946.
[19] G. Rieley, Derivatization of organic compounds prior to gas chromatographic–combustion–isotope ratio mass spectrometric analysis: identification of isotope fractionation processes, Analyst 119 (1994) 915–919.
[20] B.D. Gunter, J.D. Gleason, Isotope fractionation during gas chromatographic separations, J. Chromatogr. Sci 9 (1971) 191.
[21] W. Meier-Augenstein, Applied gas chromatography coupled to isotope ratio mass spectrometry, J. Chromatogr. 842 (1999) 351.
[22] K.A. van Leeuwen, P.D. Prenzler, D. Ryan, F. Camin, Gas chromatography-combustion-isotope ratio mass spectrometry for traceability and authenticity in food stuffs and beverages, Compr. Rev. Food Sci. Food Saf. 13 (2014) 814.
[23] B.O. Aguilar-Cisneros, M.G.L. Pez, E. Richling, F. Heckel, P. Schreier, Tequila authenticity assessment by headspace SPME-HRGC-IRMS analysis of $^{13}C/^{12}C$ and $^{18}O/^{16}O$ ratios of ethanol, J. Agric. Food Chem. 50 (2002) 7520.
[24] C. Guillou, J. Koziet, A. Rossmann, G.J. Martin, Determination of the C-13 contents of organic acids and sugars in fruit juices: an inter-comparison study, Anal. Chim. Acta 388 (1999) 137.
[25] O. Bréas, F. Reniero, G. Serrini, G.J. Martin, A. Rossmann, Isotope ratio mass spectrometry: analysis of wines from different european countries, Rapid Commun. Mass Spectrom. 8 (1994) 967–970.
[26] L. Schipilliti, I. Bonaccorsi, A. Cotroneo, P. Dugo, L. Mondello, Evaluation of gas chromatography-combustion-isotope ratio mass spectrometry (GC-C-IRMS) for the quality assessment of citrus liqueurs, J. Agric. Food Chem. 61 (8) (2013) 1661–1670.
[27] L.A. Neves, G.F. Sarmanho, V.S. Cunha, R.J. Daroda, D.A.G. Aranda, M.N. Eberlin, M. Fasciotti, Anal. Methods 7 (2015) 4780.
[28] W.A. Brand, H. Geilmann, E.R. Crosson, C.W. Rella, Cavity ring-down spectroscopy versus high-temperature conversion isotope ratio mass spectrometry; a case study on δ^2H and $\delta^{18}O$ of pure water samples and alcohol/water mixtures, Rapid Commun. Mass Spectrom. 23 (2009) 1879–1884.
[29] C.V. von Eckstaedt, K. Grice, M. Ioppolo-Armanios, G. Chidlow, M. Jones, δD and δ13C analyses of atmospheric volatile organic compounds by thermal desorption gas chromatography isotope ratio mass spectrometry, J. Chromatogr. A 1218 (2011) 6511.
[30] N. Gentile, L. Besson, D. Pazos, O. Delemont, P. Esseiva, On the use of IRMS in forensic science: proposals for a methodological approach, Forensic Sci. Int. 212 (2011) 260.
[31] C. Lennard, P. Maynard, C. Roux, S. Benson, Forensic applications of isotope ratio mass spectrometry – a review, Sci. Int. 157 (2006) 1–22.
[32] A.T. Cawley, U. Flenker, The application of carbon isotope ratio mass spectrometry to doping control, J. Mass Spectrom 43 (2008) 854–864.
[33] N. Baume, C. Saudan, A. Desmarchelier, E. Strahma, P. Sottas, C. Bagutti, M. Cauderay, Y.O. Schumacher, P. Mangin, M. Saugy, Use of isotope ratio mass spectrometry to detect doping with oral testosterone undecanoate: inter-individual variability of $^{13}C/^{12}C$ ratio, Steroids 71 (2006) 364.
[34] B.J. Smallwood, R.P. Philp, J.D. Allen, Stable carbon isotopic composition of gasoline determined by isotope ratio monitoring gas chromatography mass spectrometry, Org. Geochem. 33 (2002) 149.
[35] R.M. Alonso-Salces, J.M. Moreno-Rojas, M.T.V. Holland, F. Reniero, C. Guillou, K. Berger, Virgin olive oil authentication by multivariate analyses of ^{1}HNMR fingerprints and $\delta^{13}C$ and δ^2H data, J. Agric. Food Chem. 58 (2010) 5586–5596.
[36] F. Angerosa, O. Bréas, Contento C. Guillou, F. Reniero, E. Sada, Application of stable isotope ratio analysis to the characterization of the geographical origin of olive oils, J. Agric. Food Chem 47 (1999) 1013–1017.
[37] H.T. Slover, E. Lanza, Quantitative analysis of food fatty acids by capillary gas chromatography, J. Am. Oil Chem. Soc. 56 (1979) 933.
[38] K.-S. Liu, Preparation of fatty acid methyl esters for gas-chromatographic analysis of lipids in biological materials, J. Am. Oil Chem. Soc. 71 (11) (1994) 1179–1187.
[39] G. Rieley, R.J. Collier, D.M. Jones, G. Eglinton, P.A. Eakin, A.E. Fallick, Sources of sedimentary lipids deduced from stable carbon-isotope analyses of individual compounds, Nature 352 (1991) 425–427.
[40] S.E. Woodbury, R.P. Evershed, J.B. Rossell, R.E. Griffith, P. Famell, Detection of vegetable oil adulteration using gas chromatography combustion/isotope mass spectrometry, Anal. Chem. 67 (1995) 2685–2690.
[41] R. Hrastar, M.G. Petrisaica, N. Ogrinc, I.J. Kosair, Fatty acid and stable carbon isotope characterization of camelina sativa oil: implications for authentication, J. Agric. Food Chem. 57 (2009) 579.
[42] J.E. Spangenberg, N. Ogrinc, Authentication of vegetable oils by bulk and molecular carbon isotope analyses with emphasis on olive oil and pumpkin seed oil, J. Agric. Food Chem. 49 (2001) 1534.
[43] (a) F. Angerosa, O. Bréas, S. Contento, C. Guillou, F. Reniero, E. Sada, Application of stable isotope ratio analysis to the characterization on the geographical origin of olive oils, J. Agric. Food Chem. 47 (1999) 1013–1017.
[44] P.S. Nigam, A. Singh, Production of liquid biofuels from renewable resources, Prog. Energy Combust. Sci. 37 (1) (2011) 52–68.
[45] A.K. Tiwari, A. Kumar, H. Raheman, Biodiesel production from jatropha oil (*Jatropha curcas*) with high free fatty acids: an optimized process, Biomass Bioenergy 31 (2007) 569–575.
[46] M.Y. Koh, T.I.M. Ghazi, A review of biodiesel production from *Jatropha curcas* L. oil, Renew. Sustain. Energy Rev. 15 (5) (2011) 2240–2251.
[47] D.J. Morrison, K. Cooper, T. Preston, Reconstructing bulk isotope data from CSIA, Rapid Commun. Mass Spectrom. 24 (2010) 1799–1804.
[48] https://www.en-standard.eu/csn-en-14103-fat-and-oil-derivatives-fatty-acid-methyl-esters-fame-determination-of-ester-and-linolenic-acid-methyl-ester-contents/ (Accessed in 23 November 2016).
[49] R. Panetta, H. Jahren, Single-step transesterification with simultaneous concentration and stable isotope analysis of fatty acid methyl esters by chromatography-combustion-isotope ratio mass spectrometry, Rapid Commun. Mass Spectrom. 25 (2011) 1373–1381.
[50] J.C. Goding, D.Y. Ragon, J.B. O'Connor, S.J. Boehm, A.M. Hupp, Comparison of GC stationary phases for the separation of fatty acid methyl esters in biodiesel fuels, Anal. Bioanal. Chem. 405 (2013) 6087–6094.

2.2.1. Material suplementar

Support information

Title: "Two-point normalization using internal and external standards for a traceable determination of $\delta^{13}C$ values of fatty acid methyl esters by gas chromatography/combustion/isotope ratio mass spectrometry"

Table S1. Yields (%) of oil extraction from seeds of *J. curcas* from different states/cities of Brazil.

Sample code and city of origin	Extraction	Weight of seeds (g)	Weight of oil (g)	Yield (%)	Average yield (%)
DOURADOS (264)	1	30.1281	9.1750	30.4	34.4
	2	30.1027	10.5380	35.0	
	3	30.5500	11.6010	37.9	
LAVRAS (201)	1	30.0174	10.7690	35.9	35.2
	2	30.1610	9.0611	30.1	
	3	30.3570	12.0663	39.7	
MARANHÃO (136)	1	30.5856	13.0807	42.8	42.9
	2	30.0550	11.5745	38.5	
	3	30.1114	14.2409	47.3	
RIO GRANDE DO SUL (299)	1	30.7965	14.1387	45.9	43.7
	2	30.5889	11.1104	36.3	
	3	30.6230	14.9845	48.9	
PETROLINA (112)	1	30.0762	9.772	32.5	34.7
	2	30.1463	8.7472	29.0	
	3	30.3139	12.9422	42.7	
Unknown (813)*	1	30.5682	13.7824	45.1	40.3
	2	30.2924	11.8396	39.1	
	3	30.0781	11.0951	36.9	

*The origin of sample number 813 could not be confirmed.

Table S2. Isotopic values from 3 different oil extractions of the same seed (sample 813).

Extraction	Sample code_extraction_ replicate	$\delta^{13}C_{VPDB}$ (‰)	Mean(‰)	Standard deviation (‰)	RSD (%)	Mean of extractions (‰)	Standard deviation (‰)	RSD (%)
	813_1_1	-28.67	-28.69	0.03	0.09	-28.70	0.03	0.09
1	813_1_2	-28.68						
	813_1_3	-28.72						
	813_2_1	-28.62	-28.68	0.06	0.21			
2	813_2_2	-28.74						
	813_2_3	-28.69						
	813_3_1	-28.74	-28.73	0.02	0.07			
3	813_3_2	-28.74						
	813_3_3	-28.71						

Table S3. Ester content and ester composition determined with GC/MS of derivatized *J. curcas* oil using the ultrasonic method with methanol-BF_3.

	Total ester content and its distribution (g / 100 g)								
	Samples								
Ester	**136**	**813**	**299**	**112**	**201**	**264**	**100**	**101**	**102**
C16:0	15.06	15.37	14.39	15.10	14.06	14.82	13.94	13.48	14.09
C16:1	0.93	1.05	0.77	0.99	0.85	0.85	0.78	0.70	0.76
C18:0	5.94	5.75	5.51	5.52	6.20	5.59	7.36	6.70	6.55
***cis*-C18:1**	36.19	37.78	35.49	35.60	38.14	37.36	45.05	40.72	40.13
***trans*-C18:1**	1.29	1.38	1.09	1.33	1.32	1.24	0.97	1.09	1.13
C18:2	40.59	38.66	42.75	41.45	39.43	40.15	31.91	37.32	37.33
Total ester content (g / 100 g)	96.44	103.03	95.25	98.35	96.71	96.80	97.77	96.77	95.02

2.2.2. Autorização para reprodução do artigo

Copyright Clearance Center RightsLink®

Home | Create Account | Help

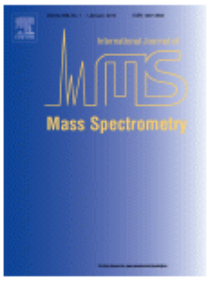

Title: Two-point normalization using internal and external standards for a traceable determination of δ13C values of fatty acid methyl esters by gas chromatography/combustion/isotope ratio mass spectrometry

Author: Maíra Fasciotti,Thays V.C. Monteiro,Alexandre A. Ferreira,Marcos N. Eberlin,Laura A. Neves

Publication: International Journal of Mass Spectrometry

Publisher: Elsevier

Date: July 2017

LOGIN

If you're a copyright.com user, you can login to RightsLink using your copyright.com credentials.

Already a RightsLink user or want to learn more?

Please note that, as the author of this Elsevier article, you retain the right to include it in a thesis or dissertation, provided it is not published commercially. Permission is not required, but please ensure that you reference the journal as the original source. For more information on this and on your other retained rights, please visit: https://www.elsevier.com/about/our-business/policies/copyright#Author-rights

BACK | CLOSE WINDOW

2.3. Microalgae biomass characterization using ion mobility-mass spectrometry

O artigo a seguir, em formato de manuscrito, encontra-se em fase de submissão para revista internacional da área de química analítica.

Journal title

Article

Title: “Microalgae biomass characterization using ion mobility-mass spectrometry”

Authors: Maíra Fasciotti[1,5]*, Gustavo H. M. F. Souza[2], Giuseppe Astarita[3], Ingrid C. R. Costa[1], Thays. V. C. Monteiro[1], Claudia M. L. L. Teixeira[4], Marcos N. Eberlin[5,6], Amarijt S. Sarpal[1]

[1] National Institute of Metrology, Quality and Technology (INMETRO), Division of Chemical Metrology, Laboratory of organic analysis, 25250-020, Duque de Caxias, RJ, Brazil

[2] MS Applications & Development Laboratory, Waters Corporation, Barueri, SP, Brazil;

[3] Department of Biochemistry and Molecular & Cellular Biology, Georgetown University, Washington, DC, USA;

[4] Instituto Nacional de Tecnologia (INT), Rio de Janeiro, Rio de Janeiro, Brazil;

[5] ThoMSon Mass Spectrometry Laboratory, Institute of Chemistry, University of Campinas – UNICAMP, Campinas, SP, Brazil.

[6] Mackenzie Presbyterian University, School of Engineering, 01302-907 São Paulo, SP Brazil

*corresponding author: M. Fasciotti, mfasciotti@inmetro.gov.br

ABSTRACT

Algae biomass displays an extremely complex set of metabolites and its molecular characterization has been very challenging. We are reporting strategies to characterize microalgae extracts via traveling wave ion mobility – mass spectrometry (TWIM-MS). First, we analyzed microalgae extracts by direct infusion to an electrospray ion source (ESI) with no previous chromatographic separation (DI-ESI-TWIM-MS). Second, we screened metabolites and lipids in the extracts via an untargeted high throughput method by ultra-performance liquid chromatography (UPLC) coupled to TWIM using data independent analysis (DIA) – MS^E (UPLC-$HDMS^E$). Sixteen different microalgae biomasses were evaluated by both approaches. DI-TWIM-MS was able, via distinct drift times, to set apart different classes of metabolites, making microalgae typification more evident. UPLC-$HDMS^E$, identified 1251 different metabolites, providing their lipid profiles, serving, therefore, as a powerful tool to determine best biotechnological applications for algae samples. Collision-cross section determinations was able to discriminate triacylglycerol, increasing the confidence in their identifications, serving, therefore, as a guide for biofuels production. These two approaches seem to offer powerful tools for the algae industry identifying ideal strains and culture conditions for specific biotechnology applications, saving time in the analysis, and providing a wider number of identified species.

INTRODUCTION

Algae are a diverse group of predominantly aquatic organisms that have the ability to efficiently perform photosynthesis. They are responsible for close to 90% of photosynthesis performed on the planet [1,2,3] and form a diversified polyphyletic group, that is, they in fact form a group of an expanded set of organisms belonging to different phylogenetic groups.[4,5] Algae have been for decades widely studied within several fields of science. With the advent of modern biotechnology, algae have received even more attention, especially with the emergence of third- and fourth-generation fuels. [6,7,8,9,10] After it was realized that algae were able to provide better yields than processes with other biomasses - and through theoretically simpler production - biofuels made from algae were framed as more promising 3rd-generation fuels. [11] Intensive research followed for the quest of more efficient production of different types of biofuels and chemicals from algae. [12,13] A very interesting advantage of algae as source of biomass is that they can be grown in waste and salty waters, [14,15] acting simultaneously as a bioremediation strategy. [16,17,18,19]

Currently, major studies have focused on applications of algae to produce biohydrogen through solar energy and water; [20] bioisoprene (2-methyl-1,3-butadiene); [21] and of bioethanol, mainly produced by cyanobacteria with yields comparable to the classic microorganism of alcoholic production, the famous *Saccharomyces cerevisiae*. [22,23] Butanol and isobutanol have also been directly produced from CO_2 via algae bioprocesses. [24,25] However, biodiesel is perhaps the most promising biofuel to be produced via algae, since some oleaginous algae have 30-60% (w/w) of triacylglycerols on a dry basis. [26,27,28] To obtain better yields to produce biodiesel precursor lipids – mainly triacylglycerols – the algae species have

been cultivated in different culture media, containing different nutrients and under physical-chemical conditions. These parameters strongly influence biomass composition. [29] Cell growth, lipid productivity, composition and nature of components are dependent on several parameters such as types of algae species/strains, culture medium composition, light flux, feed used for their cultivation and temperature. [30,31] For instance, it has been shown that stressful culture conditions such as nitrogen limitation or nutrient imbalance can be implemented to stimulate the increase in the neutral lipid content in the microalgae cells, and it can be used for the growth of high biodiesel potential algae strains. [32,33] The type of cultivation systems (e.g. open pond, closed or hybrid bioreactor), also play an important role in the process. [34,35,36]

Although algae-based biofuels are quite promising, major improvements in the technology to grow and harvest the algae, to enhance the extraction of the neutral lipid content and to transform it in biofuels have been the main factors slowing their wider implementation. Several improvements are being tested, especially for downstream and upstream processes optimization. [37,38]

Alongside the algae production processes, the characterization of the resulting biomass is extremely important to ensure that the growth conditions are actually affecting the biomass composition as desired. [39] The detailed chemical compositional characterization of algae biomass is therefore a fundamental step to ensure that the best biotechnological applications are being given by the developer, either for the production of biofuels, biogas, bio-based chemicals, bioremediation or even for the area of nutraceutical and food supplements, that are being frequently used as dietary products. [40,41,42]

The characterization of the algae biomass has been performed using several analytical techniques, from classical physical-chemical methods such as elemental

analysis, gravimetric determination of total lipid content or classical methods for total protein or carbohydrate measurements, [43] to more complex instrumental techniques such as NMR [44,45], FTIR, [46] laser-based techniques [47] and chromatography. [48, 49] Classical physical-chemical methods offer the advantage of being less expensive, faster (but often laborious regarding sample preparation) and often requiring less operator training. They can be adequate for the purpose depending on the information desired.

Nevertheless, as algae biomass composition is extremely complex [50] in terms of classes of chemical compounds and in the number of total compounds itself, and speciation is of great importance to fully understand what metabolic pathways are taking place in some specific cultivation condition, and what is the main factor influencing the alterations.

Mass spectrometry (MS) has been established as a powerful and versatile analytical technique for both quantitation of target compounds as well as identification of a massive number of unknown compounds at once in a wide variety of matrices and samples. Due to these interesting features, MS-based analytical methods have been successfully applied for algae characterization for more than four decades. Peptides such as microcystins, [51,52,53] proteins, [54,55, 56,57] several classes of toxins, [58 ,59,60, 61] isoflavones, [62] lipids, [63,64,65,66,67,68] fatty acids,[69,70,71,72] sterols,[73] polysaccharides[74,75] hydrocarbons,[76,77] aldehydes,[78] and other classes of specific metabolites of biological or environmental importance [79,80,81,82,83] have already been successfully determined using MS-based methodologies, most of them by using liquid or gas chromatography coupled to tandem (triple quadrupole) or high resolution mass spectrometers.

The versatility of MS also comes from a quite diverse set of ion sources and mass analyzers, allied with the proper hyphenation with other analytical separation techniques such as chromatography, electrophoresis and ion mobility. These couplings provide enhanced peak detectability and capacity due to its multidimensional separation processes based on different molecules/ions properties, which gives all the compounds in a complex mixture many chances to be "seen", *i.e.* detected, characterized, identified and quantified, as a single "individual".

With the introduction of commercially available instruments, [84] ion mobility coupled with high resolution mass spectrometry (IM-HRMS), has recently become the technique of choice in omics sciences (especially in proteomics, lipidomics and metabolomics studies). [85, 86] The technique is frequently coupled with liquid chromatography leading to multidimensional data, combining the compounds' parameters of retention times *versus* ions *m/z* ratios *versus* ions drift times, the former being achieved in a few minutes and the latter at the millisecond scale of time.

Ion mobility (IM) is a technique that separates gaseous ions while they travel through a buffer gas under the influence of an electrical field. [87] There are several modalities and instrumental arrangements of IM, and they differ in the size of the drift cell, its format and how the electrical field is applied and interacts with the ions.[88] The drift gas plays a crucial role in the separation, being introduced in different scales of pressure depending on the IM modality. IM separation is based on parameters such as the tridimensional shape/size of the ions, i.e. collision cross section (CCS), charge, and ion-dipole interactions of the ions with the neutral drift gas molecules. [89] The lighter, more compact and the species with weaker interactions with the mobility gas (because they have lower charge states or dipole moments) will be faster and,

therefore, will exhibit a lower drift time, a parameter measured by the IMS technique. Three-dimensional spectra (*m/z* x drift time x intensity) are obtained for the data. As the intensity axis is often represented by a color-scale, IMS data are often called two-dimensional drift time *versus m/z* spectrum or simply drift plots.

Previous studies have demonstrated the excellent performance of the technique for isomers and isobars separation, characterization of complex mixtures, [90,91,92,93] as well as for increasing the selectivity of lipidomics and metabolomics analyses. [85] This new dimension of the data is very useful, because species that are not resolved by chromatography can be separated by IMS, which increases the detection capacity of the technique. In complex mixtures, different classes of compounds are distributed forming sets of characteristic tendencies, that is, drift time regions that are characteristic of classes of compounds or their analogues.

This work aimed to explore the potential of ion mobility coupled to high resolution mass spectrometry to characterize different microalgae biomasses. Two approaches were used: direct infusion (DI) of algae extracts directly into the electrospray (ESI) source of the TWIM-MS instrument, the DI-ESI-TWIM-MS approach; and a untargeted metabolomics screening using ultra performance liquid chromatography analysis (UPLC) coupled to TWIM using data independent analysis (DIA) – MS^E – as method of MS acquisition with the objective of performing a comprehensive and detailed lipid and metabolite identification, the UPLC-$HDMS^E$ approach.

EXPERIMENTAL SECTION

Chemicals

Methanol and chloroform (LC grade) were purchased from Tedia Brazil (Rio de Janeiro, Brazil). Analytical grade phosphoric acid (85% w/w), formic acid

(98–100%), LC grade leucine enkephalin, poly-D-alanine and ammonium formate were purchased from Sigma-Aldrich (Merck Sigma-Aldrich, KGaA, Darmstadt, Germany). Mobile phases acetonitrile and propan-2-ol (MS grade) were purchased from J. T. Backer (Sao Paulo, Brazil). Water was purified using a Millipore Milli-Q system (Merck Millipore, KGaA, Darmstadt, Germany).

Samples

In total, 16 microalgae biomasses were analyzed, including 5 from different genera (*Tetraselmis* aff. *chuii, Spirulina platensis, Dunaliella salina, Chlorella vulgaris, Scenedesmus ecornis*), and obtained under different cultivation times and/or culture media composition or light source (Scheme 1). See SI for detailed cultivation conditions. For comparison with microalgae extracts, commercial samples of refined soybean, corn, rapeseed, sunflower and olive oils were purchased in the local market.

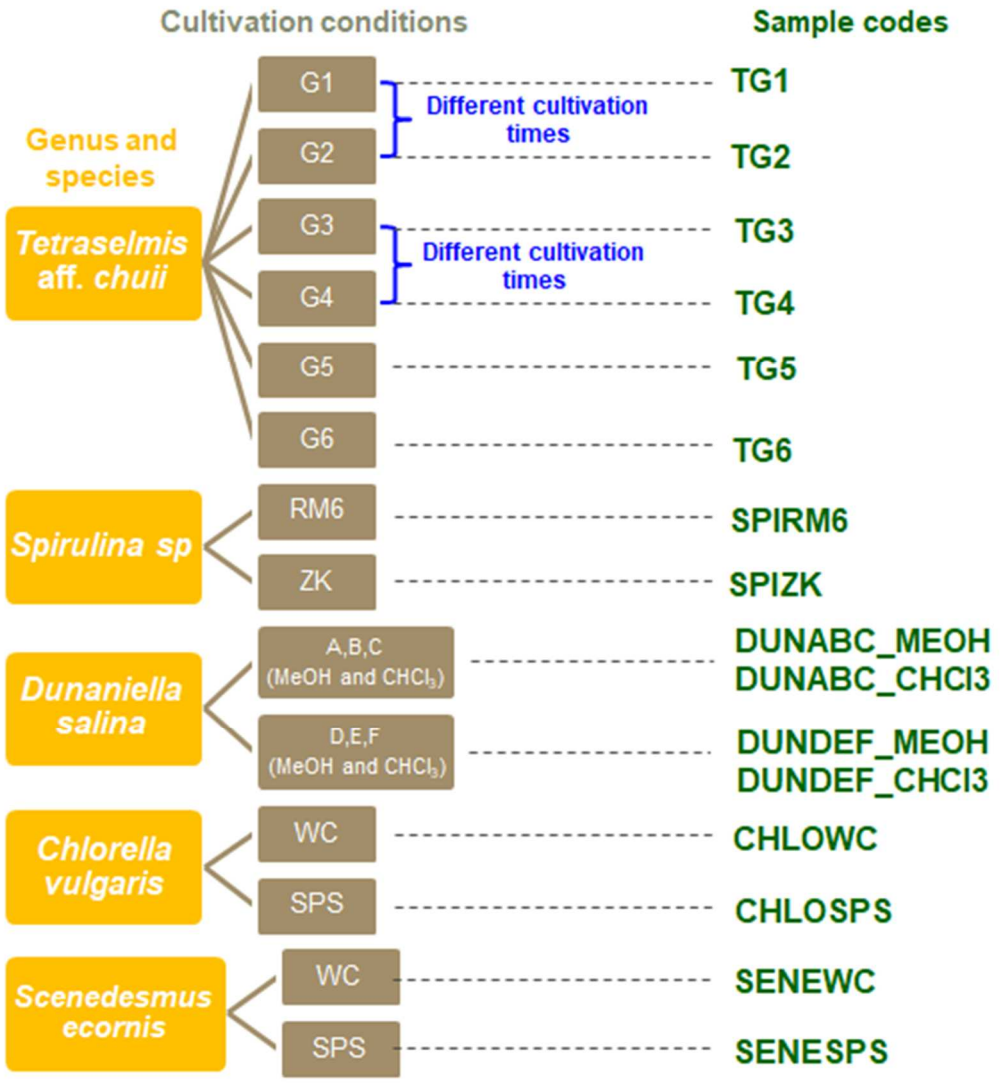

SHEME 1. Sixteen different microalgae biomasses analyzed in this work.

Sample preparation

Lyophilized biomasses of different algae were extracted using the Bligh and Dyer like method [94] with some modifications. [95] For *Tetraselmis* aff. *chuii, Spirulina platensis, Chlorella vulgaris and Scenedesmus ecornis* samples, 0.1 g of each lyophilized biomass was homogenized with 15 mL of chloroform: methanol: H_2O (2:1:0.5, v/v) and put in an ultrasonic bath (200W, 50 Hz) for one hour at 30 ℃. The lipid fractions were filtered using filter paper and then dried under water vapor heat set to 60 ℃. The dried lipid fractions were determ ined gravimetrically. For the

Dunaliella salina samples (ABC and DEF culture media) the protocol was different due to the high concentration of salts in the dried biomass. The lipid extraction was then performed in two steps: the first consisted in the dry biomass extraction using pure chloroform (20 mL) under ultrasonic agitation also for 1h at 30 ℃. The solid was decanted and the liquid phase was transferred to a beaker. Then, in the second step, a volume of 20 mL of methanol was used with 300 µL of H_2O to extract the solid residue of the first step (with pure chloroform), under the same extraction conditions. The chloroform and methanol extracts were also evaporated under 60 ℃ and the dried extracts were gravimetrically determined. All the lipid extracts for all samples were then re-dissolved in pure methanol at an approximate concentration of 2 mg $\cdot$ mL^{-1}. Then, 20 µL of the lipid fraction in methanol were diluted in 1 mL of methanol with 0.1 % of formic acid for the direction infusion approach and in mobile phase B for the UPLC-$HDMS^E$ analysis.

METHODS

DI-ESI-TWIM-MS approach

Direct infusion approach was performed on a Traveling Wave Ion Mobility Mass Spectrometer (TWIM-MS, Synapt HDMS, Waters, UK). The samples were direct infused at a flow rate of 20 µL / min using an external syringe pump into the ESI source operated under positive ion mode, 3.5 kV of capillary, 40 and 5.0 V of cone and extractor cone, respectively. The source and desolvation temperatures were 80 and 150 ℃, and the nitrogen nebulizer gas was used at a flow rate of 400 L / h. Parameters such as the drift gas pressure (N_2, 1.05 mbar), height (30V) and wave velocity (650 m/s) were optimized to obtain the same spectra as when only QTOF mode is used, avoiding any distortion or sensitivity loss, in a range of *m/z* 50 – 1,500.

The mass spectrometer was mass calibrated in ESI(+) mode at 10,000 resolution (FWHM) over acquisition mass ranges of *m/z* 50 – 2000, using a solution of phosphoric acid 0.1% (v/v) in acetonitrile:H_2O (1:1). The characterization of the most important ions of the spectra was performed by fragmentation of manually selected precursor ions by collision induced dissociation (CID) using argon as collision gas (collisions energies 20 – 35 eV), and the identification was done by comparison of the MS/MS data with data bases such as LIPID MAPS [96] and Human Metabolome Database.[97]

UPLC-HDMS ^{E}

UPLC-HDMS^{E} was performed in a Synapt HDMS G2-S*i* mass spectrometer with an ACQUITY™ UPLC *i*-Class as chromatograph (both Waters, UK). The separation was carried out using an ACQUITY CSH™ C_{18}, 2.1 mm x 100 mm column kept at 55 ˚C during analysis. Mobile phase consisted of solvent A (acetonitrile:H_2O 60:40 + 10mM ammonium formate + 0.1% formic acid); and solvent B (propan-2-ol:acetonitrile 90:10 +10 mM ammonium formate + 0.1% formic acid). The gradient elution program was as follows: 0 – 0.99 min from 60:40 A:B to 57:43 A:B; 0.99 - 1.24 min from 57:43 A:B to 50:50 A:B; 1.24 – 5.39 min from 50:50 A:B to 1:99 A:B; 5.39 – 5.64 min from 1:99 A:B to 60:40 A:B, then remaining constant until 8 min. Flow rate was 0.7 mL.min^{-1} and sample injection volumes were 4 µL (FTN AutoSampler). Total run time was 8 min. The mass spectrometer was equipped with an ESI source, also in positive ion mode, operating under 3.5 kV of capillary and 40 V of cone. The source and the desolvation temperature were 110 and 450 ℃, respectively, and the nitrogen nebulizer gas was used at flow rate of 900 L / h at a pressure of 6 bar. The mass spectrometer was operated in ion-mobility (HDMS^{E})

mode, which is a method acquisition of MS and MS/MS spectra in an automated way. The mass analyzer operates in both low energy (for precursors ions) and high energy (for fragments) mode to promote collision induced dissociation (CID) of non-selected precursor ions, leading to spectra of products fragments aligned to the precursor ion. In this technique, the term “HD” comes from "high definition", because in this case the MS^E acquisition technique is also coupled to the ion mobility. Trap collision energy (low) was 4 eV, and transfer collision energy (high) was a ramp from 25 to 65 eV, also using argon as collision gas. The IMS cell was filled with N_2 under a pressure of 3.65 mbar. The IM cell was calibrated using poly-DL-alanine (10 mg/L) in H_2O: acetonitrile (50:50 + 0.1% of formic acid) to allow the calculation of the analytes CCS values. Both MS calibration and lock mass correction during analysis was performed using a leucine enkephalin (theoretical *m/z* 554.2620) solution in H_2O:acetonitrile (50:50 + 0.1% formic acid) at a concentration of 100 pg/µL and infused at a flow rate of 0.010 mL/min. The acquisitions in $HDMS^E$ mode ranged from *m/z* 50 to 1500. Default IMS conditions were used for IMS screening (T-wave velocity ramp start of 1000 m/s and end of 300 m/s; and T-wave pulse height of 40 V).

Data processing and statistics

Both DI–TWIM-MS and UPLC-$HDMS^E$ data were collected using the software MassLynx 4.1v (SCN 639 for Synapt HDMS and SCN 932 for Synapt G2-S*i,* Waters, UK). The DI-ESITWIM-MS data were evaluated using the software DriftScope 2.7v and HDMS Compare 1.0v, and the chemometric analysis for samples statistical comparison was performed using the software EZinfo 2.0v (Umetrics, USA) appended into MarkerLynx (Waters, UK).

For UPLC-HDMS^E data, processing and analysis was conducted by using Progenesis QI Informatics (Nonlinear Dynamics, Newcastle, U.K.) in a standard protocol [85] in which each UPLC–MS run was imported as a raw file to obtain the ion-intensity map, including *m/z* and retention time. As default, these ion maps were then aligned in the retention-time direction. From the aligned runs, an aggregate run representing the compounds in all samples was used for peak picking. This aggregate was then compared with all runs, to ensure that the same ions are detected in every run. Isotope and adduct deconvolution was applied, to reduce the number of features detected. Data were normalized according to total ion intensity. Metabolites were identified by database searches against their accurate masses in publicly available databases, including the LIPIDMAPS database and the Human Metabolome database (HMDB), and MetaScope (CCS database provided in Progenesis QI software), as well as by fragmentation patterns, retention times, and CCS values, when available. The platform LipidCCS [98] was also used for additional CCS comparison.

RESULTS AND DISCUSSION

DI-TWIM-MS of microalgae extracts

Researchers and biorefineries must have robust analytical tools for the detailed analysis of microalgae biomasses, in order to determine the best application for a specific biomass, and also to evaluate the process of algae production. We report two different strategies for performing a quite challenging molecular characterization of algae biomass extracts by using IM-MS, focusing on triacylglycerols (TAGs), as they are the the major transesterifiable lipids precursors of fatty acid methyl esters (FAMEs) for biodiesel production. [26, 27]

Figure 1 shows the full scan mass spectrum obtained by DI-ESI-TWIM-MS of the algae *Tetraselmis* aff*. chui* TG4. It highlights the sample complexity, and some examples of expected lipid classes that could be present in specific *m/z* ranges. For all other spectra, see Figures S1-S16. Quite different profiles are indeed observed which shows that the composition of the algal biomass is considerably altered as a function of the culture media and species or strains, and that these changes are easily detected through the present approach. Note that determining how specific classes of compounds vary more pronouncedly as a function of algae growth parameters is critical to optimize production conditions.

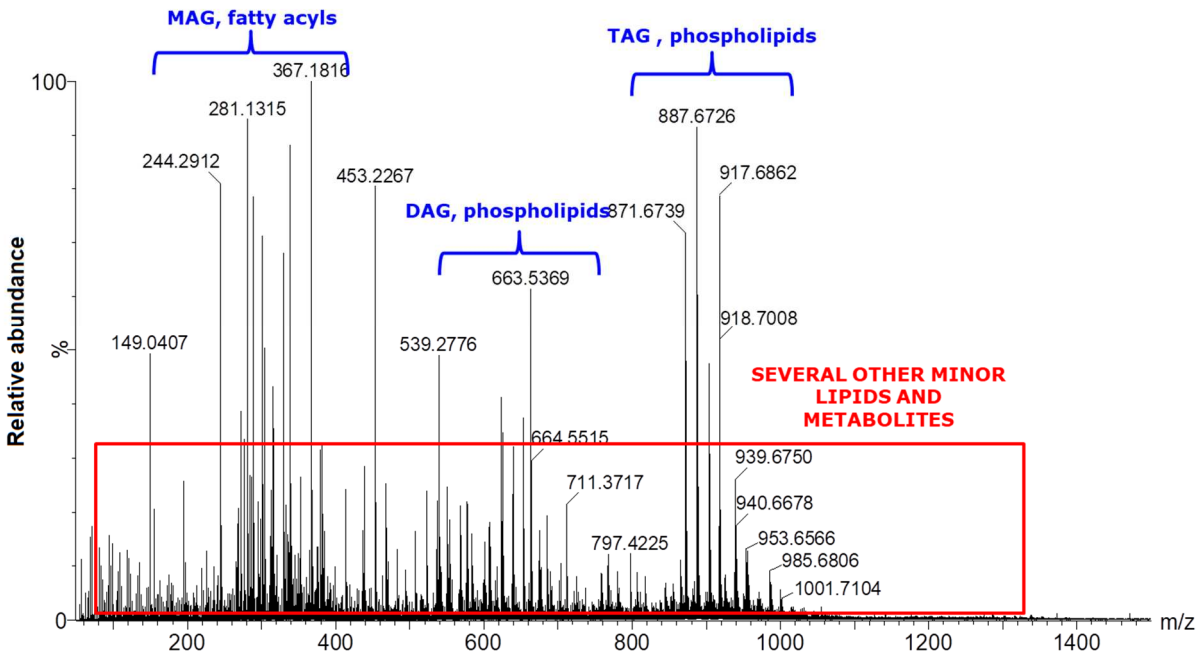

FIGURE 1. DI- ESI(+)-TWIM-MS data of an extract of *Tetraselmis* aff*. chui* cultivated in culture media G4 (Sample "TG4").

All 16 DI-ESI-TWIM-MS mass spectra for each microalgae extract were statistically evaluated by chemometrics (Figure 2) using principal component analysis. Grouping was primarily due to the microalgae genera, confirming that microalgae metabolite profile is indeed a mainly characteristic feature of this genera.

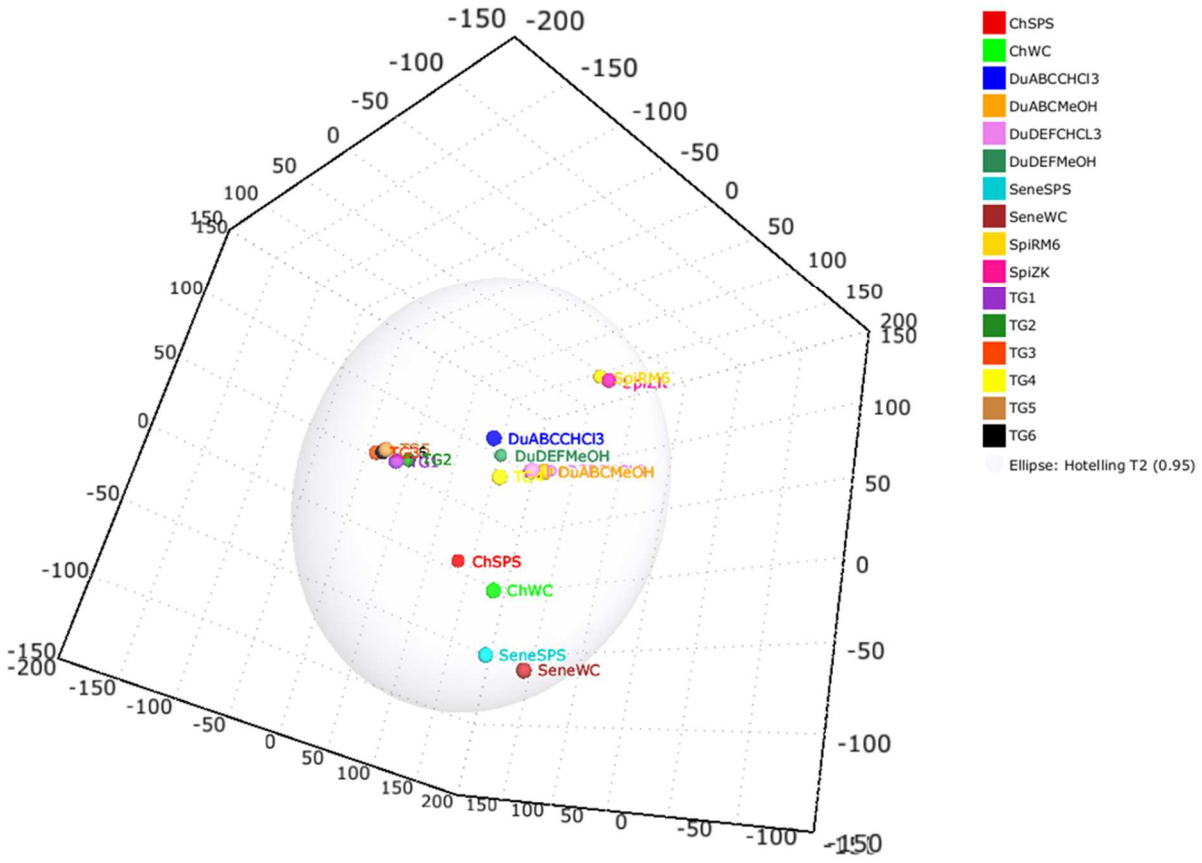

FIGURE 2. Statistical comparison of the 16 algal extracts using principal component analysis (PCA). Note the grouping by algae genus.

The algae extracts were also evaluated by their two-dimensional drift time versus *m/z* spectra, considering the TWIM separation of the ionized lipids and metabolites in samples.

Figure 3 shows representative examples of two-dimensional drift time *versus* *m/z* spectra for some microalgae species. The spectra for all samples are also included in the Supporting Information (Figures S17-S32) of this work.

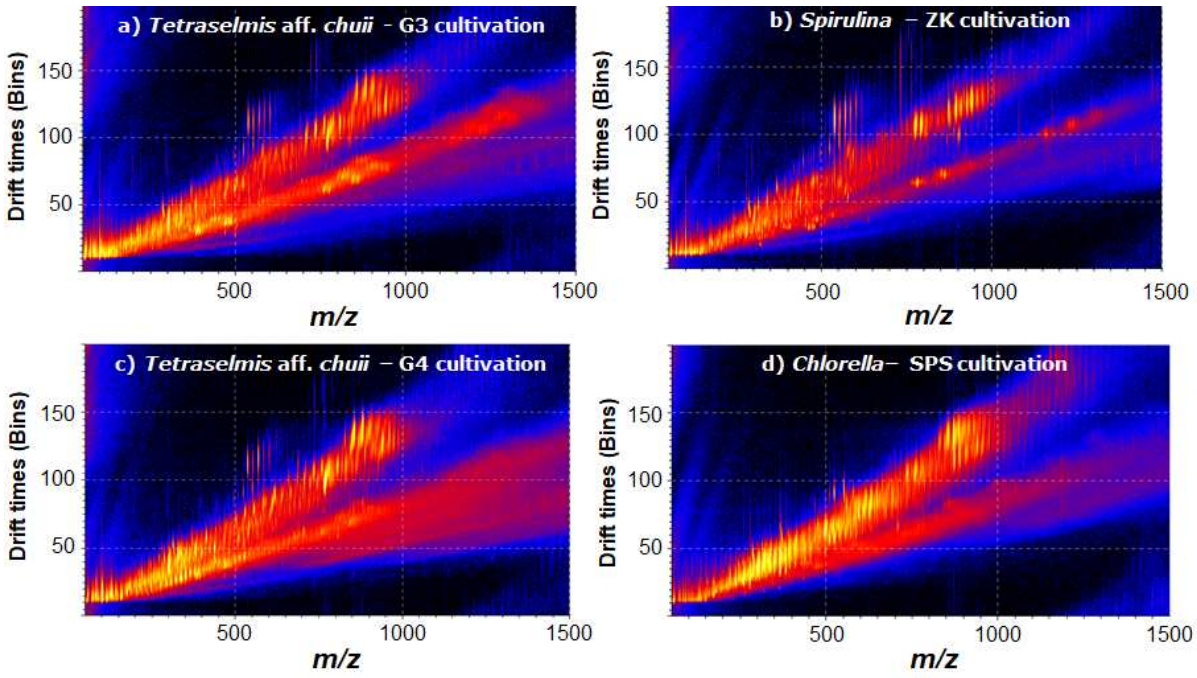

FIGURE 3. Representative two-dimensional drift time *versus m/z* for the samples extracts of **a)** TG3; **b)** SPIZK, **c)** TG4 and **d)** CHLOSPS.

Note that, in fact, there are classes of compounds that separate through different tendencies of drift time, even if they are overlapped in the same *m/z* range. The visualization of the differences in the profiles of each algae is, therefore, more evident. This approach allows the lipid profile screening in the sample. For example, for the investigation of the TAG content in a lipid extract, since this class of compounds will be distributed within a certain *m/z* range, (which, however, may be superimposed with several other classes of lipids and metabolites, making difficult the detection of this class), and distributed in a tendency of characteristic drift times, for a given experimental condition. Therefore, this approach provides a rapid response to decision-making in algae culture studies, or even to interrupt or continue processes in algae biorefineries.

The principal ions distributed in characteristics mobility tendencies can also be further characterized by their MS/MS spectrum, and identified by comparison with databases like LIPID MAPS. [96] Figure S33 shows an example of MS/MS of an isolated ion with a nominal *m/z* 885.7 from sample "DUNDEF_CHCL3" identified by its exact mass and fragments as a triacylglycerol TG(18:1_18:1_18:1), plus several other overlapped isomers distinguished by their fragments, indicating how complex the algae extracts in fact are.

High-throughput lipids and metabolites identification by UPLC-HDMS^E

Carry out a comprehensive characterization of the different components present in samples by manually interpreting MS/MS spectra obtained by DI-ESI-TWIM-MS of the extracts is laborious and time consuming due to the ultimate complexity of the samples that present different classes of lipids, besides other metabolites. For this, a second approach by UPLC-HDMS^E technique was used to analyze the lipids and metabolites of samples. Thus, in addition to the exact mass data for precursor ions and fragments, CCS data are also obtained for the precursor ion by calibration using substances whose CCS is known, thereby increasing data selectivity. Moreover, adding one more intrinsic physical-chemical ion property such as the CCS, significantly increases the confidence of metabolite/lipid identification.[99] One of the most common calibrants for CCS values is a solution of poly-DL-alanine, whose singly charged oligomers already have their CCS values well determined in nitrogen as drift gas.

Each chromatographic run, together with the MS, MS/MS and IMS spectra associated to it, was imported to Progenesis QI software, which, through the comparison with the LIPIDMAPS, HMDB, and a search engine with a CCS database provided by Waters – MetaScope - performs the identification by theoretical /

experimental comparison of the precursors and fragments exact mass, isotope distribution, fragmentation profile (*in silico* fragmentation or known experimental fragmentation pathways) and CCS values. The combination of all these identification parameters results in an overall compound identification score for each identified compound.

From the 16 analyzed samples, all in the same conditions of analysis, 1251 different compounds were collectively identified, within an *m/z* error of 10 ppm for both precursor ion and fragments. Among these 1251 compounds: 1) only 158 could not be identified by their fragments; 2) 30 of them were also identified by their CCS, assuming a theoretical / experimental error of lower than 4%; 3) the isotope similarities were from 30.4 to 99.4, with an average of 82.1; 4) among the fragmented ions, the average fragmentation score was 41.9 (ranging from 1 to 99.4); and finally, 5) the identification score ranged from 30 to 59.1, with an average of 39.5. The identifications with the highest scores were accepted and described in the spreadsheet with the metabolomics and lipidomics description of this study, provided as supplementary material of this work. The number of compounds also identified by the CCS is relatively low (i.e. 30 compounds) limited by the database used as it is not as broad as the LIPID MAPS or the HMDB. Among these 1251 accepted compound identifications, 210 were identified exclusively as lipids and the others categorized as “other metabolites”. The lipids were also categorized into fatty acyls (FA), glycerolipids (GL), glycerophospholipids (GP), sphingolipids (SP), sterol lipids (ST), prenol lipids (PR), saccharolipids (SL) categories. Although TAG are glycerolipids, this class was categorized separately, as we are discussing and emphasizing its importance for biodiesel production.

From the normalized abundances of each deconvoluted compound identified per sample, several interpretations can be made. Figure 4 shows the lipidomics and metabolomics results interpretations for all the samples. Figure 4a shows the sum of the normalized abundance for each class of lipids and other metabolites, and Figure 4b shows only the normalized abundances for different lipid classes in the samples. Figure 4c shows the percentage abundance of compounds identified as lipids and as other metabolites, and Figure 4d shows the percentage abundance of lipid classes distributed in each sample.

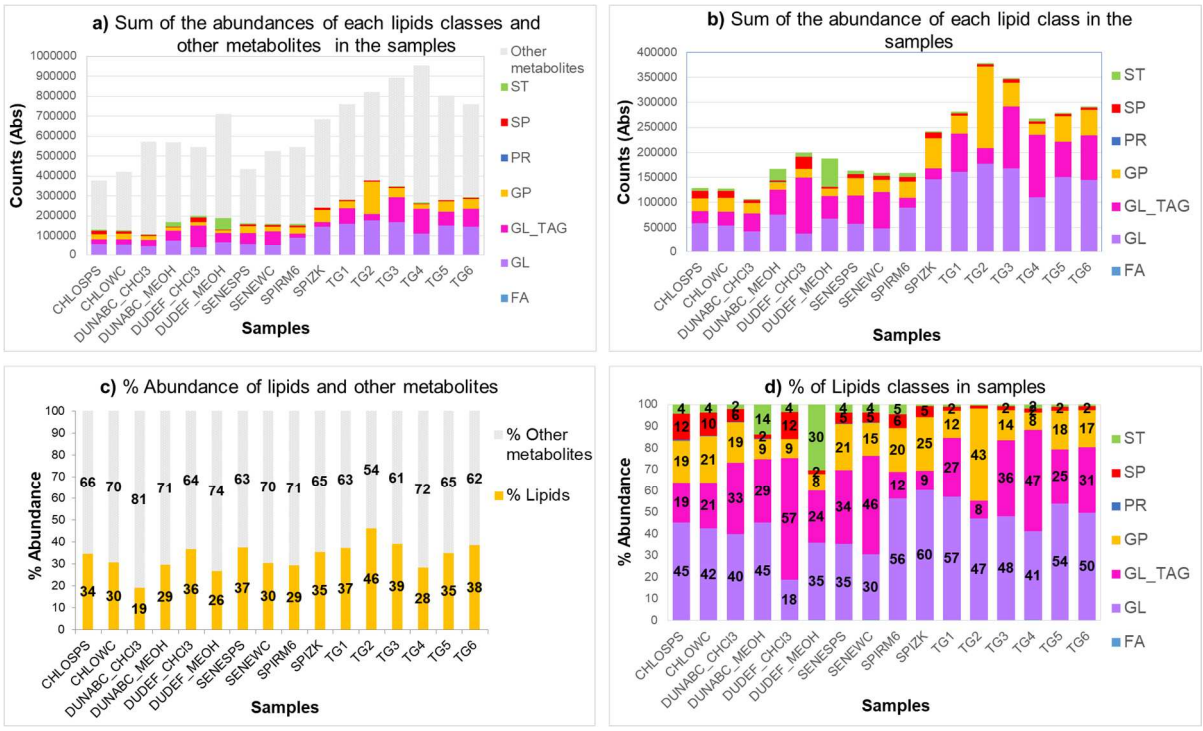

FIGURE 4. a) Sum of the normalized abundances of each lipids classes and other metabolites identified in the samples; a) sum of the normalized abundance of each lipid class identified in the samples; c) Relative abundance of lipids and metabolites for each sample; d) Relative distribution of lipid classes in each sample. Legends: fatty acyls (FA), glycerolipids (GL), glycerophospholipids (GP), sphingolipids (SP), sterol lipids (ST), prenol lipids (PR), saccharolipids (SL).

The results presented in the Figure 4 are not quantitative, meaning that they cannot be considered as a “weight by weight %” measurement in the sample extracts, because not all the reported compounds have the same ionization behavior, which implies that they have different response factors. Moreover, none lipidomics or metabolomics data covers 100% of the compounds that are indeed present in the samples. It is expected that several other compounds remained undetected and/or unidentified. And in fact, as recently reported by Dorrestein and co-workers [82] in a recent metabolomics study of algae and cyanobacteria, approximately 86% of the metabolomics signals detected were not found in other available datasets, concluding that even using a very diverse datasets, algae and cyanobacteria have unique features and families of metabolites that are still uncharacterized. However, the normalized abundance of each class of known compounds is a very suitable way to perform a detailed screening about the algae biomass composition and to understand how different processes may be affecting algae composition.

Figures 4a and 4c points out that the abundance of compounds identified as metabolites is higher than the compounds identified as lipids, as indeed expected, as the number of potential metabolites is indeed much higher than the number of compounds of the lipid class. The sample with the highest abundance of lipids was the sample TG2 (Fig 4c), mainly distributed between GL (excepting GL_TAG – that is highlighted separately) and GP. The sample with the highest % of GL_TAG was DUNDEF_CHCl3 (Fig. 4d), but when comparing the sum of the normalized abundance (Fig. 4b), It can be noted also that the samples DUDEF_CHL3, TG3 and TG4 were the ones presenting the highest abundances of compounds identified as TAGs. It indicates that they would – at least in theory – provide better yields for the

biodiesel production, if it was a real case of a study of algae prospecting for biodiesel production.

The detection of some metabolites and ST compounds may have important implications when algae biomass is used for nutraceutical products. When the untargeted approach detects toxins or sterols compounds (i.e. testosterone), or other classes of biologically active compounds, it is important to state at this point that further studies must be conducted, and these compounds must be characterized using targeted analysis to confirm the primary assumption of the untargeted analysis.

Another approach that may assist in comparing the lipid profile of algal samples is the binary comparison of drift time x *m/z* spectra through the HDMS compare software. In this approach, the ion mobility spectra are superimposed, highlighting the classes of compounds that are more abundant in each sample, generating a map in which each sample is marked with a color. Figure 5 shows the comparison of the spectra of TG3 and a blend of commercial vegetable oils (a mixture of soybean, corn, rapeseed, sunflower and olive oils in even proportions). It can be seen that the results converge with the results obtained through the lipid analysis shown in Fig. 4, and clearly the TAG abundance in sample TG3 are superimposed with the TAGs of the vegetable oil blend, as shown in the insert of Figure 5. Another binary comparison of samples TG4 and SPIKZ is shown in Figure S34, being evident the differences in their drift plots which are also confirmed by the results shown in Figure 4, in which among all samples SPIKZ had the lowest abundance of TAG, and in fact the TAG region for SPIZK is much less abundant if compared to sample TG4 (Figure S34).

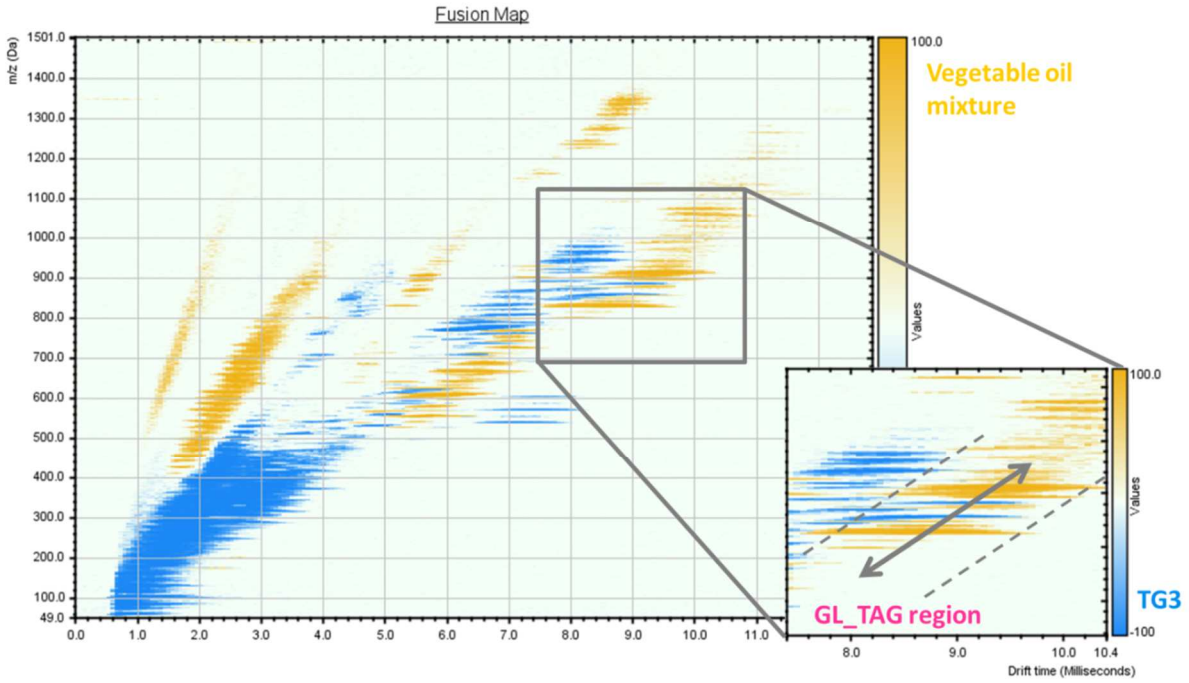

FIGURE 5. Fusion map comparing the "DT *versus* m/z" spectrum of sample TG3 and a blend of commercial edible oils obtained with the DI-TWIM-MS approach, highlighting the insert, that zooms the superimposed drift time regions for GL_TAG class in both samples.

In fact, the DI-TWIM-MS data really converge with the CCS values determined by UPLC-HDMS^E. Comparing the drift time *versus m/z* plot for a sample obtained by the DI approach with the plot of all the experimental CCS values *versus m/z* measured for all identified compounds, we can observe the same drift time tendencies showing up in both cases. To illustrate that, Figure 6 shows a comparison of the TG3 sample drift time plot, and the experimental CCS values determined for all the 1251 identified compounds. We can highlight at least 4 different areas: I – a low abundance very separated tendency, probably minor metabolites; II – the compounds identified as TAGs, mainly from *m/z* 700 – 1000 and slightly higher CCS values; III – a very busy region with several superimposed lipids and other

metabolites; and IV – also a low abundant separated tendency. We can also observe in what regions the lipid classes tend to appear, which is helpful to detect misleading identification if some of them appear in a very distinct region. It can also help to choose classes of compounds and take a closer look at their identification. It is worth noting also that the separation of distinct tendencies in the sample TG3 are more evident because not all of the 1251 compounds are present in sample TG3. The use of more polarizable drift gasses such as CO_2 has been proven to be an alternative to increase the selectivity and classes separations in complex mixtures such as crude oil, and it could also be helpful in this case. [91]

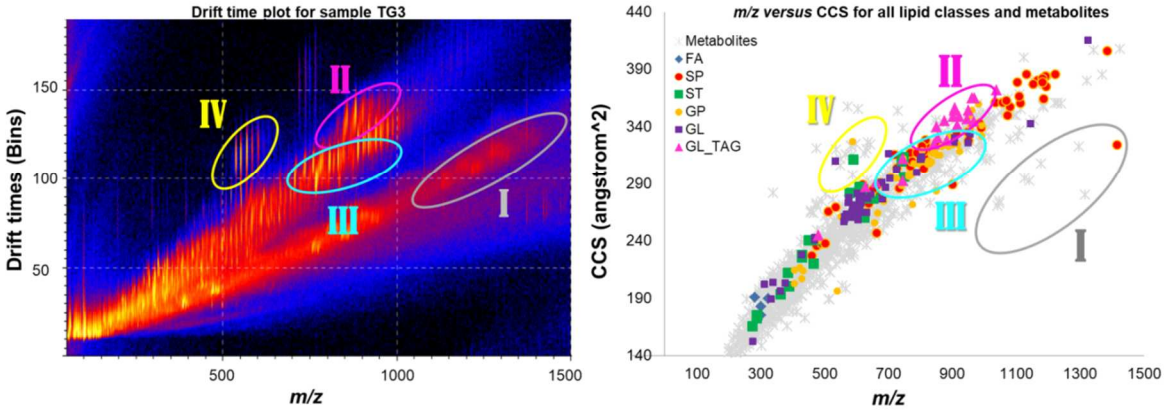

FIGURE 6. Comparison of the two dimensional drift time *versus m/z* plot for sample TG3 with the collision cross sections experimentally determined by UPLC-HDMS^E for all the 1251 compounds, highlighting the areas I, II, III and IV that could be detected in both plots.

On the other hand, databases of CCS values in CO_2 or CCS calibrants (such as poly-d-alanine) values in this gas are not yet available, as the determination of this parameter in CO_2 is much more complex.[100] However, if only the separation of classes of different compounds are needed, and no CCS values must be determined,

the use of CO_2 can be a good alternative to better detect different classes of lipids and metabolites in complex mixtures such as microalgae extracts.

Additional TAGs confirmation was made by comparing the experimental data of measured CCS values with the ones available in the recently released CCS data base, LipidsCCS, [98] and the results are shown in Table S1. Both the measured and the LipidsCCS theoretical values were determined in N_2, as drift gas, so they are comparable. Only two compounds identified as TAG had no theoretical CCS value available in LipidCCS dataset, which were TG(10:0_8:0_8:0) and TG(21:0_22:6_22:6). For the other TAGs, the experimental *versus* theoretical CCS error was mostly bellow to 10%, with 6.7% average. The experimental values tended to be around 20 Å^2 positively biased, that is, 20 Å^2 on average larger than the theoretical values. Even though the experimental data presented this minor systematic error, which probably comes from the Synapt G2-S*i* CCS calibration with poly-d-alanine step, the CCS were mostly in accordance with LipidCCS data base, which shows that this parameter is actually very useful and helps further identification and confirmation of compounds.

All the approaches demonstrated here have the potential to be applied as methodologies for lipids and metabolites screening in real cases of microalgae prospecting and can be implemented as routine both for research and in microalgae biorefineries.

CONCLUSIONS

This work has demonstrated that the technique of ion mobility mass spectrometry allowed obtaining a fast profile of microalgae extracts, in which the new dimension of ion mobility separation helps the visualization of distinct classes of

compounds, especially for the triacylglycerol class. The variability of the lipids in the algae is incredibly high and sensitive to the cultivation parameters, but the statistical classification among the samples indicated that the main parameter that influences the composition of the extracts is the genus of the algae. Genus seems therefore to be an initial variable to be considered in a study of algae prospecting for a specific biotechnological application. For example, after defining the best genera, the culture medium and cultivation conditions could be studied and optimized.

Statistical or binary comparison of the samples drift time plots spectra can be very useful, especially for comparison with reference samples, that is, microalgae that have been already shown to be suitable for a particular application, or whose lipid profile has already been characterized. It is a simple and fast approach and provides a good response for an initial profiling of a given set of samples.

However, through the DI-ESI-TIWIM-MS approach of the extracts, carrying out the comprehensive identification of all the ions of the samples is laborious. The high level of complexity of the samples requires a more powerful methodology to perform a more global and detailed sample screening. For this, the UPLC-HDMS^E technique was used to tentatively identify over 1200 compounds collectively in the 16 samples, based on intrinsic parameters of the detected ions (exact mass, fragmentation pattern, isotope distribution and CCS). More than 200 were identified as lipids of several classes. Among the 16 samples evaluated in this study, *Tetraselmis* aff*. chuii*, cultivated in F/2 medium plus fertilizers for 12 (TG3) and 16 days (TG4), as well as biomass of *Dunaliella salina* produced in reduced Shaish medium and extracted with $CHCl_3$ (DUDEF_CHL3), were the ones with the highest TAGs abundances. For sure, the methodologies explored in this work can be applied to algae biorefineries to predict whether some specific algae will be viable for

biodiesel production or for other biotechnology applications, as well as help in studies of microalgae cultivation improvements.

AKNOWLEDGEMENTS

We thank the State of São Paulo Research Foundation (FAPESP), State of Rio de Janeiro Research Foundation (FAPERJ), the Brazilian National Council for Scientific and Technological Development (CNPq) and the Financing Agency of Studies and Projects (FINEP) for financial assistance. We gratefully acknowledge Waters Brazil managers for opening their demo laboratory (Barueri, Brazil) to run the UPLC-HDMS^E experiments. We also thank the National Institute of Technology for microalgae biomasses donation and the referees of this work to contribute for its quality improvement.

REFERENCES

(1) Raven, J. A.; Giordano, M. Algae, *Current Biology*, **2014**, *24(13)*, R590–R595.

(2) Nigel, D. H.; Lloyd, D. T.; Canvin, D. A. Culver Photosynthesis and Photorespiration in Algae, *Plant Physiology*, **1977**, *59 (5)*, 936–940.

(3) Pedersen, O.; Colmer, T.D.; Sand-Jensen, K. Underwater Photosynthesis of Submerged Plants – Recent Advances and Methods, *Frontiers in Plant Science*, **2013**, *4*, 1–19.

(4) Bhattacharya, D.; Medlin, L. Algal Phylogeny and the Origin of Land Plants, Plant Physiology, **1998**, *116 (1)*, 9–15.

(5) Radmer, R. J. Algal Diversity and Commercial Algal Products, *BioScience*, **1996**, *46*, 263–270.

(6) Fasciotti, M. Perspectives for the use of biotechnology in green chemistry applied to biopolymers, fuels and organic synthesis: from concepts to a critical point of view, *Sustainable Chemistry and Pharmacy*, **2017**, *6*, 82–89.

(7) Cuellar-Bermudez, S. P.; Garcia-Perez, J. S.; Rittmann, B. E.; Parra-Saldivar, R. Photosynthetic bioenergy utilizing CO_2: an approach on flue gases utilization for third generation biofuels, *Journal of Cleaner Production*, **2015**, *98*, 53–65.

(8) Maity, J.P.; Bundschuh, J.; Chen, C.-Y.; Bhattacharya, P. Microalgae for third generation biofuel production, mitigation of greenhouse gas emissions and wastewater treatment: Present and future perspectives – A mini review, *Energy*, **2014**, **78**, 104–113.

(9) Lü J.; Sheahan C.; Sheahan, C.; Fu, P. Metabolic engineering of algae for fourth generation biofuels production, *Energy & Environmental Science*, **2011**, *4*, 2451–2466.

(10) Alam, F.; Mobin, S.; Chowdhury, H. Third Generation Biofuel from Algae, *Procedia Engineering*, **2015**, *105* , 763–768.

(11) Singh, A.; Nigam, P. S.; Murphy, J.D. Renewable fuels from algae: An answer to debatable land based fuels, *Bioresource Technology*, **2011**, *102 (1)*, 10–16.

(12) Scott, S. A.; Davey, M. P.; Dennis, J. S.; Horst, I.; Howe, C. J.; Lea-Smith, D.J.; Smith, A. G. Biodiesel from algae: challenges and prospects, *Current Opinion in Biotechnology*, **2010**, *21 (3)*, 277–286.

(13) Giordano, M.; Wang Q.; Microalgae for Industrial Purposes. In: Vaz Jr. S. (eds) *Biomass and Green Chemistry*, **2018**, Springer, Cham.

(14) Sun, X.; Wang, C.; Li, Z.; Wang, W.; Tong, Y. Wei, J. Microalgal cultivation in wastewater from the fermentation effluent in riboflavin (B2) manufacturing for biodiesel production, *Bioresource Technolgy*, **2013**, *143*, 499–504.

(15) Miazek, K.; Kratky, L.; Sulc, R., *et al.* Effect of Organic Solvents on Microalgae Growth, Metabolism and Industrial Bioproduct Extraction: A Review. *International Journal of Molecular Sciences*, **2017**, *18(7)*, 1429 (1-31).

(16) Ramanna, L.; Guldhe, A.; Rawat, I.; Bux, F. The optimization of biomass and lipid yields of Chlorella sorokiniana when using wastewater supplemented with different nitrogen sources. *Bioresource Technology*, **2014**, *168*, 127–135.

(17) Cuellar-Bermudez, S. P. *et al.* Nutrients utilization and contaminants removal. A review of two approaches of algae and cyanobacteria in wastewater, *Algal Research*, **2017**, *24*, 438–449.

(18) Kligerman, D.C.; Bouwer. E. J. Prospects for biodiesel production from algae-based wastewater treatment in Brazil: A review. *Renewable and Sustainable Energy Reviews,* **2015**, *52*, 1834–1846.

(19) Delrue, F.; Álvarez-Díaz, P. D.; Fon-Sing, S.; Fleury, G.; Sassi, J.-F. The environmental biorefinery: Using microalgae to remediate wastewater, a win-win paradigm. *Energies,* **2016**, *9*, 132.

(20) Kruse, O.; Hankamer, B. Microalgal hydrogen production. *Current Trends in Biotechnology*, **2010**, *21*, 238–243.

(21) Yang, J.; Xian M, Su S, *et al.* Enhancing Production of Bio-Isoprene Using Hybrid MVA Pathway and Isoprene Synthase in E. coli. Williams, *PLoS ONE,* **2012**, 7(4), e33509.

(22)John, R. P.; Anisha, G.S.; Nampoothiri, K. M.; Pandey, A.; Micro and macroalgal biomass: A renewable source for bioethanol, *Bioresource Technology*, **2011**, *102(1)*, 186–193.

(23) Kim, N.-J.; Li, H.; Jung, K.; Chang, H. N.; Lee, P. C. Ethanol production from marine algal hydrolysates using Escherichia coli KO11, *Bioresource Technology*, **2011**, *102(16)*, 7466–7469.

(24) Astumi, S.; Can, A. F.; Connor, M. R. *et al.*, Metabolic Engineering of Escherichia coli for 1-butanol production, *Metab. Eng.*, **2008**, *10*, 305–311.

(25) Atsumi, S.; Higashide, W.; Liao J. C.; Direct photosynthetic recycling of carbon dioxide to isobutyraldehyde, *Nature Biotechnology*, **2009**, *27*, 1177–1180.

(26) Beer, L. L.; Boyd, E. S.; Peters, J. W.; Posewitz, M. C. Engineering algae for biohydrogen and biofuel production, *Current Opinion in Biotechnology,* **2009**, *20*, 264–271.

(27) Mata, T. M.; Martins, A. A.; Caetano, N. S.; Microalgae for biodiesel production and other applications: A review. *Renewable and Sustainable Energy Reviews*, **2010**, *14(1)*, 217–232.

(28) Chisti, Y. Biodiesel from microalgae beats bioethanol. *Trends in Biotechnology*, **2008**, 26 (3), 126–131.

(29) Kerkhoven, E. J.; Pomraning, K. R.; Baker, S. E.; Nielsen, J. Regulation of amino-acid metabolism controls flux to lipid accumulation in Yarrowia lipolytica. *npj Systems Biology and Applications*, **2016**, *2*, 16005.

(30) Tuchman, N.; Schollett, M.; Rier, S. & Geddes, P. Differential Heterotrophic Utilization of Organic Compounds by Diatoms and Bacteria under Light and Dark Conditions. Hydrobiologia, **2006**, *561*, 167–177.

(31) Boroda, A.; Aizdaicher, N.; Odintsova, N.; The influence of ultra-low temperatures on marine microalgal cells, *Journal of Applied Phycology,* **2014**, *26*, 387–397.

(32) Ma, N.-L.; Aziz, A.; Teh, K.-Y.; Lam S. S.; Cha T.-S.; Metabolites Re-programming and Physiological Changes Induced in *Scenedesmus regularis* under Nitrate Treatment, *Nature Scientific Reports*, **2018**, *8*, 9746. DOI:10.1038/s41598-018-27894-0

(33) Markou, G.; Nerantzis, E. Microalgae for high-value compounds and biofuels production: A review with focus on cultivation under stress conditions. *Biotechnology Advances*, **2013**, *31*, 1532–1542.

(34) Michael A. Borowitzka, Commercial production of microalgae: ponds, tanks, and fermenters, *Progress in Industrial Microbiology*, **1999**, 35, 313–321.

(35) Brennan, L.; Owende, P. Biofuels from microalgae — A review of technologies for production, processing, and extractions of biofuels and co-products, *Renewable and Sustainable Energy Reviews*, **2010**, *14 (2)*, 557–577.

(36) Carvalho A.P.; Meireles, L. A.; Malcata, F. X. Microalgal Reactors: A Review of Enclosed System Designs and Performances, *Biotechnology Progress* , **2006**, *22(6)*, 1490–1506.

(37) Sharma, A. K.; Sahoo, P. K.; Singhal, S.; Joshi, G. Exploration of upstream and downstream process for microwave assisted sustainable biodiesel production from microalgae *Chlorella vulgaris*, *Bioresource Technology*, **2016,** *216*, 793–800.

(38) V. Ashokkumar, Zainal Salam, Palanivel Sathishkumar, Tony Hadibarata, Abdull Rahim Mohd Yusoff, Farid Nasir Ani, Exploration of fast growing *Botryococcus sudeticus* for upstream and downstream process in sustainable biofuels production, *Journal of Cleaner Production*, **2015**, *92*, 162–167.

(39) Lieve, M.L.; Laurens, S. V.; Wychen, J. P.; McAllister, S. A., Dempster, T. A.; McGowen, J.; Pienkos, P.T. Strain, biochemistry, and cultivation-dependent measurement variability of algal biomass composition, *Analytical Biochemistry*, **2014**, *452*, 86–95.

(40) Singh, S.; Kate, B. N.; Banerjee, U. C. Bioactive Compounds from Cyanobacteria and Microalgae: An Overview. *Critical Reviews in Biotechnology*, **2005**, *25*, 73–95.

(41) Sinéad. L.; Paul, R.R.; Catherine, S. Marine bioactives as functional food ingredients: potential to reduce the incidence of chronic diseases, *Marine Drugs*, **2011**, *9(6)*,1056–1100.

(42) Spolaore, P.; Joannis-Cassan, C.; Duran, E.; Isambert, A. Commercial applications of microalgae, *J Biosci Bioeng*, **2006**, *101(2)*, 87–96.

(43) Slocombe, S. P.; Zhang, Q.; Ross, M.; Anderson, A.; Thomas, N. J.; Lapresa, A.; Rad-Menéndez, C.; Campbell, C. N.; Black, K. D.; Stanley M. S.; Day. J. G. Unlocking nature's treasure-chest: screening for oleaginous algae. *Nature Scientific Reports*, **2015**, *9844*, 1–17.

(44) Pollesello, P.; Toffanin, R.; Murano, E.; Paoletti, S.; Rizzo, R.; Kvam, B. J. Lipid extracts from different algal species: ^{1}H and ^{13}C-NMR spectroscopic studies as a new tool to screen differences in the composition of fatty acids, sterols and carotenoids, *Journal of Applied Phycology,* **1992**, *4*, 315–322.

(45) Sarpal, A. S.; Silva, P. R. M.; Martins, J. L.; Amaral, J. J.; Monnerat, M. M.;. Cunha, V. S.; Daroda, R. J.; de Souza, W. Biodiesel Potential of Oleaginous Yeast Biomass by NMR Spectroscopic Techniques, *Energy Fuels*, **2014**, *28(6)*, 3766–3777.

(46) Dean, A. P.; Sigee, D. C.; Estrada, B.; Pittman, J. K.; Using FTIR spectroscopy for rapid determination of lipid accumulation in response to nitrogen limitation in freshwater microalgae. *Bioresource Technology* , **2010**, *101*, 4499–4507.

(47) Pavel Pořízka, *et. al.* Algal Biomass Analysis by Laser-Based Analytical Techniques—A Review, *Sensors (Basel)*, 2014,*14(9)*, 17725–17752.

(48) Sarpal, A.S.; Teixeira, C.M.; Silva, P.R.; Lima, G. M.; Silva S.R.; Monteiro, T.V.; Cunha, V.S.; Daroda, R.J. Determination of lipid content of oleaginous microalgal biomass by NMR spectroscopic and GC-MS techniques, *Analytical and Bioanalytical Chemistry* **2015**, *407(13)*,3799–3816.

(49) Chopra, A.; Tewari, A. K.; Vatsala, S.; Kumar, R.; Sarpal, A. S.; Basu, B. Determination of Polyunsaturated Fatty Esters (PUFA) in Biodiesel by GC/GC–MS and 1H-NMR Techniques, *Journal of the American Oil Chemists' Society*, **2011**, *88*, 1285–1296.

(50) Collard, F.; Blin, J. A review on pyrolysis of biomass constituents: Mechanisms and composition of the products obtained from the conversion of cellulose, hemicelluloses and lignin, *Renewable and Sustainable Energy Reviews*, **2014**, *38*, 594–608.

(51) Lawrence, J. F.; Niedzwiadek, B.; Menard, C.; Lau, B. P.Y.; Lewis, D.; Kuper-Goodman, T.; Carbone, S.; Holmes, C. Comparison of Liquid Chromatography/Mass Spectrometry, ELISA, and Phosphatase Assay for the Determination of Microcystins in Blue-Green Algae Products, *Journal of AOAC International*, **2001**, 84, 1035–1044.

(52) S.; Bogialli, M.; Bruno, R.; Curini, A.; Di Corcia, C.; Fanali, A. Laganà, Monitoring Algal Toxins in Lake Water by Liquid Chromatography Tandem Mass Spectrometry *Environ. Sci. Technol.*, **2006**, *40 (9)*, 2917–2923.

(53) Beltrán, E.; Ibáñez, M.; Sancho, J. V.; Hernández, F. Determination of six microcystins and nodularin in surface and drinking waters by on-line solid phase extraction–ultra high pressure liquid chromatography tandem mass spectrometry, *Journal of Chromatography A*, **2012**, *1266*, 61–68.

(54) Krishnamurthy, T.; Szafraniec, L.; Hunt, D. F.; Shabanowitz, J.; Yates 3rd, J. R.; Hauer, C. R.; Carmichael, W. W.; Skulberg, O.; Codd, G. A.; Missler S.; Structural characterization of toxic cyclic peptides from blue-green algae by tandem mass spectrometry PNAS, **1989**, *86 (3)*, 770–774.

(55) Sun, M.-M.; Sun, J.; Qiu, J.-W.; Jing, H.; Liu, H. Characterization of the proteomic profiles of the brown tide alga Aureoumbra lagunensis under phosphate- and nitrogen-limiting conditions and of its phosphate limitation-specific protein with

alkaline phosphatase activity, *Applied and environmental microbiology*, **2012**, *78(6)*, 2025–33.

(56) Lee, H.-W.; Roh, S.W.; Cho, K.; Kim, K.-N. ; Cha, I.-T.; Yim, K. J.; Song, H. S.; Nam, Y.-D.; Oda, T. ; Chung, Y.-H. ; Kim, S. J.; Choi, J.-S.; Kim, D., Phylogenetic analysis of microalgae based on highly abundant proteins using mass spectrometry, *Talanta*, **2015**, *132*, 630–634.

(57) Khan, A.; Eikani, C. K.; Khan, H.; Iavarone, A.T.; Pesavento, J. J. Characterization of Chlamydomonas reinhardtii Core Histones by Top-Down Mass Spectrometry Reveals Unique Algae-specific Variants and Post-translational Modifications, *Journal of proteome research*, **2017**, *17(1)*, 23–32.

(58) Dahlmann, J.; Budakowski, W. R.; Luckas, B. Liquid chromatography electrospray ionisation-mass spectrometry based method for the simultaneous determination of algal and cyanobacterial toxins in phytoplankton from marine waters and lakes followed by tentative structural elucidation of microcystins, *Journal of Chromatography A*, **2003**, *994*, 45–57.

(59) Gerssen, A.; Mulder, P. P.J.; de Boer, J. Screening of lipophilic marine toxins in shellfish and algae: Development of a library using liquid chromatography coupled to orbitrap mass spectrometry, *Analytica Chimica Acta*, **2011**, *685 (2)*, 176–185.

(60) Lajeunesse, A.; Segura , P. A. ; Malorie, G.; Hudon , C. ; Thomas , K.; Quilliam, M. A. ; Gagnon, C. Detection and confirmation of saxitoxin analogues in freshwater benthic Lyngbya wollei algae collected in the St. Lawrence River (Canada) by liquid chromatography–tandem mass spectrometry, *Journal of chromatography*, **2012**, *1219*, 93–103.

(61) Zendong, Z.; McCarron, P.; Herrenknecht, C.; Sibat, M.; Amzil, Z.; Cole, R. B., Philipp Hess, High resolution mass spectrometry for quantitative analysis and untargeted screening of algal toxins in mussels and passive samplers, *Journal of Chromatography A*, **2015**, *1416*, 10–21.

(62) Klejdus, B.; Lojková, L.; Plaza, M.; Šnóblová, M.; Štěrbová, D. Hyphenated technique for the extraction and determination of isoflavones in algae: Ultrasound-assisted supercritical fluid extraction followed by fast chromatography with tandem mass spectrometry, *Journal of Chromatography A*, **2010**, *1217(51)*, 7956–7965.

(63) Jones, J.; Manning S.; Montoya, M.; Keller K.; Poenie, M.; Extraction of Algal Lipids and Their Analysis by HPLC and Mass Spectrometry, *Journal of the American Oil Chemist's Society*, **2012**, *89(8)*, 1371–1381.

(64) He, H.; Rodgers, R. P.; Marshall, A. G.; Hsu, C. S. Algae Polar Lipids Characterized by Online Liquid Chromatography Coupled with Hybrid Linear

Quadrupole, Ion Trap/Fourier Transform Ion Cyclotron Resonance Mass Spectrometry, *Energy & Fuels*, **2011**, *25(10)*, 4770–4775.

(65) Guschina, I. A.; Harwood, J. L. Lipids and lipid metabolism in eukaryotic algae, *Progress in Lipid Research*, **2006**, *45(2)*, 160–186.

(66) Danielewicz, M. A.; Anderson L. A.; Franz, A. K. Triacylglycerol profiling of marine microalgae by mass spectrometry, *The Journal of Lipid Research*, **2011**, *52(11)*, 2101–2108.

(67) MacDougall, K.M.; McNichol, J.;McGinn, P.J. *et al.* Triacylglycerol profiling of microalgae strains for biofuel feedstock by liquid chromatography–high-resolution mass spectrometry, *Analytical and Bioanalytical Chemistry*, **2011**, *401*, 2609–2616.

(68) Kind, T.; Meissen, J. K.; Yang, D.; Nocito, F.; Vaniya, A.; Cheng, Y.-S.; VanderGheynst, J. S.; Fiehn, O. Qualitative analysis of algal secretions with multiple mass spectrometric platforms, *Journal of Chromatography A*, **2012**, *1244*, 139–147.

(69) Akoto, L.; Stellaard, F.; Irth, H.; Vreuls, R. J.J.; Pel, R. Improved fatty acid detection in micro-algae and aquatic meiofauna species using a direct thermal desorption interface combined with comprehensive gas chromatography–time-of-flight mass spectrometry, *Journal of Chromatography A*, **2008**, *1186(1–2)*, 254–261.

(70) Řezanka, T.; Vokoun, J.; Slavíček, J.; Podojil, M.; Determination of fatty acids in algae by capillary gas chromatography—mass spectrometry, *Journal of Chromatography A*, **1983**, *268*, 71–78.

(71) Ross, M. M.; Neihof, R. A.; Campana, J. E. Direct fatty acid profiling of complex lipids in intact algae by fast-atom-bombardment mass spectrometry, *Analytica Chimica Acta*, **1986**, 18, 149–157.

(72) Samburova V.; Lemos M. S.; Hiibel S.; Hoekman S. K.; Cushman, J. C.; Zielinska, B. Analysis of Triacylglycerols and Free Fatty Acids in Algae Using Ultra-Performance Liquid Chromatography Mass Spectrometry, *Journal of the American Oil Chemist's, Society,* **2013**, *90(1),* 53–64.

(73) Řezanka, T., Vyhnálek, O.; Podojil, M. Identification of sterols and alcohols produced by green algae of the genera *Chlorella* and *Scenedesmus* by means of gas chromatography—mass spectrometry, *Folia Microbiol*, **1986**, 31:44. doi.org/10.1007/BF02928678

(74) Anastyuk, S. D.; Shevchenko, N. M.; Nazarenko, E. L.; Dmitrenok, P. S.; Zvyagintseva, T. N. Structural analysis of a fucoidan from the brown alga Fucus evanescens by MALDI-TOF and tandem ESI mass spectrometry, *Carbohydrate Research*, **2009**, *344 (6)*, 779-787.

(75) Anastyuk, S. D.; Shevchenko, N. M.; Eugene L. Nazarenko, Tatyana I. Imbs, Vladimir I. Gorbach, Pavel S. Dmitrenok, Tatyana N. Zvyagintseva, Structural analysis of a highly sulfated fucan from the brown alga Laminaria cichorioides by tandem MALDI and ESI mass spectrometry, *Carbohydrate Research*, **2010**, 345(15), 2206–2212.

(76) Han, J.; Calvin M. Hydrocarbon distribution of algae and bacteria, and microbiological activity in sediments, *PNAS*, **1969**, *64(2)*, 436–443.

(77) Barupal, D. K.; Kind, T.; Kothari, S. L.; Lee D. Y.; Fiehn, O. Hydrocarbon phenotyping of algal species using pyrolysis-gas chromatography mass spectrometry, *BMC Biotechnology*, **2010**, 10:40. doi.org/10.1186/1472-6750-10-40.

(78) Ma J.; Xiao R.; Li J.; Li J.; Shi B.; Liang Y.; Lu, W.; Chen, L. Headspace solid-phase microextraction with on-fiber derivatization for the determination of aldehydes in algae by gas chromatography–mass spectrometry, *Journal of Separation Science,* **2011***, 34(12)*, 1477–83.

(79) Klejdus, B.; Lojková, L.; Plaza, M.; Šnóblová, M.; Štěrbová, D.; Hyphenated technique for the extraction and determination of isoflavones in algae: Ultrasound-assisted supercritical fluid extraction followed by fast chromatography with tandem mass spectrometry, *Journal of Chromatography A*, **2010**, *1217(51)*, 7956–7965.

(80) Kadam, S.U.; Tiwari, B. K.; O'Donnell, C.P. Application of Novel Extraction Technologies for Bioactives from Marine Algae, Journal of Agricultural and Food Chemistry, **2013**, *61 (20)*, 4667–4675.

(81) Murugaiyan J.; Ahrholdt J. ; Kowbel V.; Roesler, U. Establishment of a matrix-assisted laser desorption ionization time-of-flight mass spectrometry database for rapid identification of infectious achlorophyllous green micro-algae of the genus Prototheca *Clinical Microbiology and Infection*, **2012**; *18*, 461–467.

(82) Luzzatto-Knaan , T.; Garg, N.; Wang, M.; Glukhov, E.; Peng, Y.; Ackermann, G.; Amir, A.; Duggan, B. M.; Ryazanov, S.; Gerwick, L.; Knight, R.; Alexandrov, T.; Bandeira, N.; Gerwick, W.H.; Dorrestein, P. C. Digitizing mass spectrometry data to explore the chemical diversity and distribution of marine cyanobacteria and algae, *eLife*, **2017**, *6*, e24214.

(83) Garg, N.; Kapono, C.; Lim, Y.W.; Koyama, N.; Vermeij, M. J.; Conrad, D.; Rohwer, F.; Dorrestein, P.C. Mass spectral similarity for untargeted metabolomics data analysis of complex mixtures, *International Journal of Mass Spectrometry*, **2015**, *377*, 719-727.

(84) Giles K.; Pringle, S.D.; Worthington, K.R.; Little, D.; Wildgoose J.L.; Bateman RH. Applications of a travelling wave-based radio-frequency-only stacked ring ion guide. *Rapid Communications in Mass Spectrometry*, **2004**, *18(20)*, 2401-2414.

(85) Paglia, G.; Astarita, G. Metabolomics and lipidomics using traveling-wave ion mobility mass spectrometry. *Nature Protocols*, **2017**, *12*, 797–813.

(86) Souza, G.H.M.F.; Guest, P.C.; Martins-de-Souza D. LC-MS(E), Multiplex MS/MS, Ion Mobility, and Label-Free Quantitation in Clinical Proteomics. Methods in Molecular Biology, **2017**, *1546*, 57–73.

(87) Kanu, A. B.; Dwivedi, P.; Tam, M.; Matz, L.; Hill Jr. H. H. Ion mobility mass spectrometry. *Journal of Mass Spectrometry*, **2008**, *43*, 1–22.

(88) Cumeras, R.; Figueras, E.; Davis, C. E.; Baumbach, J. I.; Gràcia, I. Review on Ion Mobility Spectrometry. Part 1: current instrumentation, *Analyst*, **2015**, 140, 1376–1390.

(89) Fasciotti, M.; Lalli, P. M.; Heerdt, G.; Steffen, R. A.; Corilo, Y. E.; Sá, G. F.; Daroda, R. J.; Reis, F. A. M.; Morgon, N. H.; Pereira, R. C. L.; Eberlin, M. N.; Klitzke, C. F. Structure-drift time relationships in ion mobility mass spectrometry, *International Journal for Ion Mobility Spectrometry*, **2013**, *1*, 1–16.

(90) Valentine, S. J.; Kulchania, M.; Barnes, C. A. S.; Clemmer, D. E. Multidimensional separations of complex peptide mixtures: a combined high-performance liquid chromatography/ion mobility/time-of-flight mass spectrometry approach, *International Journal of Mass Spectrometry*, **2001**, *212*, 97–109.

(91) A) Fasciotti, M.; Lalli, P. M.; Klitzke, C. F.; Corilo, Y. E.; Pudenzi, M. A.;. Pereira, R. C. L.; Bastos, W.; Daroda, R. J.; Eberlin, M. N. Petroleomics by Traveling Wave Ion Mobility–Mass Spectrometry Using CO_2 as a Drift Gas, *Energy & Fuels*, **2013**, *27 (12)*, 7277–7286; B) Santos, J. M.; Galaverna, R. S.; Pudenzi, M. A.; Schmidt, E. M.; Sanders, N. L.; Kurulugama, R. T.; Mordehai, A.; Stafford, G. C.; Wisniewski Jr, A.; Eberlin, M. N. Petroleomics by ion mobility mass spectrometry: resolution and characterization of contaminants and additives in crude oils and petrofuels, *Analytical Methods*, **2015**, *7*, 4450–4463.

(92) McCullagh, M.; Douce, D.; Van Hoeck, E.; Goscinny, S. Exploring the Complexity of Steviol Glycosides Analysis Using Ion Mobility Mass Spectrometry, *Analytical Chemistry*, **2018**, 90 (7), 4585–4595.

(93) Benigni, P.; Thompson, C. J.; M. E.; Ridgeway, M. A.; Park, Fernandez-Lima, F. Targeted High-Resolution Ion Mobility Separation Coupled to Ultrahigh-Resolution Mass Spectrometry of Endocrine Disruptors in Complex Mixtures, *Analytical Chemistry*, **2015**, *87(8)*, 4321–4325.

(94) Bligh, E. G.; Dyer, W. J. A rapid method of total lipid extraction and purification. *Canadian Journal of Biochemistry and Physiology*, **1959**, *37*, 911–917

(95) Sarpal, A. S., Costa, I. C. R., Teixeira, C. M. L. L., Filocomo, D., Candido R, et al. Investigation of Biodiesel Potential of Biomasses of Microalgaes Chlorella, Spirulina and Tetraselmis by NMR and GC-MS Techniques. Journal of Biotechnology and Biomaterials, **2016**, *6(1)*, doi:10.4172/2155-952X.1000220.

(96) The LIPID MAPS Lipidomics Gateway, http://www.lipidmaps.org.

(97) a) Wishart D. S., Tzur D. , Knox C, et al., HMDB: the Human Metabolome Database. Nucleic Acids Res. 2007Jan;35 (Database issue):D521-6. 17202168; b) Wishart DS, Knox C, Guo AC, et al., HMDB: a knowledgebase for the human metabolome. Nucleic Acids Res. 2009 37(Database issue):D603-610. 18953024; c) Wishart DS, Jewison T, Guo AC, Wilson M, Knox C, et al., HMDB 3.0 — The Human Metabolome Database in 2013. Nucleic Acids Res. 2013. Jan 1;41(D1):D801-7. 23161693; d) Wishart DS, Feunang YD, Marcu A, Guo AC, Liang K, et al., HMDB 4.0 — The Human Metabolome Database for 2018. Nucleic Acids Res. 2018. Jan 4;46(D1):D608-17.

(98) Zhou, Z.; Tu, J.; Xin, X.; Shen, X.; Zhu, Z.-J. LipidCCS: Prediction of Collision Cross-Section Values for Lipids with High Precision to Support Ion Mobility-Mass Spectrometry based Lipidomics, *Analytical Chemistry*, **2017**, *89*, 9559–9566.

(99) Zhou, Z.; Tu J.; Zhu, Z.-J. Advancing the large-scale CCS data base for metabolomics and lipidomics at the machine-learning era, *Current Opinion in Chemical Biology*, **2018**, *42*, 34–41.

(100) Smith, S. D. P.; Knapman, T. W.; Campuzano, I.; Malham, R. W.; Berryman, J. T.; Radford, S. E.; Ashcroft, A. E. Deciphering drift time measurements from travelling wave ion mobility spectrometry-mass spectrometry studies. *European Journal of Mass Spectrometry*, **2009**, *15*, 113–130.

2.3.1. Material suplementar

Supporting information

Article: "Microalgae biomass characterization using ion mobility-mass spectrometry"

Authors: Maíra Fasciotti[1,5]*, Gustavo H. M. F. Souza[2], Giuseppe Astarita[3], Ingrid C. R. Costa[1], Thays. V. C. Monteiro[1], Claudia M. L. L. Teixeira[4], Marcos N. Eberlin[5], Amarijt S. Sarpal[1]

[1] National Institute of Metrology, Quality and Technology (INMETRO), Division of Chemical Metrology, Laboratory of organic analysis, 25250-020, Duque de Caxias, RJ, Brazil

[2] MS Applications & Development Laboratory, Waters Corporation, Barueri, SP, Brazil;

[3] Department of Biochemistry and Molecular & Cellular Biology, Georgetown University, Washington, DC, USA;

[4] Laboratory of Microalgae Biotechnology, National Institute of Technology (INT), Rio de Janeiro, Rio de Janeiro, Brazil;

[5] ThoMSon Mass Spectrometry Laboratory, Institute of Chemistry, University of Campinas – UNICAMP, Campinas, SP, Brazil.

*corresponding author: M. Fasciotti, mfasciotti@inmetro.gov.br

1) Detailed cultivation conditions of each microalgae biomass:

Chlorella vulgaris (CCMA-UFSCar 012) and *Scenedesmus ecornis* (CCMA-UFSCar 088) were kindly provided by Prof Armando Vieira from Federal University of São Carlos and their isolates are kept in the collection of microalgae cultures of the Department of Botany, Federal University of São Carlos (CCMA-UFSCar, WDCM 835). *Tetraselmis* aff. *chuii* and *Arthrospira* (*Spirulina*) *platensis* were kindly provided by Prof Gleyci Moser from University of State of Rio de Janeiro and by Prof Sergio Lourenço from Fluminense Federal University, respectively. *Dunaliella salina* was collected and isolated by the group of the Laboratory of Microalgae Biotechnology and identified in collaboration with UFSCar, being deposited in this culture collection as CCMA-UFSCar 711. *Chlorella vulgaris* and *Scenedesmus ecornis* were maintained in modified WC (Guillard & Lorenzen, 1972), *Tetraselmis* aff. *chuii*, *Dunaliella salina* and

Arthrospira (*Spirulina*) *platensis* in F/2 (GUILLARD, 1975), Shaish et al (1992) and modified Zarrouk (George, 1976) media, respectively, in Erlenmeyer flasks with 300 mL, density of photonic flux around 135 $\mu E.m^{-2}.s^{-1}$ of white fluorescent light, and temperature of 25 ± 2 ºC, until the transferring to PET bottles or Erlenmeyer flasks. New cultures were prepared for each species using 10 % (v/v) of inoculums for a total volume of 4 L or of 300 mL (in the case of *C vulgaris*). In the cultivations in bottles, the air was used as source of CO_2, which was passed in the culture medium through air pumping at 3.0 L min^{-1}; in the case of cultivation in Erlenmeyer flasks, CO_2 from air was provided by agitation of the flasks which were maintained in an orbital shaker. The light source was fluorescent light, except in the case of *Dunaliella salina* cultivations where cool white LED were used in all cultivations and in the case of *Tetraselmis* aff. *chuii* where half of the cultivations were carried out with cool white LED and half with fluorescent light, in which: G1 and G2 culture medium F/2 and LED light, for 12 and 16 days of cultivation, respectively; G3 and G4 culture medium F/2 with fertilizers and LED light, for 12 and 16 days of cultivation, respectively; G5 e G6: fluorescent light, for 12 days, in culture medium F/2 and culture medium F/2 with fertilizers, respectively. In all cultivations photonic flux density was around 120-150 µmol photons m^{-2} s^{-1} except for *C. vulgaris* and *Dunaliella salina*, for which 300 and 200 µmol photons m^{-2} s^{-1} were used, respectively. Temperature was maintained at 25 ± 2 ℃, except for *Arthrospira* (*Spirulina*) *platensis* cultivation whose temperature was 32 ± 1 ℃.

WC, WC medium designated WCSPS (where P was replaced by superphosphate at 0.007 g L^{-1} and the source of nitrogen by Chilean saltpeter at 0.12 g.L-1), and medium designated WCSP (where P was replaced by superphosphate at 0.007 g L^{-1}) were used for *Chlorella vulgaris* cultivations. For *Tetraselmis* aff. *chuii* cultivations, were used Guillard F/2 and this same medium modified by replacement of the source of nitrate and phosphate with agricultural fertilizers in the same concentration of F/2 in terms of N and P; the source of nitrate was replaced by Chilean Saltpeter (Simple Mineral Fertilizer - VITAPLAN®) and phosphate source by Simple Superphosphate (Mineral Fertilizer - HERINGER®). RM6 modified by our group (data are being submitted to publication) and Zarrouk medium modified by George (1976) were used for *Arthrospira* (Spirulina) *platensis* cultivation; this RM6 modified medium is different from RM6 (Raoof et al. 2006) basically by the addition of microelements solution and $FeSO_4$. *Dunalilella salina* suspensions designated as ABC and DEF were cultivated in

Shaish medium (Shaish et al., 1992) and Shaish medium with reduced nitrate (by ten times), respectively. The cultures were monitored daily through cell count under a microscope (Olympus CX31) or by optical density readings (at 730 nm) in order to determine the growth phases. When the chosen growth phase was attained, the cultivation was interrupted and the cultures were centrifuged in a Rotixa 50RS centrifuge (Hettich) at 4 ºC and 3500 rpm for 10 minutes, except in the case of *Arthrospira* (*Spirulina*) *platensis* that was filtered in a filter screen (120-micron). In the case of *Tetraselmis* aff *chuii*, cultivation was interrupted in two different stages: at linear growth phase and at the final of this phase. The biomasses were collected and frozen. The frozen biomass was lyophilized in an Enterprise IID lyophilizer (Terroni). After lyophilization, the samples were kept in the refrigerator at -20 ºC to protect from degradation until analysis.

References for cultivation conditions:

George, E. A., (1976) Culture Centre of algae and protozoa. List of strains 1976, 3rd Edition. Inst. Terr. Ecol., Nat Environment Res. Counc., Cambridge, 120pp.

Guillard, R.R.L. (1975) Culture of phytoplankton for feeding marine invertebrates. Culture of Marine Invertebrates Animals. Plenum Publishing. p. 29–60.

Guillard, R.R.L., Lorenzen CJ (1972) Yellow-green algae with chlorophyllide c. J Phycol 8, p.10–14.

Raoof B., Kaushik B.D., Prasanna R. (2006): Formulation of a low-cost medium for mass production of *Spirulina*. Biomass and Bioenergy, 30, p. 537–542.

Shaish A, Ben-Amotz A.; Avron M. (1992). Biosynthesis of β-carotene in *Dunaliella*. Methods in Enzymology. 213, p. 439–444.

2) Direct infusion ESI(+)-QTOF (Synapt HDMS) mass spectra for all samples:

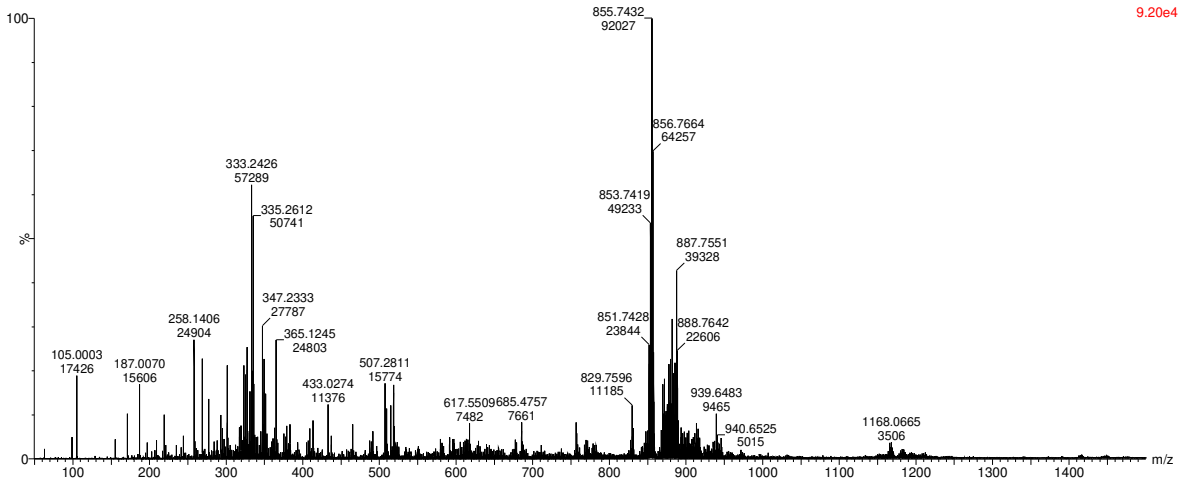

FIGURE S1. Direct infusion ESI(+)-QTOF mass spectrum for CHLOSPS.

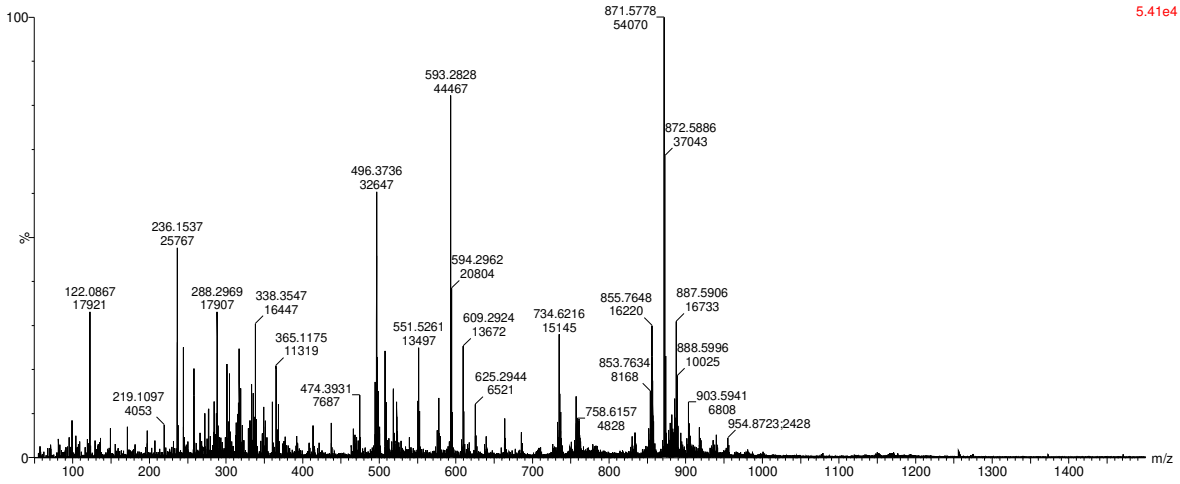

FIGURE S2. Direct infusion ESI(+)-QTOF mass spectrum for CHLOWC

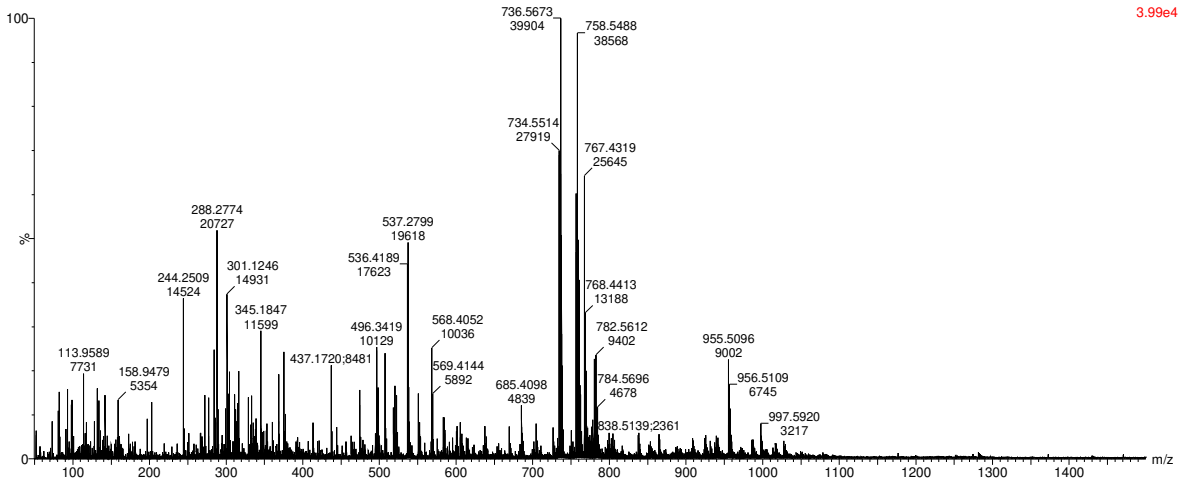

FIGURE S3. Direct infusion ESI(+)-QTOF mass spectrum for DUNABC_CHCl3

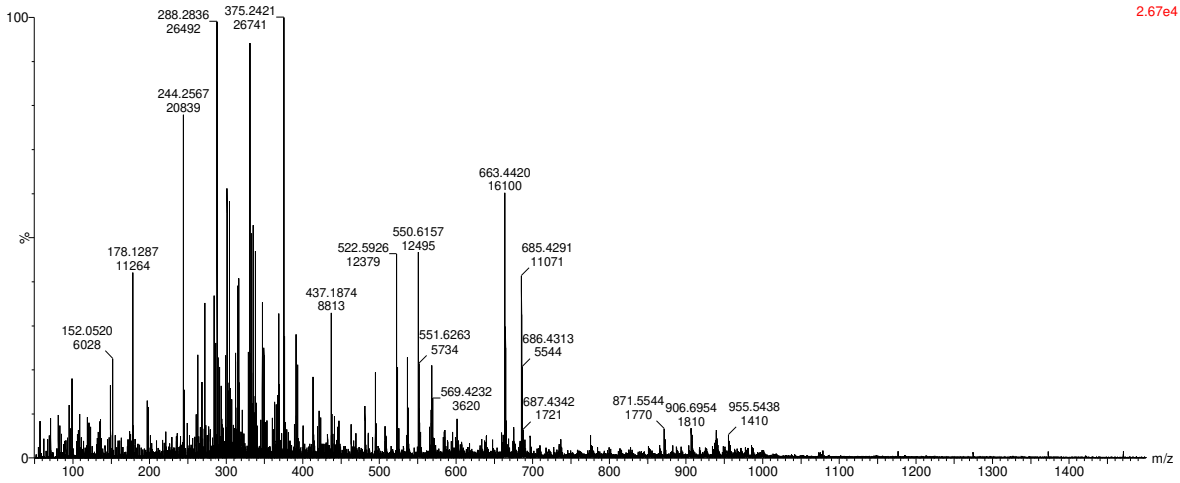

FIGURE S4. Direct infusion ESI(+)-QTOF mass spectrum for DUNABC_MEOH

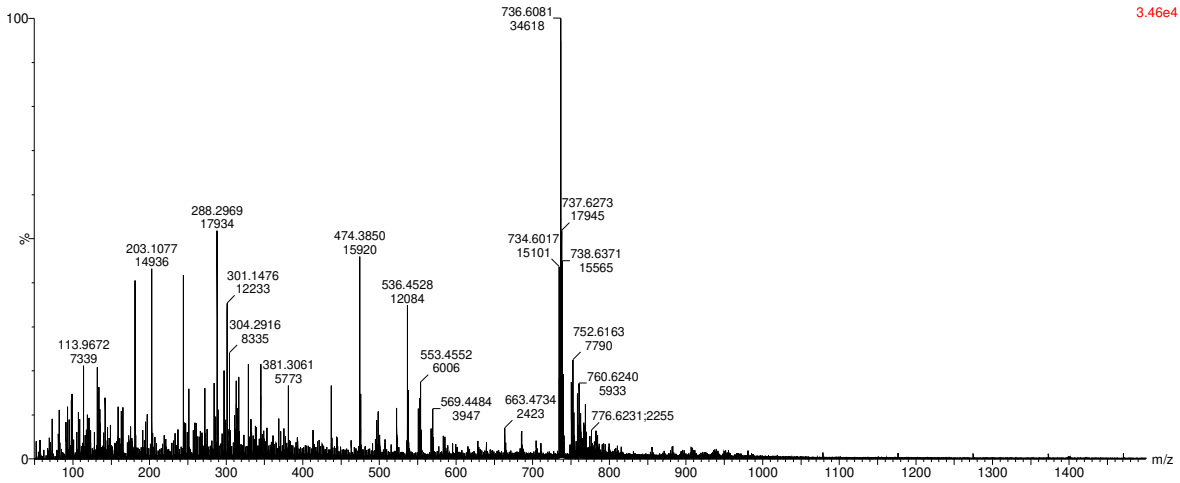

FIGURE S5. Direct infusion ESI(+)-QTOF mass spectrum for DUDEF_CHCl3

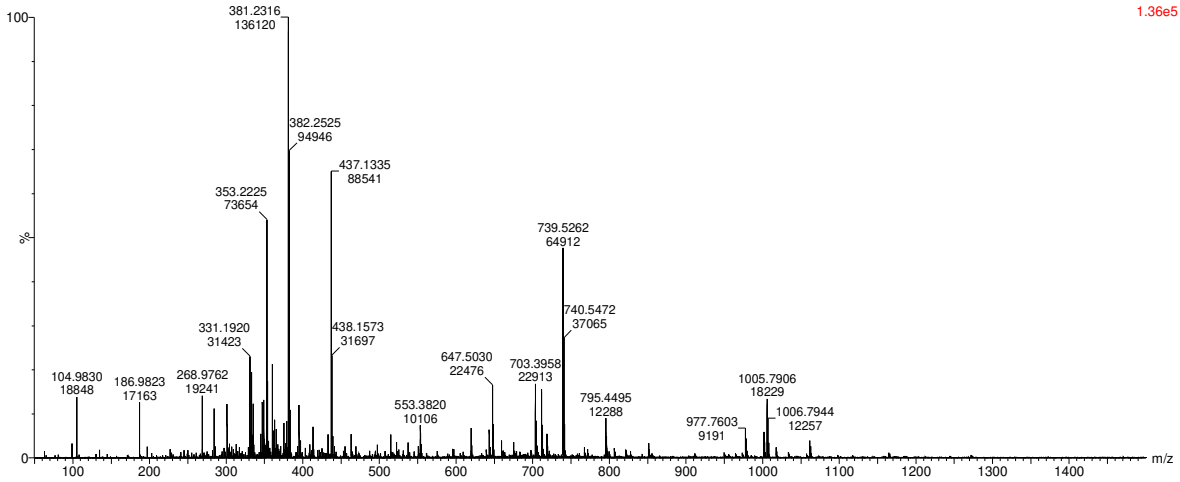

FIGURE S6. Direct infusion ESI(+)-QTOF mass spectrum for DUDEF_MEOH

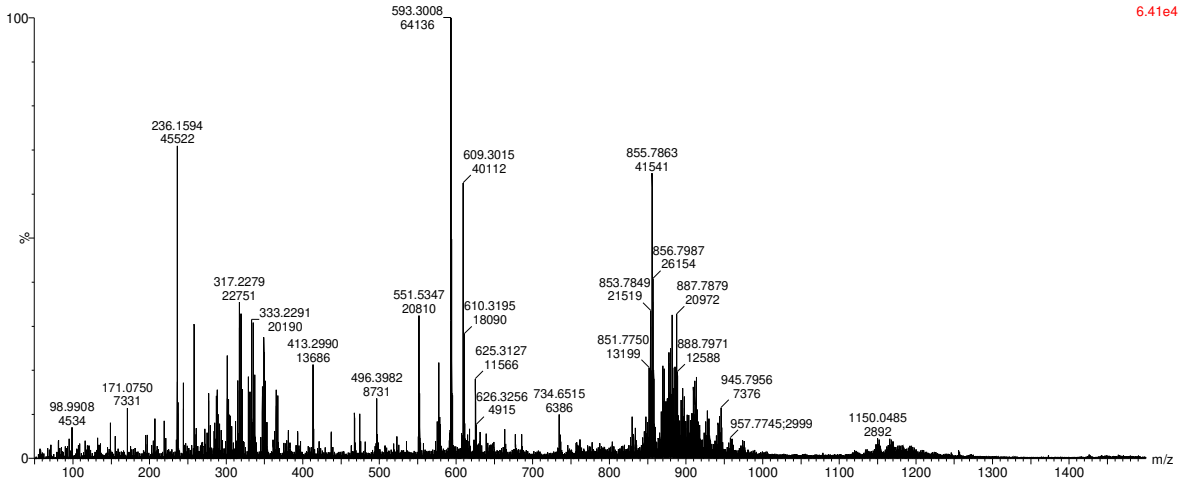

FIGURE S7. Direct infusion ESI(+)-QTOF mass spectrum for SENESPS

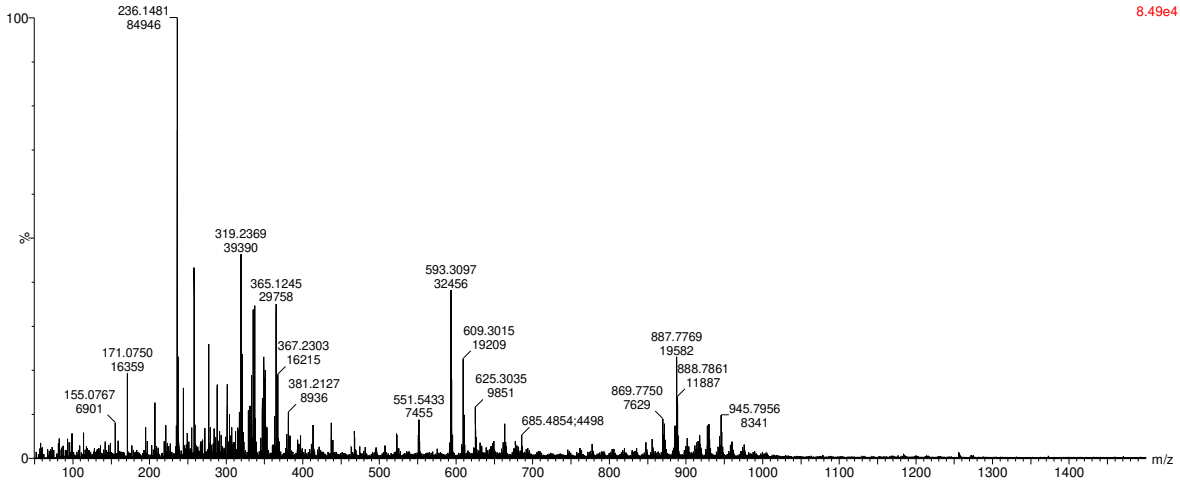

FIGURE S8. Direct infusion ESI(+)-QTOF mass spectrum for SENEWC

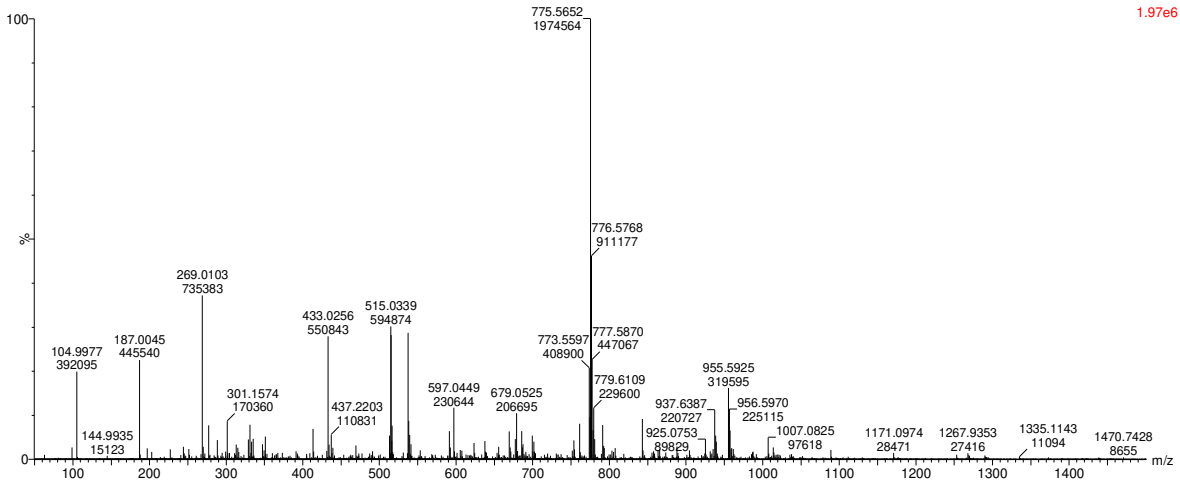

FIGURE S9. Direct infusion ESI(+)-QTOF mass spectrum for SPIRM6

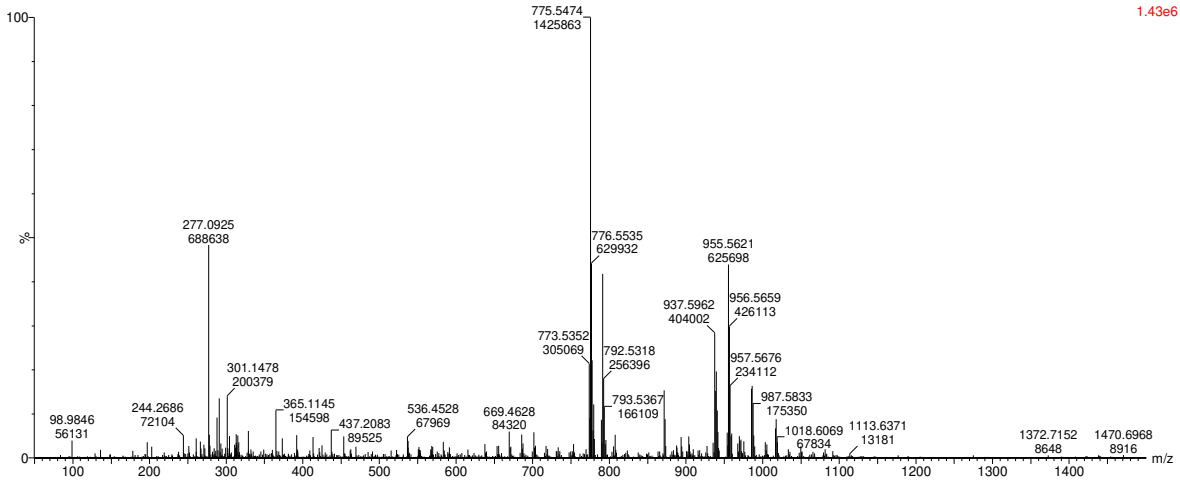

FIGURE S10. Direct infusion ESI(+)-QTOF mass spectrum for SPIZK.

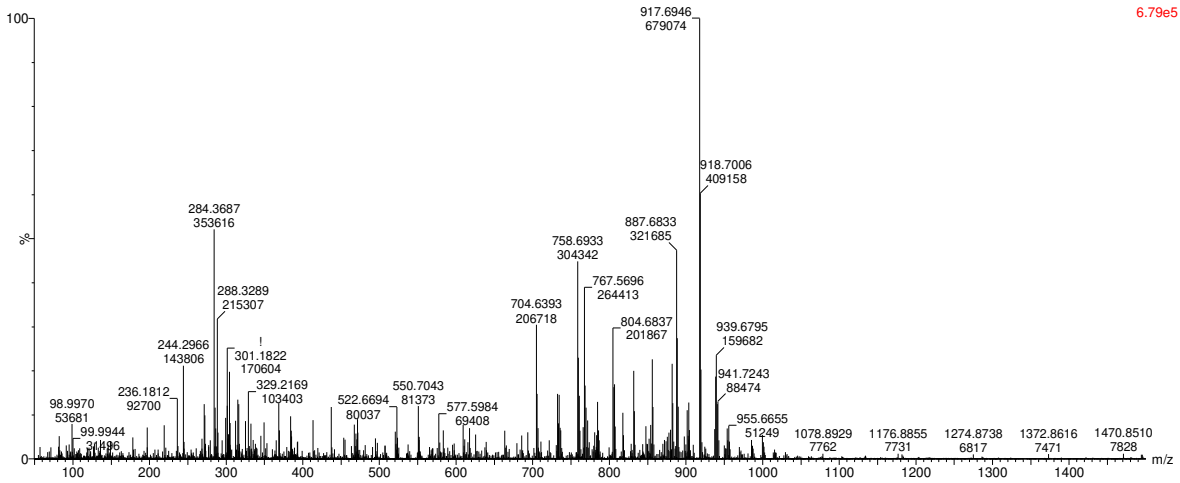

FIGURE S11. Direct infusion ESI(+)-QTOF mass spectrum for TG1.

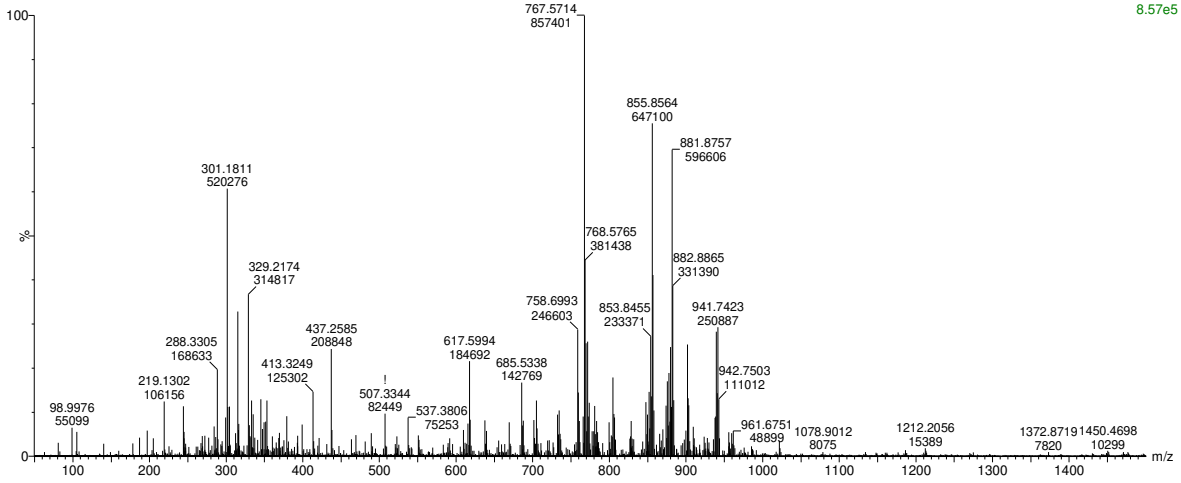

FIGURE S12. Direct infusion ESI(+)-QTOF mass spectrum for TG2.

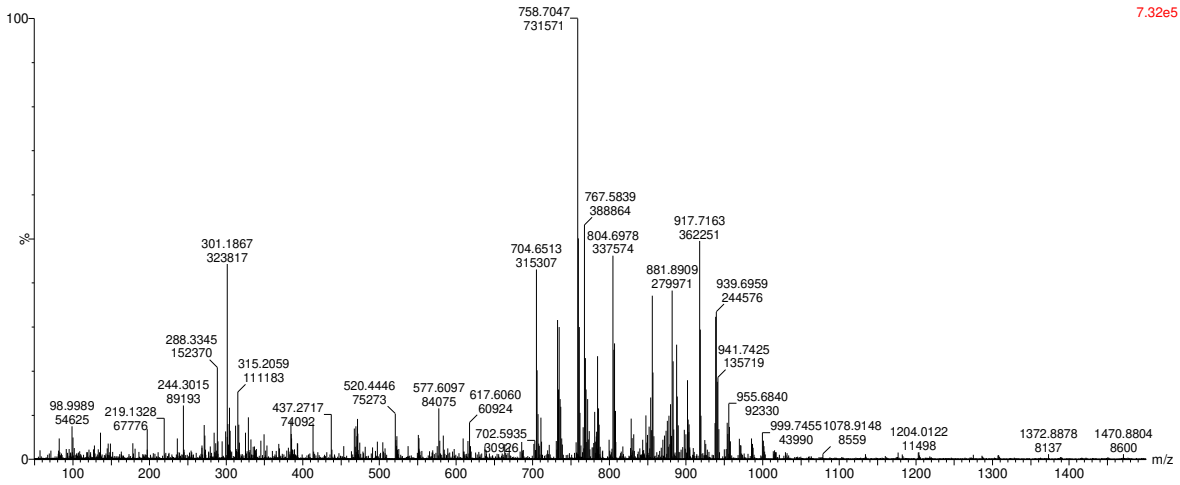

FIGURE S13. Direct infusion ESI(+)-QTOF mass spectrum for TG3.

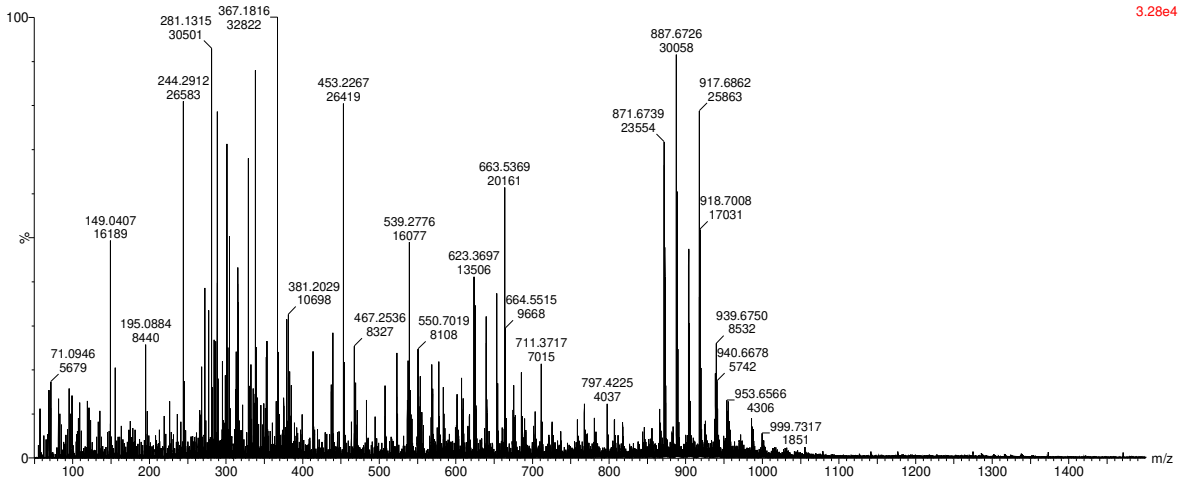

FIGURE S14. Direct infusion ESI(+)-QTOF mass spectrum for TG4.

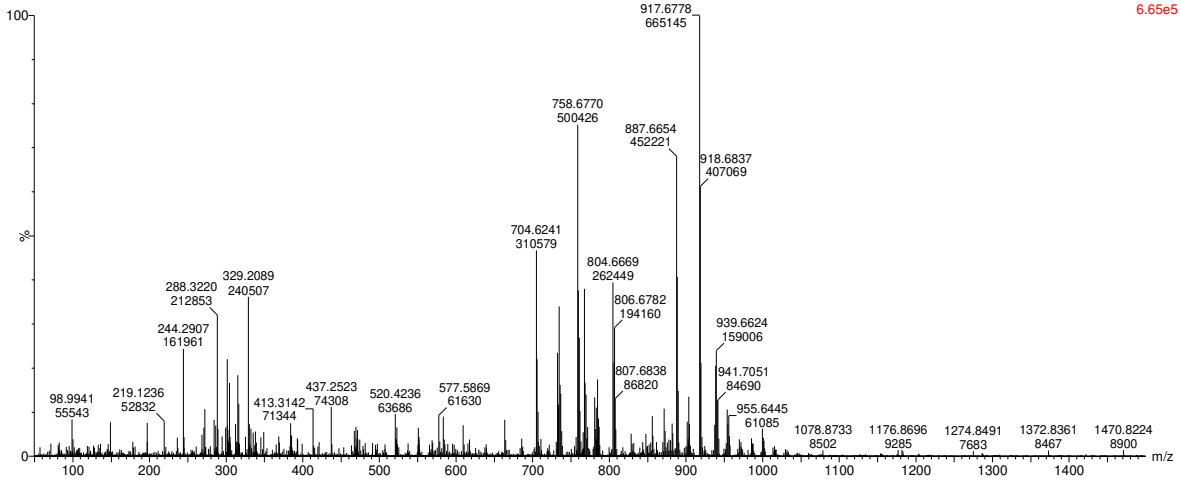

FIGURE S15. Direct infusion ESI(+)-QTOF mass spectrum for TG5.

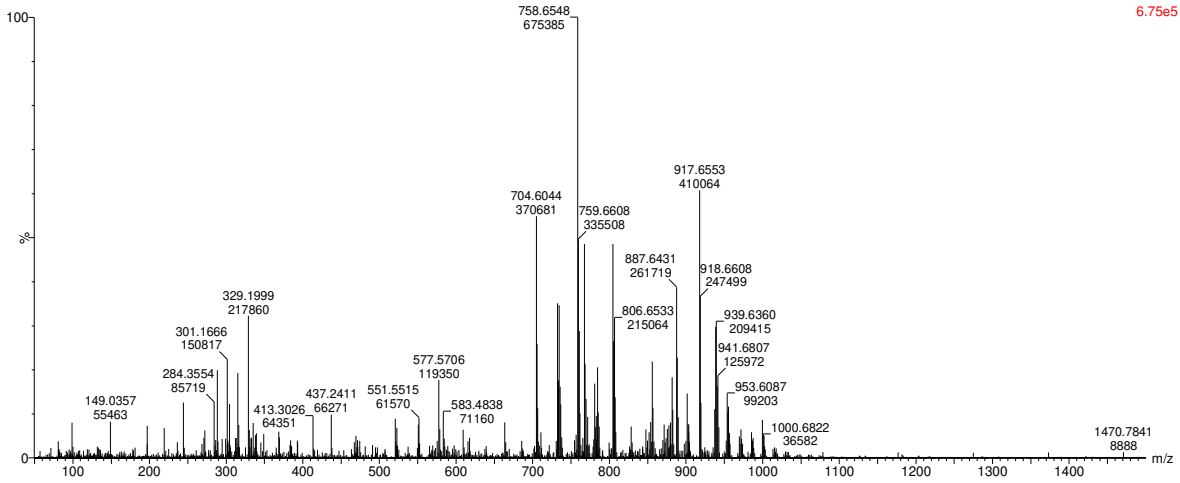

FIGURE S16. Direct infusion ESI(+)-QTOF mass spectrum for TG6.

3) Two-dimensional drift time versus *m/z* for all algae samples:

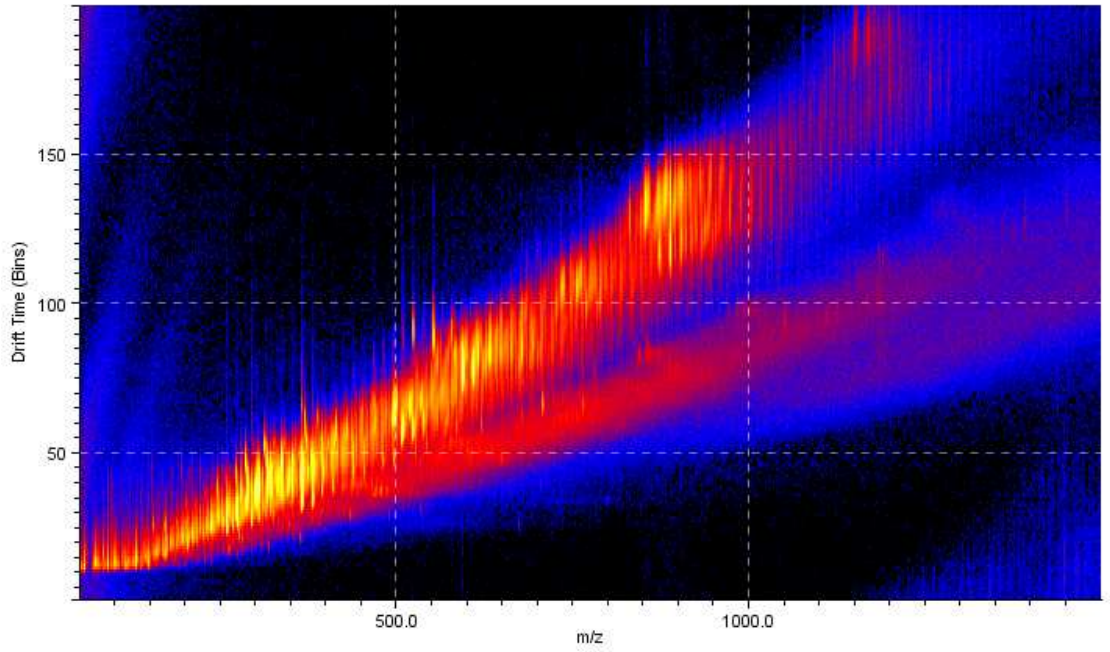

FIGURE S17. Two-dimensional drift time versus *m/z* for **CHLOSPS.**

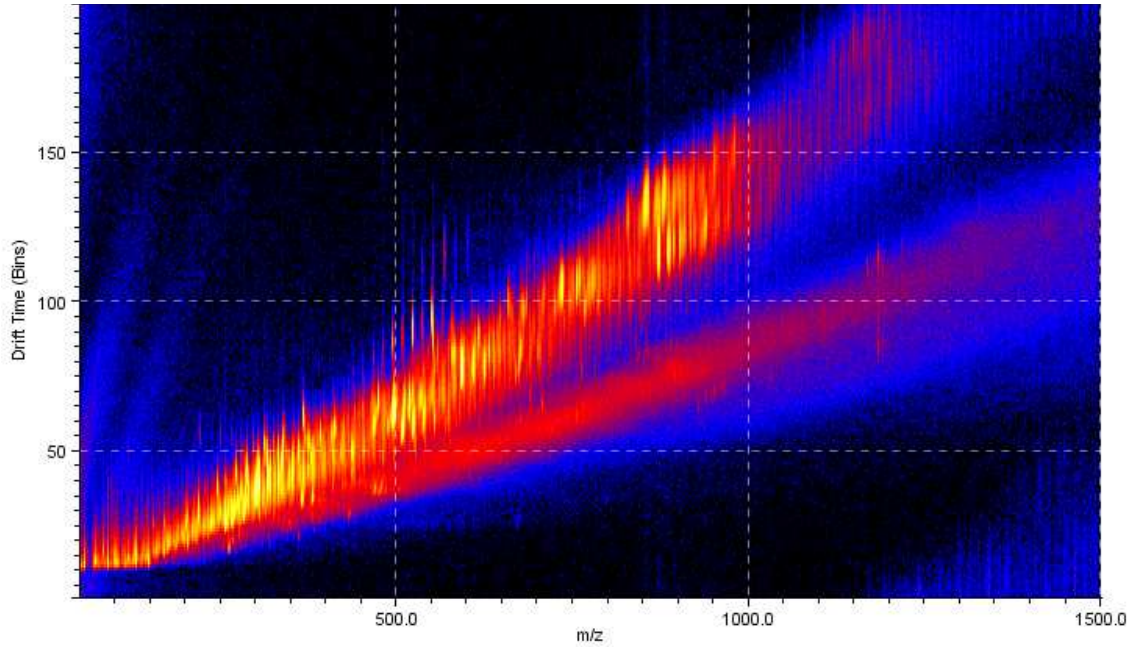

FIGURE S18. Two-dimensional drift time versus *m/z* for **CHLOWC.**

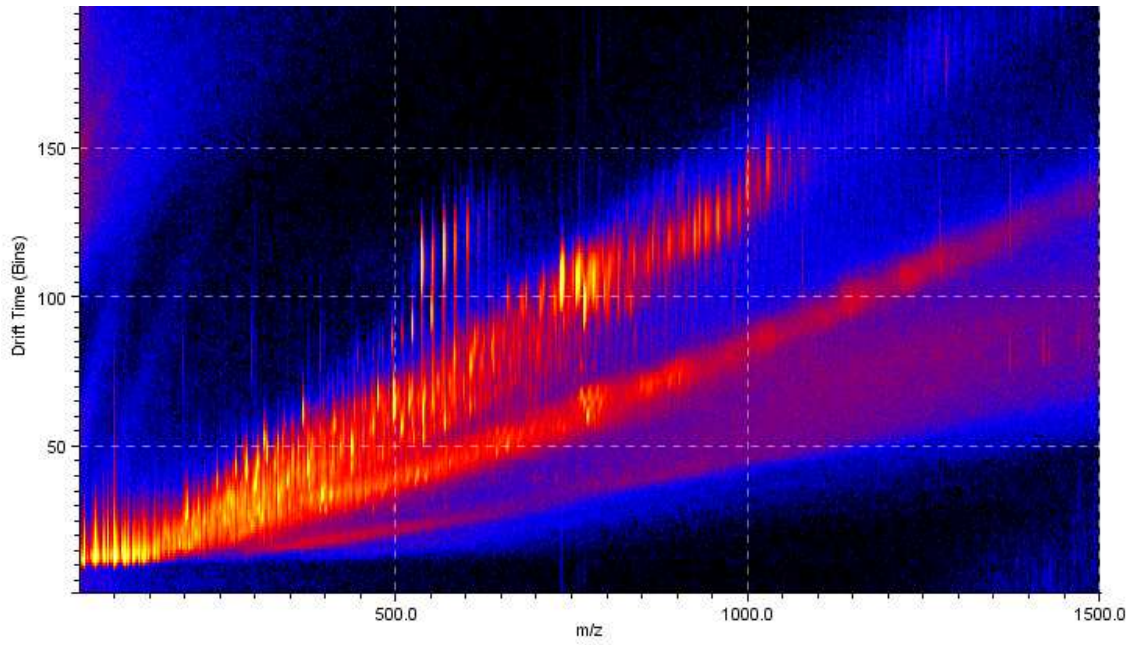

FIGURE S19. Two-dimensional drift time versus *m/z* for **DUNABC_CHCl3.**

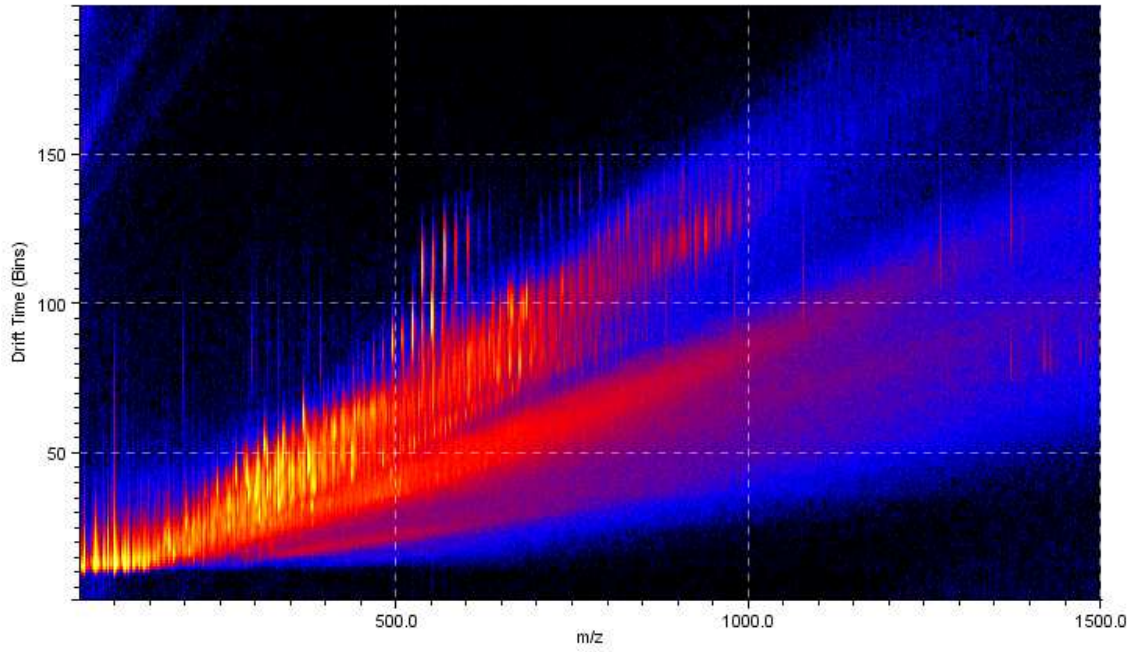

FIGURE S20. Two-dimensional drift time versus *m/z* for **DUNABC_MEOH.**

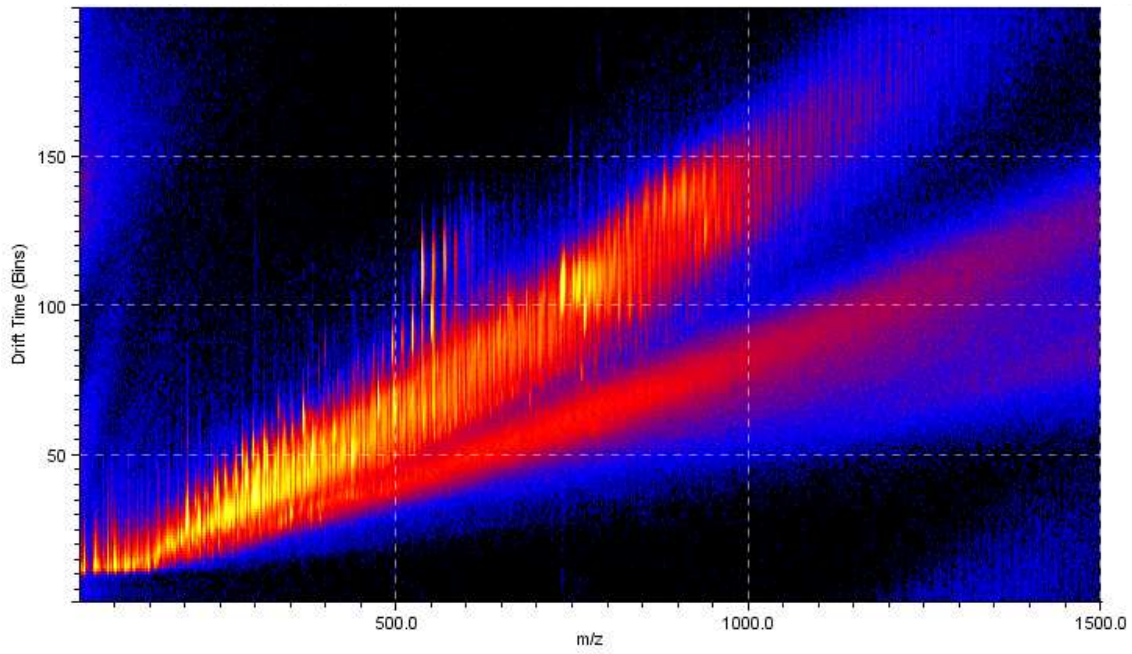

FIGURE S21. Two-dimensional drift time versus *m/z* for **DUDEF_ CHCl3.**

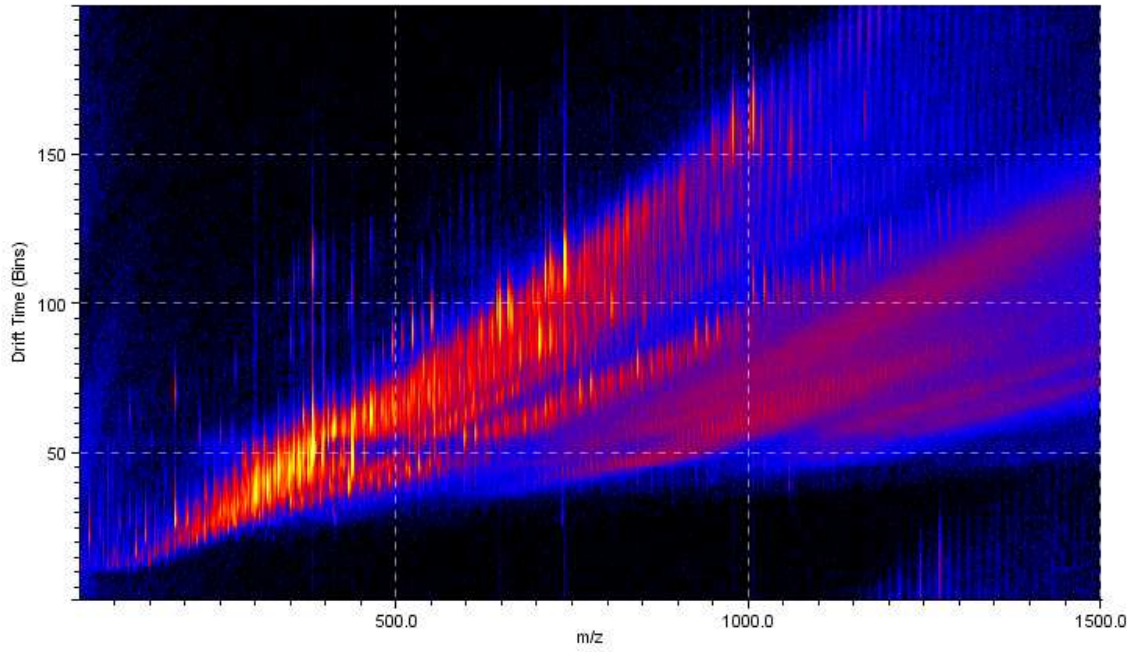

FIGURE S22. Two-dimensional drift time versus *m/z* for **DUDEF_MEOH.**

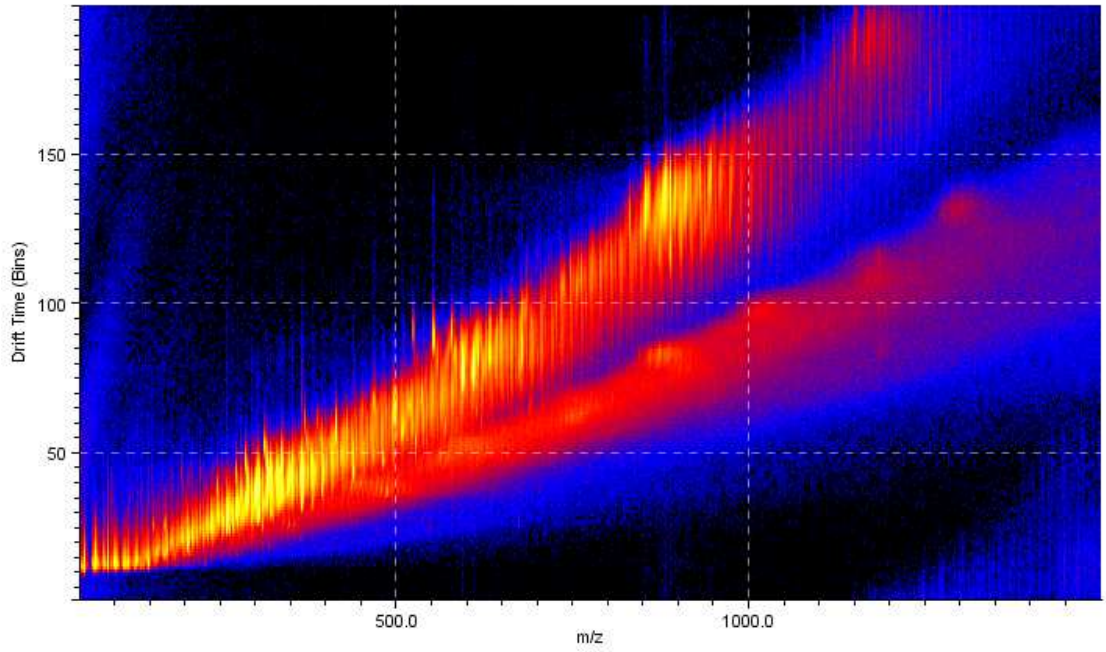

FIGURE S23. Two-dimensional drift time versus *m/z* for **SENESPS.**

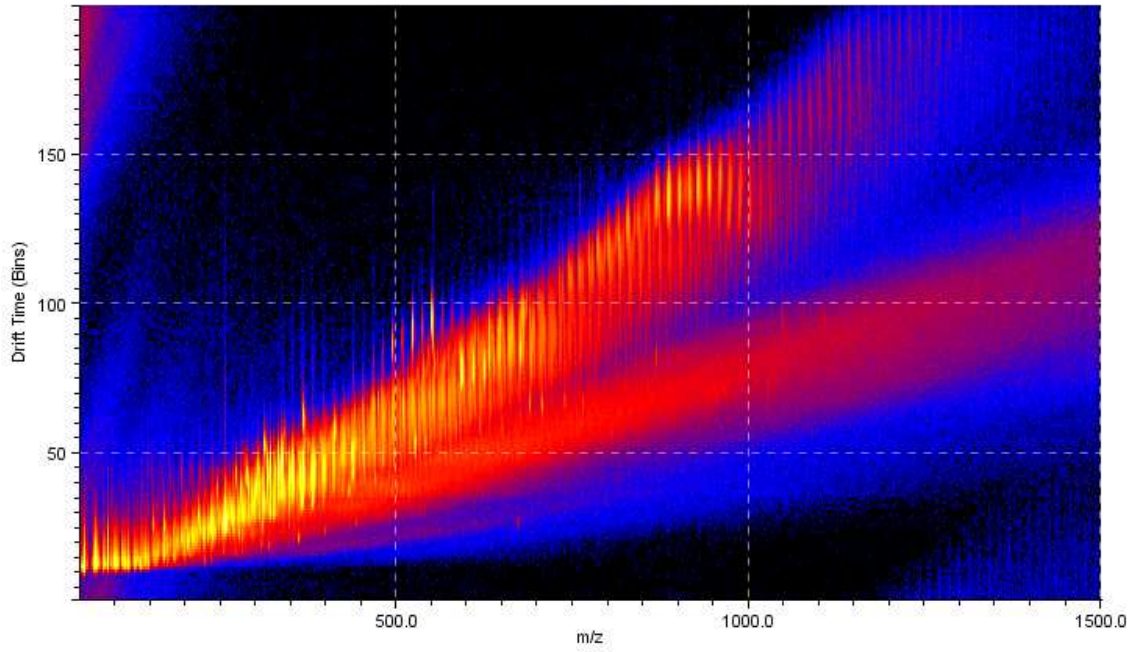

FIGURE S24. Two-dimensional drift time versus *m/z* for **SENEWC.**

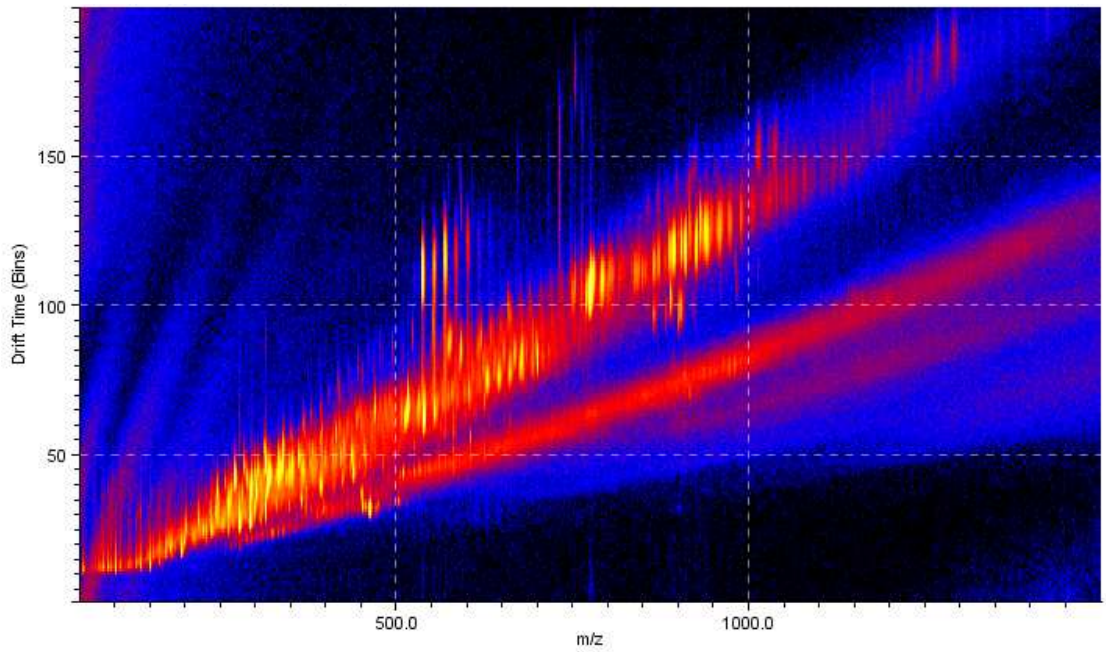

FIGURE S25. Two-dimensional drift time versus *m/z* for **SPIRM6.**

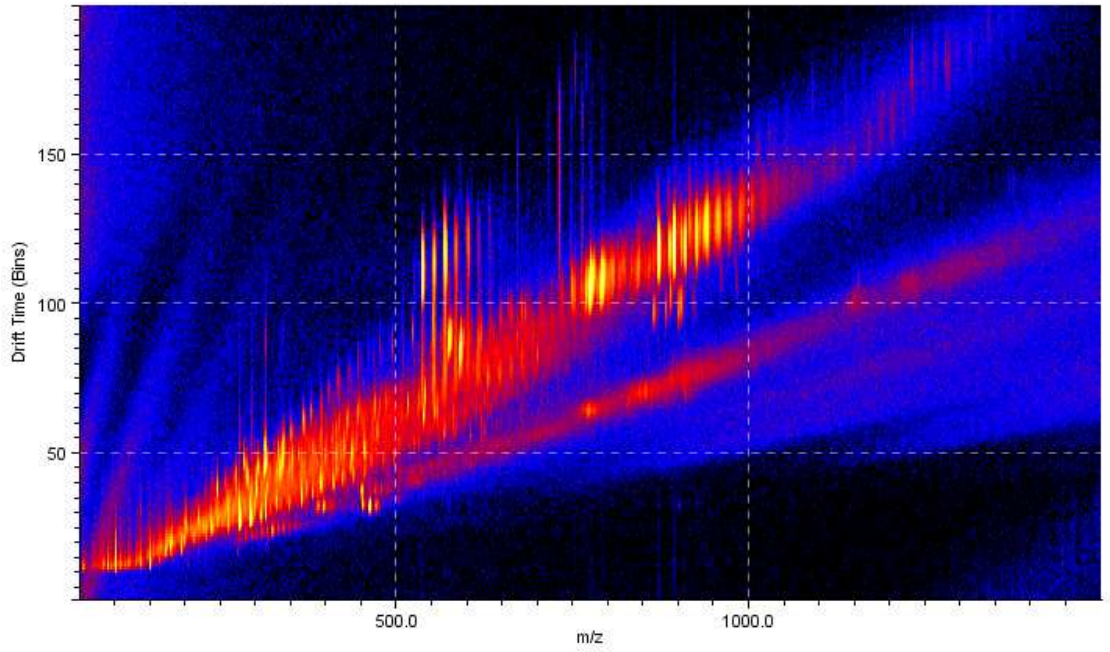

FIGURE S26. Two-dimensional drift time versus *m/z* for **SPIZK.**

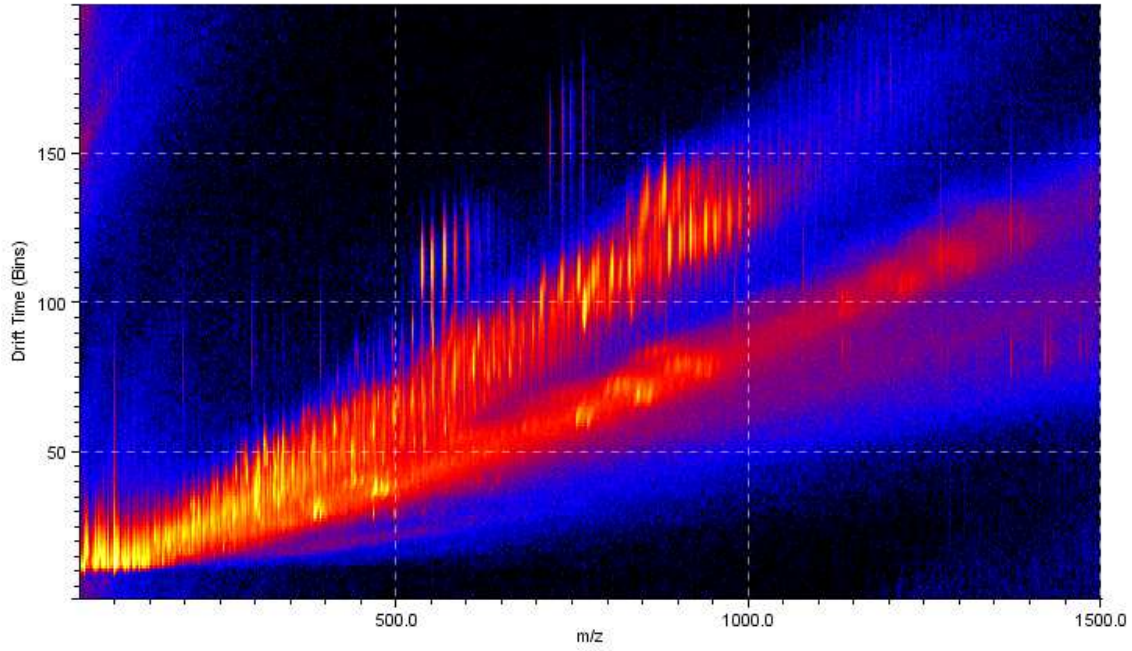

FIGURE S27. Two-dimensional drift time versus *m/z* for **TG1.**

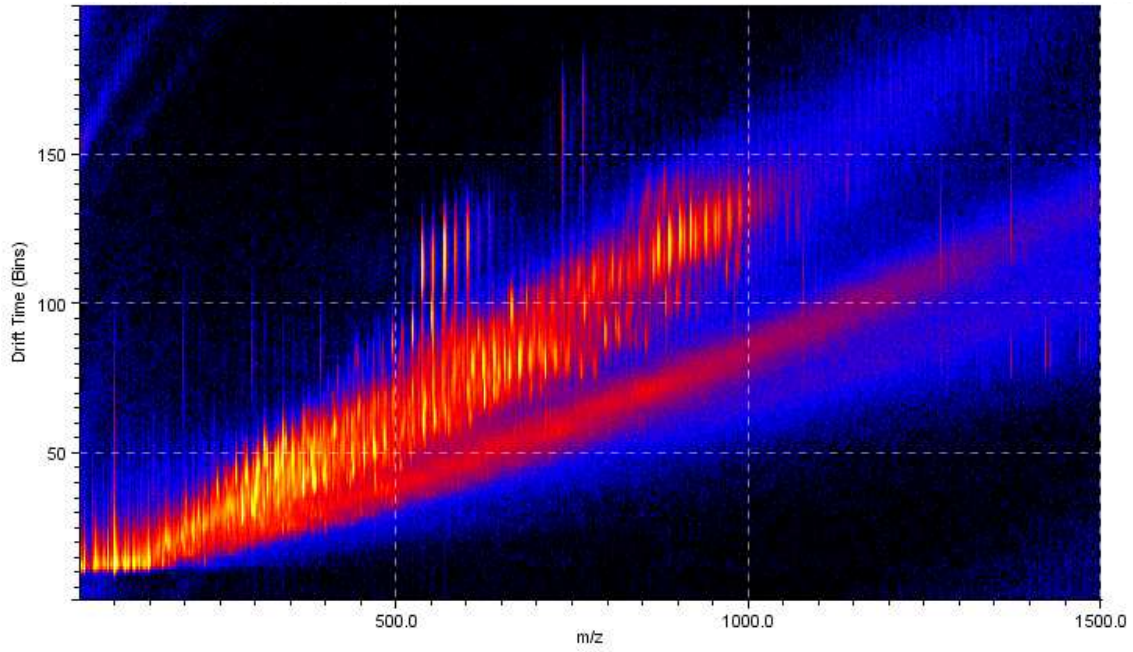

FIGURE S28. Two-dimensional drift time versus m/z for **TG2.**

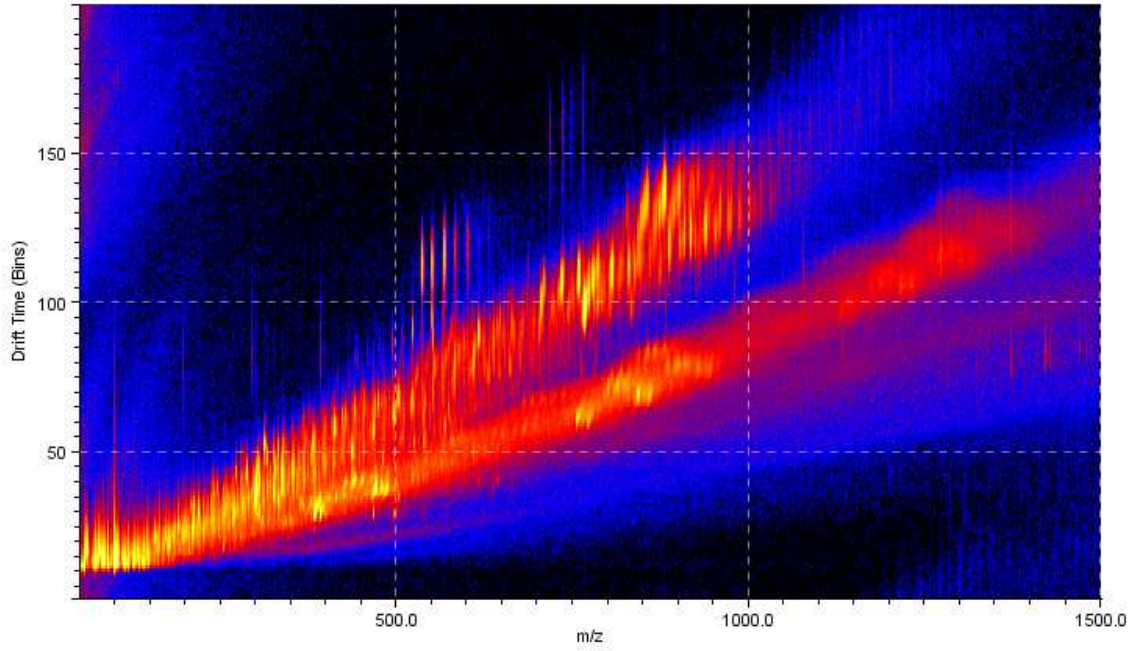

FIGURE S29. Two-dimensional drift time versus m/z for **TG3.**

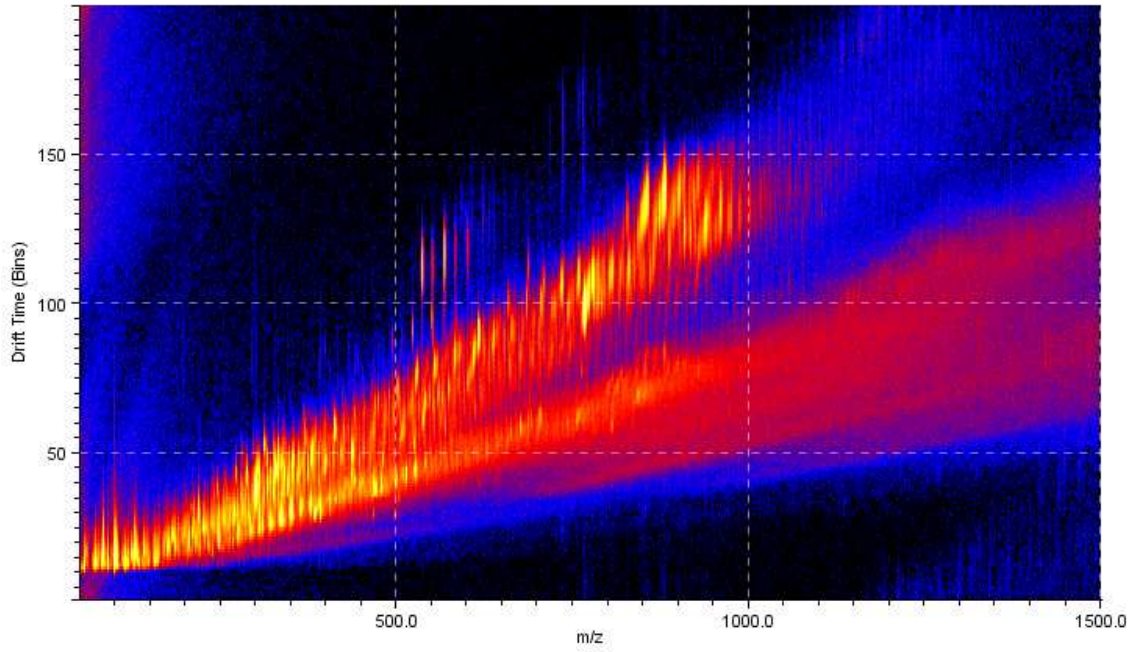

FIGURE S30. Two-dimensional drift time versus m/z for **TG4.**

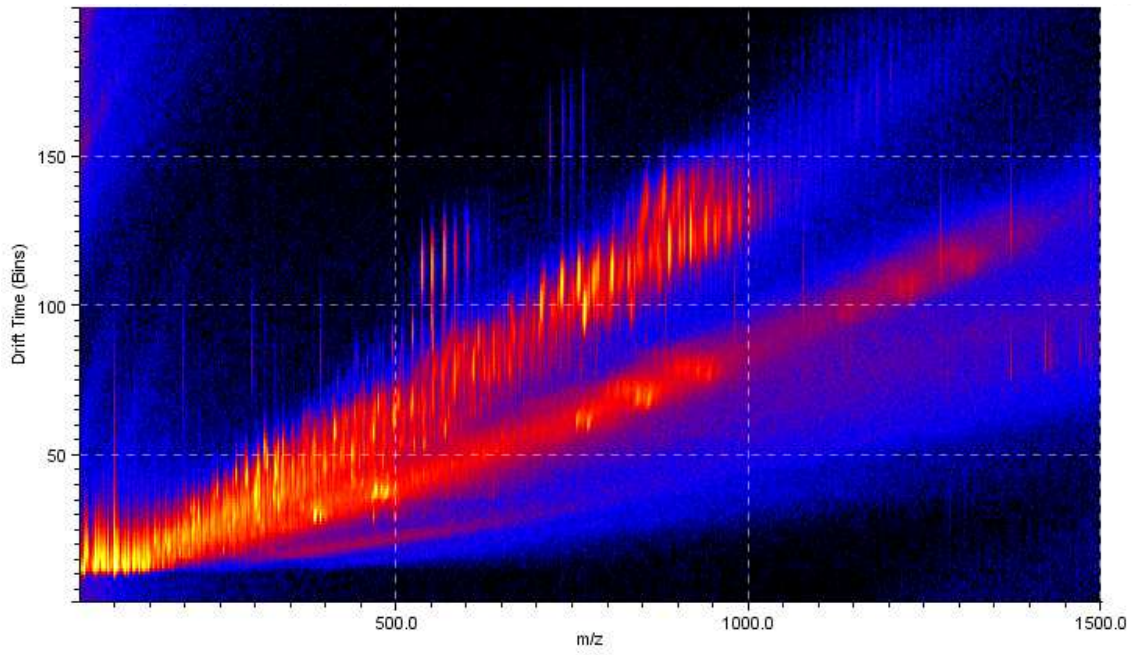

FIGURE S31. Two-dimensional drift time versus m/z for **TG5.**

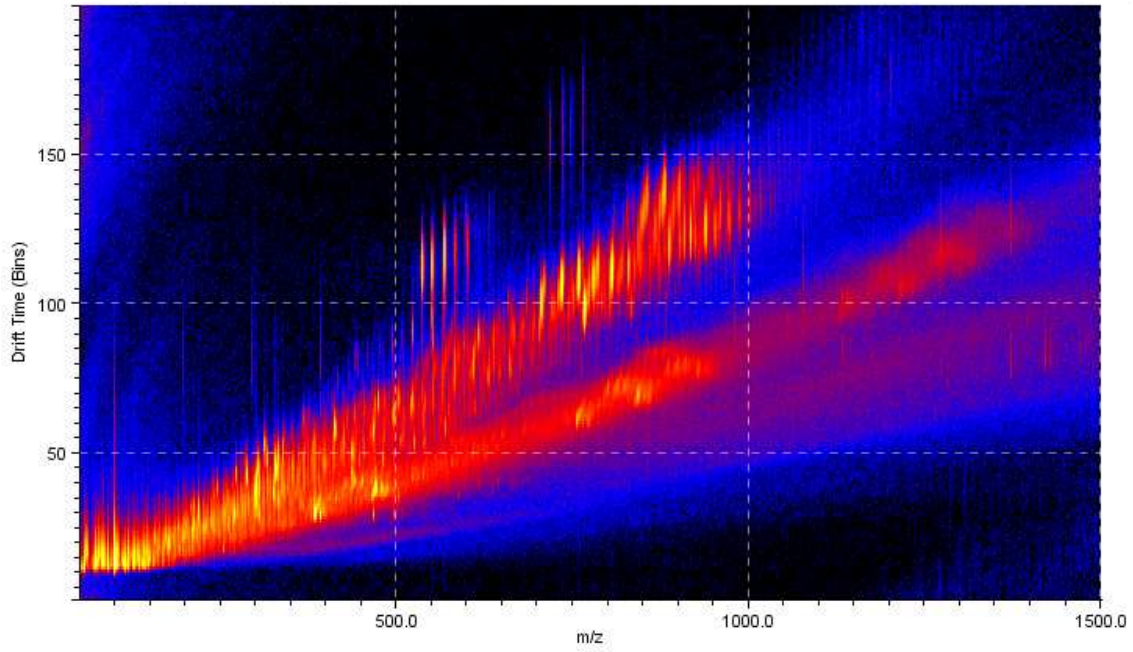

FIGURE S32. Two-dimensional drift time versus *m/z* for **TG6.**

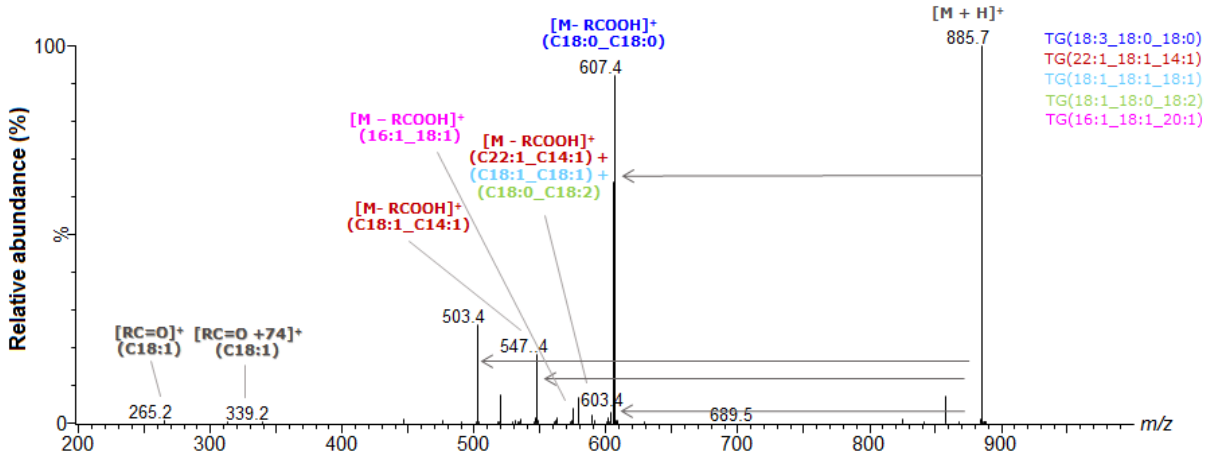

FIGURE S33. MS/MS spectrum of the ion of *m/z* 885.7 and all the identified TAGs isomers

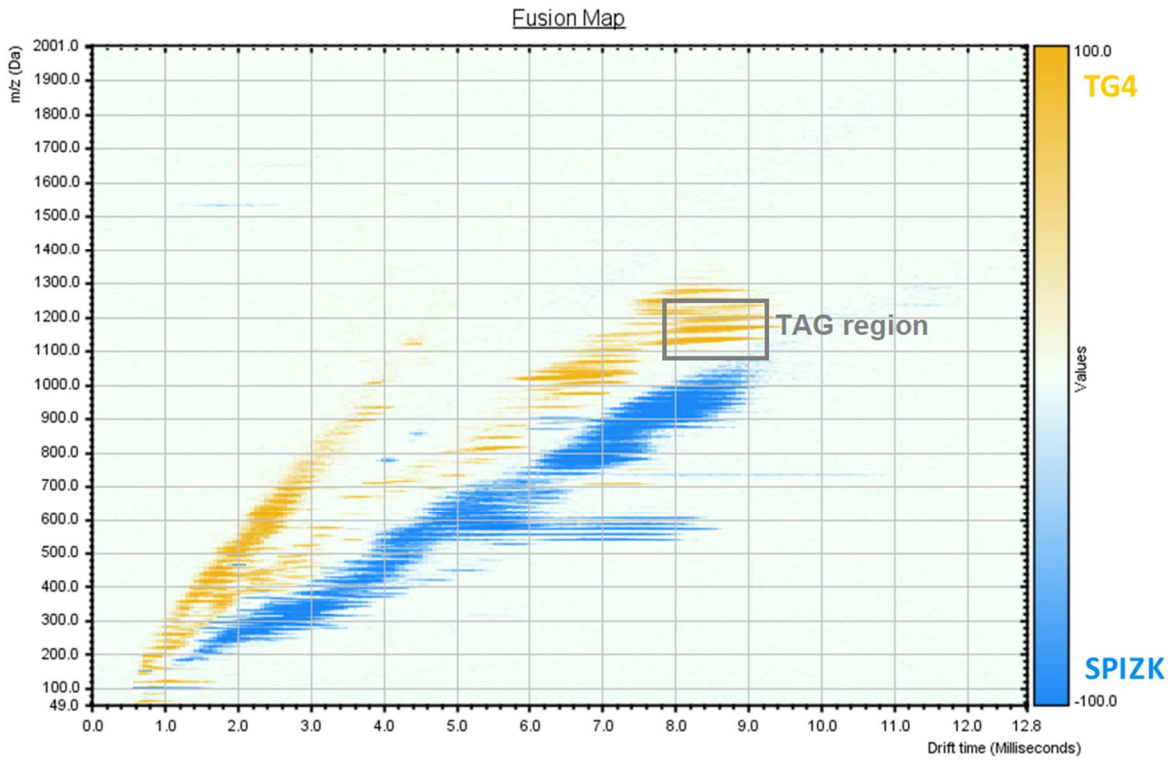

FIGURE S34. Fusion map comparing samples TG4 and SPIZK

Table S1. Additional TAGs confirmation by comparing the experimental data of measured CCS values with LipidsCCS theoretical values. (ND = not determined; *Not fragmented)

m/z	Experimental CCS (angstrom^2)	Theoretical CCS LipidCCS	$\Delta\Omega^2$	Error (%)	LipidCCS ion	Accepted Compound ID	Accepted Description
745.6244	291.5	294.2	-2.7	-0.9	M+Na	11148	Glyceryl Trimyristate :: Lipids :: Lipids :: 2,3-di(tetradecanoyloxy)propyl tetradecanoate
902.8201	348.4	323.1	25.3	7.8	M+NH4	5497163	TG 54:3 (18:1_18:1_18:1) :: Glycerolipids :: Lipids :: 2,3-bis[[(Z)-octadec-9-enoyl]oxy]propyl (Z)-octadec-9-enoate
481.3890	244.0	NA	ND	ND	M+H-H2O	HMDB72193	TG(10:0_8:0_8:0)
745.6330	311.3	272.7	38.6	14.2	M+Na	HMDB71106	TG(10:0_a-17:0_15:0)
855.7469	329.9	314.7	15.2	4.8	M+H	HMDB48185	TG(14:1_22:2_16:1)
850.7894	339.4	315.7	23.7	7.5	M+NH4	HMDB10416	TG(16:0_16:0_18:1)
906.8513	353.9	326.7	27.2	8.3	M+NH4	HMDB44083	TG(16:0_18:1_20:0)
962.9140	364.6	336.9	27.7	8.2	M+NH4	HMDB44085	TG(16:0_18:1_24:0)
876.8054	344.8	319.3	25.5	8.0	M+NH4	TG(16:0_18:1_18:1)	TG(16:0_18:1_18:1)
916.7429	340.8	322.8	18.0	5.6	M+NH4	TG(16:0_20:5_20:5)	TG(16:0_20:5_20:5)
969.8848	364.6	339.1	25.5	7.5	M+H	HMDB49167	TG60:3*
950.8195	353.7	330.4	23.3	7.0	M+NH4	HMDB50126	TG(18:1_22:4_18:2)
922.7890	348.3	324.4	23.9	7.4	M+NH4	TG(18:1_18:2_20:4)	TG(18:1_18:2_20:4)
843.6514	324.2	304.9	19.3	6.3	M+Na	HMDB52943	TG(18:3_14:1_18:3)
884.6803	327.8	311.6	16.2	5.2	M+Na	HMDB55501	TG(18:4_18:4_18:4)
947.7142	346.3	326.9	19.4	5.9	M+Na	HMDB55695	TG(20:5_16:0_22:6)
967.6830	344.3	327.1	17.2	5.3	M+Na	TG(20:5_20:5_20:5)	TG(20:5_20:5_20:5)
908.8665	355.8	328.6	27.2	8.3	M+NH4	HMDB66803	TG(21:0_18:0_15:0)
1038.8583	371.5	NA	ND	ND	M+NH4	TG(21:0_22:6_22:6)	TG65:12*
661.5394	290.2	275	15.2	5.5	M+Na	HMDB71162	TG(8:0_12:0_16:0)
628.5525	286.4	272.7	13.7	5.0	M+NH4	HMDB72772	TG(8:0_i-14:0_12:0)
		Average	**21**	**6.7**			

2.4. Compendium on Amazon oils composition. Part I - Triacylglycerols characterization and comparison with commercial trivial vegetable oils and fats

O artigo a seguir, em formato de manuscrito, encontra-se em fase de submissão para revista internacional da área de química analítica.

Journal title

Article

Title: "Compendium on Amazon oils composition. Part I - Triacylglycerols characterization and comparison with commercial trivial vegetable oils and fats"

Authors: Maíra Fasciotti,[1,5*] Thays V. C. Monteiro,[1] Michael Murgu,[2] Werickson F.C. Rocha,[1] Simone C. Chiapetta,[4] Luiz R. Moraes,[3] Alessandra Sussulini,[5] Marcos N. Eberlin,[5] Valnei S. Cunha[1]

[1] National Institute of Metrology, Quality and Technology (INMETRO), Division of Chemical Metrology, Laboratory of organic analysis, 25250-020, Duque de Caxias, RJ, Brazil

[2] MS Applications & Development Laboratory, Waters Corporation, Barueri, SP, Brazil;

[3] Amazon Oil, Ananindeua, PA, Brazil;

[4] Instituto Nacional de Tecnologia (INT), Rio de Janeiro, Rio de Janeiro, Brazil;

[5] University of Campinas (UNICAMP), Institute of Chemistry, Campinas, SP, Brazil.

*corresponding author: M. Fasciotti, mfasciotti@inmetro.gov.br

ABSTRACT

The Amazon forest concentrates one of the most important and richest biodiversity on planet. Its oleaginous native species are specially being exploited due to the worldwide tendency to invest in natural and sustainable products. Because of this, the Amazon biodiversity is in the focus of attention of cosmetics, pharmaceutical and food industries, since oils from its native species have shown beneficial potential for human health. There are several studies in the literature about the composition of oils from Amazonian species, as well as many popular beliefs about their beneficial properties. However, conducting a comprehensive and ultra-detailed analysis of the composition of these oils is a challenging task due to their complexity. In this way, this compendium aims to elucidate the composition of different Amazon oils using a powerful technique such as mass spectrometry, to ensure their authenticity and quality, corroborating the understanding of their properties, through the identification of bioactive compounds. In this first part of the compendium, a detailed fatty acids and intact triacylglycerols (TAGs) from fifteen oleaginous Amazon species are reported, by using gas chromatography-mass spectrometry and electrospray high resolution mass spectrometry. The TAGs were characterized by their MS/MS spectrum resulting in a detailed study about TAGs composition in these samples. Over 40 different TAGs were identified and the occurrence of isomers was remarkable, showing that TAGs complexity in these samples is much higher than reported in some previous literature about Amazon oils composition. For samples such as babassu, murumuru and tucuma butter, the mass spectra were almost identical, presenting only minimal variations in some TAGs relative abundances. Patawa and buriti oils also displayed identical mass spectra profiles. All the Amazon samples were compared to trivial oils such as soybean, corn, coconut and olive oil, and their mass spectra were statistically evaluated using principal component analysis. The results showed a formation of three main groups: butters, high oleic acid oils and high linoleic acids oils, plus some disconnected butters such as bacuri and cupuaçu with compositions closer to oils than to other butters. By generating a greater knowledge about the chemical composition of these oils is easier to detect possible adulterations in products that employ them in their composition, and additionally, encourage the sustainable production and appropriate use of Amazon forest resources.

INTRODUCTION

With the largest area of tropical rainforest in America, the Brazilian Amazon forest has a unique biodiversity, sheltering one of the richest varieties of animal and plant species on the planet. [1,2] Such biodiversity is an important basis for increasing the knowledge about the functioning of life on the planet and the interactions between physical-biotic systems and human beings, contributing to a better life quality. The preservation and sustainable use of this natural patrimony is of interest not only of Brazil, but also as of all humanity. Investing in the sustainable exploitation of the Amazon's biodiversity, one guarantees its preservation, placing the Amazon in the focus of world attention, avoiding the extinction of this natural patrimony. [3,4]

The Amazon oleaginous native species are being increasingly exploited due to the worldwide tendency to invest in products that appeals as being from a "natural" origin, petrochemicals free, made of "organic" materials, "vegan", "sustainable" and "cruelty free", meaning that they are not made of any animal raw materials and not tested in animals as well. [5,6] Because of this, the Amazon biodiversity is even more in the focus of the attention of the cosmetics, pharmaceutical and food industries, since oils from its native species have shown beneficial potential for health from several points of view. [7] The National Cancer Institute (NCI) of United States estimates that 70% of the anti-cancer plants identified until now are native from rain forests. [8,9]

Oils are important components for many industries, being used for different purposes. In the cosmetics industry, for instance, they are employed in the oily phase of creams, emulsions, lotions with moisturizing, emollient, antioxidant and nourishing properties for the skin and hair, in dairy use products such as shampoos, conditioners, soaps and body lotions. [10] Vegetable oils are also being widely used as a substitute for mineral oil in the cosmetics industry, in order to increase the efficacy and safety of these production inputs. In the food industry, the importance of vegetable oils is quite remarkable, as the search for healthier fats is a permanent goal for nutraceutical foods research. As known, the intake of certain types of fats can be associated with coronary heart disease, or some others may have beneficial properties such as cholesterol decrease levels. [11]

From the sustainability point of view, investing in the oil and fats industry from the Amazon biodiversity is interesting, since this ensures the protection and maintenance of these native species, because these oils are extracted from seeds, almonds and pulp of the fruits of Amazon trees. Encourage the use of the fruit of these species adds value to it and inhibits the (often illegal) wood extractivism, minimizing the risks of a native species to become extinct. As an example of this situation, the ucuuba-based (*Virola surinamensis*) products can be highlighted. The ucuuba tree wood used to be widely employed for making broomsticks in the region of Pará state, in Brazil. When purchasing an Ucuuba fruit-based product, the end user automatically directs the market and the economic benefits for the production of this raw material, instead of its wood extractivism, as the Ucuuba fruits will be more profitable than its wood.

The introduction of sustainable and environmentally friendly exploitation models also helps to bring attention to the Amazon territory, as one of the main problems in this region nowadays is the lack of government oversight. [12,13,14] In addition, the trade of native oils helps in the socioeconomic development of riverine families that inhabit productive areas in the Amazon, improving their life quality. [15]

Data from the Brazilian Institute of Geography and Statistics (IBGE) indicate that the production of fruits of oilseeds in the Amazon region generates about R$ 1.5 billion per year, according to data from 2006. The amount of production and its values for some Amazonian species are presented in Table 1. It is estimated that, at the present days, this production has increased, although there is no more recent data collected by IBGE.

Two important companies in the region of Belém, Amazonoil and Beraca, produce tons of Amazon oils annually that are marketed in Brazil and exported. [16,17] Due to the high commercial value and the importance of these vegetable oils in the cosmetic and food industry, the possibility of fraud involving mixtures of low-value commercial oils, such as soybean oil, is very frequent. Then, it is necessary the development of selective, sensitive and fast techniques to evaluate the chemical composition of the Amazon oils.

Table 1. Quantity harvested and production value for some Amazon oil seeds in the year of 2006

Amazon oil seed	Quantity harvested (tons)	Values of production (x 1,000 R$ - BRL)
Açaí	267,499	176,380
Andiroba	878	1,272
Babaçu	163,420	109,060
Bacuri	3,159	1.401
Buriti	6,450	5,409
Castanha-do-Pará	20,920	18,990
Cupuaçu	3,026	3,980
Murumuru	71	45
Ucuuba	21	14
Tucuma	4,040	3,259

Source: Adapted from IBGE, Agricultural Census, 2006.

There are several studies in the literature about the composition of oils from Amazon species regarding some specific classes of compounds, as well as many "popular" beliefs about their beneficial properties to human health. However, conducting a comprehensive and detailed analysis of the composition of these oils is a challenging task due to the complexity of these matrices and the wide variety of polarities and chemical features that the compounds may have. Mass spectrometry (MS) has been at least for the last thirty years the technique of choice successfully applied for the characterization of vegetable oils from many origins and with different objectives. [18,19,20,21] The methods include from the classical fatty acid methyl esters (FAMEs) analysis by gas chromatography coupled to mass spectrometry to electrospray ionization with high resolution mass spectrometry (HRMS). In this way, MS-based methods can help to elucidate the composition of these native species, guaranteeing their authenticity and quality, corroborating the understanding of their properties, through the identification of bioactive compounds. By generating a greater knowledge about the chemical composition of these oils, is easier to detect possible adulterations in products that employ them, additionally protecting the sustainable production and appropriate use of Amazon forest resources.

The general purpose of this work was to apply state-of-art methodologies using several MS techniques to perform an ultra-detailed characterization of both major and minor compounds in samples of oils and butters from native oleaginous species from Amazon forest. At the end, it is intended to obtain a comprehensive compendium regarding the chemical composition of these oils. The part I of this compendium will focus on the major composition characterization, which are the triacylglycerols, and also will compare the composition of these oils with other oils and fats of vegetable and animal origin whose use is more trivial, highlighting similarities and differences between them, thus encouraging new applications or corroborating the ones already being implemented.

EXPERIMENTAL

Chemicals

Methanol, toluene and hexane (LC grade) were purchased from Tedia Brazil (Rio de Janeiro, Brazil). Analytical grade phosphoric acid (85% m/m), formic acid (98–100%), potassium hydroxide, ammonium bicarbonate, sodium chloride and BF_3-methanol reagent and nonadecanoic acid methyl ester (analytical standard) were purchased from Sigma-Aldrich (Merck Sigma-Aldrich, KGaA, Darmstadt, Germany).

Samples

Samples of oils and butters from Amazon were donated by Amazon Oil company (www.amazonoil.com). When possible, at least two lots of each species (produced at different years) were analyzed. Samples were frozen (-4 °C) and stored out of the light as soon as they were received. All samples have certificate of traceability, that is, they are traceable from the extraction until the moment of packaging, which guarantees their authenticity. All the Amazon samples analyzed in this work are reported in Table 2, as well as they scientific name, type (oil or butter), the main traditional and medicinal uses and a brief collection of previously reported composition and properties in the literature. All the samples are guaranteed pure and natural, obtained by cold pressing dry extraction,

without passing 60 ºC, free of preservatives, additives, pesticides, fertilizers, and of another chemical substance; they are wild species that grow naturally in the Amazon rainforest, sustainably produced.

The Amazon samples were also compared with commercially available samples of oils, fats and butters that are commonly used, as follows: soybean oil (n = 3), corn (*Zea mays L.*, n = 3), sunflower (n = 3), canola (*Brassica sp.*, n = 3), milk butter (n = 3), commercial margarine (n = 3), extra virgin olive oil (mixture of species, n = 3), coconut oil (*Cocos nucifera*, n = 2), beef tallow (n= 1) and lard (n = 1).

METHODS

Fatty acids methyl esters (FAME) quantification by GC-MS

The Amazon oils and butters samples listed in Table 2 were converted into FAME through a transesterification reaction in which to an approximately 0.8 g of each sample was added 5 mL of a 1 mol $\cdot$ L^{-1} KOH/methanol solution that was heated under reflux for three hours. Then, 5 mL of BF_3-methanol reagent was added to the reaction and kept again under reflux for one more hour. After the reaction time, 1 mL of a saturated NaCl aqueous solution and 10 mL of hexane were added to the reaction media. After the liquid-liquid extraction and phase separation, the hexane upper phase was transferred to 25 mL becker. The solvent was completely evaporated at 50 ^{o}C, resulting in the mixture of FAME. For GC-MS analyses, 5 mg of the internal standard C19:0 and 5 mg of the FAME mixture were precisely weighted in GC vials. Then, approximately 1 mL of toluene was added to the vial, and precisely weighted as well. The mixture was vortexed for approximately 15 seconds until complete dissolution, and then the vials were placed on the autosampler of the GC for the analysis.

The identification and quantification of the FAME content produced from the transesterification of the Amazon oils were performed using gas chromatography with mass spectrometer detector (GC/MS - Shimadzu GCMS-QP2010, Tokyo, Japan) according to a validated standard procedure – “EN 14103:2011: Determination of ester and linolenic acid methyl ester contents”, with some modifications. The

chromatographic separation of methyl ester was performed in an Rtx-Wax (Varian, 30 m x, 0.25 mm i.d. x 0.32 µm film thickness) column. 1 µL of sample was injected in split mode, 1:150 ratio. The splitless injector temperature was set to 250 ℃. The oven temperature program starts at 60 ℃ hold for 2 minutes, to 200 ℃ at 10 ℃ min^{-1}, and to 240 ℃ at 5 ℃ min^{-1}, hold for 7 minutes, with a total run time of 31 min. Helium was used as the carrier gas at a constant flow rate of 3 mL min^{-1}. Samples were analyzed in instrumental triplicates.

Triacylglycerols (TAGs) characterization by ESI-QTOF-MS

For the characterization of intact TAGs, 2 mg of each sample was precisely weighted and dissolved with 1.5 mL of toluene in glass vials. Then, 10 µL of this solution was diluted in 1 mL of methanol with 10 mmol · L^{-1} ammonium bicarbonate, to induce the formation of ammonium adducts. The samples solutions were direct infused (flow rate of 10 µL · min^{-1}) using an external syringe pump into the ESI source of a QTOF mass spectrometer (Synapt HDMS, Waters, UK), operated under positive ion mode, 3.0 kV of capillary, 40 and 3.0 V of cone and extractor cone, respectively. The source and desolvation temperatures were 80 and 150 ℃, and the nitrogen nebulizer gas was used at a flow rate of 300 L h^{-1}. The mass spectrometer was mass calibrated in ESI(+) mode at 10,000 resolution (FWHM) over acquisition mass ranges of *m/z* 50 – 2000, using a solution of phosphoric acid 0.1% (v/v) in acetonitrile:H_2O (1:1). Samples full scan mass spectra were also acquired over an *m/z* range of 50 – 2000.

The characterization of the main TAG ions in the spectra was performed by fragmentation of manually selected precursor ions (selection window of 1 Da) by collision induced dissociation (CID) using argon as collision gas (collisions energies from 20 to 35 eV). TAG identification was done by comparison of the MS/MS spectra with LIPID MAPS database, [22] using the search database of glycerolipid precursor/product ions tool. Some filtering criteria were adopted to accept the TAG identification: minimum of 10 out of 18 fragments detected; all the three possible acyl group neutral losses detected; and at least 2 other fragments for each acyl chain detected as well, under an *m/z* deviation of 0.02 Da.

Data analysis and statistics

Direct infusion data were acquired using the software MassLynx 4.1v (SCN 639 for Synapt HDMS, Waters, UK). Each mass spectrum was exported as peak lists (*m/z versus* counts) combining the same number of scans for all samples. For principal component analysis (PCA), all the data were aligned in *m/z* axis and normalized. For that, several pre-processing and their combinations were tested. The results showed that the best estimation was variable alignment (COW, slack = 5), normalize (inf-Norm, Maximum = 1), and mean center. A preliminary PCA model was performed to study the data. For the construction of the PCA model, the PLS toolbox version 3.51 (Eigenvector Research, Manson, WA) was used, running in MATLAB R2015b.

RESULTS AND DISCUSSIONS

Chemically, vegetable oils and butters consist mainly of triacylglycerol (TAGs), small amounts of mono and diacylglycerols and minor unsaponifiable constituents such as sterols, vitamins, polyphenols, fatty alcohols, tocopherols, terpene alcohols, hydrocarbons, and several other compounds from different chemical classes. [23] These constituents have a pronounced effect on the stability and on its nutritional properties. [24] The fatty acids content varies according to the oleaginous species and their distribution in the TAG molecules is responsible for chemical, physical and biological properties of the oils and fats. Minor compounds such as hydrocarbons, polyphenols and terpenes with contribute for several organoleptic and medicinal properties. [23]

This work describes the detailed triacylglycerol composition of sixteen different virgin and certified Amazon oils and butters, characterized by GC-MS and ESI-MS. Amazon oils have being the focus of an intensive research during the last decades and several properties and compositional data have been already described. Table 2 summarizes the samples studied in this work, their commercial and scientific names, a collection of their principal popular and medicinal uses, and previously reported compounds and properties in the literature for the species.

Table 2. Samples of oils and butter analyzed in this work, their principal popular and medicinal uses and previously reported compounds and properties in the literature for the species

Commercial name	Scientific name	Samples analyzed in this work	Number of lots	Traditional and medicinal uses	Principal compounds and parameters reported in previous literature
Açaí	*Euterpe oleraceae*	Pulp virgin oil	2	Brain stimulation; foods and beverages preparations (acai "wine"); hair and skin repair; natural antioxidant; natural anti-inflammatory [29,33]	Pectic polysaccharides;[25] xylan polysaccharides;[26] anthocyanins and non-anthocyanin polyphenolics;[27,28] lignoids, flavonoids, phenolics; [29] minerals, total lipids, proteins and carbohydrates;[27] antioxidant activity; [30,31] fatty acids; [31] tocopherols and tocotrienols;[32] pharmacological activities [29,33]
Andiroba	*Carapas guianensis*	Nut virgin oil	2	Natural anti-inflammatory for throat infection and joint pain;[40] fungicide, antiparasitics and antimalarials;[34] skin moisturizing and bleaching agent; mosquito and insects repellent [35]	Triterpenes, steroids, coumarins, flavonoids, limonoids, fatty acids, triacylglycerols; [32,36,37,38] carapanolides;[39] tetranortriterpenoids;[40] carapanosins [41]
Babassu	*Orbignya Oleifera, Arecaceae*	Nut virgin butter	1	High temperature frying and cooking; antimicrobial; skin moisturizing and soothing for atopic dermatitis and itching;[42,43] natural anti-inflammatory[44]	Fatty acids and glycerydes [45,46]
Bacaba-de-leque	*Oenocarpus distichus, Arecacea*	Virgin oil	1	Organoleptic properties compared to olive oil; hair and skin repair and moisturizing; beverages preparations ("bacaba wine"); natural antioxidant [47]	Phenolic composition, antioxidant activity; [48] total lipids, carotene and steroids, fatty acids; [49] insoluble fibers, vitamins, minerals; [50] total phenolic, flavonoids and flavonols compounds, monomeric anthocyanins [51]

Bacuri	*Platonia insignis, Clusiaceae*	Seed virgin butter	2	Powerful skin and hair moisturizing; used to treat stingray sting; food and beverages preparations; pulmonary congestion; joint pain;[52] hair tonic and anti-dandruff; [53] leishmanicidal activities [54,61]	Carbohydrates, protein, fat, ash, dietary fiber, sugars, amino acids, fatty acids and minerals; [55] volatile compunds; [32,56,57,58] xanthones (alpha- and gamma-mangostin);[54] α-carotene and β-carotene, pro-vitamin A carotenoids; [59, 60] garcinielliptone [61]
Buriti	*Mauritia venifera*	Pulp virgin oil	2	Skin and hair moisturizing; post-sunburn treatment; skin anti-aging and healing effect [62,63]	Pectic polysaccharides;[64] carotenoids (α-carotene, β-carotene, ɣ-carotene, zeaxanthin, tocopherols; [32,65,66] acylglycerols, fatty acids, [66,38] phenolic compounds [32,67]
Castanha-do-para	*Bertholletia Excelsa H. B. K.*	Nut virgin oil	2	Skin and hair moisturizing; food preparations; natural antioxidant; skin anti-aging; anti-cancer [68]	Squalene, tocopherol, phenolic compounds, antioxidant activity; [32,69] fatty acids;[70,71,72] minerals, macronutrients, aminoacids,[71] phospholipids, sterols;[72] Se-containing proteins,[73] TAGs; [74,38] volatile compounds; [75] proteins [76]
Cupuaçu	*Theobroma grandiflorum*	Seed virgin butter	2	Dermatitis treatment and skin healing; hair treatment;[77] foods and beverages preparations [78]	Xanthine alkaloids, flavonoids, fatty acids, TAGs;[32,79,38] aglycones; [80] volatile compounds; [81,82] β-carotene; [83] TAGs; [84] polyphenol compounds; [78,85]
Graviola	*Annona muricata, Annonaceae*	Nut virgin oil	1	Powerful natural antioxidant, anticancer and antitumoral effects, anti-arthritic, antidiabetic;[86] foods and beverages preparations; vermifuge and anthelmintic against worms, parasites and lice [87]	Total phenolics, annonacin, squamocin; [88] acetogenins; [86] volatile compounds; [89] minerals, proteins, carbohydrates, fatty acids;[90,91] antioxidant activity, α-tocopherol [91]
Murici	*Byrsonima crassifolia*	Seed virgin oil	1	Natural antioxidant;[92] foods and beverages preparations; antibacterial and antifungal; [93] natural medicine the gastrointestinal tract;	Volatile compounds; [56,81, 95,96] ethyl and methyl methylthiopropanoate, methionol [95]

				anti-inflammatory and fever inhibitor [94]	
Murumuru	*Astrocarium murumuru*	Nut virgin butter	2	Food preparation; skin and hair moisturizing; [97] cosmetics [98]	Total lipids, carotenes and steroids, fatty acids; [49, 99] TAGs [38]
Patawa	*Oenocarpus bataua, Arecaceae*	Pulp virgin oil	1	Skin and hair moisturizing; anti-dandruff and for hair growing; foods and beverages preparations (pataua "wine"); anti-cancer [100]	Total lipids, total carotene, fatty acids; [49] TAGs, Δ^5-avenasterol, stilbenes, phenolic acids, condensed tannins; [32] Phenolic composition, antioxidant activity; [101] vitamins, anthocyanins [102]
Pracaxi	*Pentaclethra Filamentosa*	Seed virgin oil	2	Skin treatments against erysipelas, burns and stretch marks; [103,104]	Behenic acid; [32] fatty acids [100]
Tucuma	*Astrocaryum vulgare, Arecaceae*	Nut virgin butter and pulp virgin oil	2 (butter); 1 (oil)	Powerful skin and hair moisturizing; foods and beverages preparations; antihyperglycemic;[105] biodiesel production[106]	Total lipids, total carotene, total steroids, fatty acids; [49,107,108] total protein, carbohydrates,TAGs; [107] tocopherols, carotenoids, phytosterols [109]
Ucuuba	*Virola sebifera*	Virgin butter	2	Skin treatment; [110] the best substitute for beef tallow and petrolatum; used for treatment of rheumatism, arthritis, cramps, mouth sores and hemorrhoids; [111]antiviral [112]	Fatty acids, lignans (aryltetralone dibenzylbutyrolactone arylindan, furofuran, etc); [32,113,114] TAGs; [38] triacontane, tetratriacontane [115]

The quantification of fatty acids by GC is the most usual methodology for lipid profile characterization. For all analyzed samples of oils and butters, the total ester content ranged from 85 to 103%, confirming the high saponifiable lipid content. Table 3 presents the average results obtained for the percentage of each FAME found in the Amazon samples and Table 4 presents the approximated amount of saturated, monounsaturated and polyunsaturated fats in the samples, which is an important data specially for the food industry. The results show the average profile of fatty acids distribution, which differs principally according to the species. Note the presence of medium chain saturated fatty acids in butter samples of babassu, murumuru, and tucuma butter, as well as the high content of oleic acid (C18:1) in the samples of açaí, andiroba, bacaba-de-leque, graviola,

buriti, patauá and oil of tucuma oil. This is an interesting aspect, as it is known that the intake of monosaturated fats brings benefits to human health, and this is also a common feature of olive oils. [116] There is a remarkable difference between the tucuma oil and its butter, even though they are from the same species, as the butter is extracted from the seeds and the oil from the pulp. This fact shows a different lipid accumulation profile in different parts of the fruits.

Table 3. Fatty acids profile in Amazon oils and butters determined by GC-MS

Samples	% FAME (g / 100 g)*													
	C8:0	C10:0	C12:0	C14:0	C16:0	C16:1	C18:0	C18:1	C18:2	C18:3	C20:0	C20:1	C22:0	C24:0
Açaí			2	1	25	4	2	57	9	1				
Andiroba					27	1	9	52	9	2				
Babassu		2	45	17	10		3	19	4					
Bacaba-de-leque					23	1	2	53	20	1				
Bacuri			1	2	60	7	1	28	2					
Buriti					17		2	79	2	1				
Brazil nut					15		12	41	32					
Cupuaçu					7		36	39	3		12	<1	2	
Graviola					21	1	6	41	28	1	1			
Murici					10		8	38	42		1			
Murumuru		1	45	31	8		3	8	3					
Patawa			1	1	11	<1	6	76	5	1				
Pracaxi					2		4	52	11		1	2	17	11
Tucuma (butter)	1	2	51	28	6		3	7	3					
Tucuma (oil)			2	2	25		4	61	3	2				
Ucuuba			16	74	5	<1	1	4	1					

Table 4. Saturated, monounsaturated and polyunsaturated fat distribution in Amazon oils and butters

Samples	% (g / 100 g)		
	Saturated fat	Monounsaturated fat	Polyunsaturated fat
Açaí	29	61	10
Andiroba	36	53	11
Babassu	78	19	4
Bacaba-de-leque	25	54	21
Bacuri	64	34	2

Buriti	18	79	3
Brazil nut	27	41	32
Cupuaçu	57	40	3
Graviola	28	43	29
Murici	20	38	42
Murumuru	88	8	4
Patawa	18	76	6
Pracaxi	35	54	11
Tucuma (butter)	90	10	0
Tucuma (oil)	33	62	5
Ucuuba	95	4	1

The quantification of fatty acids is the standard approach to obtain a simplified profile of the samples. However, the intact TAG analysis in native form offers more information about the oils composition and can reveal a more characteristic profile for each sample. Moreover, by reducing the major components analysis to the simple fatty acid profile determination, some information can be lost, because when a wide variety of species is considered, which is the case of this work, the fatty acids profile may provide unclear answers to describe a more specific profile for each samples.

In TAG molecules, the fatty acids are 3 by 3 transesterified with the glycerol molecule. Therefore, for a given set of fatty acids, there is a much greater number of possible precursor TAGs. Thus, the TAG analysis provides a greater volume of information regarding the oil composition. Besides, the direct analysis of intact TAGs excludes the sample derivatization step, which is laborious, chemicals and time consuming. TAGs can be AAA type, when all the fatty acids are the same; ABA or AAB when they have two different fatty acids; or ABC, ACB or BAC when the 3 acyl groups are different. In the first case, only one fragment due to a neutral loss of acyl group will be detected, in the second case, two fragments, and for the last case, 3. If more than 3 fragments are detected, more than one TAG isomer is present in a given selected precursor ion. [117]

The use of ammonium bicarbonate as an additive for ESI ionization also helped the TAGs detection and in the interpretation of the results, as there was practically only the formation of ammonium adducts (avoiding the formation of other adducts such as sodium or the TAGs protonated molecule). Moreover, the formation of ions with even *m/z*

ratios facilitates the detection of TAGs, differentiating them from other classes of substances also present in the samples, such as minor compounds or background ions.

Samples of the same species, but different lots (year of production) also presented an identical spectral profile (mass spectra for duplicated samples are shown in supporting information), indicating that the TAG profile is in fact a signature for each Amazon species. The ESI(+)-QTOF mass spectra present a great complexity due to the large structural variability of the TAGs molecules. Thus, the MS/MS analysis of the main detected ions in the samples was performed, in order to elucidate the composition of the TAGs in each sample.

The product ion mass spectra obtained via CID for each TAG ion detected in the samples were compared to LIPID MAPS database. The fragmentation of TAG molecules is ordered (it does not differ from one TAG to the other, always following the same major pathways) and its mechanism is well known.[118] Each ammonium adduct of a single TAG molecule generates eighteen possible ions after fragmentation: one precursor ion $[M+NH_4]^+$ plus seventeen fragments, being the ones of neutral loss of the acyl radicals the major fragments detected in the MS/MS spectra of a TAG. For the unambiguous identification through the comparison with the LIPID MAPS database some filters were considered: minimum of 10 out of 18 ions detected; all the 3 fragments due to the acyl radical neutral loss, and at least two more fragments for each of the three radicals in *sn*1, *sn*2 and *sn*3. In this way, it is possible to obtain information about the composition of each acyl radical present in a particular TAG ion. On the other hand, it is not possible to state the position in which they are bound in the precursor TAG molecule, nor the double bonds *E/Z* stereochemistry and its position in the acyl chain.

It was possible to perform the characterization of the most abundant TAG ions, as well as the TAG ions with relative abundances of less than 0.1%. As proof-of-concept, an ultra-comprehensive TAG identification was performed for açaí oil, pracaxi oil and ucuuba butter and the results are electronically available in supporting information in spreadsheets. For instance, it was possible to characterize 76 different TAGs in pracaxi oil, 71 in ucuuba butter and 26 in açaí oil. However, in this work, only the top 10 most abundant ions for each sample will be described, as it corresponds from 70 to 98% of the total TAGs in the samples.

It should be highlighted the high occurrence of isomers: at least 2 TAGs with different acyl radicals compositions were detected in each fragmented ion. This number came to be up to 10 different isomeric TAGs for some TAG precursor ions. It is expected that there are even more possible isomers, which are not being reported after the filtering criteria used for identification in LIPID MAPS. It is also interesting to note that the MS/MS mass spectrum of the same TAG in different samples may vary or not. Figure 1 shows the product ion scan for the TAG of *m/z* 628.7 in three different samples: Fig. 1a tucuma butter, Fig.1b babassu butter and Fig. 1c murumuru butter. Note that the *m/z* 628.7 MS/MS spectra for all samples are quite similar, being the relative abundances for the fragments of *m/z* 383.3, 411.3, 439.3 and 467.4 almost identical, indicating that probably these TAGs are the same and in approximated equal abundances in these different samples. However, Figure 2 shows the MS/MS mass spectra for the ion of *m/z* 902.8 (the inserted zooms in the mass spectrum from *m/z* 600 to 606 allow to better observe the main fragments). Note that the relative abundances of the fragments with *m/z* 601.5, 603.5 and 605.5 differ more for one sample to another, indicating that the proportion of TAG isomers are not the same in these three distinct samples. It means that the isomer TG(18:1_18:1_18:1) is more abundant than the other isomers in tucuma oil (Fig. 2a), while other TAGs as TG(18:0_18:1_18:2) were detected by their fragments (*m/z* 601.5 and 605.5) with higher relative abundances in murici (Fig. 2b) and graviola oils (Fig. 2c).

The representative full scan ESI(+)-QTOF mass spectrum for each Amazon oils and butters, as well the identification of the principal TAGs and their relative abundances are reported in the following sections for each sample considering: the *m/z* of the $[M+NH_4]^+$ precursor ion (experimental and theoretical), its relative abundance (in low energy mass spectrum), the nominal *m/z* of the fragments detected in the MS/MS spectrum, the number of fragments detected by comparison with the LIPID MAPS. The fragments are also obtained with high resolution and accuracy, with an average mass error bellow 20 ppm, but are reported with only one decimal place to avoid excess of information in the tables.

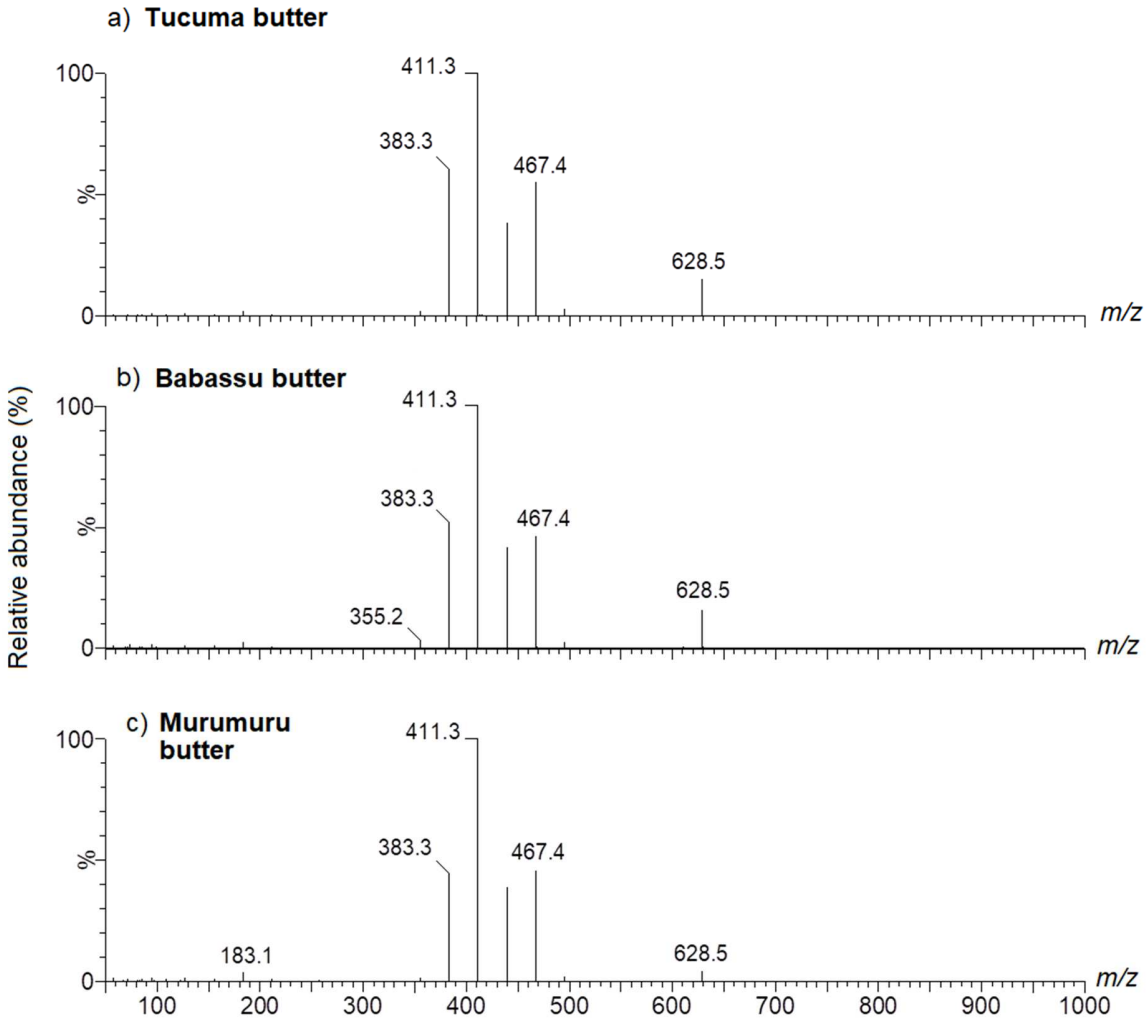

Figure 1. ESI(+)-MS/MS product ion scan via CID for the precursor ion of *m/z* 628.5 of a) tucuma, b) babassu and c) murumuru butters.

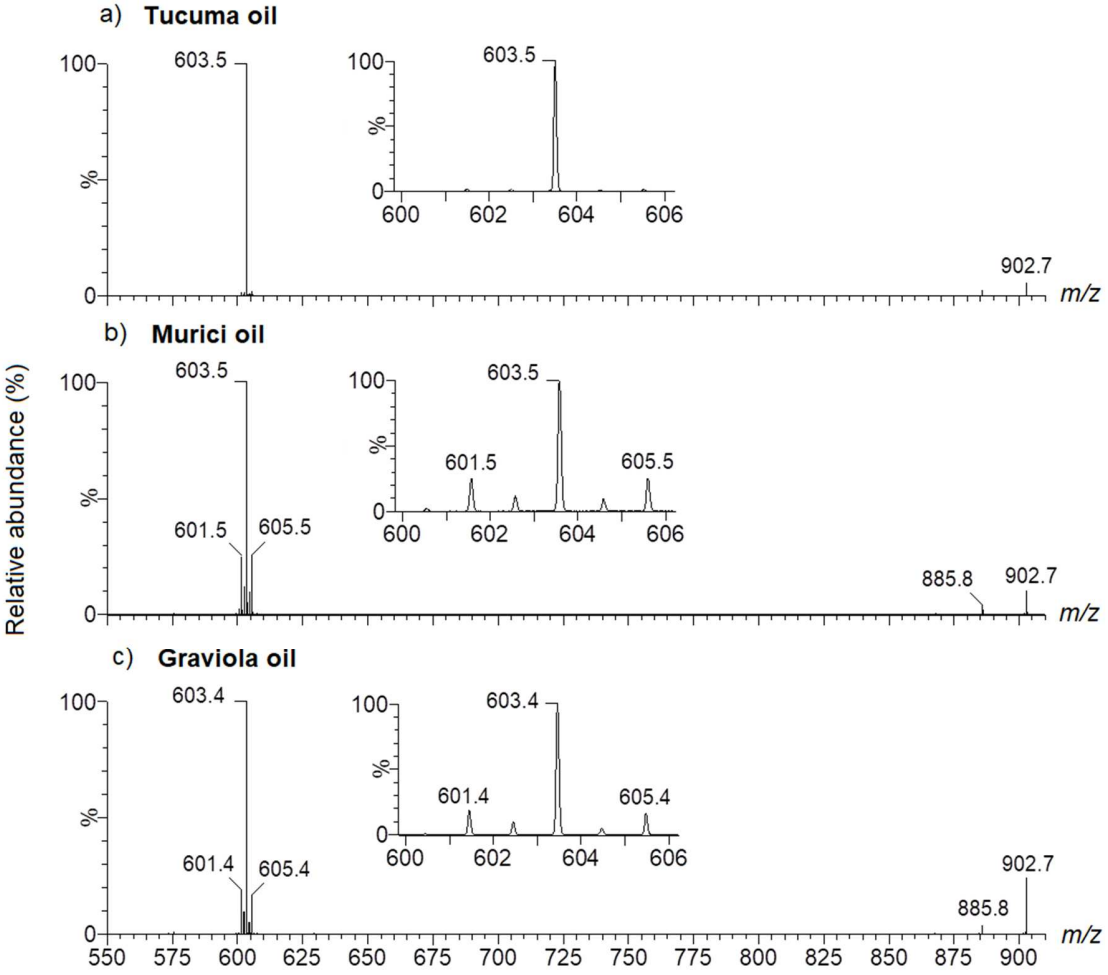

Figure 2. ESI(+)-MS/MS product ion scan via CID for the precursor ion of *m/z* 902.7 of a) tucuma, b) murici and c) graviola oils.

Açaí oil

Figure 3 shows a representative full scan ESI(+)-QTOF mass spectrum of açaí oil. The principal TAGs ions are present from *m/z* 840 to 910, and some DAG detected in *m/z* from 550 to 650. The fatty acids composition for açaí oil is on average C12:0 (2%), C14:0 (1%), C16:0 (25%), C16:1 (4%), C18:0 (2%), C18:1 (57%), C18:2 (9%) and C18:3 (1%), as shown in Table 5, as well as all the identified TAGs.

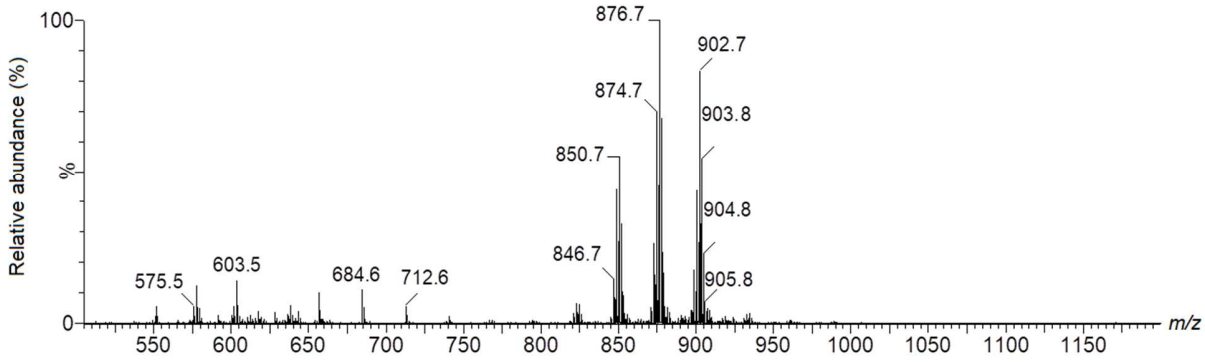

Figure 3. Representative full scan ESI(+)-QTOF mass spectrum of açaí oil.

In total, 20 different TAGs constitute the top 10 most abundant ions, and they account to 98.1% of the total TAGs ions abundances. All the TAGs are mainly formed by the previously mentioned fatty acids. The most abundant ions, *m/z* 876.7 and 902.7, are TG(16:1_18:0_18:1), TG(18:2_16:0_18:0) and TG(18:1_16:0_18:1); and triolein - TG(18:1_18:1_18:1) - and its isomer TG(18:1_18:2_18:0), respectively. Açaí is a high oleic acid and, indeed, this fatty acid is present in most of the identified TAGs.

1 **Table 5**. Identification of the principal TAGs of açaí oil and their relative abundances (%)

Experimental *m/z* $[M+NH_4]^+$	Theoretical *m/z* $[M+NH_4]^+$	Detected fragments (CE 25-30 eV)	Number of detected fragments per TAGs	Identified TAGs	Relative abundance (%)
848.7726	848.7702	848.77; 831.7; 813.7; 577.5; 575.5; 549.5; 339.3; 321.3; 313.3; 311.3; 295.3; 293.2; 265.3; 263.2; 247.2; 245.2; 239.2; 237.2; 221.22; 219.2	18; 18	TG(16:0_16:1_18:1); TG(16:0_16:0_18:2)	2.9
850.7859	850.7858	833.8 815.7; 577.5; 551.5; 339.28; 321.3; 313.3; 295.3; 265.3; 247.3; 239.2; 221.2	18	TG(18:1_16:0_16:0)	4.1
872.7675	872.7702	855.7; 855.7; 601.5; 575.5; 573.4; 339.2; 337.2; 321.2; 319.2; 311.2; 293.2; 265.2; 263.2; 247.2; 245.2; 237.2; 219.2; 335.2; 317.2; 313.2; 295.2; 261.2; 243.2; 239.2; 221.2	18; 18; 18	TG(16:1_18:2_18:1); TG(18:3_16:0_18:1); TG(18:2_18:2_16:0)	7.2
874.7805	874.7858	857.7; 839.7; 601.5; 577.5; 575.5; 339.2; 337.2; 321.2; 319.2; 313.2; 295.2; 265.2; 263.2; 247.2; 245.2; 239.2; 221.2; 603.5; 311.2; 293.2; 237.2; 219.2	18;18	TG(18:2_18:1_16:0); TG(18:1_16:1_18:1)	11.1
876.7939	876.8015	859.8; 841.8; 605.6; 577.5; 575.5; 341.3; 339.3; 323.3; 321.3; 311.3; 293.2; 267.3; 265.3; 249.3; 247.3; 237.2; 219.2; 603.5; 579.5; 337.3; 319.3; 313.3; 295.3; 263.2; 245.2; 239.2; 221.2	18; 18; 18	TG(16:1_18:0_18:1); TG(18:2_16:0_18:0); TG(18:1_16:0_18:1)	16.3
896.7657	896.7702	879.7; 861.7; 601.5; 599.5; 597.4; 339.3; 337.3; 335.3; 321.3; 319.3; 317.2; 265.3; 263.2; 261.2; 247.2; 245.2; 243.2	18	TG(18:3_18:1_18:2)	5.6
898.7744	898.7858	881.75; 863.7; 603.5; 599.50; 339.28; 321.27; 317.24; 265.2; 261.2; 247.2; 245.2; 243.2; 337.3; 319.3; 263.2; 245.2	18;18	TG(18:1_18:3_18:1); TG(18:2_18:1_18:2)	9.5
900.7914	900.8015	883.8; 865.8; 603.5; 601.5; 339.3; 337.3; 321.3; 319.3; 319.3; 263.2; 247.2; 247.2; 605.5; 245.2; 599.5; 341.3; 335.2; 317.2; 267.26; 261.2; 249.2; 247.2; 243.2	18; 17	TG(18:1_18:1_18:2); TG(18:0_18:1_18:3)	13.0

902.8036	902.8171	885.79; 867.78; 603.5; 339.28; 321.27; 265.25; 247.24; 605.55; 601.5; 341.3; 337.27; 323.29; 319.26; 267.26; 263.2; 249.25; 247.2; 245.2	18; 18	TG(18:1_18:1_18:1); TG(18:1_18:2_18:0)	19.4
904.8238	904.8328	887.8; 869.79; 605.5; 603.5; 341.3; 339.28; 323.29; 321.27; 267.26; 265.25; 249.25; 247.2; 607.56; 337.27; 319.26; 263.2; 245.2	18; 18	TG(18:0_18:1_18:1); TG(18:2_18:0_18:0)	9.0
				TOTAL	98.1

Andiroba oil

Figure 4 shows a representative full scan ESI(+)-QTOF mass spectrum of andiroba oil. The principal TAGs ions are present from *m/z* 810 to 910, and the DAGs in this sample were detected in a considerably high abundance in *m/z* from 550 to 650. The fatty acids composition for andiroba oil is on average C16:0 (27%), C16:1 (1%), C18:0 (9%), C18:1 (52%), C18:2 (9%) and C18:3 (2%), as shown in Table 5.

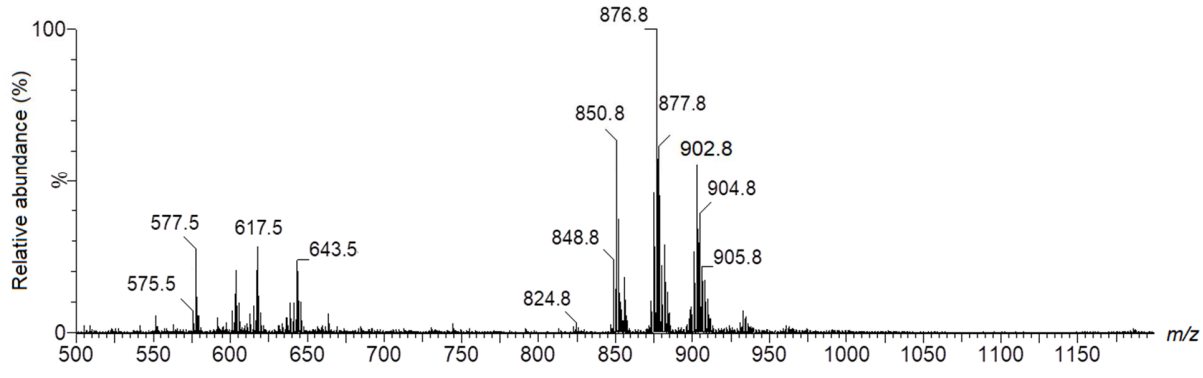

Figure 4. Representative full scan ESI(+)-QTOF mass spectrum of andiroba oil.

All the identified TAGs in andiroba oil are reported in Table 6. In total, 21 different TAGs compose the top 10 most abundant TAG ions, and they account to approximately 90.6% of the total TAGs ions abundances. All the TAGs are mainly formed by the above mentioned fatty acids, but few TAGs also presented the fatty acids C20:0 and C22:1, as observed for the TAGs TG(16:1_20:0_18:1), TG(18:1_20:0_16:0), and

TG(22:1_16:0_16:0). The most abundant ions, *m/z* 850.7 and 876.7, are TG(16:0_18:1_16:0), and TG(16:0_18:1_18:1) and TG(18:2_16:0_18:0), respectively. Andiroba is also high oleic acid oil and, indeed, this fatty acid is presented in the majority of the identified TAGs, followed by TAGs with C16:0, combined in the TAGs in multiple ways and forming different isomers as it could be detected. Triolein - TG(18:1_18:1_18:1) - and its isomer TG(18:1_18:2_18:0) were also identified in andiroba oil.

Table 6. Identification of the principal TAGs of andiroba oil and their relative abundances (%)

Experimental *m/z* $[M+NH_4]^+$	Theoretical *m/z* $[M+NH_4]^+$	Detected fragments (CE 25-30 eV)	Number of detected fragments per TAGs	Identified TAGs	Relative abundance (%)
848.7665	848.7702	831.7; 813.7; 577.5; 575.5; 551.5; 549.5; 339.3; 337.3; 319.3; 313.3; 311.2; 265.3; 263.2; 245.2; 239.2; 237.2; 221.2	16; 13	TG(18:2_16:0_16:0); TG(16:1_18:1_16:0)	5.1
850.7778	850.7858	833.75; 815.7; 577.5; 551.5; 339.3; 321.27; 313.2; 295.26; 265.2; 247.2; 239.2; 221.2	18	TG(16:0_18:1_16:0)	13.3
872.7686	872.7702	855.7; 837.7; 601.5; 599.5; 577.5; 575.5; 573.48; 337.3; 319.26; 317.2; 313.27; 265.2; 263.2; 261.2; 247.2; 245.2; 243.2; 239.2; 221.2	17; 15	TG(16:0_18:2_18:2); TG(18:3_16:0_18:1); TG(18:2_18:1_16:1); TG(18:2_18:1_16:1)	2.3
874.7788	874.7858	857.75; 839.7; 603.5; 601.5; 577.5; 575.5; 339.3; 337.3; 321.3; 319.3; 313.3; 311.2; 265.2; 263.2; 247.2; 245.2; 239.2	16; 15	TG(18:2_18:1_16:0); TG(16:1_18:1_18:1)	9.8
876.7791	876.8015	859.8; 841.8; 603.5; 579.5; 577.5; 575.5; 341.3; 339.3; 321.3; 319.2; 313.3; 265.3; 263.2; 247.2; 245.2; 239.2; 221.2	17; 14	TG(16:0_18:1_18:1); TG(18:2_16:0_18:0)	21.2
878.8022	878.8171	861.8; 843.8; 607.6; 605.55; 579.5; 577.5; 341.3; 339.3; 323.3; 321.3; 313.3; 311.3; 267.3; 265.3; 249.3; 247.2; 239.2; 221.2; 219.2	17; 16	TG(18:0_18:1_16:0); TG(18:0_18:0_16:1)	9.6

900.7949	900.8015	883.8; 865.8; 605.6; 603.5; 601.5; 599.5; 341.3; 339.3; 337.3; 335.3; 323.3 321.3; 319.3; 317.2; 265.6; 263.2; 261.2; 247.2; 245.2; 243.2	18; 16	TG(18:1_18:2_18:1); TG(18:3_18:1_18:0)	5.7
902.809	902.8171	885.8; 867.8; 605.6; 603.5; 601.5; 339.3; 337.3; 321.3; 319.3; 267.3; 265.3 263.2; 247.2; 245.2	18; 16	TG(18:1_18:1_18:1); TG(18:0_18:1_18:2)	11.9
904.8232	904.8328	887.8; 869.8; 633.6; 607.6; 605.6; 603.5; 575.5; 369.3; 341.3; 339.3; 337.3; 323.3; 321.3; 319.3; 293.2; 277.3; 267.3; 265.3; 263.2; 249.3; 247.3; 245.2; 237.2	18; 18; 14	TG(18:1_18:0_18:1); TG(18:0_18:2_18:0); TG(16:1_20:0_18:1)	8.3
906.8435	906.8484	889.8; 871.8; 633.6; 607.6; 605.6; 577.5; 551.5; 341.3; 339.3; 323.3; 321.3; 313.3; 303.3; 295.3; 277.3; 267.3; 265.3; 249.3; 247.2; 239.2; 221.2	18; 17; 16	TG(18:0_18:1_18:0); TG(18:1_20:0_16:0); TG(22:1_16:0_16:0)	3.6
				TOTAL	90.6

Babassu butter

The ESI(+)-QTOF mass spectrum of babassu butter is shown in Figure 5. As babassu fatty acids profile is C10:0 (2%), C12:0 (45%), C14:0 (17%), C16:0 (10%), C18:0 (3%), C18:1 (19%) and C18:2 (4%), as shown in Table 3, it is expected that the babassu TAGs appear in a lower *m/z* range compared to the preciously discussed oils. In fact, the main TAGs are in the range of *m/z* from 500 to 900.

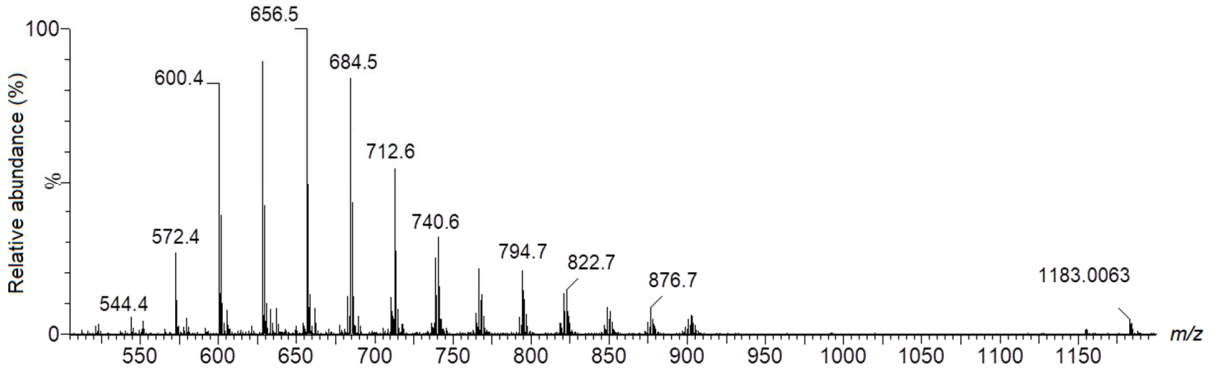

Figure 5. Representative full scan ESI(+)-QTOF mass spectrum of babassu butter.

Note in Table 7, a higher occurrence of isomers for each TAG $[M+NH_4]^+$ ion, in which the top 10 most abundant TAG ions accounts to approximately 78.6% of the total TAGs ions abundances, and 38 different TAGs were identified. This may be due to the higher number of different fatty acids, which obviously leads to several isomers possibilities. Fig. 1b shows the MS/MS spectrum of the precursor ion of *m/z* 628.5, in which a least six different fragments due to the neutral loss of an acyl group can be easily observed. In fact, at least six different TAG isomers were identified in this precursor ion, as reported in Table 6. Most of the identified TAGs are composed by the fatty acids reported in Table 3, but also some less abundant TAGs containing C6:0, C8:0, C14:1 and C20:0 were also detected. We can observe all the combinations of fatty acids forming a wider variety of TAGs. The base peak of *m/z* 656.5 is characterized as a mixture trilaurin - TG(12:0_12:0_12:0) – with several other isomers identified by their different fragments, as TG(10:0_14:0_12:0), TG(16:0_12:0_8:0), TG(16:0_10:0_10:0) and TG(20:0_6:0_10:0), all in the same precursor ion. Babassu is a high lauric acid butter, and in fact, the most abundant TAGs are composed mainly by this fatty acid in at least one of the sn glycerol position. The occurrence of TAGs with oleic acid in babassu butter increases with the TAG molecular mass.

Table 7. Identification of the principal TAGs of babassu oil and their relative abundances (%)

Experimental *m/z* $[M+NH_4]^+$	Theoretical *m/z* $[M+NH_4]^+$	Detected fragments (CE 25-30 eV)	Number of detected fragments per TAGs	Identified TAGs	Relative abundance (%)
572.4884	572.4885	555.5; 537.4; 439.4; 411.3; 383.3; 355.3; 257.2; 229.2; 211.2; 201.2; 183.2; 165.2; 155.1; 127.1; 109.1; 99.1; 81.1	16; 15	TG(8:0_12:0_10:0); TG(6:0_12:0_12:0)	3.9
600.5139	600.5198	583.5; 467.4; 439.4; 411.3; 383.3; 355.3; 285.2; 257.2; 211.2; 201.2; 183.2; 165.2; 155.1; 127.1; 109.1; 99.1; 81.1	15; 13; 13	TG(12:0_8:0_12:0); TG(8:0_14:0_10:0); TG(14:0_12:0_6:0)	12.1
628.5420	628.5511	611.5; 593.5; 495.4; 467.4; 439.4; 411.3; 383.3; 355.3; 341.3; 327.3; 323.3; 313.3; 295.3; 285.3; 267.2; 257.2; 239.2; 229.2; 211.2; 201.1; 193.2; 183.2; 165.2; 155.1; 137.1; 127.1; 109.1; 99.1; 81.1	18; 18; 18; 17; 17	TG(8:0_12:0_14:0); TG(14:0_10:0_10:0); TG(10:0_12:0_12:0); TG(10:0_16:0_8:0); TG(14:0_14:0_6:0); TG(18:0_8:0_8:0)	13.2
656.5691	656.5824	639.6; 523.5; 495.4; 467.4; 439.4; 411.3; 383.3; 351.3; 327.2; 257.2; 239.2; 229.2; 211.2; 183.2; 165.2; 155.2; 137.1; 99.1; 81.1	17; 14; 14; 14; 13	TG(12:0_12:0_12:0); TG(10:0_14:0_12:0); TG(16:0_12:0_8:0). TG(16:0_10:0_10:0); TG(20:0_6:0_10:0)	14.7
684.6163	684.6137	523.5; 495.4; 467.4; 439.4; 411.4 383.3; 285.2; 267.2; 257.2; 249.2; 239.2; 229.2; 201.1; 211.2; 183.2; 165.2; 155.1; 137.1; 109.1	15; 14; 14; 14; 13	TG(12:0_12:0_14:0); TG(10:0_18:0_10:0); TG(8:0_18:0_12:0); TG(14:0_14:0_10:0); TG(16:0_10:0_12:0)	12.3
712.6417	712.6450	695.6; 523.5; 495.4; 467.4; 439.4; 411.3; 313.3; 295.3 295.3; 285.2; 267.2; 257.2; 239.2; 229.2; 221.2; 211.2; 183.2; 165.2; 155.1; 137.1	17; 16; 14	TG(16:0_12:0_12:0); TG(16:0_10:0_14:0); TG(18:0_12:0_10:0)	7.9
738.6608	738.6606	695.6; 577.5; 523.5; 495.4; 493.4; 467.4; 465.4; 439.4; 411.3; 339.3; 313.3; 295.3; 285.2; 267.2; 265.3; 257.2; 239.2; 229.2; 221.2; 211.2; 209.2; 191.2; 183.2; 165.2; 155.1; 137.1; 127.1; 109.1	13; 13; 13; 12; 12	TG(12:0_18:1_12:0); TG(12:0_16:0_14:1); TG(10:0_14:0_18:1); TG(18:1_8:0_16:0); TG(14:1_14:0_14:0)	3.6
740.6744	740.6763	723.6; 579.5; 523.5; 495.4; 467.4; 439.4; 341.3; 313.3; 267.3; 257.2; 239.2; 211.2; 183.3; 109.1	13; 12; 11; 11	TG(18:0_12:0_12:0); TG(12:0_16:0_14:0); TG(14:0_14:0_14:0); TG(8:0_18:0_16:0)	4.7

766.6925	766.6919	749.7; 731.7; 605.6; 577.5; 549.5; 521.4; 493.4; 467.4; 465.4; 341.3; 339.3; 321.3; 285.2; 265.2; 257.2; 249.3; 247.2; 239.2; 211.2; 183.1; 155.1 137.1; 127.1117 109.1	15; 15; 14	TG(8:0_18:1_18:0); TG(14:0_18:1_12:0); TG(18:1_10:0_16:0)	3.1
794.7233	794.7232	777.7; 605.6; 577.5; 549.5; 521.5; 495.4; 493.4; 339.3; 313.3; 285.2; 267.2; 265.3; 257.2; 249.3; 247.2; 239.2; 229.2; 221.2; 211.2; 183.2; 165.2; 155.1	15; 14; 13	TG(12:0_16:0_18:1); TG(14:0_14:0_18:1); TG(10:0_18:1_18:0)	3.0
				TOTAL	78.6

Bacaba oil

Figure 6 shows a representative full scan ESI(+)-QTOF mass spectrum of bacaba-de-leque oil. Note that the mass spectrum profile for this oil is very similar to the açaí mass spectrum (Fig. 3), as their fatty acid distribution is quite similar as well, being C16:0 (23%), C16:1 (1%), C18:0 (2%), C18:1(53%), C18:2 (20%) and C18:3 (1%) for bacaba oil, as shown in Table 3.

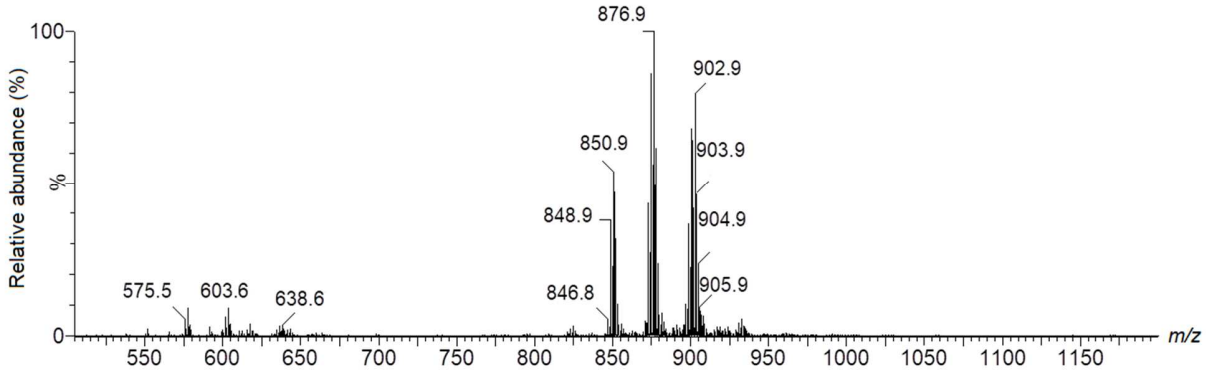

Figure 6. Representative full scan ESI(+)-QTOF mass spectrum of Bacaba oil.

For bacaba-de-leque oil, 26 different TAGs were identified in the top 10 most abundant ions in this sample that totalized 95.5% of all TAGs ions detected. This sample is also a high oleic acid oil, and all its TAGs are described in Table 8. As expected, the majority of the TAGs are mixtures of the reported fatty acids and in only in *m/z* 904.8 two

isomeric TAGs - TG(18:1_20:1_16:0) and TG(18:2_20:0_16:0) - presented C20:1 and C20:0 in their composition, but their fragments have low abundances in the MS/MS spectrum. Also for the base peak of *m/z* 902.8, in addition to triolein, 3 other isomers were also detected: TG(18:1_22:1_14:1), TG(18:1_18:0_18:2) and TG(18:3_18:0_18:0), and two of them without any oleic acid in the composition, which shows the importance of fragmentation to proper characterize and identify the native TAGs in oils. The presence of fatty acids C22:1 and C14:1 was also detected, but with low abundances as well.

Table 8. Identification of the principal TAGs of bacaba oil and their relative abundances (%)

Experimental *m/z* $[M+NH_4]^+$	Theoretical *m/z* $[M+NH_4]^+$	Detected fragments (CE 25-30 eV)	Number of detected fragments per TAGs	Identified TAGs	Relative abundance (%)
748.7661	848.7702	831.8; 813.7; 575.5; 551.5; 319.3; 313.3; 295.3; 263.2; 245.2; 239.2	15	TG(16:0_18:2_16:0)	6.7
850.7798	850.7858	815.7; 577.5; 551.5; 339.3; 321.3; 313.3; 265.3; 247.2; 239.2; 221.2	15	TG(18:1_16:0_16:0)	9.6
872.7633	872.7702	855.7; 837.7; 601.5; 599.5; 577.5; 575.5; 573.5; 339.3; 337.3; 335.3; 321.3; 319.3; 317.2; 313.3; 311.3 293.2; 265.3; 263.2; 261.2; 247.2; 245.2; 243.2; 239.2; 221.2	17; 17; 17	TG(18:1_18:3_16:0); TG(18:2_18:2_16:0); TG(18:2_16:1_18:1)	7.7
874.7723	874.7858	857.7; 839.7; 603.5; 601.5; 579.5; 577.5; 575.5; 573.5; 339.3; 335.3; 337.3; 323.3; 321.3; 319.2; 313.3; 311.3; 295.3; 267.3; 265.3; 263.2; 261.2; 249.3; 247.2; 245.2; 243.2; 239.2; 237.2; 221.2; 219.2	18; 17; 16: 16	TG(16:0_18:2_18:1); TG(16:1_18:1_18:1); TG(18:2_18:0_16:1); TG(18:3_18:0_16:0)	15.3
876.7785	876.8015	859.8; 841.8; 605.5; 603.5; 579.5; 577.5; 575.5; 341.3; 339.3; 337.3; 323.3; 321.3; 319.3; 313.3; 311.3; 295.3; 293.2; 267.3; 265.3; 263.2; 249.6; 247.2; 245.2; 239.2; 237.2; 221.2; 219.2	18; 18; 18	TG(18:1_18:0_16:1); TG(18:1_16:0_18:1); TG(18:2_16:0_18:0)	17.8

898.7770	898.7858	881.8; 863.7; 603.5; 601.5; 599.5; 339.3; 337.3; 335.2; 321.3; 319.2; 317.2; 265.2; 263.2; 261.2; 247.2; 245.2; 243.2	18; 18	TG(18:1_18:3_18:1); TG(18:1_18:2_18:2)	6.5
900.7914	900.8015	900.8; 883.8; 605.5; 603.5; 601.5; 599.5; 341.3; 339.3; 337.3; 335.2; 323.3; 321.3; 319.3; 265.3 263.2; 261.2; 249.3; 247.2; 245.2	17; 17; 16	TG(18:1_18:2_18:1); TG(18:2_18:2_18:0); TG(18:0_18:3_18:1)	12.2
902.8090	902.8171	885.8; 867.8; 659.6; 607.6; 605.5; 603.5; 601.5; 547.5; 395.3; 377.3; 341.3; 339.3; 337.3; 335.3; 323.3; 321.3; 319.3; 317.2; 303.3; 283.2; 267.3; 265.3; 263.2; 261.2; 249.3; 247.2; 245.2; 209.2; 191.2	18; 18; 18; 17	TG(18:1_18:1_18:1); TG(18:1_22:1_14:1); TG(18:1_18:0_18:2); TG(18:3_18:0_18:0)	14.2
904.8221	904.8328	887.8; 631.6; 607.6; 605.6; 603.5; 577.5; 575.5; 369.3; 351.3; 349.3; 341.3; 339.3; 337.3 323.3; 321.3; 319.3; 313.3; 293.3; 277.3; 275.3; 267.3; 265.3; 263.2; 247.2; 249.3; 247.2; 245.2; 239.2; 221.2	17; 17; 15; 15	TG(18:1_18:0_18:1); TG(18:0_18:0_18:2) ; TG(18:1_20:1_16:0); TG(18:2_20:0_16:0)	4.2
903.8385	906.8484	607.6; 605.6; 341.3; 339.3; 323.3; 321.3; 267.3; 265.3; 249.3; 247.2	16	TG(18:0_18:0_18:1);	1.2
				TOTAL	95.5

Bacuri butter

A representative full scan ESI(+)-QTOF mass spectrum of bacuri butter is presented in Figure 7. Differently from the babassu butter, the TAGs in bacuri butter are mainly distributed in the range of *m/z* from 810 to 910, which is a region of TAGs in the previously described oils. However, it is also possible to detect the TAG ions of *m/z* 656.5, 684.6 and 712.6 also present in babassu butter. Nevertheless, the bacuri butter is a high palmitic acid sample, presenting the fatty acid composition of C12:0 (1%), C14:0 (2%), C16:0 (60%), C16:1 (7%), C18:0 (1%), C18:1 (28%) and C18:2 (2%), as reported in Table 3. Note that what makes bacuri a butter is the higher proportion of palmitic acid.

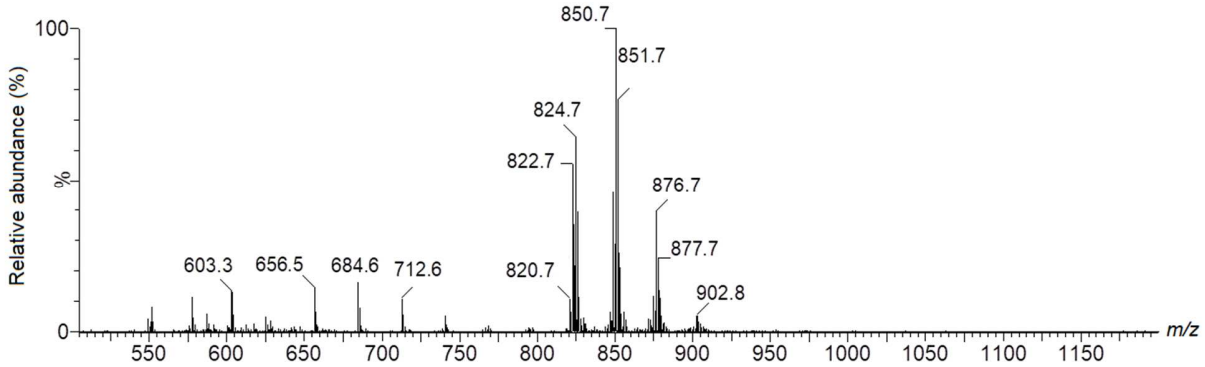

Figure 7. Representative full scan ESI(+)-QTOF mass spectrum of bacuri butter.

All the identified TAGs in bacuri butter are reported in Table 9. In total, 25 different TAGs composes the top 10 most abundant ions, and they account to a total of 94.9% of the total TAGs ions abundances. All the TAGs are mainly formed by the previously mentioned fatty acids, but several other TAGs displayed different fatty acids in their compositions, as in the TAGs such as TG(26:0_6:0_6:0), TG(22:0_8:0_8:0), TG(8:0_22:0_10:0), TG(20:1_12:0_16:1) and TG(18:1_20:0_14:1), but all in relatively low abundances. The base peak of *m/z* 850.7 is a mixture of TG(18:0_16:1_16:0), TG(16:0_16:0_18:1) and TG(20:0_12:0_18:1), this last one being the less abundant TAG, based on its fragments intensities. The tripalmitin TG(16:0_16:0_16:0) in *m/z* 824.4 was the only TAG detected for this precursor ion, with a relative abundance of approximately 20%.

Table 9. Identification of the principal TAGs of bacuri butter and their relative abundances (%)

Experimental *m/z* $[M+NH_4]^+$	Theoretical *m/z* $[M+NH_4]^+$	Detected fragments (CE 25-30 eV)	Number of detected fragments per TAGs	Identified TAGs	Relative abundance (%)
684.6162	684.6137	551.5; 523.5; 467.4; 453.4; 439.4; 435.4; 379.4; 361.4; 327.3; 305.3; 285.2; 271.2; 257.2; 239.2; 211.2; 201.1; 193.2; 183.2; 165.2; 155.1; 127.1; 109.1; 99.1; 81.1	15; 14; 14	TG(14:0_12:0_12:0); TG(26:0_6:0_6:0); TG(22:0_8:0_8:0)	1.5

712.6461	712.6450	551.5; 523.5; 495.4; 467.4; 439.4; 397.4; 379.4; 355.3; 323.3; 313.3; 305.3; 295.3; 257.2; 239.2; 211.2; 183.2; 137.1; 109.1	13; 12; 10	TG(12:0_12:0_16:0); TG(8:0_22:0_10:0); TG(16:0_14:0_10:0)	2.3
820.739	820.7389	803.7; 785.7; 603.5; 575.5; 549.5; 547.5; 521.5; 493.4; 367.3; 339.3; 313.3; 311.3; 293.2; 265.3; 257.2; 239.2; 237.2; 237.2; 221.2; 219.2; 211.2; 183.2	17; 15; 13	TG(16:1_16:0_16:1); TG(20:1_12:0_16:1); TG(16:1_14:0_18:1)	2.5
822.7479	822.7545	805.7; 787.7; 605.6; 577.5; 551.5; 549.5; 521.5; 495.4; 367.3; 349.3; 313.3; 311.3; 293.2; 257.2; 249.3; 239.2; 237.2; 221.2; 219.2; 211.2; 193.2; 165.2	16; 15	TG(16:1_16:0_16:0); TG(16:0_12:0_20:1); TG(14:0_16:1_18:0)	13.2
824.7496	824.7702	551.5; 313.3; 239.2; 221.2	13	TG(16:0_16:0_16:0)	19.9
848.7642	848.7702	603.5; 577.5; 575.5; 551.5; 549.5; 339.3; 337.3; 321.3; 319.3; 313.3; 311.3; 295.3; 293.2; 285.2; 267.2; 265.3; 263.2; 247.2; 245.2; 239.2; 237.2; 221.2; 219.2; 211.2; 193.2	16; 16	TG(18:1_14:0_18:1); TG(16:1_18:1_16:0); TG(18:2_16:0_16:0)	11.1
850.7493	850.7858	833.8; 815.7; 633.6; 579.5; 577.5; 551.5; 549.5; 521.5; 341.3; 339.3; 323.3; 321.3; 313.3; 311.3; 295.3 293.3; 277.3; 267.3; 265.3; 257.2; 249.3; 247.2; 239.2; 237.2; 221.2; 219.2; 183.2 165.2	18; 18; 16	TG(18:0_16:1_16:0); TG(16:0_16:0_18:1); TG(20:0_12:0_18:1)	26.0
852.7936	852.8015	607.6; 579.5; 551.5; 341.3; 313.3; 295.3; 267.3; 249.3; 239.2; 221.2	15; 11	TG(18:0_16:0_16:0); TG(14:0_18:0_18:0)	6.1
874.7856	874.7858	857.8;603.5; 601.5; 577.5; 575.5; 573.5; 339.3; 337.3; 323.3; 321.3; 319.3; 313.3; 311.3; 265.3; 263.2; 247.2; 245.2; 239.2; 237.2; 221.2; 219.2	16; 16; 13	TG(16:0_18:2_18:1); TG(18:1_16:1_18:1); TG(16:1_18:0_18:2)	2.6

876.7952	876.8015	859.8; 841.8; 633.6; 603.5; 579.5; 577.5; 575.5; 547.5; 351.3; 341.3; 339.3; 337.3; 321.3; 319.3; 313.3; 295.3; 283.2; 277.3; 267.3; 265.3; 263.2; 247.2; 245.2; 239.2; 221.2; 191.2	18; 16; 16	TG(18:1_18:1_16:0); TG(18:1_20:0_14:1); TG(16:0_18:0_18:2)	9.6
				TOTAL	94.9

Buriti oil

The ESI(+)-QTOF mass spectrum of buriti oil is shown in Figure 8. Buriti oil fatty acids profile is C16:0 (17%), C18:0 (2%), C18:1 (79%) and C18:2 (3%) and C18:3 (1%), as shown in Table 3, and its mass spectrum profile also very similar to other high oleic acids oils such as açaí (Fig. 3) and bacaba oil (Fig. 6), but with a higher abundance of the ion of *m/z* 902.7, due to the higher oleic acid content in this oil.

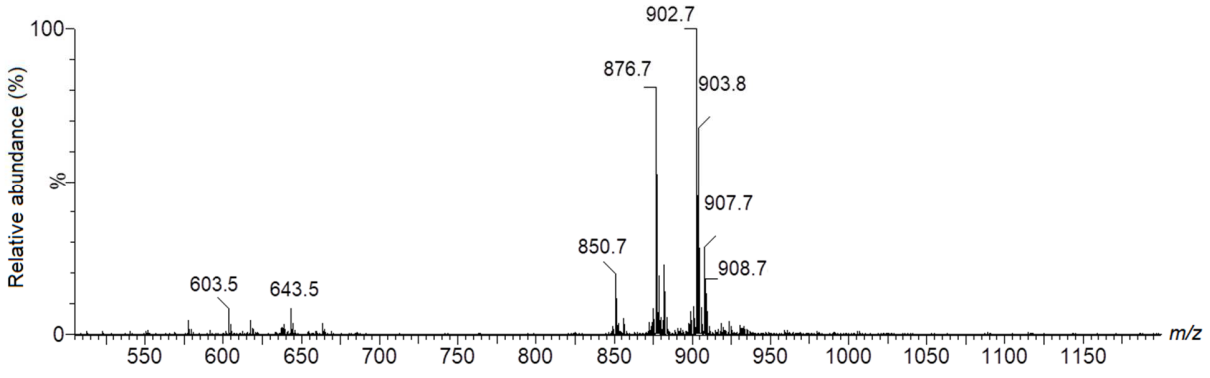

Figure 8. Representative full scan ESI(+)-QTOF mass spectrum of Buriti oil.

For buriti oil, 32 different TAGs were identified in the top 10 most abundant ions in this sample, totalizing 97.3% of all TAGs ions detected, and are all described in Table 10. Some low abundant TAGs with different fatty acids as the one reported for this oil in Table 3 were also detected, which is the case of the case of the fatty acids C14:1, C20:0 C20:1, C22:0, C22:1 and C22:2, detected in TAGs as TG(14:1_18:1_18:0), TG(14:1_16:0_22:1), TG(18:0_14:1_22:2); TG(22:0_18:2_14:1); TG(20:0_16:1_18:2) TG(22:0_18:1_14:1), TG(14:1_18:0_22:1) and TG(16:0_20:1_18:1), but again, all with low abundances as

observed by the intensity of their characteristic fragments. The base peak has also *m/z* 902.7, which for buriti oil is a mixture of 6 different isomers, but being the triolein and the isomer TG(18:2_18:0_18:1) the most abundant among them. The other TAGs identified in this sample are basically several combinations of the reported fatty acids.

Table 10. Identification of the principal TAGs of buriti oil and their relative abundances (%)

Experimental *m/z* $[M+NH_4]^+$	Theoretical *m/z* $[M+NH_4]^+$	Detected fragments (CE 25-30 eV)	Number of detected fragments per TAGs	Identified TAGs	Relative abundance (%)
848.7770	848.7702	831.7; 813.7; 605.6; 577.5; 575.5; 551.5; 549.5; 547.5; 341.3; 339.3; 321.3; 319.3; 313.3; 293.2; 293.2; 265.3; 263.2; 245.2; 239.2; 237.2; 221.2; 219.2; 209.2; 191.2	15; 15; 13; 13	TG(16:1_16:0_18:1); TG(18:2_16:0_16:0); TG(18:0_16:1_16:1); TG(14:1_18:1_18:0)	1.7
850.7881	850.7858	833.8; 815.7; 577.5; 551.5; 339.3; 321.3; 313.3; 265.3; 247.2; 239.2; 221.2	16	TG(16:0_18:1_16:0)	9.6
872.7728	872.7702	855.7; 837.7; 629.6; 601.5; 599.5; 577.5; 575.5; 573.5; 543.4; 351.3; 339.3; 337.3; 335.3; 321.3; 319.3; 317.2; 313.3; 311.3; 295.3; 277.3; 265.3; 263.2; 261.2; 247.2; 245.2; 243.2; 239.2; 237.2; 221.2; 219.2; 209.2; 191.2	18; 18; 17; 16	TG(18:1_18:3_16:0); TG(16:0_18:2_18:2); TG(16:1_18:2_18:1); TG(14:1_18:3_20:0)	3.3
874.7894	874.7858	857.8; 839.7; 603.5; 601.5; 577.5; 575.5; 339.3; 337.3; 319.3; 313.3; 311.3; 265.3; 263.2; 247.2; 245.2; 239.2; 237.2; 221.2; 219.2	16; 15	TG(18:2_16:0_18:1); TG(18:1_18:1_16:1)	5.6
876.8002	876.8015	859.8; 841.8; 633.6; 603.5; 579.5; 577.5; 575.5; 521.5; 339.3; 337.3; 323.3; 321.3; 319.3; 313.3; 267.3; 265.3; 263.2; 247.2; 245.2; 239.2; 221.2; 209.2; 191.2	17; 15; 15	TG(18:1_18:1_16:0); TG(18:0_16:0_18:2); TG(14:1_16:0_22:1)	26.4
896.7781	896.7702	879.8; 861.7; 603.5; 601.5; 599.5; 597.5; 339.3; 337.3; 335.3 333.2; 321.3; 319.3 317.3; 315.2; 265.3 263.2; 261.2; 259.2 ; 247.2; 245.2; 243.2	18; 17	TG(18:1_18:2_18:3); TG(18:4_18:1_18:1)	1.5
898.7781	898.7858	881.8; 603.5; 601.5; 599.5; 339.3; 337.3; 335.2; 321.3; 319.3; 317.2; 265.3; 263.2; 261.2; 247.2; 245.2; 243.2	17; 17	TG(18:1_18:_18:3); TG(18:2_18:1_18:2)	4.4

900.8060	900.8015	883.8; 865.8; 607.6; 605.6; 603.5; 601.5; 599.5; 341.3; 339.3; 337.3; 335.3; 333.2; 323.3; 321.3; 319.3; 317.2; 267.3; 265.3; 263.2; 261.2; 249.3; 247.2; 245.2; 243.21	18; 18; 17	TG(18:3_18:0_18:1); TG(18:0_18:2_18:2); TG(18:0_18:4_18:0)	5.9
902.8094	902.8171	885.8; 867.8; 659.6; 631.6; 607.6; 605.5; 603.5; 601.5; 573.5; 549.5; 545.5; 393.3; 379.4; 369.3; 337.3; 375.3; 341.3; 339.3; 335.3; 323.3; 321.3; 319.3; 317.2; 305.3; 301.3; 293.2; 283.2; 277.3; 267.3; 265.3; 263.2; 261.2; 249.3; 247.2; 245.2; 243.2; 237.2; 219.2; 209.2; 191.2	18; 18; 18; 18; 17; 16	TG(18:1_18:1_18:1); TG(18:2_18:0_18:1); TG(18:0_18:0_18:3); TG(18:0_14:1_22:2); TG(22:0_18:2_14:1); TG(20:0_16:1_18:2)	28.7
904.8272	904.8328	887.8; 869.8; 661.6; 631.6; 607.6; 605.6; 603.6; 577.5; 547.5; 379.4; 349.3; 341.3; 339.3; 337.3; 323.3; 321.3; 319.3; 313.3; 305.3; 283.2; 295.3; 293.3; 275.3; 267.3 265.3; 263.2; 249.3; 247.3; 245.2; 239.2; 209.2; 221.2; 191.2	18; 18; 17; 17; 17	TG(18:0_18:1_18:1); TG(18:0_18:2_18:0); TG(22:0_18:1_14:1); TG(14:1_18:0_22:1); TG(16:0_20:1_18:1)	10.3
				TOTAL	**97.3**

Brazil nut oil

A representative full scan ESI(+)-QTOF mass spectrum of Brazil nut oil is presented in Figure 9. As described in Table 3, its fatty acid profile is C16:0 (15%), C18:0 (12%), C18:1 (41%) and C18:2 (32%), therefore Brazil nut oil has a balanced composition between oleic and linoleic acid.

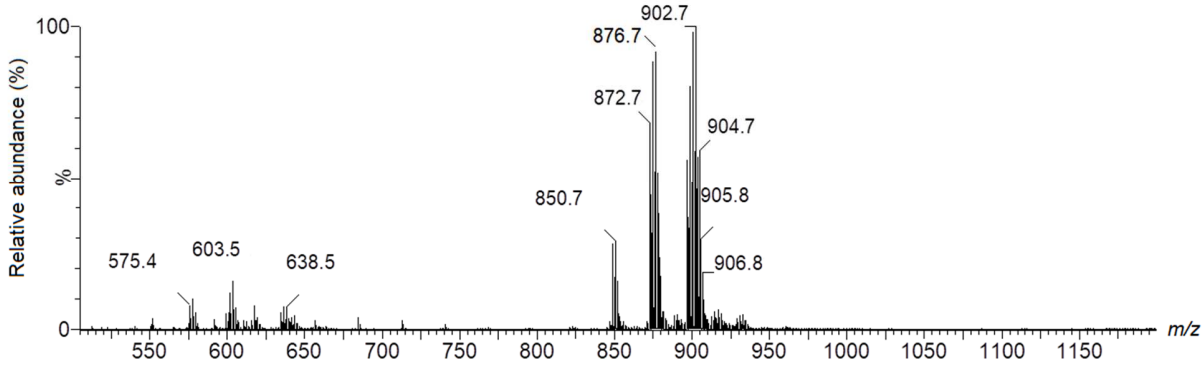

Figure 9. Representative full scan ESI(+)-QTOF mass spectrum of Brazil nut oil.

On the other hand, several TAGs were identified with others fatty acids, as described in Table 11. For instance, all the isomers detected in *m/z* 872.7, that were identified by all its possible fragments. This points out that the TAG composition in Brazil nut oil is more complex than expected if we consider only the previously mentioned fatty acid composition. In Brazil nut oil, 35 different TAGs were identified in the top 10 most abundant ions in this sample, totalizing 87.8% of all TAGs ions detected. The TAGs of *m/z* 874.7, 876.7, 898.7, 900.8 and 902.8 presented relatively even proportions, and are composed by combinations of the most abundant fatty acids in Brazil nut oil.

Table 11. Identification of the principal TAGs of Brazil nut oil and their relative abundances (%)

Experimental *m/z* $[M+NH_4]^+$	Theoretical *m/z* $[M+NH_4]^+$	Detected fragments (CE 25-30 eV)	Number of detected fragments per TAGs	Identified TAGs	Relative abundance (%)
848.7674	848.7702	831.7; 813.7; 603.5; 577.5; 575.5; 551.5; 549.5; 339.3; 337.3; 319.3; 313.3; 265.3; 263.2; 247.2; 245.2; 239.2; 221.2; 211.2; 193.2	16; 14; 13	TG(16:0_16:0_18:2); TG(14:0_18:1_18:1); TG(16:0_18:1_16:1)	3.3
872.7632	872.7702	855.7; 837.7; 629.6; 601.5; 599.5; 577.5; 575.5; 573.5; 571.5; 549.5; 547.5; 543.4; 519.4; 369.3; 365.3; 363.3; 351.3; 347.3; 345.3; 341.3; 339.3; 337.3; 335.3; 323.3; 321.3; 319.3; 317.2; 313.3; 311.3; 295.3; 293.3; 291.3; 289.3; 283.2; 277.3; 273.3 271.2; 267.3; 265.3; 263.2; 261.2; 249.3; 247.2; 245.2; 243.2; 239.2; 237.2; 221.2 219.2; 209.2; 191.2	18; 18; 18; 18; 18; 18; 18; 18	TG(18:3_16:1_18:0); TG(16:1_18:2_18:1); TG(16:0_18:1_18:3); TG(16:1_20:3_16:0); TG(22:2_ 14:1_16:1); TG(20:0_14:1_18:3); TG(20:2_14:1_18:1); TG(16:0_18:2_18:2); TG(18:1_18:3_16:0)	9.5
874.7783	874.7858	857.8; 839.7; 603.5; 601.5; 579.5; 577.5; 575.5; 573.5; 341.3; 339.3; 337.3; 335.3 323.3; 321.3; 319.3; 317.2; 313.3; 311.3; 265.3; 263.2; 261.2; 249.3; 247.3; 245.2; 243.2; 239.2; 237.2; 221.2; 219.2	17; 17; 16; 16	TG(16:0_18:1_18:2); TG(16:1_18:1_18:1); TG(18:3_18:0_16:0); TG(18:2_16:1_18:0)	10.8
876.7960	876.8015	859.8; 841.8; 605.6; 603.5; 579.5; 577.5; 575.5; 341.3; 339.3; 337.3; 321.3; 319.3; 313.3; 267.3; 265.3; 263.2; 249.3; 247.2; 245.2; 239.2; 221.2	17; 16; 14	TG(16:0_18:1_18:1) TG(16:0_18:2_18:0); TG(16:1_18:1_18:0)	10.4
878.8102	878.8171	861.8; 843.8; 605.6; 579.5; 577.5; 341.3; 339.3; 323.3; 321.3; 313.3; 267.3; 265.3; 249.3; 247.3; 239.2; 221.2	17	TG(16:0_18:0_18:1)	4.0

896.7603	896.7702	879.7; 861.7; 603.5; 601.5; 599.5; 597.5; 339.3; 337.3; 335.3; 321.3; 319.3; 317.2; 265.3; 263.2; 261.2; 259.2; 247.2; 245.2; 243.2	18; 18; 15	TG(18:2_18:2_18:2); TG(18:3_18:1_18:2); TG(18:1_18:1_18:4)	8.5
898.7698	898.7858	881.8; 863.7; 603.5; 601.5; 599.5; 597.5; 339.3; 337.3; 335.3; 323.3; 321.3; 319.3; 317.2; 265.2; 263.2; 261.2; 249.3; 247.2; 245.2; 243.2	18; 18; 16	TG(18:1_18:1_18:3); TG(18:1_18:2_18:2); TG(18:0_18:3_18:2)	10.9
900.7858	900.8015	883.8; 865.8; 605.6; 603.5; 601.5; 599.5; 341.3; 339.3; 337.3; 335.3; 323.3; 321.3; 319.3; 317.2; 267.3; 265.3; 263.2; 261.2; 249.3; 247.2; 245.2; 243.2	18; 18; 18	TG(18:1_18:0_18:3); TG(18:2_18:1_18:1); TG(18:2_18:2_18:0)	12.4
902.8007	902.8171	885.8; 867.8; 607.6; 605.6; 603.5; 601.5; 341.3; 339.3; 337.3; 321.3; 319.3; 317.2; 267.3; 265.3; 263.2; 249.3; 247.2; 245.2	18; 17; 14	TG(18:1_18:1_18:1); TG(18:2_18:0_18:1); TG(18:0_18:3_18:0)	11.4
904.8149	904.8328	887.8; 869.8; 631.6; 607.6; 605.6; 603.5; 577.5; 575.5; 351.3; 341.3; 339.3; 337.3; 323.3; 321.3; 319.3; 313.3; 293.3; 277.3; 275.3; 267.3; 265.3; 263.2; 249.3; 247.2; 245.2; 239.2; 221.2	18; 18; 15; 15	TG(18:0_18:1_18:1); TG(18:0_18:0_18:2); TG(20:0_18:2_16:0); TG(20:1_16:0_18:1)	6.5
				TOTAL	87.8

Cupuaçu butter

The ESI(+)-QTOF mass spectrum of a representative sample of cupuaçu butter is shown in Figure 10. The presence of TAGs in a higher *m/z* range can be noted, due to the presence of fatty acids with long (and very long) chains, as C20:0 (12%), C20:1 (<1%) and C22:0 (2%). Cupuaçu is a butter with a high oleic acid content (39%), but also high amounts of saturated fatty acids, principally C18:0 (36%) and the ones with longer carbon chains, as described in Table 3 and 4, makes it a butter.

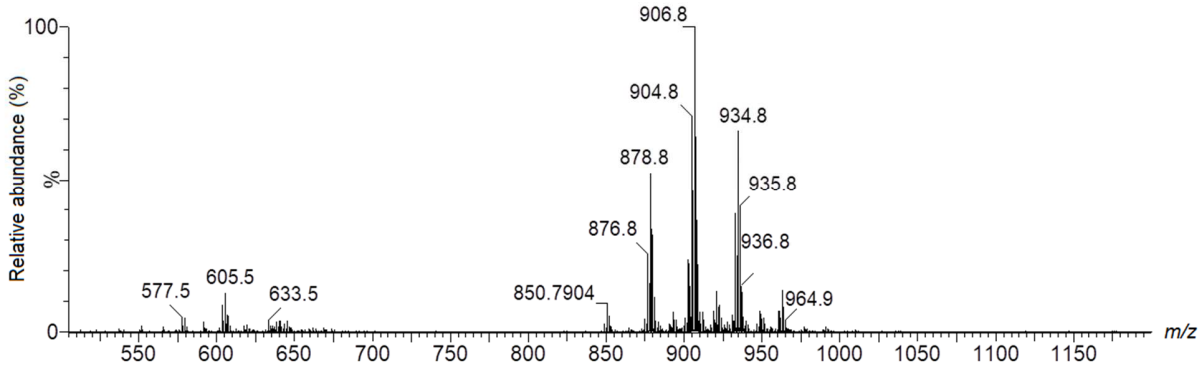

Figure 10. Representative full scan ESI(+)-QTOF mass spectrum of cupuaçu butter.

The detailed TAG identification for cupuaçu butter is described in Table 12. In total, 40 different TAGs compose the top 10 most abundant ions, being 87.6% of the total TAGs ions abundances. All the TAGs are formed by the above mentioned fatty acids and there is a high occurrence of isomeric TAGs in each fragmented $[M+NH_4]^+$ precursor ion. For instance, in *m/z* 904.8, 6 different isomers were identified by their exclusive fragments. On the other hand, for the base peak of *m/z* 906.8, only 2 isomers were identified as TG(18:0_18:1_18:0) and TG(20:0_16:0_18:1).

Table 12. Identification of the principal TAGs of cupuaçu butter and their relative abundances (%)

Experimental *m/z* $[M+NH_4]^+$	Theoretical *m/z* $[M+NH_4]^+$	Detected fragments (CE 25-30 eV)	Number of detected fragments per TAGs	Identified TAGs	Relative abundance (%)
850.7856	850.7858	833.8; 815.8; 577.5; 551.5; 339.3; 321.3; 313.3; 295.3; 265.3; 247.2; 239.2; 221.2	18	TG(16:0_16:0_18:1)	2.0
876.7955	876.8015	859.8; 841.8; 605.6; 603.5; 579.5; 577.5; 575.5; 341.3; 339.3; 321.3; 319.3; 313.3; 267.3; 265.3; 263.2; 247.2; 245.2; 239.2; 237.2; 221.2; 219.2	17; 15; 14	TG(16:0_18:1_18:1); TG(16:0_18:0_18:2); TG(18:1_16:1_18:0)	6.9
878.8108	878.8171	861.8; 843.8; 605.6; 579.5; 577.5; 341.3; 339.3; 323.3; 321.3; 313.3; 295.3; 267.3; 265.3; 249.3; 247.2; 239.2; 221.2	18	TG(16:0_18:0_18:1)	10.6

902.8094	902.8171	885.8; 867.8; 659.6; 629.6; 607.6; 605.6; 603.5; 01.5; 573.5; 545.5; 379.4; 369.3; 351.3; 341.3; 339.3; 337.3; 335.3; 323.3; 321.3; 319.3; 317.3; 277.3; 67.3; 265.3; 263.2; 261.2; 249.3; 247.2; 245.2; 243.2; 239.2; 221.2; 191.2	18; 18; 18; 15; 14	TG(18:1_18:1_18:1); TG(18:0_18:1_18:2); TG(18:3_18:0_18:0); TG(18:3_20:0_16:0); TG(18:2_14:1_22:0)	7.5
904.8113	904.8328	887.8; 869.8; 633.6; 631.6; 607.6; 605.6; 603.5; 577.5; 575.5; 369.3; 367.3; 341.3; 339.3; 337.3; 321.3; 319.3; 313.3; 295.3; 293.3; 277.3; 275.3; 267.3; 265.3; 263.2; 249.3; 247.2; 245.2; 239.3; 221.2; 219.2	17; 17; 17; 17; 16; 16	TG(20:0_18:2_16:0); TG(20:1_16:0_18:1); TG(18:1_18:1_18:0); TG(18:2_16:0_20:0); TG(18:0_18:0_18:2); TG(20:0_16:1_18:1)	16.9
906.8221	906.8484	889.8; 871.8; 633.6; 607.6; 605.6; 577.5; 369.3; 351.3; 341.3; 339.3; 323.3; 321.3; 313.3; 295.3; 277.3; 267.3; 265.3; 249.3; 247.2; 239.2; 221.2	18; 18	TG(18:0_18:1_18:0); TG(20:0_16:0_18:1)	18.7
930.8478	930.8484	913.8; 895.8; 635.6; 633.6; 631.6; 629.6; 603.5; 601.5; 369.3; 367.3; 351.3; 341.3; 339.3; 337.3; 335.3; 321.3; 319.3; 317.2; 295.3; 293.3; 277.3; 275.3; 265.3; 263.2; 261.2; 249.3; 247.2; 245.2; 243.2	18; 17; 16	TG(18:1_20:0_18:2); TG(18:1_20:1_18:1); TG(18:3_20:0_18:0)	2.0
932.8564	932.8641	915.8; 897.8; 659.6; 635.6; 633.6; 631.6; 607.6; 605.6; 603.5; 577.5; 575.5; 397.4; 393.3; 369.3; 367.3; 351.3; 41.3; 339.3; 337.3; 323.3; 21.3; 319.3; 313.3; 301.3; 303.3; 295.3; 293.3; 91.3; 277.3; 273.3; 267.3; 265.3; 263.3; 249.3; 247.3; 245.2; 239.2; 221.2	18; 18; 17; 16; 16; 16; 16; 16	TG(18:0_20:0_18:2); TG(18:1_18:1_20:0); TG(16:0_18:0_22:2); TG(20:2_18:0_18:0); TG(18:1_20:1_18:0); TG(20:2_20:0_16:0); TG(22:0_18:2_16:0); TG(16:0_22:1_18:1)	9.5
934.8705	934.8797	917.8; 899.8; 663.6; 661.6; 635.6; 633.6; 607.6; 605.6; 577.5; 549.5; 425.4; 397.4; 379.4; 369.3; 367.3; 351.3; 349.3; 341.3; 339.3; 333.4; 323.3; 321.3; 313.3; 311.3; 305.3; 295.3; 293.2; 277.3; 275.3; 267.3; 265.3; 249.3; 247.2; 239.2; 237.2; 221.2; 219.2	18; 18; 18; 18; 18; 18; 18; 17	TG(16:1_18:0_22:0); TG(20:0_18:0_18:1); TG(18:1_22:0_16:0); TG(16:0_20:1_20:0); TG(20:0_20:0_16:1); TG(18:0_20:1_18:0); TG(20:0_20:1_16:0); TG(16:1_16:0_24:0)	11.1
962.9087	962.9110	945.9; 927.9; 663.6; 661.6; 635.6; 633.6; 605.6; 397.4; 369.3; 367.3; 351.3; 341.3; 339.3; 323.3; 321.3; 305.3; 295.3; 293.3; 277.3; 275.3; 267.3; 265.3; 249.3; 247.3	18; 17; 17	TG(18:1_20:0_20:0); TG(18:1_18:0_22:0); TG(18:0_20:0_20:1)	2.2
				TOTAL	87.6

1

Graviola oil

The ESI(+)-QTOF mass spectrum of graviola oil is shown in Figure 11. A very similar spectral profile compared to bacaba oil (Fig. 6) is observed, which may point out that a unique fingerprint for each sample of oils and butters are truly impossible to obtain, especially when a wider number of different samples are being considered, because some samples have quite similar mass spectra. Some DAG can also be observed in the *m/z* range of 500 to 600. The fatty acid composition for graviola oil, described in Table 3, is C16:0 (21%), C16:1 (1%), C18:0 (6%), C18:1 (41%), C18:2 (28%), C18:3 (1%) and C20:0 (1%), being graviola a high oleic oil, but also with a considerably high content of linoleic and palmitic acids.

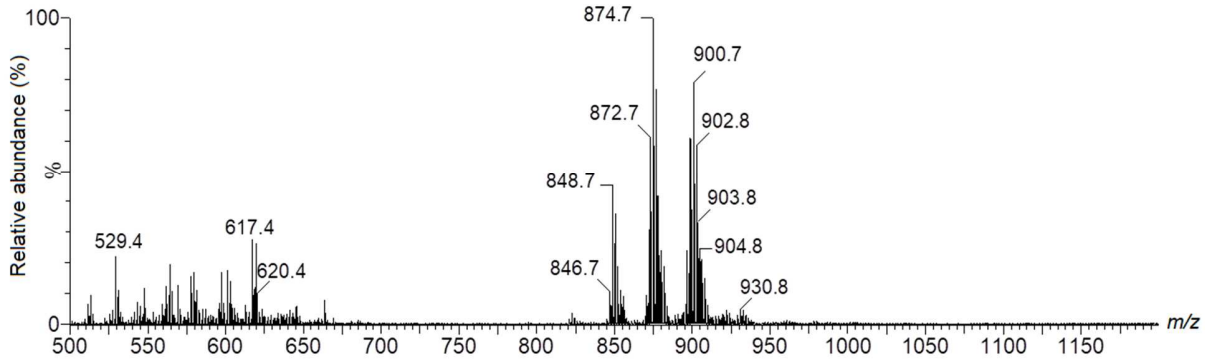

Figure 11. Representative full scan ESI(+)-QTOF mass spectrum of graviola oil.

The detailed TAG identification for graviola oil is described in Table 13, and 55 different TAGs constitutes the top 10 most abundant ions, and they account to a total of 81.8% of the total TAGs ions abundances. Graviola is the oil with the highest complexity among the ones already described and up to ten different TAG isomers were detected for each $[M+NH_4]^+$ precursor ion. For example, the ion of *m/z* 876.8, including TAGs with other fatty acids, as in TG(22:2_16:1_14:1), TG(20:1_18:0_14:1), TG(18:3_22:2_14:0) and TG(18:2_22:2_14:1) detected by their fragments. As shown in Fig. 2c and in Table 12, triolein in *m/z* 902.8 was detected with four other isomers also identified by their fragments.

Table 13. Identification of the principal TAGs of graviola oil and their relative abundances (%)

Experimental *m/z* $[M+NH_4]^+$	Theoretical *m/z* $[M+NH_4]^+$	Detected fragments (CE 25-30 eV)	Number of detected fragments per TAGs	Identified TAGs	Relative abundance (%)
848.7706	848.7702	831.7; 813.7; 577.5; 575.5; 551.5; 549.5; 339.3; 337.3; 319.3; 313.3; 311.3; 295.3 265.3; 263.2; 247.2 245.2; 239.2; 237.22 221.2; 219.2	18; 16	TG(16:0_16:0_18:2); TG(16:0_16:1_18:1);	6.5
850.7864	850.7858	833.8; 815.7; 605.6 579.5; 577.5; 551.5 549.5; 341.3; 339.3 323.3; 321.3; 313.3 311.3; 295.3; 285.2; 267.3; 265.3; 247.2; 239.2; 237.2; 221.2; 219.2	18; 16; 15	TG(16:0_16:0_18:1); TG(16:0_16:1_18:0); TG(14:0_18:0_18:1)	5.3
872.7694	872.7702	855.7; 837.7; 629.6; 601.5; 599.5; 577.5; 575.5; 573.5; 547.5; 545.5; 519.5; 393.3; 365.3; 349.3; 347.3; 339.3; 337.3; 335.3; 321.3; 319.3; 317.2; 313.3; 311.3; 301.3; 293.2; 291.3; 283.2; 275.3; 273.3; 265.3 263.2; 261.2; 247.2; 245.2; 243.2; 239.2; 237.2; 219.2; 209.2; 191.2	18; 18; 18; 18; 15; 15	TG(18:2_16:1_18:1); TG(16:1_20:2_16:1); TG(20:2_18:1_14:1); TG(16:0_18:1_18:3); TG(22:2_16:1_14:1); TG(18:2_14:1_20:1)	8.8
874.7806	874.7858	857.8; 839.8; 713.7; 631.6; 629.6; 603.5 601.5; 579.5; 577.5 575.5; 573.5; 549.5 491.4; 423.4; 405.4 365.3; 349.3; 347.3 341.3; 339.3; 337.3 335.3; 331.3; 323.3 321.3; 319.3; 317.3 313.3; 311.3; 291.3 285.3; 283.2; 273.3 267.3; 265.2; 263.2 261.2; 249.3; 247.3 245.2; 243.2; 239.2 237.2; 221.2; 219.2 209.2; 201.1; 193.2 183.1; 127.1 ; 109.1	18; 18; 18; 17; 17; 17; 17	TG(20:2_18:0_14:1); TG(20:2_24:1_8:0); TG(24:1_14:1_14:1); TG(18:1_18:1_16:1); TG(14:0_18:1_20:2); TG(16:0_18:2_18:1); TG(18:0_18:3_16:0)	14.4

876.7996	876.8015	859.8; 841.8; 633.6 631.6; 605.6; 603.6 579.5; 577.5; 575.5 549.5; 547.5; 521.5 377.4; 367.3; 351.3 341.3; 339.3; 337.3 323.3; 321.3; 319.3 313.3; 311.3; 295.3 293.3; 305.3; 303.3 295.3; 293.2; 285.2 283.2; 275.3; 267.3 265.3; 263.2; 249.3 247.2; 245.2; 239.2 237.2; 221.2; 219.2; 211.2; 209.2; 193.2; 191.2	18; 18; 18; 17; 17; 17; 17; 17; 17; 17	TG(18:1_18:1_16:0); TG(18:1_18:0_16:1); TG(18:2_16:0_18:0); TG(22:1_14:0_16:1); TG(18:1_14:0_20:1); TG(14:1_22:1_16:0); TG(20:1_18:0_14:1); TG(16:1_16:0_20:1); TG(14:1_16:1_22:0); TG(20:0_18:2_14:0)	11.1
896.7711	896.7702	879.7; 861.7; 653.6; 603.5; 601.5; 599.5; 597.5; 543.4; 393.3; 339.3; 337.3; 335.3; 333.2; 321.3; 319.3; 317.2; 315.2; 301.3 283.2; 265.3; 263.2; 261.2; 259.2; 247.2; 245.2; 243.2; 241.2; 209.2; 191.2	18; 18; 18; 17	TG(18:2_18:2_18:2); TG(18:1_18:2_18:3); TG(18:4_18:1_18:1); TG(22:2_18:3_14:1)	3.5
898.7824	898.7858	881.8; 863.8; 655.6 653.6; 627.5; 605.5; 603.5; 601.5; 599.5; 597.5; 575.5; 571.5 545.5; 393.3; 375.3; 367.3; 363.3; 349.3; 345.3; 341.3; 339.3 337.3; 335.3; 333.2 323.3; 321.3; 319.3 317.3; 311.3; 301.3 293.3; 289.3; 285.2 275.3; 271.2; 265.3 263.2; 261.2; 259.2; 249.3; 247.2; 245.2; 243.2; 219.2; 193.2; 191.2	18; 18; 17; 17; 16; 16; 16; 16; 16	TG(18:3_18:1_18:1); TG(18:2_18:1_18:2); TG(18:3_16:1_20:1); TG(18:2_18:0_18:3); TG(20:3_18:1_16:1); TG(18:4_18:0_18:1); TG(20:3_14:1_20:1); TG(18:3_22:2_14:0); TG(18:2_22:2_14:1)	8.8
900.7973	900.8015	883.8; 865.8; 605.6; 603.5; 601.5; 599.5 341.3; 339.3; 337.3 335.3; 321.3; 319.3 317.3; 267.3; 265.3 263.2; 261.2; 247.2 245.2; 243.2	18; 16; 16	TG(18:1_18:1_18:2); TG(18:0_18:3_18:1); TG(18:0_18:2_18:2)	11.4
902.8157	902.8171	885.8; 867.8; 631.7 629.6; 607.6; 605.6 603.5; 601.5; 575.5 367.3; 349.3; 341.3; 339.3; 337.3; 335.3 323.3; 321.3; 319.3 317.3; 313.3; 311.3 293.3; 267.3; 275.3 265.3; 263.3; 261.2 249.3; 247.2; 245.2 243.2; 239.2; 237.2 219.2; 221.2	18; 18; 18; 18; 17	TG(18:1_18:1_18:1); TG(18:1_18:0_18:2); TG(18:0_18:3_18:0); TG(18:1_20:1_16:1); TG(18:2_16:0_20:1)	8.5

904.8310	904.8328	887.8; 869.8; 633.6; 631.6; 607.6; 605.6; 603.5; 577.5; 575.5; 369.3; 351.3; 349.3; 341.3; 339.3; 337.3; 323.3; 321.3; 319.3; 313.3; 311.3; 293.2; 277.3; 275.3; 267.3; 265.3; 263.2; 249.3; 247.2; 245.2; 239.2	18; 18; 15; 15; 15; 15	TG(18:1_18:0_18:1); TG(18:0_18:2_18:0); TG(16:1_18:1_20:0); TG(18:1_16:0_20:1); TG(16:0_18:2_20:0); TG(16:1_18:0_20:1)	3.5
				TOTAL	81.8

Murici oil

Figure 12 shows a representative full scan ESI(+)-QTOF mass spectrum of murici oil. As for Brazil nut oil (Fig. 9), graviola oil has also a balanced proportion between oleic and linoleic acids, being its fatty acid composition (Table 3), as follows: C16:0 (10%), C18:0 (8%), C18:1 (42%), C20:0 (1%), but murici oil can be considered more as a high linoleic oil.

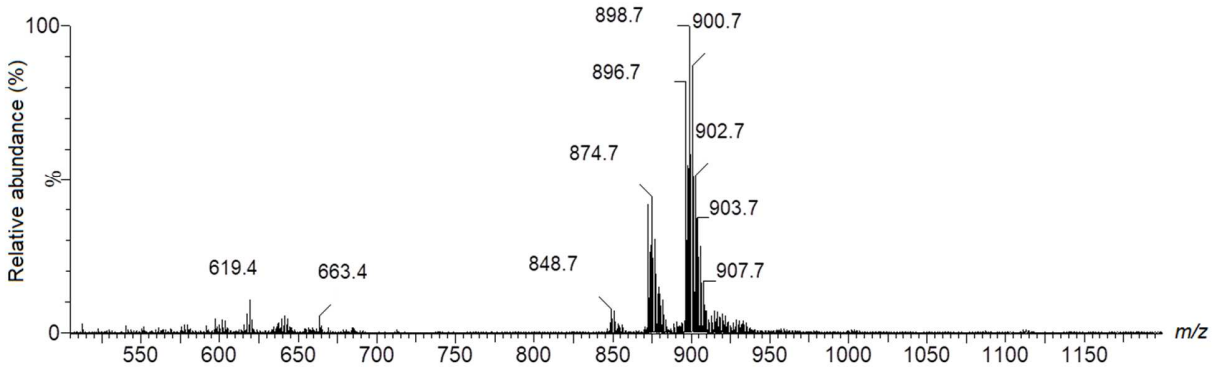

Figure 12. Representative full scan ESI(+)-QTOF mass spectrum of murici oil.

In total, 37 distinct TAGs were identified within the 10 most abundant ions in the mass spectrum, as reported in Table 14, which totalizes 83.5% of the total TAGs ions abundances. The base peak of *m/z* 898.8 is a mixture of TAGs containing the most abundant fatty acids, but also C18:3, C14:1 and C22:1 detected in a relative high abundance by their fragments, and also present in other $[M+NH_4]^+$ of TAGs precursors ions. Different fatty acids were identified in less abundant TAGs as well, corroborating the oil samples complexity in terms of native TAGs composition. As shown in Fig. 2b, the

MS/MS spectrum of the precursor ion of *m/z* 902.7 indicates the presence of the isomer TG(18:0_18:1_18:2) in a relative high proportion together with triolein (TG(18:1_18:1_18:1)), as indicated by the abundances of the fragments of *m/z* 601.5 and 605.6. Another isomer, TG(16:0_18:2_20:1), was also detected in a low abundance in this same precursor ion.

Table 14. Identification of the principal TAGs of murici oil and their relative abundances (%)

Experimental *m/z* $[M+NH_4]^+$	Theoretical *m/z* $[M+NH_4]^+$	Detected fragments (CE 25-30 eV)	Number of detected fragments per TAGs	Identified TAGs	Relative abundance (%)
872.7695	872.7702	855.7; 837.7; 599.5; 577.5; 575.5; 573.5; 339.3; 337.3; 335.3; 319.3; 317.2; 313.3; 265.3; 263.2; 261.2; 245.2; 243.2; 239.2; 221.2	17; 15; 14	TG(16:0_18:2_18:2); TG(16:0_18:3_18:1); TG(16:1_18:1_18:2)	7.2
874.7837	874.7858	857.7; 839.7; 603.5; 601.5; 579.5; 577.5; 575.5; 573.5; 341.3; 339.3; 337.3; 335.3; 321.3; 319.3; 313.3; 311.3 295.3; 293.2; 265.3; 263.2; 261.2; 249.3 247.2; 245.2; 243.2; 239.2; 221.2; 219.2	18; 17; 15; 15	TG(16:0_18:2_18:1); TG(18:1_18:1_16:1); TG(18:2_16:1_18:0); TG(16:0_18:0_18:3)	7.6
876.8029	876.8015	859.8; 841.8; 603.5; 579.5; 577.5; 575.5; 339.3; 321.3; 313.3; 295.3; 265.3; 247.2; 239.2; 221.2	18; 17	TG(16:0_18:1_18:1); TG(16:0_18:0_18:2);	5.2
896.7649	896.7702	879.7; 861.7; 623.5; 603.5; 601.5; 599.5; 597.5; 573.5; 363.3; 345.3; 339.3; 337.3 335.3; 333.3; 321.3; 319.3; 317.3; 315.2; 313.3; 295.3; 289.3; 265.3; 263.2; 261.2 259.2; 247.2; 245.2; 243.2; 241.2; 221.2	18; 18; 16	TG(18:1_18:2_18:3); TG(18:1_18:1_18:4); TG(16:0_18:3_20:3)	14.1
898.7739	898.7858	881.8; 863.7; 655.6; 603.5; 601.5; 599.5; 597.5; 543.5; 395.4; 377.3; 341.3; 339.3; 337.3; 335.3; 323.3; 321.3; 319.3; 317.2; 303.3; 265.3; 263.2; 261.2; 249.3; 247.2; 245.2; 245.2; 243.2 191.2	18; 18; 17; 16	TG(18:1_18:1_18:3); TG(18:1_18:2_18:2); TG(18:0_18:2_18:3); TG(14:1_18:3_22:1)	17.1
900.7910	900.8015	883.8; 865.8; 657.6; 629.5; 607.6; 605.6; 603.5; 601.5; 599.5; 547.5; 545.5; 395.4; 393.3; 377.3; 375.3; 341.3; 339.3; 337.3; 335.3; 323.3; 321.3; 319.3; 317.2; 303.3; 301.3; 283.2; 267.3; 265.3; 263.2;	18; 18; 18; 18; 18; 18; 15	TG(18:2_18:1_18:1); TG(18:0_18:2_18:2); TG(18:1_18:0_18:3); TG(18:0_18:4_18:0); TG(18:1_14:1_22:2); TG(22:1_14:1_18:2); TG(22:2_16:1_16:1)	14.9

		261.2; 249.3; 247.2; 245.2; 243.2; 209.2; 191.2			
902.8131	902.8171	885.8; 867.8; 629.6; 605.6; 603.5; 601.5; 575.5; 367.3; 341.3; 339.3; 337.3; 323.3 321.3; 319.3; 295.3; 293.3; 275.3; 267.3; 265.3; 263.2; 249.3; 247.2; 245.2; 239.2	18; 18; 16	TG(18:1_18:1_18:1); TG(18:0_18:1_18:2); TG(16:0_18:2_20:1)	8.8
904.8281	904.8328	887.8; 869.8; 633.6; 631.6; 607.6; 605.6 603.5; 577.5; 575.5; 369.3; 351.3; 349.3; 341.3; 339.3; 337.3; 323.3; 321.3; 319.3; 313.3; 295.3; 293.2; 277.3; 275.3; 267.3; 265.3; 263.2; 249.3; 247.2; 245.2; 219.2	18; 18; 16; 16; 15; 15	TG(18:0_18:1_18:1); TG(18:2_18:0_18:0); TG(16:0_18:2_20:0); TG(16:1_18:1_20:0); TG(18:0_16:1_20:1); TG(20:1_18:1_16:0)	4.2
906.8445	906.8484	889.8; 871.8; 635.6; 633.6; 607.6; 605.6; 577.5; 369.3; 351.3; 341.3; 339.3; 313.3; 295.3; 293.2; 277.3; 267.3; 265.3; 249.3; 247.2; 239.2369	16; 15; 14	TG(16:0_18:1_20:0); TG(18:0_18:0_18:1); TG(16:1_18:0_20:0)	2.8
908.8752	908.8641	891.83; 873.8; 635.6; 607.56; 579.5; 351.3; 341.3; 313.3; 295.3; 277.3; 267.3; 239.2	14; 12	TG(16:0_18:0_20:0); TG(18:0_18:0_18:0);	1.5
				TOTAL	83.5

Murumuru butter

Figure 13 presents the full scan ESI(+)-QTOF mass spectrum for murumuru butter. Note that the murumuru mass spectrum is almost identical of babassu butter (Fig. 5), with small differences in the relative abundance of some ions, but a quite similar spectral profile indicates that an unique fingerprint for these samples may not be obtained, since oils and butters from different species are displaying similar profiles. As for babassu butter, the murumuru butter has also a medium chain fatty acids profile, being C10:0 (1%), C12:0 (45%), C14:0 (31%), C16:0 (8%), C18:0 (3%), C18:1 (8%) and C18:2 (3%), being a high lauric acid butter (Table 3).

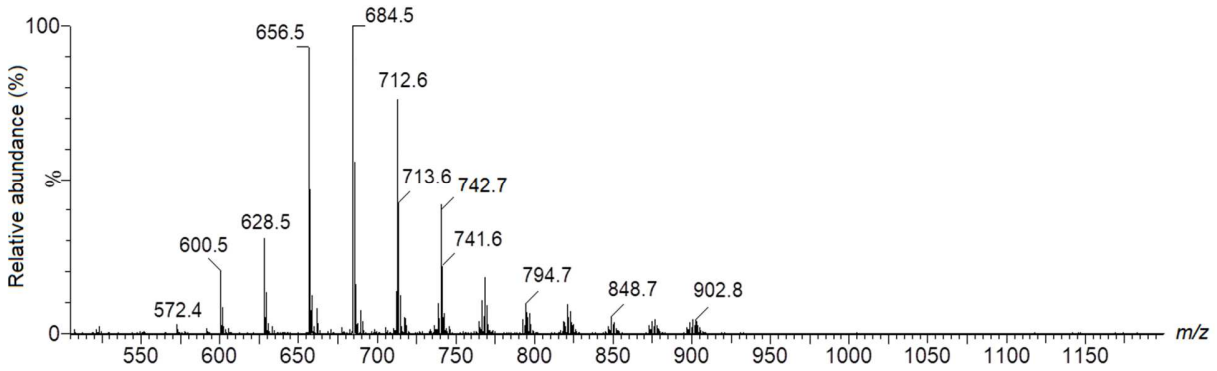

Figure 13. Representative full scan ESI(+)-QTOF mass spectrum of murumuru butter.

It is possible to observe in Table 15 a high occurrence of isomers for all TAG $[M+NH_4]^+$ ions, and the top 10 most abundant TAG ions account to approximately 77.7% of the total TAGs ions abundances, with 46 different identified TAGs. This is also due to the higher number of different fatty acids, leading to the possibility of more diverse isomers. In murumuru butter, most of the identified TAGs are composed by the fatty acids reported in Table 3, but also some less abundant TAGs containing C6:0, C8:0 and C20:1 were also detected. Fig. 1c shows the MS/MS spectrum of the precursor ion of *m/z* 628.5, but in this case five isomers were identified by their different fragments due to the neutral loss of acyl groups could be easily observed. The base peak of *m/z* 684.5 is characterized as a mixture of AAB and ABC type TAGs, such as TG(10:0_14:0_14:0), TG(12:0_12:0_14:0), TG(10:0_12:0_16:0) and TG(8:0_16:0_14:0). The ion of *m/z* 656.5, with a relative abundance of 17%, was identified as trilaurin, plus 7 other TAG isomers, all identified by their exclusive fragments.

Table 15. Identification of the principal TAGs of murumuru butter and their relative abundances (%)

Experimental *m/z* $[M+NH_4]^+$	Theoretical *m/z* $[M+NH_4]^+$	Detected fragments (CE 25-30 eV)	Number of detected fragments per TAGs	Identified TAGs	Relative abundance (%)
600.5203	600.5198	583.5; 565.5; 467.4; 439.4; 411.3; 383.3; 355.3; 341.3; 327.3; 313.3; 299.2; 285.2; 257.2; 221.2; 211.2; 201.1; 183.2; 165.2; 155.1; 137.1; 127.1; 109.1; 99.1; 81.0	16; 16; 15; 15; 14; 14	TG(8:0_12:0_12:0); TG(16:0_8:0_8:0); TG(14:0_8:0_10:0); TG(10:0_12:0_10:0); TG(6:0_12:0_14:0); TG(6:0_8:0_18:0); TG(8:0_6:0_18:0)	3.6
628.5497	628.5511	611.5; 593.5; 495.4; 467.4; 439.4; 411.3; 383.3; 355.3; 313.3; 285.2; 257.2; 239.2; 229.2; 221.2; 211.2; 201.1; 193.2; 183.2; 165.2; 155.1; 137.1; 127.1; 109.1; 99.1; 81.1	18; 17; 17; 17; 16	TG(10:0_12:0_12:0); TG(12:0_8:0_14:0); TG(8:0_16:0_10:0); TG(10:0_10:0_14:0); TG(12:0_6:0_16:0)	5.7
656.5758	656.5824	639.6; 621.5; 523.5; 495.4; 467.4; 439.4; 411.3; 383.3; 369.3; 355.3; 341.3; 327.3; 313.3; 285.2; 267.2; 257.2; 239.2; 229.2; 221.2; 211.2; 201.1; 193.2; 183.1; 165.2; 155.1; 137.1; 127.1 ; 109.1; 99.1; 81.1	18; 18; 18; 18; 17; 16; 16; 16	TG(12:0_12:0_12:0; TG(8:0_14:0_14:0); TG(14:0_12:0_10:0); TG(10:0_16:0_10:0); TG(8:0_12:0_16:0) ; TG(14:0_6:0_16:0); TG(8:0_18:0_10:0); TG(8:0_8:0_20:0)	17.0
684.6053	684.6137	667.6; 649.6; 523.5; 495.4; 467.4; 439.4 411.3; 313.3; 295.3; 285.2; 267.2; 257.2; 239.2; 229.2; 221.2; 211.2; 193.2; 183.2; 165.2; 155.1; 137.1	18; 18; 16; 15	TG(10:0_14:0_14:0); TG(12:0_12:0_14:0); TG(10:0_12:0_16:0); TG(8:0_16:0_14:0)	18.7
712.647	712.6450	677.6; 551.5; 523.5; 495.4; 467.4; 439.4; 313.3; 285.2; 267.2; 257.2; 239.2; 221.2; 211.2; 193.2; 183.2; 165.2; 155.1; 137.1	17; 16; 15; 15	TG(12:0_14:0_14:0); TG(12:0_12:0_16:0); TG(14:0_10:0_16:0); TG(8:0_16:0_16:0)	14.8
740.6717	740.6763	723.6; 551.5; 523.5; 495.4; 467.4; 439.4; 313.3; 285.2; 267.2; 257.2; 249.3; 239.2; 211.2; 193.2; 183.2; 165.2; 137.1	17; 15; 15; 13	TG(14:0_14:0_14:0); TG(12:0_14:0_16:0); TG(12:0_12:0_18:0); TG(10:0_14:0_18:0)	8.2
766.6916	766.6919	749.7; 731.7; 605.6; 549.5; 521.4; 467.4; 465.4; 339.3; 323.3; 321.3; 285.2; 265.3; 257.2; 247.2; 211.2; 201.1; 193.2; 183.2; 165.2; 127.1; 109.1	16; 15	TG(12:0_14:0_18:1); TG(18:0_8:0_18:1)	2.2
768.7051	768.7076	751.7; 733.7; 607.6; 579.5; 551.5; 523.5; 495.4; 467.4; 439.7; 341.3; 369.3; 313.3; 285.2; 267.3; 257.2; 249.3; 239.2; 221.2; 211.2;193.2; 183.2; 165.2; 137.1; 127.1; 109.1	17; 17; 16; 15; 15; 14	TG(14:0_14:0_16:0); TG(12:0_14:0_18:0); TG(12:0_16:0_16:0); TG(18:0_18:0_8:0); TG(12:0_12:0_20:0); TG(10:0_16:0_18:0)	3.4

794.7221	794.7232	777.7; 759.7; 605.5; 577.5; 549.5; 521.4; 495.4; 467.4; 367.3; 339.3; 313.3; 285.2 265.3; 257.2; 247.2; 239.2; 211.2; 183.2; 165.2	15; 13; 10	TG(12:0_18:1_16:0); TG(14:0_14:0_18:1); TG(20:1_10:0_16:0)	2.1
820.7376	820.7389	803.7; 785.7; 603.5; 575.5; 547.5; 523.5; 521.5; 519.4; 341.3; 339.3; 337.3; 319.3 313.3; 285.3; 267.3; 265.3; 263.2; 257.2; 245.2; 239.2; 183.2 165.2	16; 14; 14; 14	TG(12:0_18:0_18:2); TG(14:0_16:0_18:2); TG(18:1_18:1_12:0); TG(18:2_16:0_14:0)	1.9
				TOTAL	77.7

Patawa oil

The ESI(+)-QTOF mass spectrum of patawa oil is shown in Figure 14. Patawa oil fatty acids profile is C12:0 (1%), C14:0 (1%), C16:0 (11%), C16:1 (<1%), C18:0 (6%), C18:1 (76%) and C18:2 (5%) and C18:3 (1%), as presented in Table 3. Its mass spectrum profile is very similar to other high oleic acid oils such as açaí (Fig. 3) and bacaba oil (Fig. 6), but more similar to buriti oil (Fig. 8), also with a very high relative abundance of the ion with *m/z* 902.7.

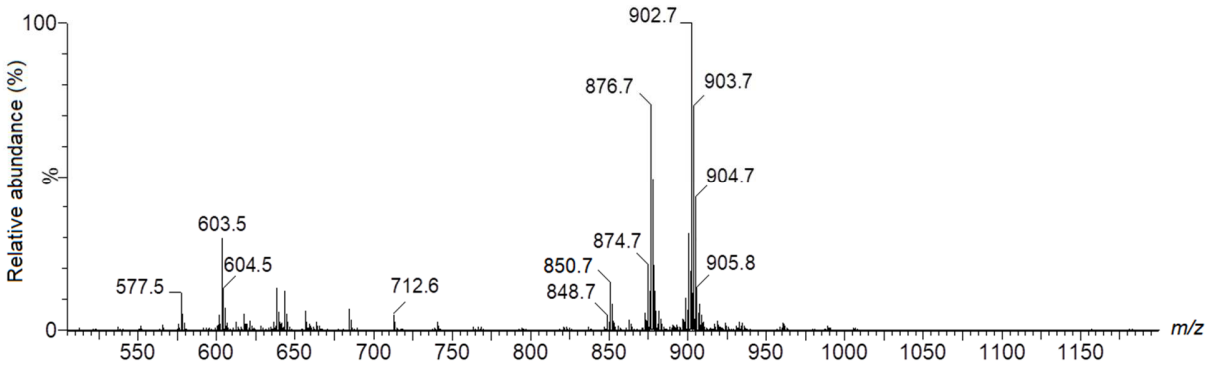

Figure 14. Representative full scan ESI(+)-QTOF mass spectrum of patawa oil.

The top 10 most abundant TAG ions for patawa oil are reported in Table 16. In total, 28 different TAGs were detected and 2 glycerolipids - TG(O-16:0_18:1_18:1) and TG(P-18:0_18:1_16:0) were also identified with a low relative abundance (1.1%). The base peak of *m/z* 902.8 was characterized as triolein - TG(18:1_18:1_18:1), plus two other

isomers, TG(18:0_18:1_18:2) and TG(18:3_18:0_18:0). Most of the identified TAGs are composed of the main fatty acids quantified for patawa oil (Table 3), and some other minor TAGs presented different fatty acids such as C22:2, C20:3, C20:1, among others.

Table 16. Identification of the principal TAGs of patawa oil and their relative abundances (%)

Experimental *m/z* $[M+NH_4]^+$	Theoretical *m/z* $[M+NH_4]^+$	Detected fragments (CE 25-30 eV)	Number of detected fragments per TAGs	Identified TAGs	Relative abundance (%)
848.7713	848.7702	831.7; 813.7; 603.5; 577.5; 575.5; 551.5; 549.5; 339.3; 337.3; 321.3; 319.3; 313.3; 285.2; 265.3; 263.2; 247.2; 245.2; 239.2; 237.2; 221.2; 219.2 211.2	17; 16; 16; 14	TG(14:0_18:1_18:1); TG(16:0_18:2_16:0); TG(18:1_16:1_16:0); TG(14:0_14:0_22:2)	1.6
850.7832	850.7858	833.8; 815.7; 577.5; 551.5; 339.3; 321.3; 313.3; 265.3; 247.2; 239.2; 221.2	16	TG(16:0_16:0_18:1)	5.0
862.8245	862.8222	845.8; 827.8; 589.6; 563.5; 339.3; 313.3; 321.3; 265.3; 247.2; 239.2	13*; 11*	TG(O-16:0_18:1_18:1); TG(P-18:0_18:1_16:0)	1.1
872.7790	872.7702	855.7; 837.7; 601.5; 599.5; 577.5; 575.5; 573.5; 549.5; 363.3; 345.3; 339.3; 337.3; 335.3; 321.3; 319.3 317.2; 313.3; 311.3; 293.2; 289.6; 271.2; 265.3; 263.2; 261.2; 247.2; 245.2; 243.2; 239.2; 237.2; 221.2; 219.2	18; 17; 17	TG(16:1_18:1_18:2); TG(18:3_16:0_18:1); TG(16:0_20:3_16:1)	1.8
874.7864	874.7858	857.8; 839.7; 631.6; 603.5; 601.5; 577.5; 575.5; 545.4; 351.3; 339.3; 337.3; 321.3 319.3; 313.3; 311.3; 293.2; 283.2; 277.3; 265.3; 263.2; 247.2; 245.2; 239.2; 237.2; 221.2; 219.2; 209.2; 191.2	18; 17	TG(16:1_18:1_18:1); TG(16:0_18:1_18:2); TG(14:1_18:2_20:0)	7.0
876.7998	876.8015	859.8; 841.8; 633.6; 605.6; 603.5; 579.5; 577.5; 575.5; 521.4; 341.3; 395.3; 339.3; 337.3; 323.3; 321.3; 319.3; 13.3; 311.3; 303.3; 295.3; 293.2; 283.2; 267.3; 265.3; 263.2; 247.2; 245.2; 239.2; 237.2; 221.2; 219.2; 191.2	18; 17; 17; 16	TG(16:0_18:1_18:1); TG(16:0_18:0_18:2); TG(16:1_18:0_18:1); TG(16:1_20:1_16:0)	24.4
896.7754	896.7702	879.7; 861.7; 603.5; 601.5; 599.5; 597.5; 339.3; 337.3; 335.2; 333.2; 321.3; 319.3; 315.2; 317.2; 265.3; 263.2; 261.2; 247.2; 245.2; 243.2;	18; 18; 18; 18	TG(18:2_18:2_18:2); TG(18:1_18:2_18:3); TG(18:4_18:1_18:1); TG(16:1_18:1_20:4)	1.2

898.7891	898.7858	881.8; 863.7; 605.6; 603.5; 601.5; 599.5; 597.5; 339.3; 337.3; 335.3; 323.3; 321.3 319.3; 317.2; 265.3; 263.2; 261.2; 247.2; 245.2; 243.2; 241.2	18; 18; 15; 14	TG(18:1_18:1_18:3); TG(18:1_18:2_18:2); TG(18:0_18:2_18:3); TG(18:1_18:4_18:0)	3.5
900.7963	900.8015	883.8; 865.8; 605.5; 603.5; 601.5; 599.5; 341.3; 339.3; 337.3; 335.3; 323.3; 321.3; 319.3; 317.2; 265.3; 263.2; 265.3; 261.2; 249.3; 247.2; 245.2; 243.2	18; 17; 17	TG(18:1_18:1_18:2); TG(18:0_18:1_18:3); TG(18:2_18:2_18:0)	10.5
902.8063	902.8171	885.8; 867.8; 607.6; 605.6; 603.5; 601.5; 341.3; 339.3; 337.3; 323.3; 321.3; 319.3 267.3; 265.3; 263.2; 261.2; 249.3; 247.2; 245.2	18; 18; 15	TG(18:1_18:1_18:1); TG(18:0_18:1_18:2); TG(18:3_18:0_18:0)	33.3
				TOTAL	89.4

* 13 possible fragments (precursor ion plus 12 fragments).

Pracaxi oil

The full scan ESI(+)-QTOF mass spectrum for pracaxi oil is presented in Figure 15. From the fatty acids composition reported in Table 3, it was indeed expected that pracaxi TAGs were heavier than the TAGs reported for the previous samples, as pracaxi oil is a source of very long chain fatty acids, as behenic acid - C22:0 (17%) and lignoceric acid C24:0 (11%) - in high amounts, so the main TAGs are in the range of *m/z* from 900 to 1000.

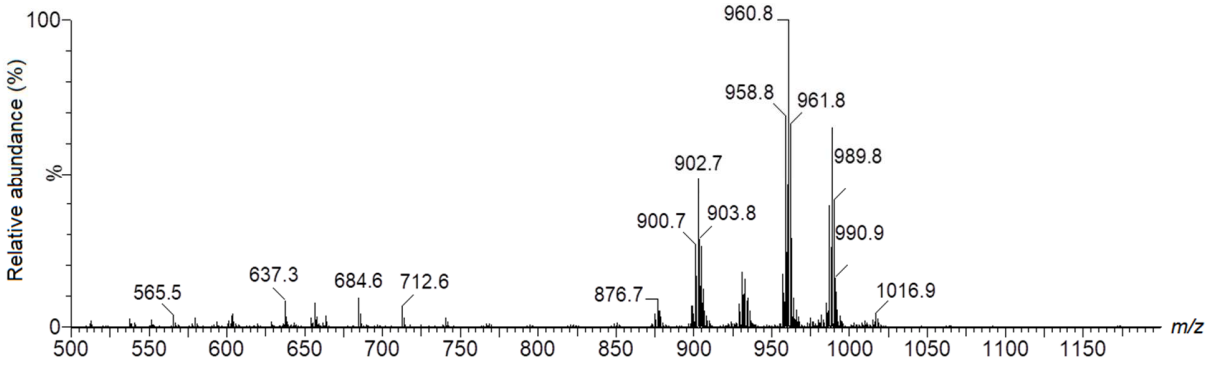

Figure 15. Representative full scan ESI(+)-QTOF mass spectrum of Pracaxi oil.

It was possible to characterize up to 76 different TAGs in pracaxi, and these data are electronically available in supporting information. However, among the top 10 most

abundant TAGs ions, 25 different TAGs were identified, accounting to 86.1% of the total TAGs ions intensities, as reported in Table 17. Pracaxi oil has also a high oleic acid content (52% - Table 3) and has triolein - and its isomer TG(18:0_18:2_18:1) - in a relative abundance of 10%. For the base peak of *m/z* 960.8, that has a relative abundance of 20%, two TAGs were identified: TG(22:0_18:1_18:1) and its isomer TG(18:2_22:0_18:0).

Table 17. Identification of the principal TAGs of pracaxi oil and their relative abundances (%)

Experimental *m/z* $[M+NH_4]^+$	Theoretical *m/z* $[M+NH_4]^+$	Detected fragments (CE 25-30 eV)	Number of detected fragments per TAGs	Identified TAGs	Relative abundance (%)
900.8026	900.8015	883.8; 865.8; 603.5; 601.5; 599.5; 341.5; 339.3; 337.3; 321.3; 319.3; 263.2; 265.3; 247.2; 245.2	18; 15	TG(18:1_18:2_18:1); TG(18:2_18:0_18:2)	5.7
902.8188	902.8171	885.8; 867.8; 605.3; 603.5; 601.3; 341.3; 339.3; 337.3; 321.3; 267.3; 265.3; 263.2; 247.2; 245.2	18; 16	TG(18:1_18:1_18:1); TG(18:0_18:2_18:1)	10.0
904.8306	904.8328	887.8; 869.8; 607.6; 605.5; 603.5; 341.3; 339.3; 337.3; 323.3; 321.3; 319.3; 267.3; 265.3; 263.3; 249.3; 247.3; 245.2	18; 18	TG(18:0_18:1_18:1); TG(18:0_18:2_18:0)	5.2
930.8510	930.8484	913.8; 895.8; 633.6; 631.6; 603.5; 601.5; 369.3; 367.3; 349.3; 339.3; 337.3; 321.3; 319.3; 295.3; 293.3; 265.3; 263.2; 247.2; 245.2	17; 16	TG(18:1_20:1_18:1); TG(18:2_18:1_20:0)	3.5
932.8647	932.8641	915.8; 897.8; 659.6; 635.6; 633.6; 631.6; 603.5; 575.5; 397.4; 341.3; 369.3; 339.3; 337.3; 323.3; 321.3; 319.3; 313.3; 295.3; 277.3; 267.3; 265.3; 263.2; 247.2; 245.2; 239.2	17; 16; 15	TG(18:1_20:0_18:1); TG(18:0_18:2_20:0); TG(18:2_16:0_22:0)	3.1
956.8686	956.8641	939.8; 921.8; 661.6; 659.6; 657.6; 601.5; 599.5; 397.4; 395.4; 377.3; 339.3; 337,3; 323.3; 321.3; 319.3; 303.3; 265,3; 263.2; 261.2; 247.2; 245.2; 243.2	18; 16; 15	TG(22:1_18:2_18:1); TG(18:2_22:0_18:2); TG(22:0_18:1_18:3)	3.5
958.8918	958.8797	941.8; 923.8; 661.6; 659.6; 603.5; 601.5; 397.4; 395.4; 379.3; 377.3; 339.3; 337.3; 323.3; 321.3; 319.3; 305; 3; 265.3; 263.2; 247.2; 245.2	18; 17	TG(18:2_18:1_22:0); TG(18:1_18:1_22:1)	14.1

960.8962	960.8954	943.9; 925.8; 663.6; 661.6; 659.6; 603.5; 397.4; 379.4; 341.3; 339.3; 337.3; 323.3; 321.3; 319.3; 305.3; 267.3; 265.3; 263.2; 249.6; 247.2 245.3	18; 18	TG(18:2_22:0_18:0); TG(22:0_18:1_18:1)	20.2
986.9156	986.9110	969.9; 951.9; 689.6; 687.6; 659.6; 629.5; 603.5; 601.5; 425.4; 423.4; 351.4; 339.3; 337.3; 333.4; 321.3; 319.3; 293.3; 265.3; 263.2; 247.2; 245.2	17; 15; 11	TG(18:2_24:0_18:1); TG(24:1_18:1_18:1); TG(22:0_20:1_18:2)	7.9
988.9346	988.9267	971.9; 953.9; 691.7; 689.6; 687.6; 661.6; 659.6; 631.6; 603.5; 425.4; 397.4; 367.3; 341.3; 351.4; 339.3; 337.3; 333.4; 323.3; 319.3; 321.3; 305.3; 293.3; 277.3; 267.3; 265.3; 263.2; 249.3; 247.2; 245.2	17; 17; 15; 15	TG(18:1_24:0_18:1); TG(18:0_24:0_18:2); TG(18:1_20:1_22:0); TG(22:0_18:2_20:0)	13.0
				TOTAL	86.1

Tucuma butter

Figure 16 shows the full scan ESI(+)-QTOF mass spectrum of tucuma butter. As for babassu and murumuru butters, tucuma butter has also a medium chain fatty acids profile, being C8:0 (1%), C10:0 (2%), C12:0 (51%), C14:0 (28%), C16:0 (6%), C18:0 (3%), C18:1 (7%) and C18:2 (3%), being a high lauric acid butter (Table 3). As expected, the mass spectrum of tucuma butter is also very similar to babassu (Fig. 5) and murumuru (Fig. 13) butters, being almost identical and impossible to differentiate.

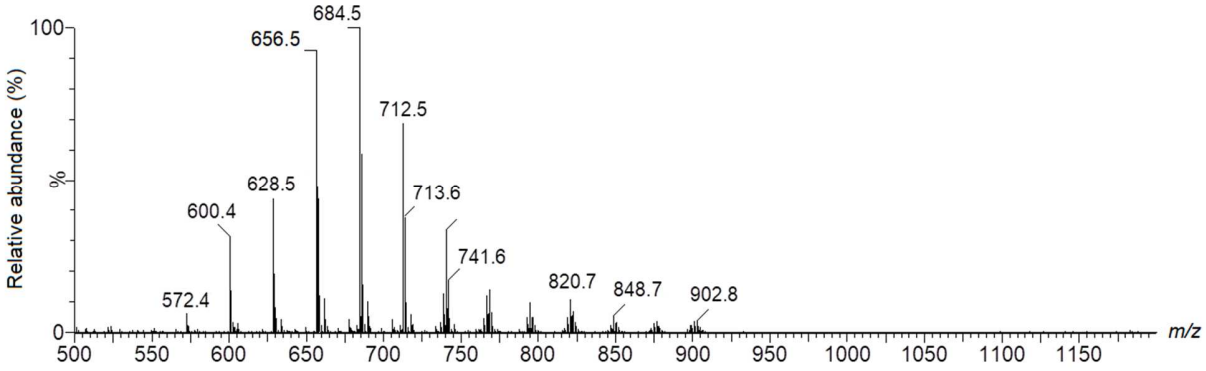

Figure 16. Representative full scan ESI(+)-QTOF mass spectrum of tucuma butter.

The detailed TAG identification for tucuma butter is described in Table 17, in which 32 different TAGs constitutes the top 10 most abundant ions, and they totalize 86% of the

total TAGs ions abundances. The characterized TAGs are composed mainly by the quantified fatty acids reported in Table 3, and some minor TAGs also presented C6:0 in the composition, but detected with low abundances. Fig. 1a shows the MS/MS spectrum of the precursor ion of *m/z* 628.5, in which six different fragments due to the neutral loss of an acyl group was also. In this case, four different TAG isomers were identified in this precursor ion, as reported in Table 18. The base peak at *m/z* 684.5 is formed by TG(12:0_12:0_14:0) and TG(14:0_14:0_10:0), and together the trilaurin in *m/z* 656.5, it was also detected the isomer TG(10:0_14:0_12:0), both contributing to a relative abundance of 19% for their precursor $[M+NH_4]^+$ ion. Up to 7 different isomers were identified for each precursor ion, as for example in *the m/z* 740.6.

Table 18. Identification of the principal TAGs of tucuma butter and their relative abundances (%)

Experimental *m/z* $[M+NH_4]^+$	Theoretical *m/z* $[M+NH_4]^+$	Detected fragments (CE 25-30 eV)	Number of detected fragments per TAGs	Identified TAGs	Relative abundance (%)
600.5146	600.5198	583.5; 565.5; 467.4; 439.4; 411.3; 383.3; 355.3; 341.3; 299.2; 285.2; 257.2; 211.2; 201.1; 183.2; 165.2; 155.1; 137.1; 127.1; 109.1; 99.1; 81.1	16; 15; 14; 14	TG(8:0_12:0_12:0); TG(8:0_10:0_14:0); TG(12:0_14:0_6:0); TG(6:0_8:0_18:0)	6.4
628.5476	628.5511	611.5; 593.5; 495.4; 467.4; 439.4; 411.3; 383.3; 285.2; 257.2; 229.2; 211.2; 201.1; 193.2; 183.2; 165.2; 155.1; 137.1; 127.1; 109.1; 99.1; 81.1	17; 16; 16; 15	TG(10:0_10:0_14:0); TG(8:0_12:0_14:0); TG(12:0_10:0_12:0); TG(6:0_14:0_14:0)	9.0
656.5765	656.5824	639.6; 621.5; 467.4; 439.4; 411.3; 285.2; 257.2; 229.2; 211.2; 183.2; 165.2; 155.1	15; 14	TG(12:0_12:0_12:0); TG(10:0_14:0_12:0)	19.0
684.6095	684.6137	667.5871 495.4408 467.4095 439.3782 285.2424 257.2111 211.2056 193.1951 183.1743 165.1638 155.1430 137.1325	14; 14	TG(12:0_12:0_14:0); TG(14:0_14:0_10:0)	20.5
712.6417	712.6450	551.5; 495.4; 467.4; 439.4; 313.3; 285.2; 257.2; 239.2; 211.2; 183.2; 109.1	12; 11; 10	TG(12:0_12:0_16:0); TG(12:0_14:0_14:0); TG(8:0_16:0_16:0)	14.1

738.6617	738.6606	721.6; 703.6; 577.5; 549.5; 521.5; 493.4; 465.4; 439.4; 339.3; 321.3; 313.3; 285.2; 265.3; 257.2; 247.2; 239.2; 229.2; 183.2; 165.2; 127.1;109.1; 155.1	18; 15; 13	TG(12:0_12:0_18:1); TG(18:1_16:0_8:0); TG(10:0_18:1_14:0)	2.6
740.6722	740.6763	723.6; 705.6; 607.6; 579.5; 551.5; 523.5; 495.4; 467.4; 439.4; 341.3; 313.3; 285.2; 267.3; 257.2; 249.3; 239.2; 221.2; 211.2; 193.2; 183.2; 165.2; 155.1; 137.1; 99.1; 81.1	18; 17; 17; 16; 15; 15; 15	TG(14:0_14:0_14:0); TG(12:0_12:0_18:0); TG(12:0_14:0_16:0); TG(10:0_14:0_18:0); TG(8:0_16:0_18:0); TG(10:0_16:0_16:0); TG(6:0_18:0_18:0)	7.0
766.6927	766.6919	749.7; 731.7; 605.5; 549.5; 521.5; 467.4; 465.4; 341.3; 339.3; 323.3; 321.3; 285.2; 265.3; 257.2; 247.2; 211.2; 183.2; 165.2; 109.1	15; 14	TG(12:0_14:0_18:1); TG(8:0_18:0_18:1)	2.5
768.7067	768.7076	751.7; 551.5; 523.5; 495.4; 467.4; 341.3; 313.3; 285.2; 267.3; 257.2; 239.2; 211.2; 193.2; 183.2; 165.2	15; 15; 13	TG(18:0_14:0_12:0); TG(16:0_14:0_14:0); TG(16:0_16:0_12:0)	2.9
794.7236	794.7232	777.7; 759.7; 577.5; 549.5; 521.5; 495.4; 339.3; 321.3; 313.3; 285.2; 265.2; 247.2; 239.2; 211.2;183.2	14; 14	TG(12:0_16:0_18:1); TG(14:0_14:0_18:1)	2.0
				TOTAL	86.0

Tucuma oil

The full scan ESI(+)-QTOF mass spectrum of tucuma oil is shown in Figure 17, and all the identified TAGs are reported in Table 18. In total, 20 different TAGs constitutes the top 10 most abundant ions, and they account to a total of 80.2% of the total detected TAGs. The principal TAGs ions are present from *m/z* 840 to 910, plus some less abundant in *m/z* from 650 to 750. Tucuma oil composition is completely different from the tucuma butter, displaying a fatty acid composition that is on average C12:0 (2%), C14:0 (2%), C16:0 (25%), C18:0 (4%), C18:1 (61%), C18:2 (3%) and C18:3 (2%), as shown in Table 3.

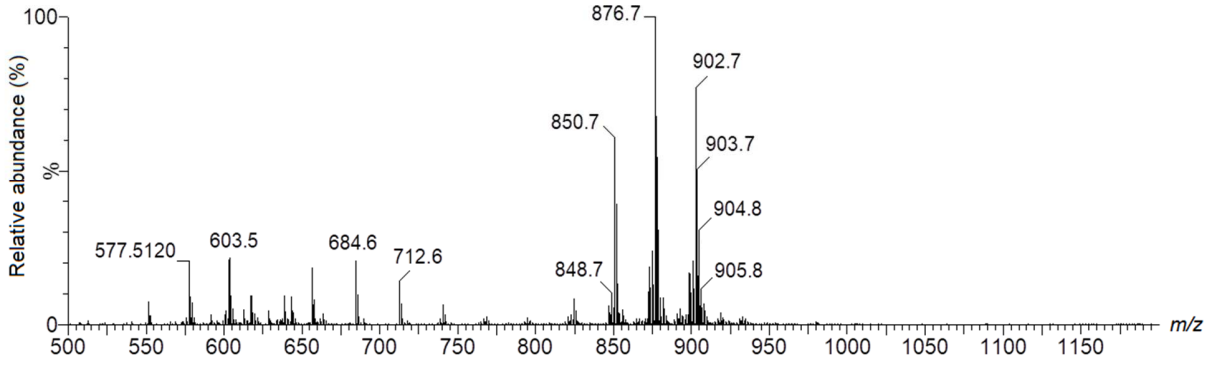

Figure 17. Representative full scan ESI(+)-QTOF mass spectrum of Tucuma oil.

Tucuma oil is also a high oleic oil and the mass spectrum is similar to andiroba (Fig. 4) and bacaba oils (Fig. 6). Some TAGs containing different the fatty acids as those described in Table 3 could also be identified. For instance, triolein in *m/z* 902.8 was identified together with other isomers, as TG(18:0_18:1_18:2), TG(16:1_18:2_20:0) and TG(14:1_22:1_18:1). However, as shown in Fig. 2a, the high abundance of the fragment of *m/z* 603.6 is by far the most abundant, indicating that triolein is the most abundant TAG in this precursor ion. In total, 39 different TAGs were identified in the top 10 most abundant ions in the mass spectrum and it account to 80.2% of the total abundance of all detected TAGs ions. The base peak of *m/z* 876.6 was characterized as TG(16:0_18:1_18:1) and the isomer TG(18:2_18:0_16:0), and they both correspond to 20.6%. For the precursor ion with *m/z* 874.7, up to 8 isomers could be identified by their fragments in Table 19.

Table 19. Identification of the principal TAGs of tucuma oil and their relative abundances (%)

Experimental *m/z* $[M+NH_4]^+$	Theoretical *m/z* $[M+NH_4]^+$	Detected fragments (CE 25-30 eV)	Number of detected fragments per TAGs	Identified TAGs	Relative abundance (%)
656.5821	656.5824	639.6; 621.5; 495.4 467.4; 439.4; 411.3; 383.3; 313.3; 295.3; 257.2; 239.2; 229.2; 221.2; 211.2; 201.1; 183.2; 165.2; 155.1; 137.1; 127.1; 109.1	18; 18; 18; 16	TG(12:0_16:0_8:0); TG(16:0_10:0_10:0); TG(12:0_12:0_12:0); TG(12:0_10:0_14:0); TG(12:0_10:0_14:0)	3.8

684.6120	684.6137	667.6; 649.6; 523.5; 495.4; 467.4; 439.4; 411.3; 313.3; 295.3; 285.2; 267.2; 257.2; 239.2; 211.2; 193.2; 183.2; 165.2; 155.1; 137.1; 127.1; 109.1	18; 17; 16; 16	TG(12:0_14:0_12:0); TG(14:0_10:0_14:0); TG(12:0_10:0_16:0); TG(16:0_8:0_14:0)	4.2
850.7788	850.7858	833.8; 815.7; 577.5; 551.5; 339.3; 321.3; 313.3; 313.3; 295.3; 295.3; 265.3; 247.2; 239.2; 221.2; 221.2	18	TG(16:0_16:0_18:1)	12.6
872.7637	872.7702	855.7; 837.7; 627.5; 601.5; 599.5; 577.5; 575.5; 573.5; 571.5; 545.4; 367.3; 349.3; 341.3; 339.3; 337.3; 335.3; 323.3; 321.3; 319.2; 317.2; 313.3; 311.3; 295.3; 293.2; 285.2; 275.3; 265.3; 263.2; 261.2; 249.3; 247.2; 245.2; 243.2; 239.2; 237.2; 221.2; 219.2; 211.2; 193.2	18; 18; 17; 17	TG(16:1_18:2_18:1); TG(18:3_16:0_18:1); TG(14:0_20:1_18:3); TG(18:3_16:1_18:0)	3.9
874.7785	874.7858	857.8; 839.7; 631.6; 603.5; 601.5; 579.5; 577.5; 575.5; 573.5; 549.5; 547.5; 521.4; 519.4; 393.3; 347.3; 341.3; 339.2; 337.3; 335.3; 323.3; 321.3; 319.3; 317.2; 313.3; 311.3; 303.3; 301.3; 295.3; 293.2; 283.2; 275.3; 273.3; 267.3; 265.3; 263.2; 261.2; 247.2; 245.2; 243.2; 239.2; 237.2; 221.2; 219.2; 209.2; 191.2	18; 18; 17; 17; 17; 16; 16; 16	TG(16:1_18:1_18:1); TG(16:0_18:2_18:1); TG(22:2_14:1_16:0); TG(16:0_18:0_18:3); TG(18:0_18:2_16:1); TG(14:1_20:1_18:1); TG(16:0_16:1_20:2); TG(22:1_14:1_16:1)	4.9
876.7922	876.8015	859.8; 841.8; 603.5; 579.5; 577.5; 575.5; 341.3; 339.3; 337.3; 323.3; 321.3; 319.3; 313.3; 295.3; 267.3; 265.3; 263.2; 247.2; 245.2; 239.2; 221.2	18; 17	TG(16:0_18:1_18:1); TG(18:2_18:0_16:0)	20.6
898.7759	898.7858	881.8; 863.7; 603.5; 601.5; 599.5; 597.5; 339.3; 337.3; 335.3; 321.3; 319.3; 317.2; 265.6; 263.2; 261.2; 247.2; 245.2; 243.2	18; 18; 15	TG(18:1_18:1_18:3); TG(18:2_18:2_18:1); TG(18:3_18:2_18:0)	3.5
900.7991	900.8015	883.8; 865.8; 607.6; 605.6; 603.5; 601.5; 599.5; 341.3; 339.3; 337.3; 335.3; 333.2; 323.3; 321.3; 319.3; 317.2; 267.3; 265.3; 263.2; 261.2; 259.2; 249.3; 247.2; 245.2; 243.2	18; 18; 18; 16	TG(18:2_18:2_18:0); TG(18:0_18:3_18:1); TG(18:1_18:1_18:2); TG(18:0_18:4_18:0)	4.3
902.8101	902.8171	885.8; 867.8; 659.6; 631.6; 605.6; 603.5; 601.5; 573.5; 547.5; 351.3; 341.3; 339.3; 337.3; 321.3; 319.3; 303.3; 295.3; 293.2; 277.3; 265.3; 263.2; 247.2; 245.2; 219.2; 209.2; 191.2	18; 16; 15; 15	TG(18:1_18:1_18:1); TG(18:0_18:1_18:2); TG(16:1_18:2_20:0); TG(14:1_22:1_18:1)	15.9

904.8393	904.8328	887.8; 869.8; 633.6; 631.6; 607.6; 605.6; 603.5; 577.5; 367.3; 351.3; 349.3; 341.3; 339.3; 337.3; 323.3; 321.3; 319.3; 313.3; 293.3; 277.3; 275.3; 267.3; 265.3; 263.2; 249.3; 247.2; 245.2; 239.2; 237.2; 219.2	18; 18; 17; 16; 15	TG(18:0_18:1_18:1); TG(18:2_18:0_18:0); TG(16:1_18:0_20:1); TG(16:0_20:1_18:1); TG(16:1_20:0_18:1)	6.3
				TOTAL	80.2

Ucuuba butter

Figure 18 presents the full scan ESI(+)-QTOF mass spectrum for ucuuba butter. Note that the ucuuba butter mass spectrum is slightly similar to the spectrum of babassu (Fig. 5), murumuru (Fig. 13) and tucuma butter (Fig. 16), but with two remarkably more intensive ions of *m/z* 712.5 and 740.6. As for other butters, the ucuuba butter has also a low medium fatty acids profile, being C12:0 (16%), C14:0 (74%), C16:0 (5%), C16:1 (<1%), C18:0 (1%), C18:1 (4%) and C18:2 (1%), so, differently from the previous reported butters, the ucuuba butter is a high myristic acid butter (Table 3), and it explains the differences in the mass spectrum.

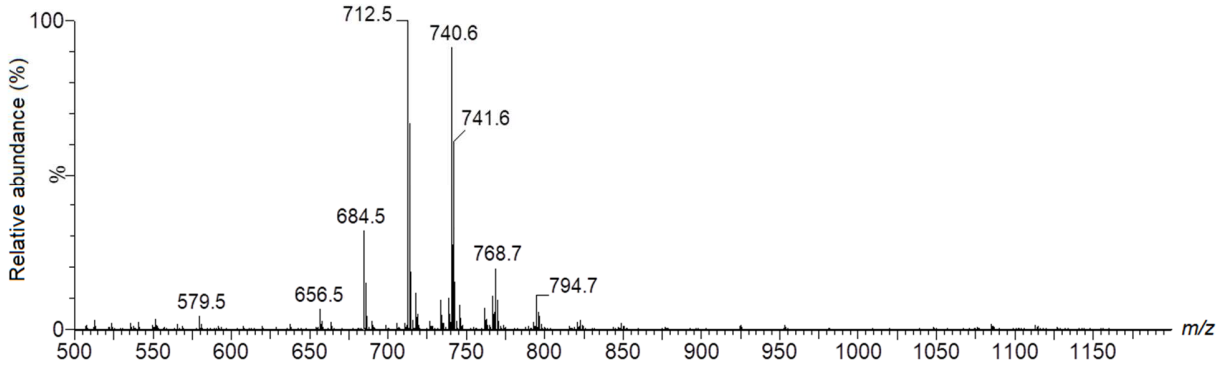

Figure 18. Representative full scan ESI(+)-QTOF mass spectrum of Ucuuba butter.

Note also in Table 20, a high occurrence of isomers for all TAG $[M+NH_4]^+$ ions, and the top 10 most abundant TAG ions account to approximately 97.3% of the total TAGs

ions abundances, and forty six different identified TAGs were identified. In ucuuba butter, most of the identified TAGs are composed by the fatty acids reported in Table 3, but in the same way as for other samples, some less abundant TAGs containing C8:0, C10:0 and C20:0 were also detected, but all the most abundant TAGs displayed at least one C14:0 in the structure. The base peak of *m/z* 712.6 is characterized as a mixture of six different isomers, being TG(12:0_12:0_14:0) and TG(14:0_14:0_10:0) the most abundant among them. The ion of *m/z* 740.6, with a relative abundance of 32%, was identified as trimyristin, plus two other TAG isomers: TG(14:0_12:0_16:0) and TG(16:0_16:0_10:0).

Table 20. Identification of the principal TAGs of ucuuba butter and their relative abundances (%)

Experimental *m/z* $[M+NH_4]^+$	Theoretical *m/z* $[M+NH_4]^+$	Detected fragments (CE 25-30 eV)	Number of detected fragments per TAGs	Identified TAGs	Relative abundance (%)
656.5750	656.5824	639.6; 621.5; 495.4; 467.4; 439.4; 411.3; 383.3; 369.3; 351.3; 327.3; 313.3; 295.3; 285.2; 257.2; 239.2; 229.2; 211.2; 201.1; 183.2; 165.2; 155.4; 137.1; 127.1; 109.1	18; 17; 17; 17; 17; 16	TG(12:0_12:0_12:0); TG(8:0_8:0_20:0); TG(16:0_8:0_12:0); TG(10:0_14:0_12:0); TG(10:0_16:0_10:0); TG(14:0_14:0_8:0)	1.7
684.6028	684.6137	667.6; 649.6; 523.5; 495.4; 467.4; 439.4; 411.3; 383.3; 355.3; 323.3; 285.2; 277.3; 267.2; 257.2; 239.2; 229.2; 211.2; 201.1; 193.2; 183.2; 165.2; 155.1; 137.1; 127.1; 109.1	18; 18; 16; 16; 15; 15; 15	TG(12:0_12:0_14:0); TG(14:0_14:0_10:0); TG(12:0_18:0_8:0); TG(18:0_10:0_10:0); TG(8:0_20:0_10:0); TG(14:0_6:0_18:0); TG(16:0_14:0_8:0)	8.8
712.6258	712.6450	695.6; 677.6; 551.5; 523.5; 495.4; 467.4; 439.4; 411.3; 369.3; 313.3; 295.3; 285.2; 277.3; 267.2; 257.2; 239.2; 229.2; 221.2; 211.2; 201.1; 193.2; 183.2; 165.2; 155.1; 137.1; 127.1; 109.1	18; 18; 18; 18; 16; 15	TG(14:0_10:0_16:0); TG(16:0_16:0_8:0); TG(16:0_12:0_12:0); TG(12:0_14:0_14:0); TG(20:0_12:0_8:0); TG(8:0_14:0_18:0)	38.3
738.6571	738.6606	721.6; 703.6; 549.5; 521.5; 495.4; 493.4; 467.4; 439.4; 339.2; 311.3; 293.4; 285.2; 283.2; 265.2; 257.2; 247.3; 239.2; 237.2; 229.2; 219.2; 211.2; 209.2; 193.2; 191.2; 183.2; 165.2; 155.1; 137.1	17; 17; 16; 16; 16	TG(16:1_12:0_14:0); TG(12:0_18:1_12:0); TG(10:0_14:0_18:1) ; TG(14:0_14:0_14:1); TG(18:1_14:0_10:0)	2.8
740.6649	740.6763	723.6; 705.6; 551.5; 523.5; 495.5; 467.4; 313.3; 285.2; 239.2; 211.2; 193.2; 137.1	15; 13; 12	TG(14:0_14:0_14:0); TG(14:0_12:0_16:0); TG(16:0_16:0_10:0)	32.0

766.6919	766.6919	749.7; 731.7; 577.5; 549.5; 521.5*; 495.4; 493.4; 467.4; 411.3; 395.3; 339.3; 321.3; 285.2; 265.3; 257.2; 239.2; 237.2; 229.2; 221.2; 211.2; 183.2; 155.1; 137.1	15; 15; 14; 12	TG(10:0_18:1_16:0); TG(12:0_10:0_22:1); TG(12:0_14:0_18:1); TG(16:0_16:1_12:0)	3.1
768.7060	768.7076	751.7; 733.7; 579.5; 551.5; 523.5*; 495.4; 467.4; 341.3; 313.3; 295.3; 285.2; 267.2; 257.2; 249.3; 239.2; 229.2; 221.2; 211.2; 193.2; 183.2; 165.2; 155.1; 137.1	18; 18; 17; 17	TG(14:0_14:0_16:0); TG(16:0_12:0_16:0); TG(18:0_10:0_16:0); TG(12:0_18:0_14:0)	5.2
792.7142	792.7076	775.7; 757.7; 575.5; 549.5; 547.4; 521.4; 519.4; 495.4; 493.4; 339.3; 319.3; 295.2; 285.2; 283.2; 265.2; 263.2; 257.2; 247.2; 245.2; 239.2; 237.2; 219.2; 211.2; 209.2; 193.2; 191.2; 183.2; 165.2	16; 16; 15	TG(18:1_14:1_14:0); TG(16:1_12:0_18:1); TG(12:0_16:0_18:2)	0.6
794.7278	794.7232	777.7; 759.7; 577.5; 549.5; 521.5; 495.4; 467.4; 367.3; 339.3; 321.3; 313.3; 293.3; 285.2; 265.3; 257.2; 247.2; 239.2; 221.2; 211.2; 193.2; 183.2; 165.2	17; 16; 15	TG(18:1_12:0_16:0); TG(14:0_18:1_14:0); TG(20:1_14:0_12:0)	2.9
796.7430	796.7389	779.7; 761.7; 579.5; 551.5; 523.5; 495.4; 341.3; 285.2; 267.3; 239.2; 211.2	14; 11; 10	TG(14:0_14:0_18:0); TG(16:0_14:0_16:0); TG(18:0_16:0_12:0)	1.2
822.7667	822.7545	805.7; 787.7; 577.5; 551.5; 549.5; 523.5; 339.3; 321.3; 313.3; 293.2; 285.2; 265.3; 247.2; 239.2; 221.2; 211.2	15; 14	TG(14:0_16:0_18:1); TG(16:0_16:0_16:1)	0.7
				TOTAL	97.3

Principal component analysis (PCA) comparing Amazon samples with trivial commercial oils and fats

All the spectra obtained by direct infusion and analysis by ESI(+)-QTOF-MS for the samples of Amazon species and for the usual oils and butters were subjected to chemometrics analysis regarding their major composition. For this, the mass range of *m/z* 500 to 1200 was selected, because it covers the range of the main TAGs for all the samples. The resulting PCA model used four principal components (PC) and explained 77.16% of the variance. The first component (PC1) explains 42.23% of the total information contained in the data, following by PC2 (18.44%), PC3 (10.88%) and PC4 (5.61%). Several heuristic and statistical criteria exist to select the appropriate number of PCs. In this work, the eigenvalues was used.

In Figure 19, two score plots from the four-component PCA model are shown. The score plots can provide information about different types of oils and the capability of mass spectrometry to describe it. The same patterns can be seen in the HCA dendrogram (see supporting information).

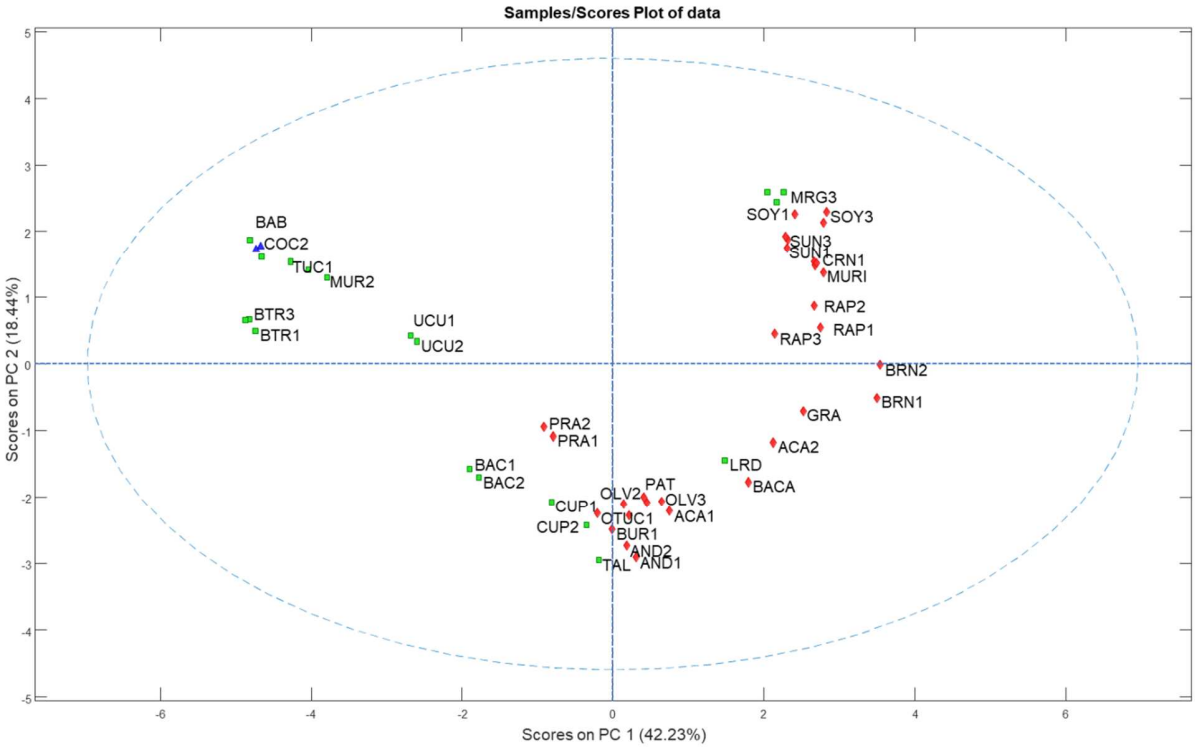

Figure 19. Two scores plots (PC1 x PC2) from a four-component PCA model for all 51 samples described in this work. (Legend: ACA = açaí oil; AND = andiroba oil; BAB = babassu butter; BAC = bacuri oil; BACA = bacaba oil; BUR = buriti oil; BRN = Brazil nut oil; CUP = cupuaçu butter; GRA = graviola oil; MURI = murici oil; MUR = murumuru butter; PAT = patawa oil; OTUC = tucuma oil; TUC = tucuma butter; PRA = pracaxi oil; UCU = ucuuba butter; SOY = soybean oil; CRN = corn oil; SUN = sunflower oil; RAP = rapeseed oil; BTR = milk butter; MRG = margarine; OLV = extra virgin olive oil; TAL = beef tallow; LRD = lard; COC = coconut oil; 1, 2, 3 = sample replicate of a different lot or brand).

The first observation from the PCA shown in Fig. 19 is that oils (in red) and butters (in green) are mostly separated along PC1 (see loadings plot in support information), and

the oils with high linoleic acyl groups are separated from the ones with the higher content of oleic acyl groups along PC2. The coconut oil (in blue) is a controversial sample because, even though it is commercially named as oil, its composition, full of saturated medium chain fatty acids, corresponds to a butter, being grouped with most of the Amazon butters (tucuma, ucuuba and murumuru) and being grouped also with milk butter. It is indeed expected if we compare the mass spectra for these samples (shown in support information) and TAGs composition mainly with medium chain saturated acyl groups.

Another interesting aspect to highlight is that for all the samples of margarine analyzed in this work (that are from the three most important brands in Brazil), the mass spectra were quite similar to the oil and other high linoleic oils such as sunflower, rapeseed, corn and the Amazon murici oil. Moreover, the samples of lard and beef tallow are quite disconnected from the butters group and close to samples like cupuaçu and bacuri butters, which points out that these samples are a balance of saturated and unsaturated fats, being an intermediate between typical butters and oils. Samples of açaí, tucuma oil, buriti, graviola and were grouped or partially with olive oil, which may highlight the nutraceutical benefit of having TAGs with high oleic content.

All the results reported in Figure 19 improve the knowledge about the oils and butters compositions and reports similarities and differences between the Amazon oils and butters and commercially available oils, helping to ensure the best applications and that the consumers have the best benefit when consuming them.

CONCLUSIONS

In this part I compendium about the chemical composition of the main Amazon oils and butters, we reported a detailed FAME and intact TAGs of sixteen different oleaginous Amazon species. The methodology employed for that was the direct infusion of methanolic solutions of these oils and analysis by ESI(+)-QTOF-MS. The TAGs were characterized by their MS/MS spectra and comparison with LIPID MAPS database. To the best of our knowledge, this is the most detailed and systematic study about TAGs composition in such samples. More than seventy different TAGs could be identified in pracaxi oil sample, for example. However, the strategy adopted in this work was to

characterize only the top ten most abundant TAGs, as they account to more than 80% of the total TAGs abundances. Over 40 different TAGs could be easily identified by their fragments, even only characterizing these most abundant ions. The occurrence of isomers is remarkable and more pronounced in butter samples, as up to ten different TAG isomers were identified in the same precursor ion. This fact points out that TAGs complexity in these samples is higher than reported in some previous literature about Amazon oils composition.

Another important observation was that an unique fingerprint for vegetable oils, at least the ones reported in this work, are difficult to obtain. For samples such as babassu, murumuru and tucuma butter, the mass spectra were almost identical, presenting only minimal variations in some TAGs relative abundances. Patawa and buriti oils also displayed identical mass spectra profiles.

All the Amazon samples were compared to commercial oils such as soybean, corn, coconut and olive oil, and their mass spectra were statistically evaluated using principal component analysis. The results presented a formation of three main groups: butters, high oleic acid oils and high linoleic acids oils. Samples such as ucuuba, tucuma, babassu and murumuru butters were grouped with coconut “oil” and milk butter. On the other hand, the high oleic samples such as açaí, andiroba, buriti and tucuma oil, were grouped with olive oil. Murici oil was the Amazon sample grouped with high linoleic acid oils such as soybean, corn, sunflower oil and margarine, and Brazil nut and graviola oil are in between the high oleic and linoleic acids oils. In addition, beef tallow and lard were more close to oily samples than butter samples.

Providing literature on a detailed composition of Amazon oils and butters, we expect to contribute to improve the applications of these products, and that the consumers have the best benefit when consuming them, since adulterations could be more easily detected, as the chemical composition of certified samples are exhaustively presented in this work. The parts II and III of this compendium will describe the volatiles and the polar minor compounds that could reveal several medicinal and biological activities and contribute to certificate its compositions, inhibiting frauds or helping to facilitate their characterization.

1
2 **REFERENCES**

[1] Mittermeier, R. A., Mittermeier, C. G., Gil, P. R., Wilson, E. O. Megadiversity: Earth's Biologically Wealthiest Nations. (CEMEX, 1997).

[2] Soares-Filho, B., Rajao, R., Macedo, M., Carneiro, A., Costa, W., Coe, M., Rodrigues, H., Alencar, A. (2014). Cracking Brazil's Forest Code. Science, 344(6182), 363–364. doi:10.1126/science.1246663

[3] Sarkar, S., Pressey, R. L., Faith, D. P., Margules, C. R., Fuller, T., Stoms, D. M., Moffett,A., Wilson, K.A., Williams,K.J., Williams, P. H. Andelman, S. (2006). Biodiversity Conservation Planning Tools: Present Status and Challenges for the Future. Annual Review of Environment and Resources, 31(1), 123–159. doi:10.1146/annurev.energy.31.042606.0

[4] Cardinale, B. J., et al. (2012). Biodiversity loss and its impact on humanity. Nature, 486(7401), 59–67. doi:10.1038/nature11148

[5] http://emais.estadao.com.br/blogs/comida-de-verdade/mercado-vegano-cresce-40-ao-ano-no-brasil/, accessed in march 2018.

[6] De Paula Pereira, N. (2009), Sustainability of cosmetic products in Brazil. Journal of Cosmetic Dermatology, 8: 160 - 161. doi:10.1111/j.1473-2165.2009.00452.x

[7] Jardim M. A. G., Medeiros, T. D. S. (2006). Oleaginous plants in the State of Pará: floristic composition and medicinal uses, Rev. Bras. Farm., 87(4): 124 – 127.

[8] Service, R. (1999). Drug industry looks to the lab instead of rainforest and reef. Science: 186.

[9] Soejarto, Djaja D. "Biodiversity prospecting and benefit-sharing: perspectives from the field." Journal of Ethnopharmacology. 1996: 1.

[10] Masson, P., Merot, F., Bardot, J. (1990). Influence of hazelnut oil phospholipids on the skin moisturizing effect of a cosmetic emulsion. International Journal of Cosmetic Science, 12(6), 243–251. doi:10.1111/j.1467-2494.1990.tb00539.x

[11] Willett, W. C., Stampfer, M. J. (2006). Rebuilding the Food Pyramid. Scientific American Sp, 16(4), 12–21

[12] https://noticias.uol.com.br/meio-ambiente/ultimas-noticias/redacao/2018/03/13/terra-de-ninguem-floresta-desprotegida-da-amazonia-e-maior-que-a-franca.htm, accessed in march of 2018

[13] Fearnside, P. M. (2016). Brazilian politics threaten environmental policies. Science, 353(6301), 746–748. doi:10.1126/science.aag0254

[14] Oliveira, U., et al. (2017). Biodiversity conservation gaps in the Brazilian protected areas. Scientific Reports, 7(1). doi:10.1038/s41598-017-08707-2

[15] https://www.institutoamazonia.org.br/ribeirinhos-transformam-riquezas-da-amazonia-de-maneira-sustentavel/ accessed in march of 2018.

[16] http://www.beraca.com/rainforest.php accessed in march of 2018.

[17] http://www.amazonoil.com.br/ accessed in march of 2018.

[18] Wu, Z., Rodgers, R. P., Marshall, A. G. (2004). Characterization of Vegetable Oils: Detailed Compositional Fingerprints Derived from Electrospray Ionization Fourier Transform Ion Cyclotron Resonance Mass Spectrometry. Journal of Agricultural and Food Chemistry, 52(17), 5322–5328. doi:10.1021/jf049596q

[19] Alves, J. O., Botelho, B. G., Sena, M. M., Augusti, R. (2013). Electrospray ionization mass spectrometry and partial least squares discriminant analysis applied to the quality control of olive oil. Journal of Mass Spectrometry, 48(10), 1109–1115. doi:10.1002/jms.3256

[20] Catharino, R. R., Haddad, R., Cabrini, L. G., Cunha, I. B. S., Sawaya, A. C. H. F., Eberlin, M. N. (2005). Characterization of Vegetable Oils by Electrospray Ionization Mass Spectrometry Fingerprinting: Classification, Quality, Adulteration, and Aging. Analytical Chemistry, 77(22), 7429–7433. doi:10.1021/ac0512507

[21] Fasciotti, M., Pereira Netto, A. D. (2010). Optimization and application of methods of triacylglycerol evaluation for characterization of olive oil adulteration by soybean oil with HPLC–APCI-MS–MS. Talanta, 81(3), 1116–1125. doi:10.1016/j.talanta.2010.02.006

[22] The LIPID MAPS Lipidomics Gateway, http://www.lipidmaps.org, accessed in May 2018.

[23] Cert, A., Moreda, W., Pérez-Camino, M. . (2000). Chromatographic analysis of minor constituents in vegetable oils. Journal of Chromatography A, 881(1-2), 131–148. doi:10.1016/s0021-9673(00)00389-7

[24] Jung, M. Y., Yoon, S. H., Min, D. B. (1989). Effects of processing steps on the contents of minor compounds and oxidation of soybean oil. Journal of the American Oil Chemists' Society, 66(1), 118–120. doi:10.1007/bf02661798

[25] Cantu-Jungles, T. M., Iacomini, M., Cipriani, T. R., Cordeiro, L. M. C. (2017). Extraction and characterization of pectins from primary cell walls of edible açaí (Euterpe oleraceae) berries, fruits of a monocotyledon palm. Carbohydrate Polymers, 158, 37–43. doi:10.1016/j.carbpol.2016.11.090

[26] Cantu-Jungles, T. M., Iacomini, M., Cipriani, T. R., Cordeiro, L. M. C. (2017). Isolation and characterization of a xylan with industrial and biomedical applications from edible açaí berries (Euterpe oleraceae). Food Chemistry, 221, 1595–1597. doi:10.1016/j.foodchem.2016.10.133

[27] Gordon, A., Cruz, A. P. G., Cabral, L. M. C., de Freitas, S. C., Taxi, C. M. A. D., Donangelo, C. M., Mattietto, R. A., Friedrich, M., Matta, V. M., Marx, F. (2012). Chemical characterization and evaluation of antioxidant properties of Açaí fruits (Euterpe oleraceae Mart.) during ripening. Food Chemistry, 133(2), 256–263. doi:10.1016/j.foodchem.2011.11.150

[28] Pacheco-Palencia, L. A., Duncan, C. E., Talcott, S. T. (2009). Phytochemical composition and thermal stability of two commercial açai species, Euterpe oleracea and Euterpe precatoria. Food Chemistry, 115(4), 1199–1205. doi:10.1016/j.foodchem.2009.01.034

[29] Yamaguchi, K. K. de L., Pereira, L. F. R., Lamarão, C. V., Lima, E. S., da Veiga-Junior, V. F. (2015). Amazon acai: Chemistry and biological activities: A review. Food Chemistry, 179, 137–151. doi:10.1016/j.foodchem.2015.01.055

[30] Garzón, G. A., Narváez-Cuenca, C.-E., Vincken, J.-P., Gruppen, H. (2017). Polyphenolic composition and antioxidant activity of açai (Euterpe oleracea Mart.) from Colombia. Food Chemistry, 217, 364–372. doi:10.1016/j.foodchem.2016.08.107

[31] Rufino, M. do S. M., Pérez-Jiménez, J., Arranz, S., Alves, R. E., de Brito, E. S., Oliveira, M. S. P., Saura-Calixto, F. (2011). Açaí (Euterpe oleraceae) “BRS Pará”: A tropical fruit source of antioxidant dietary fiber and high antioxidant capacity oil. Food Research International, 44(7), 2100–2106. doi:10.1016/j.foodres.2010.09.011

[32] Funasakia, M., Barroso, H. S., Fernandes, V. L. A., Menezes, I. S. (2016). Amazon rainforest cosmetics: chemical approach for quality control, Quim. Nova, 39 (2), 194-209, doi: 10.5935/0100-4042.20160008

[33] Heinrich, M., Dhanji, T., Casselman, I. (2011). Açai (Euterpe oleracea Mart.)—A phytochemical and pharmacological assessment of the species’ health claims. Phytochemistry Letters, 4(1), 10–21. doi:10.1016/j.phytol.2010.11.005

[34] Ferreira, M. C., Vieira, M. de L. A., Zani, C. L., Alves, T. M. de A., Junior, P. A. S., Murta, S. M. F., Rosa, L. H. (2015). Molecular phylogeny, diversity, symbiosis and discover of bioactive compounds of endophytic fungi associated with the medicinal Amazonian plant Carapa guianensis Aublet (Meliaceae). Biochemical Systematics and Ecology, 59, 36–44. doi:10.1016/j.bse.2014.12.017

[35] Ribas, J., & Carreño, A. M. (2010). Avaliação do uso de repelentes contra picada de mosquitos em militares na Bacia Amazônica. Anais Brasileiros de Dermatologia, 85(1), 33–38. doi:10.1590/s0365-05962010000100004

[36] Cabral, E. C., el al. (2013). Typification and quality control of the Andiroba (Carapa guianensis) oil via mass spectrometry fingerprinting. Analytical Methods, 5(6), 1385. doi:10.1039/c3ay25743f

[37] MINISTÉRIO DA SAÚDE. MONOGRAFIA DA ESPÉCIE Carapa guianensis Aubl. (ANDIROBA). Organização: Ministério da Saúde e Anvisa

[38] Saraiva, S. A., Cabral, E. C., Eberlin, M. N., Catharino, R. R. (2009). Amazonian Vegetable Oils and Fats: Fast Typification and Quality Control via Triacylglycerol (TAG) Profiles from Dry Matrix-Assisted Laser Desorption/Ionization Time-of-Flight (MALDI–TOF) Mass Spectrometry Fingerprinting. Journal of Agricultural and Food Chemistry, 57(10), 4030–4034.

[39] Inoue, T., Matsui, Y., Kikuchi, T., In, Y., Muraoka, O., Yamada, T., Tanaka, R. (2014). Carapanolides C–I from the seeds of andiroba (Carapa guianensis, Meliaceae). Fitoterapia, 96, 56–64. doi:10.1016/j.fitote.2014.04.006

[40] Penido, C., Conte, F. P., Chagas, M. S. S., Rodrigues, C. A. B., Pereira, J. F. G., Henriques, M. G. M. O. (2006). Antiinflammatory effects of natural tetranortriterpenoids isolated from Carapa guianensis Aublet on zymosan-induced arthritis in mice. Inflammation Research, 55(11), 457–464. doi:10.1007/s00011-006-5161-8

[41] Inoue, T., Ohmori, S., Kikuchi, T., Yamada, T., Tanaka, R. (2018). Carapanosins D—F from the Seeds of Andiroba (Carapa guianensis, Meliaceae) and Their Effects on LPS-Activated NO Production. Molecules, 23(7), 1778. doi:10.3390/molecules23071778

[42] Araujo, V.F.; Petry, A.C.; Echeverria, R.M.; Fernandes, E.C.; (2007) Plantas da Amazônia para Produção Cosmética.;

http://ec.europa.eu/consumers/cosmetics/cosing/index.cfm?fuseaction=search.details&id=57898

[43] Honorio-França, A., Pessoa, R., França, E., Ribeiro, E., Lanes, P., Chaud, N., Moraes, L. (2014). Microemulsion of babassu oil as a natural product to improve human immune system function. Drug Design, Development and Therapy, 21. doi:10.2147/dddt.s73756

[44] Reis, M. Y. F. A., et al. (2017). Anti-Inflammatory Activity of Babassu Oil and Development of a Microemulsion System for Topical Delivery. Evidence-Based Complementary and Alternative Medicine, 2017, 1–14. doi:10.1155/2017/3647801

[45] Jackson, F. L., Longenecker, H. E. (1944). The fatty acids and glycerides of babassu oil. Oil & Soap, 21(3), 73–75. doi:10.1007/bf02568011

[46] Santos, D. S., et al. (2013). Extraction and Evaluation of Fatty Acid Compositon of Orbignya phaleratаMartius Oils (Arecaceae) from Maranhão State, Brazil. Journal of the Brazilian Chemical Society, 24(2), 355–362. doi:10.5935/0103-5053.20130045

[47] Abadio Finco, F. D. B., Kammerer, D. R., Carle, R., Tseng, W.-H., Böser, S., Graeve, L. (2012). Antioxidant Activity and Characterization of Phenolic Compounds from Bacaba (Oenocarpus bacaba Mart.) Fruit by HPLC-DAD-MSn. Journal of Agricultural and Food Chemistry, 60(31), 7665–7673. doi:10.1021/jf3007689

[48] Carvalho, A. V., da Silveira, T. F., de Sousa, S. H. B., de Moraes, M. R., Godoy, H. T. (2016). Phenolic composition and antioxidant capacity of bacaba-de-leque (Oenocarpus distichus Mart.) genotypes. Journal of Food Composition and Analysis, 54, 1–9. doi:10.1016/j.jfca.2016.09.013

[49] Mambrim, M.C.T, Barrera-Arellano, D. (1997). Caracterización de aceites de frutos de palmeiras de la región amazónica del Brasil, Grasas y Aceites, 48(3), 154-158.

[50] Jaime, P. L. A., Francisca, das C. do A. S. (2018). Bacaba-de-leque (Oenocarpus distichus): A new wet tropics nutritional source. African Journal of Agricultural Research, 13(15), 803–805. doi:10.5897/ajar2018.13027

[51] Brabo de Sousa, S. H., de Andrade Mattietto, R., Campos Chisté, R., Carvalho, A. V. (2018). Phenolic compounds are highly correlated to the antioxidant capacity of genotypes of Oenocarpus distichus Mart. fruits. Food Research International, 108, 405–412. doi:10.1016/j.foodres.2018.03.056

[52] Jacomino, A. P., Pinto, P. M., & Gallon, C. Z. (2018). Bacuri— Platonia insignis. Exotic Fruits, 49–52. doi:10.1016/b978-0-12-803138-4.00008-3

[53] Lustosa, A. K. M. F., et al. (2016). Immunomodulatory and toxicological evaluation of the fruit seeds from Platonia insignis, a native species from Brazilian Amazon Rainforest. Revista Brasileira de Farmacognosia, 26(1), 77–82. doi:10.1016/j.bjp.2015.05.014

[54] Costa Júnior, J. S., et al. (2013). Cytotoxic and leishmanicidal properties of garcinielliptone FC, a prenylated benzophenone fromPlatonia insignis. Natural Product Research, 27(4-5), 470–474. doi:10.1080/14786419.2012.695363

[55] Rogez, H., Buxant, R., Mignolet, E., Souza, J. N. S., Silva, E. M., Larondelle, Y. (2004). Chemical composition of the pulp of three typical Amazonian fruits: araça-boi (Eugenia stipitata),

bacuri (Platonia insignis) and cupuaçu (Theobroma grandiflorum). European Food Research and Technology, 218(4), 380–384. doi:10.1007/s00217-003-0853-6

[56] Uekane, T. M., et al. (2017). Studies on the volatile fraction composition of three native Amazonian-Brazilian fruits: Murici (Byrsonima crassifolia L., Malpighiaceae), bacuri (Platonia insignis M., Clusiaceae), and sapodilla (Manilkara sapota L., Sapotaceae). Food Chemistry, 219, 13–22. doi:10.1016/j.foodchem.2016.09.098

[57] Borges, E. S., Rezende, C. M. (2000). Main Aroma Constituents of Genipap (Genipa americanaL.) and Bacuri (Platonia insignisM.). Journal of Essential Oil Research, 12(1), 71–74. doi:10.1080/10412905.2000.9712046

[58] Monteiro, A. R., et al. (1997). Extraction of the soluble material from the shells of the bacuri fruit (Platonia insignis Mart) with pressurized CO_2 and other solvents. The Journal of Supercritical Fluids, 11(1-2), 91–102. doi:10.1016/s0896-8446(97)00028-4

[59] Freitas de Lima, F., et al. (2016). Study on the Cytotoxic, Genotoxic and Clastogenic Potential of Attalea phalerata Mart. ex Spreng. Oil Pulp In Vitro and In Vivo Experimental Models. PLOS ONE, 11(10), e0165258. doi:10.1371/journal.pone.0165258

[60] Hiane, P. A., Bogo, D., Ramos, M. I. L., Ramos Filho, M. M. (2003). Carotenóides pró-vitamínicos A e composição em ácidos graxos do fruto e da farinha do bacuri (Scheelea phalerata Mart.). Ciência e Tecnologia de Alimentos, 23(2), 206–209. doi:10.1590/s0101-20612003000200018

[61] Costa Júnior, J. S., et al. (2013). Cytotoxic and leishmanicidal properties of garcinielliptone FC, a prenylated benzophenone fromPlatonia insignis. Natural Product Research, 27(4-5), 470–474. doi:10.1080/14786419.2012.695363

[62] Polonini, H. C., Gonçalves, K. M., Brandão, M. A. F., Chaves, M. G. A. M., Raposo, N. R. B., (2012) Amazon native flora oils: in vitro photoprotective activity and major fatty acids constituents, Rev. Bras. Farm, 93 (1), 102-108.

[63] Candido, T. L. N., Silva, M. R., & Agostini-Costa, T. S. (2015). Bioactive compounds and antioxidant capacity of buriti (L.f.) from the Cerrado and Amazon biomes. Mauritia flexuosa, Food Chemistry, 177(15), 313-319. Doi:

[64] Cantu-Jungles, T. M., Almeida, C. P. de, Iacomini, M., Cipriani, T. R., Cordeiro, L. M. C. (2015). Arabinan-rich pectic polysaccharides from buriti (Mauritia flexuosa): An Amazonian edible palm fruit. Carbohydrate Polymers, 122, 276–281. doi:10.1016/j.carbpol.2014.12.085

[65] Rodriguez-Amaya, D. B. (2000). Some Considerations in Generating Carotenoid Data for Food Composition Tables. Journal of Food Composition and Analysis, 13(4), 641–647. doi:10.1006/jfca.2000.0915

[66] Silva, S. M., Sampaio, K. A., Taham, T., Rocco, S. A., Ceriani, R., Meirelles, A. J. A. (2009). Characterization of Oil Extracted from Buriti Fruit (Mauritia flexuosa) Grown in the Brazilian Amazon Region. Journal of the American Oil Chemists' Society, 86(7), 611–616. doi:10.1007/s11746-009-1400-9

[67] Koolen, H. H. F., da Silva, F. M. A., Gozzo, F. C., de Souza, A. Q. L., de Souza, A. D. L. (2013). Antioxidant, antimicrobial activities and characterization of phenolic compounds from buriti (Mauritia flexuosa L. f.) by UPLC–ESI-MS/MS. Food Research International, 51(2), 467–473. doi:10.1016/j.foodres.2013.01.039

[68] Duke, J.A., Bogenschutz-Godwin, M.J., Ottesen, A.R., 2009. Duke's Handbook of Medicinal Plants of Latin America, 1st ed. CRC Press, Boca Raton, USA.

[69] John, J. A., Shahidi, F. (2010). Phenolic compounds and antioxidant activity of Brazil nut (Bertholletia excelsa). Journal of Functional Foods, 2(3), 196–209. doi:10.1016/j.jff.2010.04.008

[70] Rodrigues, J. E., Araújo, M. E., Azevedo, F. F. M., Machado, N. T. (2005). Phase equilibrium measurements of Brazil nut (Bertholletia excelsa) oil in supercritical carbon dioxide. The Journal of Supercritical Fluids, 34(2), 223–229. doi:10.1016/j.supflu.2004.11.018

[71] Santos, O. V., Corrêa, N. C. F., Carvalho, R. N., Costa, C. E. F., França, L. F. F., Lannes, S. C. S. (2013). Comparative parameters of the nutritional contribution and functional claims of Brazil nut kernels, oil and defatted cake. Food Research International, 51(2), 841–847. doi:10.1016/j.foodres.2013.01.054

[72] Chunhieng, T., Hafidi, A., Pioch, D.; Brochier, J.; Montet D. (2008). Detailed Study of Brazil Nut (Bertholletia excelsa) Oil Micro-Compounds: Phospholipids, Tocopherols and Sterols, J. Braz. Chem. Soc., 19, (7), 1374-1380, doi:10.1590/S0103-50532008000700021

[73] Jayasinghe, S. B., Caruso, J. A. (2011). Investigation of Se-containing proteins in Bertholletia excelsa H.B.K. (Brazil nuts) by ICPMS, MALDI-MS and LC–ESI-MS methods. International Journal of Mass Spectrometry, 307(1-3), 16–27. doi:10.1016/j.ijms.2010.12.005

[74] Funasaki, M., Oliveira, R. S., Zanotto, S. P., Carioca, C. R. F., Simas, R. C., Eberlin, M. N., & Alberici, R. M. (2012). Brazil Nut Oil: Quality Control via Triacylglycerol Profiles Provided by Easy

Ambient Sonic-Spray Ionization Mass Spectrometry. Journal of Agricultural and Food Chemistry, 60(45), 11263–11267. doi:10.1021/jf303877t

[75] Clark, R. G., Nursten, H. E. (1976). Volatile flavour components of brazil nuts Bertholletia excelsa (Humb. and Bonpl.). Journal of the Science of Food and Agriculture, 27(8), 713–720. doi:10.1002/jsfa.2740270802

[76] Sun, S. S. M., Leung, F. W., Tomic, J. C. (1987). Brazil nut (Bertholletia excelsa HBK) proteins: fractionation, composition, and identification of a sulfur-rich protein. Journal of Agricultural and Food Chemistry, 35(2), 232–235. doi:10.1021/jf00074a016

[77] Faria, L. P. Camargo, Carvalho, L. R., Paludetti, M. V., Gama, R. (2013) Hair Protective Effect of Argan Oil (Argania spinosa Kernel Oil) and Cupuassu Butter (Theobroma grandiflorum Seed Butter) Post Treatment with Hair Dye, Journal of Cosmetics, Dermatological Sciences and Applications, 3 (3A), 40-44. doi: 10.4236/jcdsa.2013.33A1006.

[78] Pugliese, A. G., Tomas-Barberan, F. A., Truchado, P., Genovese, M. I. (2013). Flavonoids, Proanthocyanidins, Vitamin C, and Antioxidant Activity of Theobroma grandiflorum (Cupuassu) Pulp and Seeds. Journal of Agricultural and Food Chemistry, 61(11), 2720–2728. doi:10.1021/jf304349u

[79] Cohen, K. de O. Jackix, M. de N. H. (2009). "Características químicas e física da gordura de cupuaçu e da manteiga de cacau" (PDF). Documentos / Embrapa Cerrados (in Portuguese) (269): 1–22.

[80] Boulanger, R. (2000). Free and bound flavour components of Amazonian fruits 3-glycosidically bound components of cupuacu. Food Chemistry, 70(4), 463–470. doi:10.1016/s0308-8146(00)00112-6

[81] Alves, S., Jennings, W. (1979). Volatile composition of certain Amazonian fruits. Food Chemistry, 4(2), 149–159. doi:10.1016/0308-8146(79)90039-6

[82] Franco, M. R. B., & Shibamoto, T. (2000). Volatile Composition of Some Brazilian Fruits: Umbu-caja (Spondias citherea), Camu-camu (Myrciaria dubia), Araça-boi (Eugenia stipitata), and Cupuaçu (Theobroma grandiflorum). Journal of Agricultural and Food Chemistry, 48(4), 1263–1265. doi:10.1021/jf9900074

[83] Gomes, G. V. L., et al. (2017). Physico-chemical stability and in vitro digestibility of beta-carotene-loaded lipid nanoparticles of cupuacu butter (Theobroma grandiflorum) produced by the

phase inversion temperature (PIT) method. Journal of Food Engineering, 192, 93–102. doi:10.1016/j.jfoodeng.2016.08.001

[84] De Azevedo, A. A., Kopcak, U., Mohamed, R. (2003). Extraction of fat from fermented Cupuaçu seeds with supercritical solvents. The Journal of Supercritical Fluids, 27(2), 223–237. doi:10.1016/s0896-8446(02)00240-1

[85] Yang, H., et al. (2003). New Bioactive Polyphenols from Theobromagrandiflorum ("Cupuaçu"). Journal of Natural Products, 66(11), 1501–1504. doi:10.1021/np034002j

[86] Moghadamtousi, S., Fadaeinasab, M., Nikzad, S., Mohan, G., Ali, H., & Kadir, H. (2015). Annona muricata (Annonaceae): A Review of Its Traditional Uses, Isolated Acetogenins and Biological Activities. International Journal of Molecular Sciences, 16(7), 15625–15658. doi:10.3390/ijms160715625

[87] Ferreira, L. E., Castro, P. M. N., Chagas, A. C. S., França, S. C., & Beleboni, R. O. (2013). In vitro anthelmintic activity of aqueous leaf extract of Annona muricata L. (Annonaceae) against Haemonchus contortus from sheep. Experimental Parasitology, 134(3), 327–332. doi:10.1016/j.exppara.2013.03.032

[88] De Moraes, I. V. M., et al. (2016). UPLC–QTOF–MS and NMR analyses of graviola (Annona muricata) leaves. Revista Brasileira de Farmacognosia, 26(2), 174–179. doi:10.1016/j.bjp.2015.12.001

[89] Pélissier, Y., Marion, C., Kone, D., Lamaty, G., Menut, C., & Bessière, J.-M. (1994). Volatile Components of Annona muricata L. Journal of Essential Oil Research, 6(4), 411–414. doi:10.1080/10412905.1994.9698410

[90] Kimbonguila, A. et al. (2010) Proximate Composition and Physicochemical Properties on the Seeds and Oil of Annona muricata grown in Congo-Brazzaville, Research Journal of Environmental and Earth Sciences, 2, 13 – 18.

[91] Elagbar, Z. A., Naik, R. R., Shakya, A. K., Bardaweel, S. K. (2016) Fatty Acids Analysis, Antioxidant and Biological Activity of Fixed Oil of Annona muricata L. Seeds, Journal of Chemistry, Volume 2016, Article ID 6948098, 6 pages, http://dx.doi.org/10.1155/2016/6948098

[92] Silva, E. M., Souza, J. N. S., Rogez, H., Rees, J. F., Larondelle, Y. (2007). Antioxidant activities and polyphenolic contents of fifteen selected plant species from the Amazonian region. Food Chemistry, 101(3), 1012–1018. doi:10.1016/j.foodchem.2006.02.055

[93] Martínez-Vázquez, M., González-Esquinca, A. ., Cazares Luna, L., Moreno Gutiérrez, M. ., & García-Argáez, A. . (1999). Antimicrobial activity of Byrsonima crassifolia (L.) H.B.K. Journal of Ethnopharmacology, 66(1), 79–82. doi:10.1016/s0378-8741(98)00155-x

[94] Maldini, M., Sosa, S., Montoro, P., Giangaspero, A., Balick, M. J., Pizza, C., & Loggia, R. D. (2009). Screening of the topical anti-inflammatory activity of the bark of Acacia cornigera Willdenow, Byrsonima crassifolia Kunth, Sweetia panamensis Yakovlev and the leaves of Sphagneticola trilobata Hitchcock. Journal of Ethnopharmacology, 122(3), 430–433. doi:10.1016/j.jep.2009.02.002

[95] Rezende, C. M., Fraga, S. R. G. (2003). Chemical and aroma determination of the pulp and seeds of murici (Byrsonima crassifolia L.). Journal of the Brazilian Chemical Society, 14(3), 425–428. doi:10.1590/s0103-50532003000300014

[96] Alves, G., Franco, M. R. (2003). Headspace gas chromatography–mass spectrometry of volatile compounds in murici (Byrsonima crassifolia L. Rich). Journal of Chromatography A, 985(1-2), 297–301. doi:10.1016/s0021-9673(02)01398-5

[97] Smith N. (2015) Astrocaryum murumuru. In: Palms and People in the Amazon. Geobotany Studies (Basics, Methods and Case Studies). Springer, Cham.

[98] Oliveira, S. F., Moura Neto, J. P., Silva, K. E. R. (2018) Uma revisão sobre a morfoanatomia e as propriedades farmacológicas das espécies Astrocaryum aculeatum Meyer e Astrocaryum vulgare Mart. Scientia Amazonia, 7 (3), CS18-CS28.

[99] Pereira Lima, R., et al. (2017). Murumuru (Astrocaryum murumuru Mart.) butter and oils of buriti (Mauritia flexuosa Mart.) and pracaxi (Pentaclethra macroloba (Willd.) Kuntze) can be used for biodiesel production: Physico-chemical properties and thermal and kinetic studies. Industrial Crops and Products, 97, 536–544. doi:10.1016/j.indcrop.2016.12.052

[100] Sosnowska, J., Balslev, H. (2009). American palm ethnomedicine: A meta-analysis. Journal of Ethnobiology and Ethnomedicine, 5(1), 43. doi:10.1186/1746-4269-5-43

[101] Tauchen, J., et al. (2016). Phenolic composition, antioxidant and anti-proliferative activities of edible and medicinal plants from the Peruvian Amazon. Revista Brasileira de Farmacognosia, 26(6), 728–737. doi:10.1016/j.bjp.2016.03.016

[102] Rezaire, A., et al. (2014). Amazonian palm Oenocarpus bataua (“patawa”): Chemical and biological antioxidant activity – Phytochemical composition. Food Chemistry, 149, 62–70. doi:10.1016/j.foodchem.2013.10.077

[103] Banov, D., Banov, F., Bassani, A. S. (2014). Case Series: The Effectiveness of Fatty Acids from Pracaxi Oil in a Topical Silicone Base for Scar and Wound Therapy. Dermatology and Therapy, 4(2), 259–269. doi: 10.1007/s13555-014-0065-y.

[104] Simmons, C. V., Banov, F., & Banov, D. (2015). Use of a topical anhydrous silicone base containing fatty acids from pracaxi oil in a patient with a diabetic ulcer. SAGE Open Medical Case Reports, 3, 2050313X1558967. doi:10.1177/2050313x15589676

[105] Baldissera, M. D., et al. (2017). Antihyperglycemic, antioxidant activities of tucumã oil (Astrocaryum vulgare) in alloxan-induced diabetic mice, and identification of fatty acid profile by gas chromatograph: New natural source to treat hyperglycemia. Chemico-Biological Interactions, 270, 51–58. doi:10.1016/j.cbi.2017.04.001

[106] Alexandre, E. C. F., Silveira, E. V., Castro, C. F. de S., Sales, J. F., de Oliveira, L. C. S., Viana, L. H., Barbosa, L. C. A. (2015). Synthesis, characterization and study of the thermal behavior of methylic and ethylic biodiesel produced from tucumã (Astrocaryum huaimi Mart.) seed oil. Fuel, 161, 233–238. doi:10.1016/j.fuel.2015.08.062

[107] Oboh, F. O. J., Oderinde, R. A. (1988). Analysis of the pulp and pulp oil of the tucum (Astrocaryum vulgare Mart) fruit. Food Chemistry, 30(4), 277–287. doi:10.1016/0308-8146(88)90114-8

[108] Dijkstra, A. J. Lauric Oils, Encyclopedia of Food and Health http://dx.doi.org/10.1016/B978-0-12-384947-2.00513-4

[109] Bony, E., et al. (2012). Awara (Astrocaryum vulgare M.) pulp oil: Chemical characterization, and anti-inflammatory properties in a mice model of endotoxic shock and a rat model of pulmonary inflammation. Fitoterapia, 83(1), 33–43. doi:10.1016/j.fitote.2011.09.007

[110] Hiruma-Lima, C. A., Batista, L. M., de Almeida, A. B. A., de Pietro Magri, L., dos Santos, L. C., Vilegas, W., Brito, A. R. M. S. (2009). Antiulcerogenic action of ethanolic extract of the resin from Virola surinamensis Warb. (Myristicaceae). Journal of Ethnopharmacology, 122(2), 406–409. doi:10.1016/j.jep.2008.12.023

[111] https://patentimages.storage.googleapis.com/bf/ca/a3/479291a41457a3/US9931366.pdf, accessed 05/10/2018

[112] Kohn, L., et al. (2015). In-Vitro Antiviral Activities of Extracts of Plants of The Brazilian Cerrado against the Avian Metapneumovirus (aMPV). Revista Brasileira de Ciência Avícola, 17(3), 275–280. doi:10.1590/1516-635x1703275-280

[113] Harrowven, D. C., Newman, N. A., Knight, C. A. (1998). On the identity of a neo-lignan from the fruits of Virola sebifera. Tetrahedron Letters, 39(37), 6757–6760. doi:10.1016/s0040-4039(98)01419-1

[114] Kato, M. J., Lopes, L. M. X., Paulino Fo, H. F., Yoshida, M., & Gottlieb, O. R. (1985). Acylresorcinols from Virola sebifera and Virola elongata. Phytochemistry, 24(3), 533–536. doi:10.1016/s0031-9422(00)80762-1

[115] Carlos, A. A., da Silva Malaquias, K., Consolmagno, R. C., Sarria, A. L. F., Fernandes, J. B., & Bueno, O. C. (2017). Virola sebifera Aubl. (Myristicaceae) leaf chemical composition and implications on leaf-cutter ant foraging choice. Arthropod-Plant Interactions, 12(3), 361–368. doi:10.1007/s11829-017-9582-9

[116] Berry, E. M., Eisenberg, S., Haratz, D., Friedlander, Y., Norman, Y., Kaufmann, N. A., & Stein, Y. (1991). Effects of diets rich in monounsaturated fatty acids on plasma lipoproteins—the Jerusalem Nutrition Study: high MUFAs vs high PUFAs. The American Journal of Clinical Nutrition, 53(4), 899–907. doi:10.1093/ajcn/53.4.899

[117] Hsu, F.-F., Turk, J. (1999). Structural characterization of triacylglycerols as lithiated adducts by electrospray ionization mass spectrometry using low-energy collisionally activated dissociation on a triple stage quadrupole instrument. Journal of the American Society for Mass Spectrometry, 10(7), 587–599. doi:10.1016/s1044-0305(99)00035-5

[118] McAnoy, A. M., Wu, C. C., Murphy, R. C. (2005). Direct qualitative analysis of triacylglycerols by electrospray mass spectrometry using a linear ion trap. Journal of the American Society for Mass Spectrometry, 16(9), 1498–1509. doi:10.1016/j.jasms.2005.04.017

2.4.1. Material suplementar

Supporting information

Article

Title: Compendium on Amazon oils composition. Part I - Triacylglycerols characterization and comparison with commercial trivial vegetable oils and fats

Authors: Maíra Fasciotti,[1,5*] Thays V. C. Monteiro,[1] Michael Murgu,[2] Werickson F.C. Rocha,[1] Simone C. Chiapetta,[4] Luiz R. Moraes,[3] Alessandra Sussulini,[5] Marcos N. Eberlin,[5] Valnei S. Cunha[1]

[1] National Institute of Metrology, Quality and Technology (INMETRO), Division of Chemical Metrology, Laboratory of organic analysis, 25250-020, Duque de Caxias, RJ, Brazil
[2] MS Applications & Development Laboratory, Waters Corporation, Barueri, SP, Brazil;
[3] Amazon Oil, Ananindeua, PA, Brazil;
[4] Instituto Nacional de Tecnologia (INT), Rio de Janeiro, Rio de Janeiro, Brazil;
[5] University of Campinas (UNICAMP), Institute of Chemistry, Campinas, SP, Brazil.
*corresponding author: M. Fasciotti, mfasciotti@inmetro.gov.br

1) **Full scan ESI(+)-QTOF mass spectrum of Amazon samples replicates (different lots, years of production):**

- **Açaí (two different lots):**

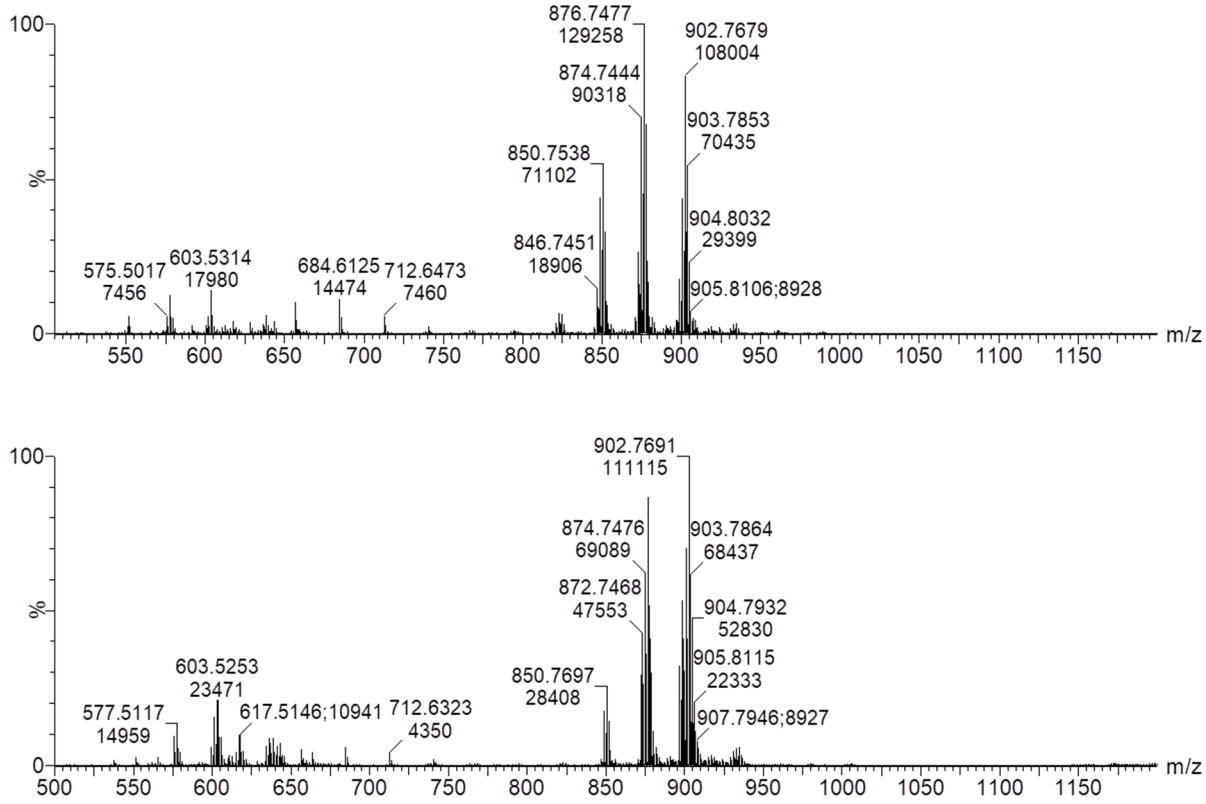

- **Andiroba (two different lots):**

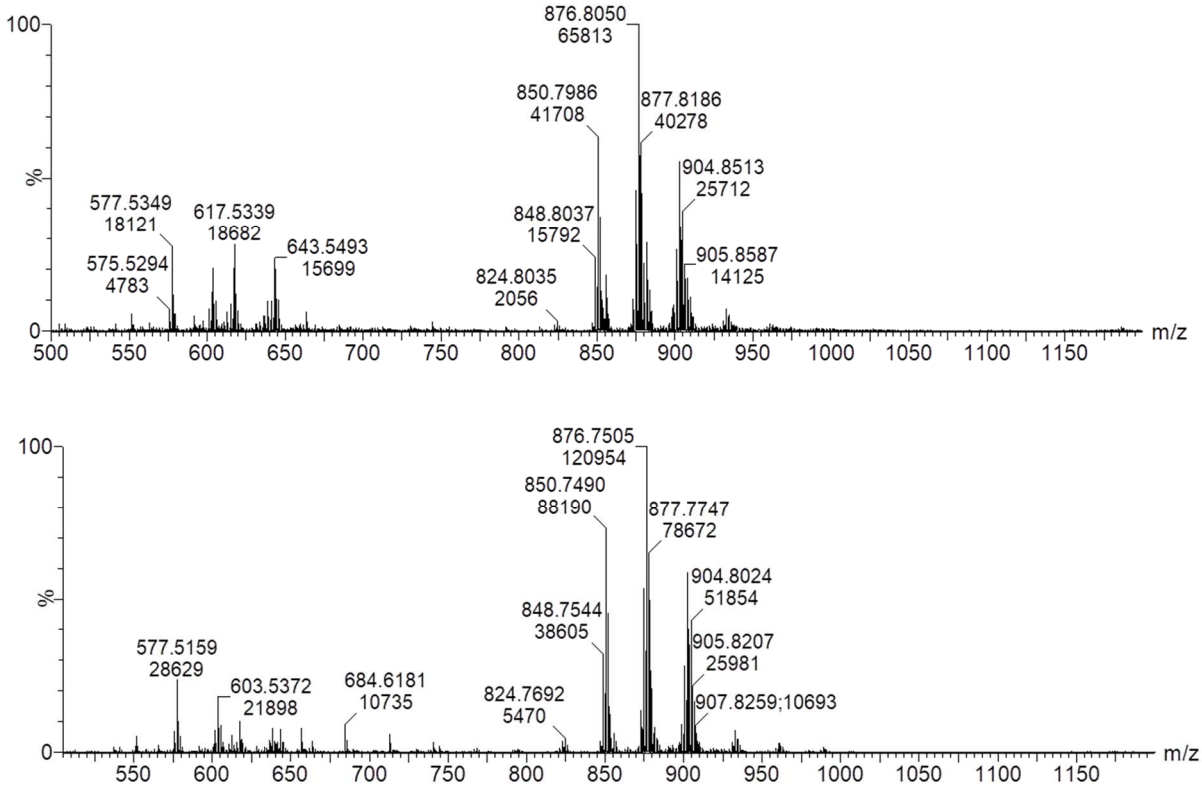

- **Bacuri (two different lots):**

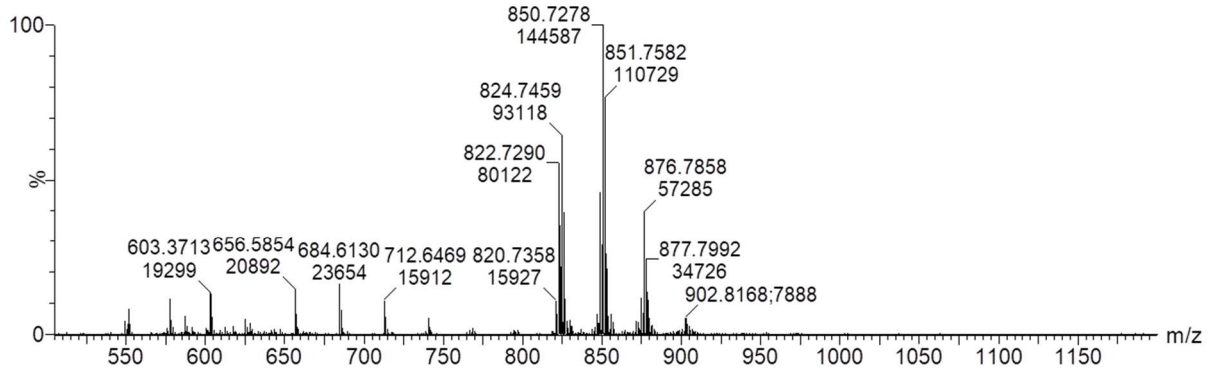

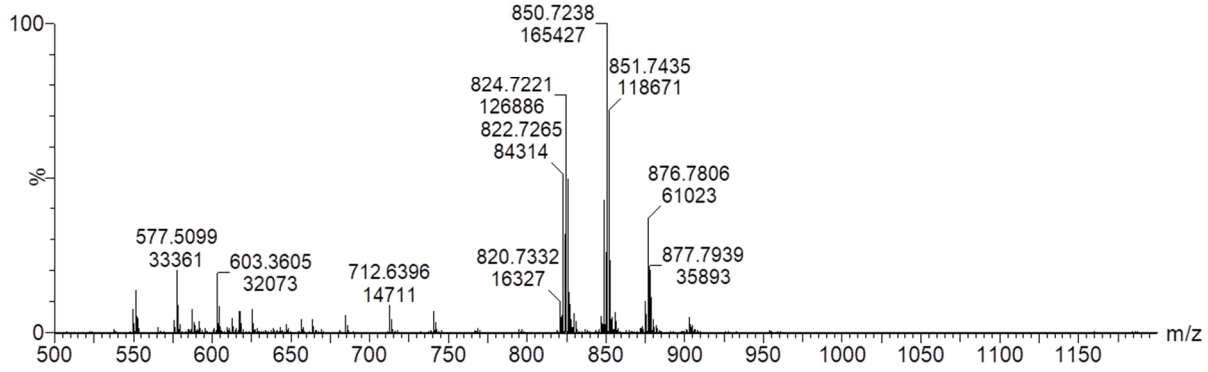

- **Brazil nut (two different lots):**

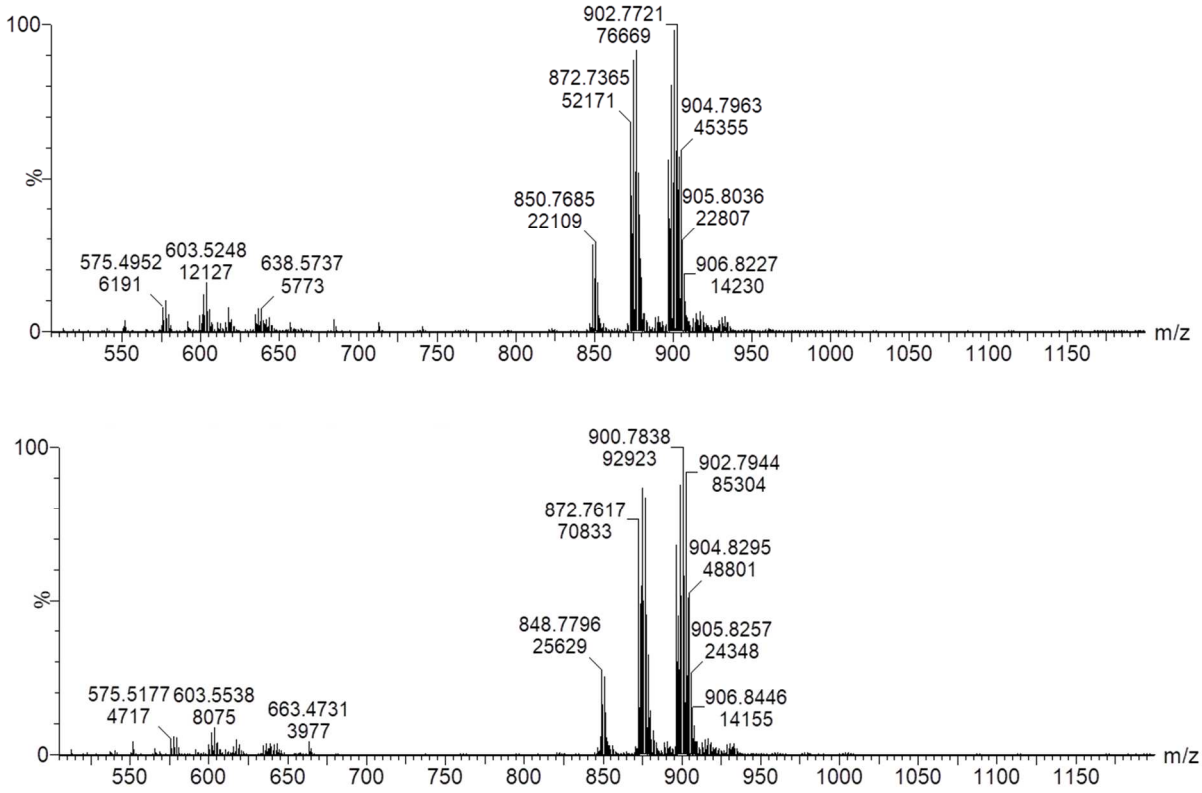

- **Buriti (two different lots):**

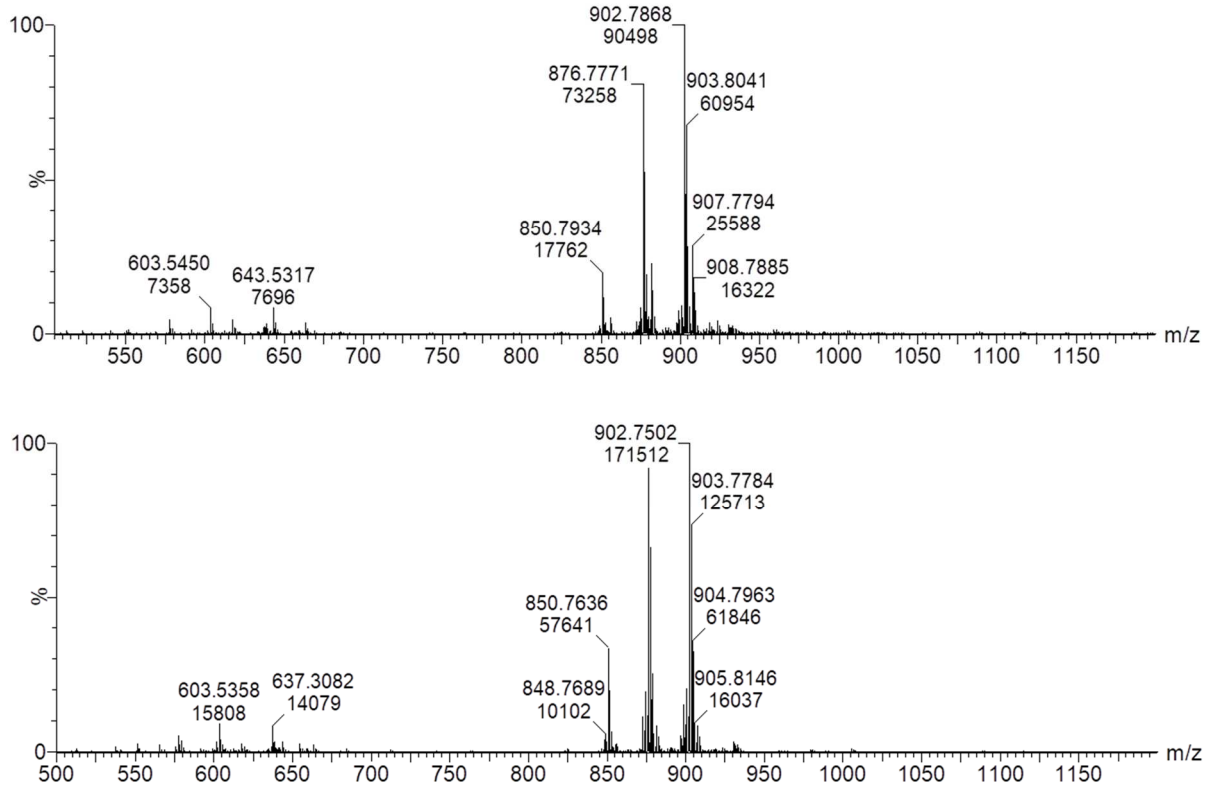

- **Cupuaçu (two different lots):**

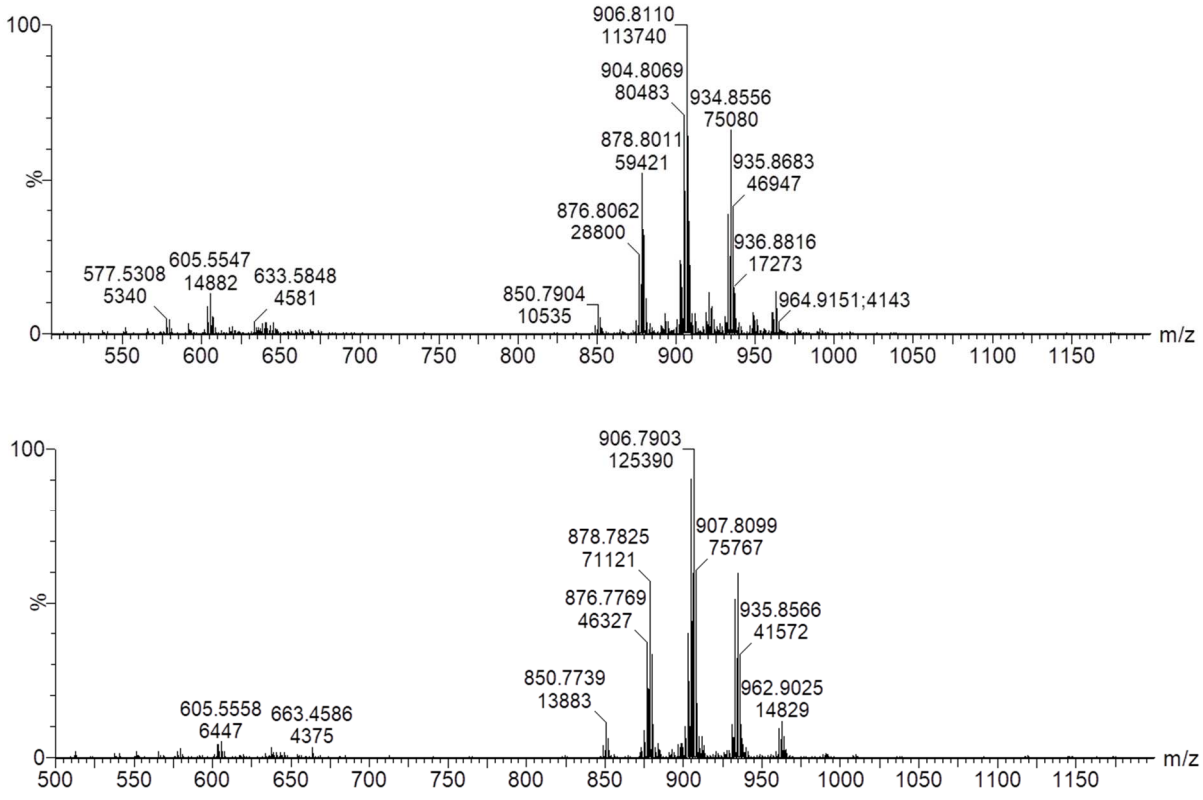

- **Murumuru (two different lots):**

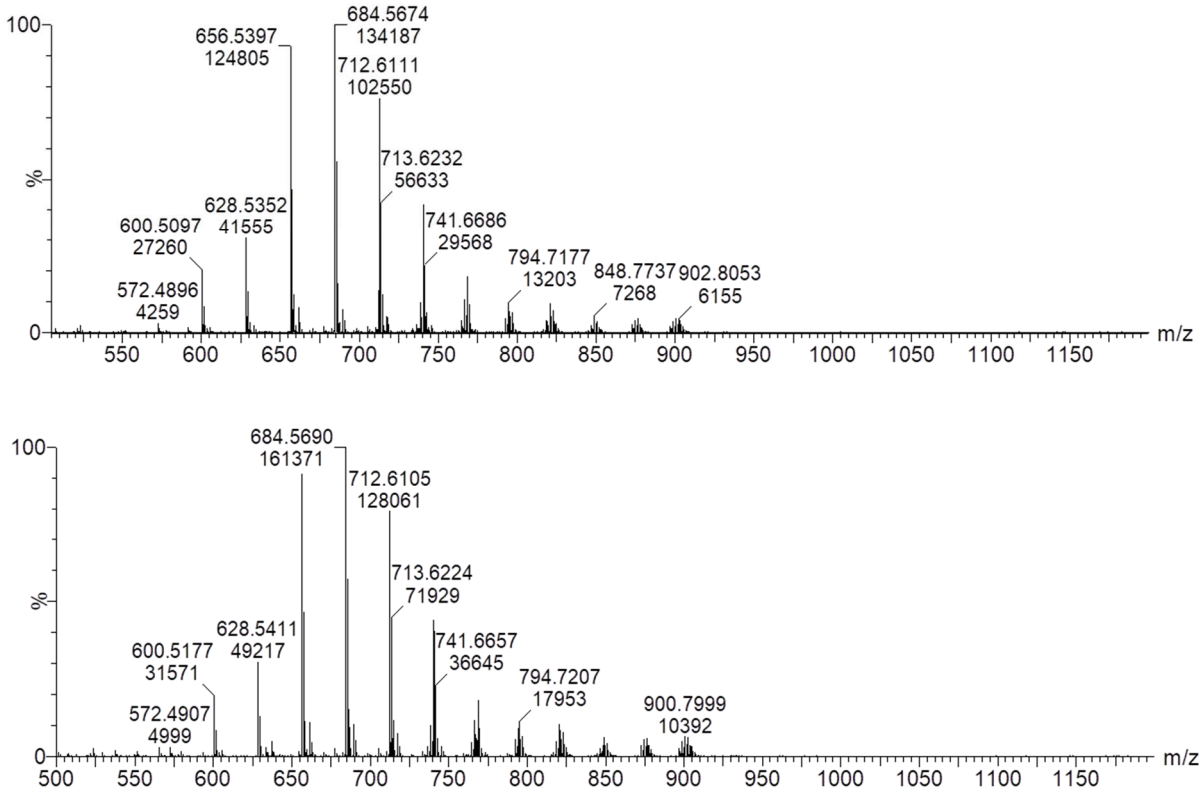

- **Pracaxi (two different lots):**

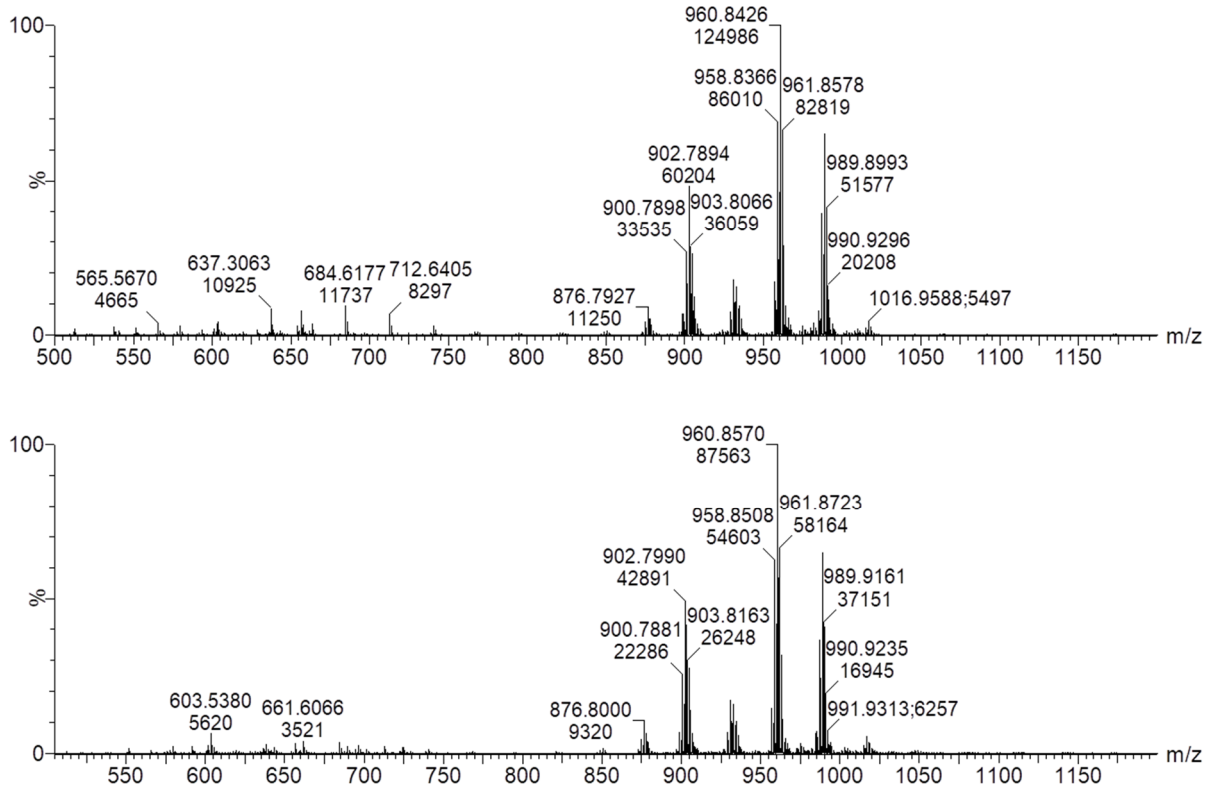

- **Tucuma (two different lots for the butter)**:

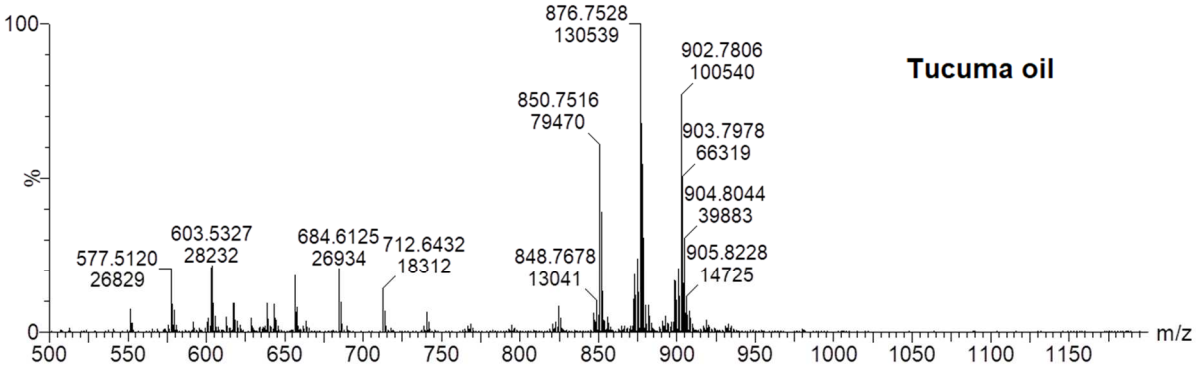

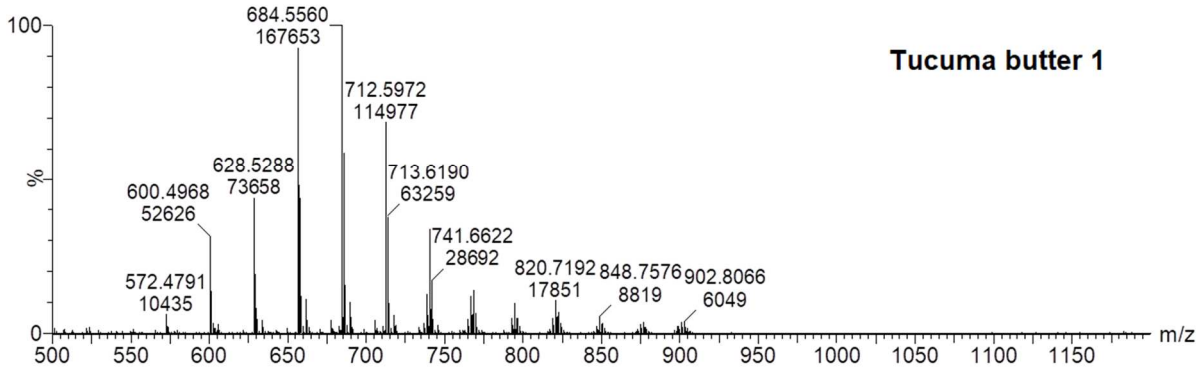

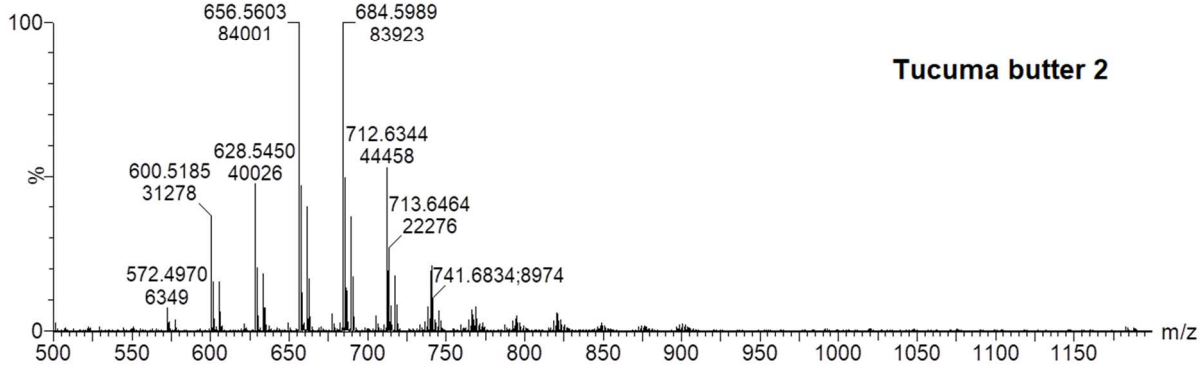

- **Ucuuba (two different lots):**

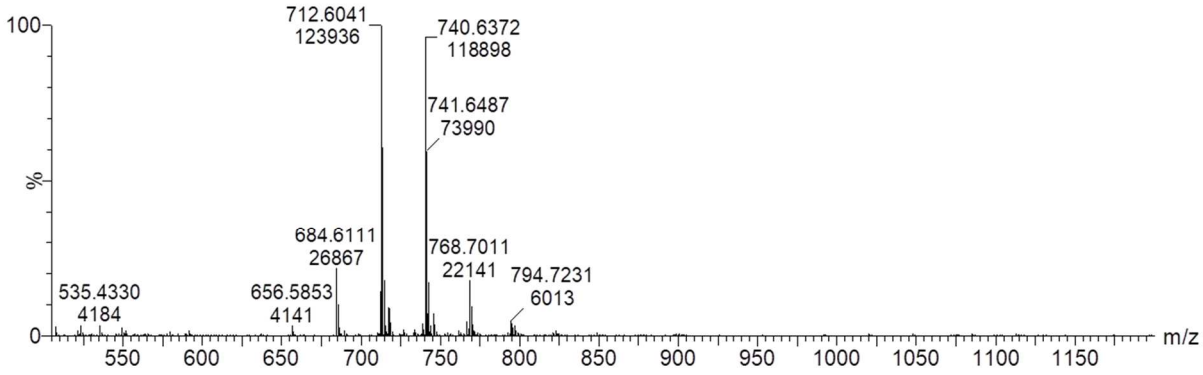

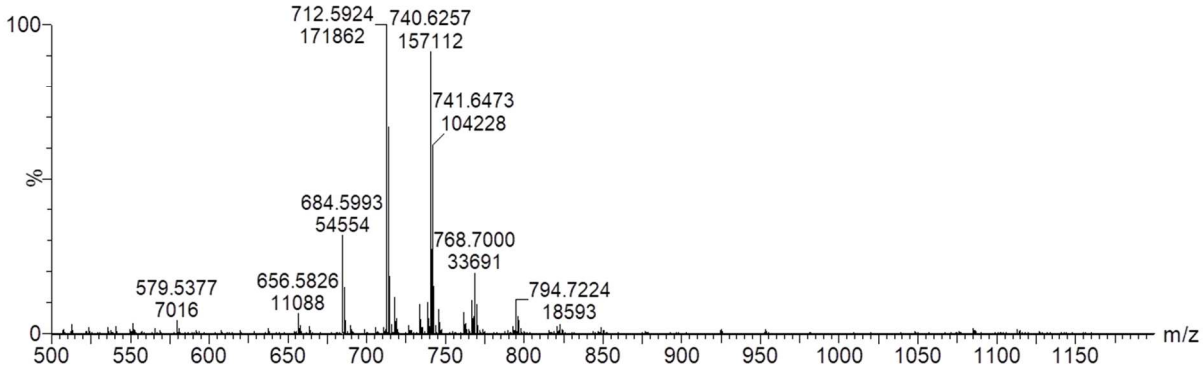

2) Full scan ESI(+)-QTOF mass spectrum of commercial commercial oils and butters:

- **Soybean oils (three different brands):**

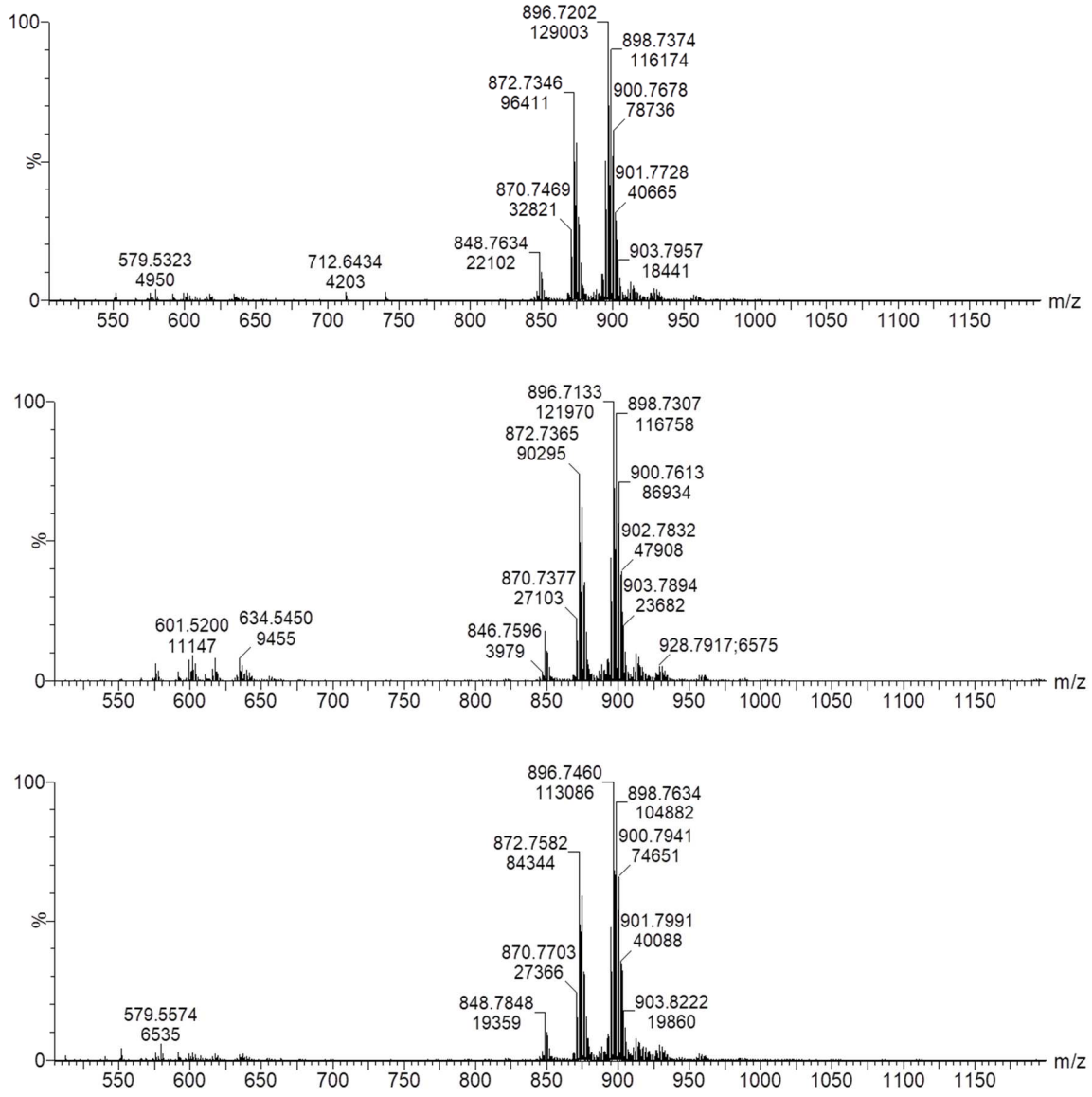

- **Corn oils (three different brands):**

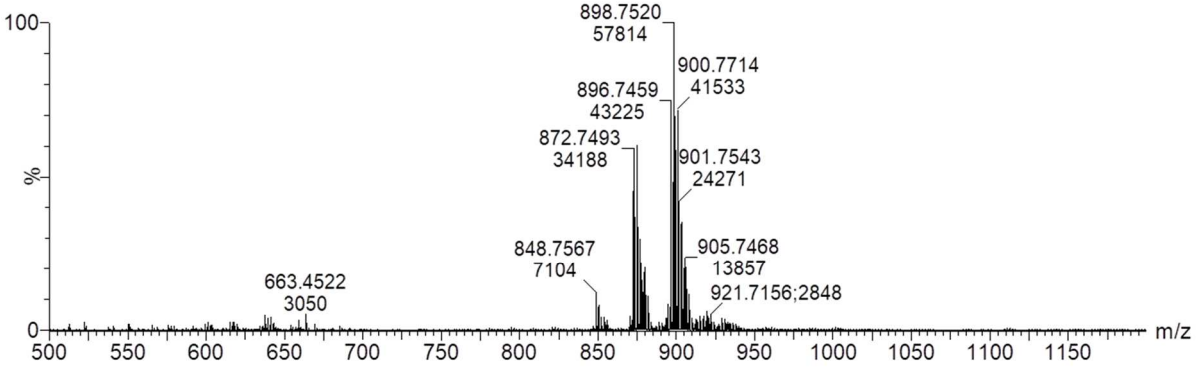

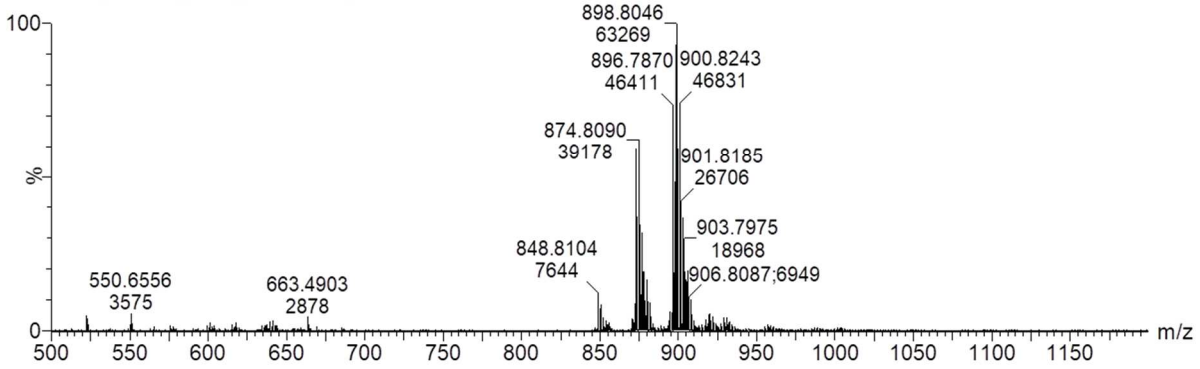

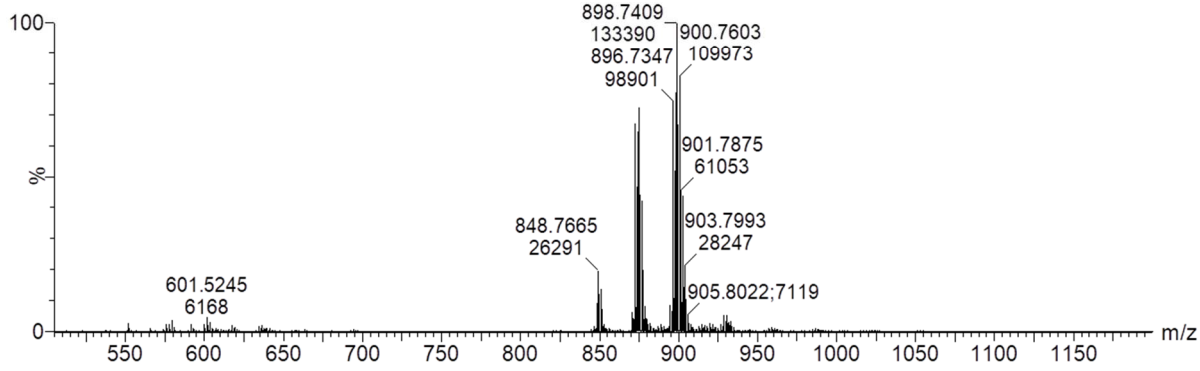

- **Sunflower oils (three different brands):**

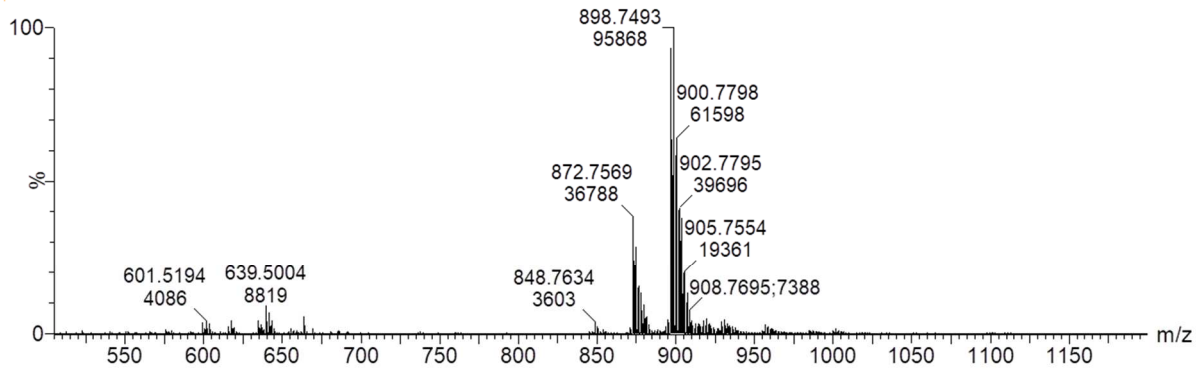

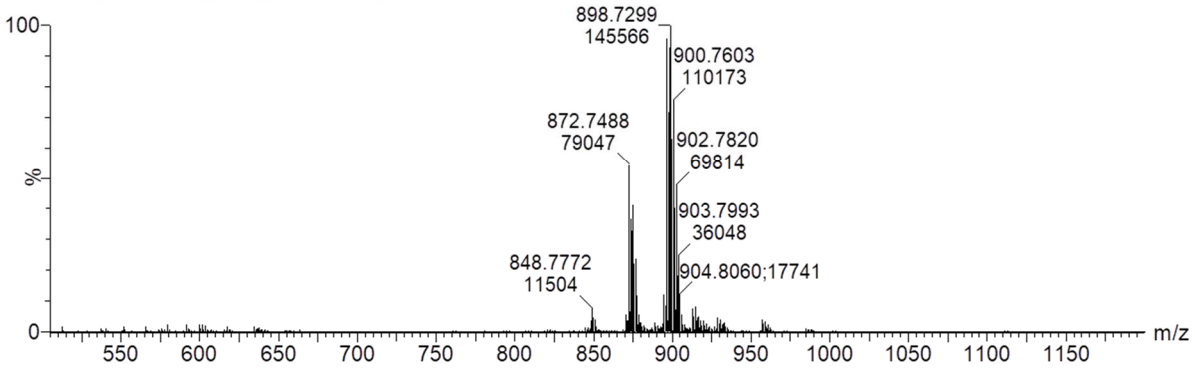

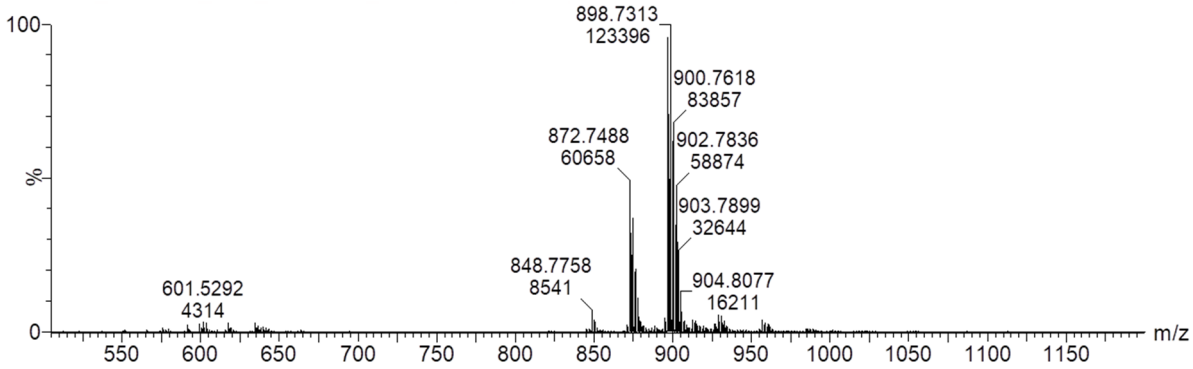

- **Rapeseed oils (three different brands):**

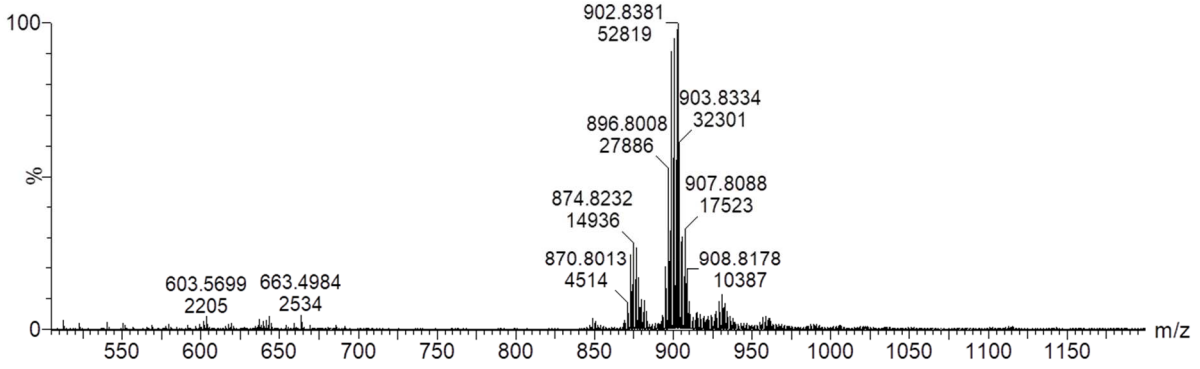

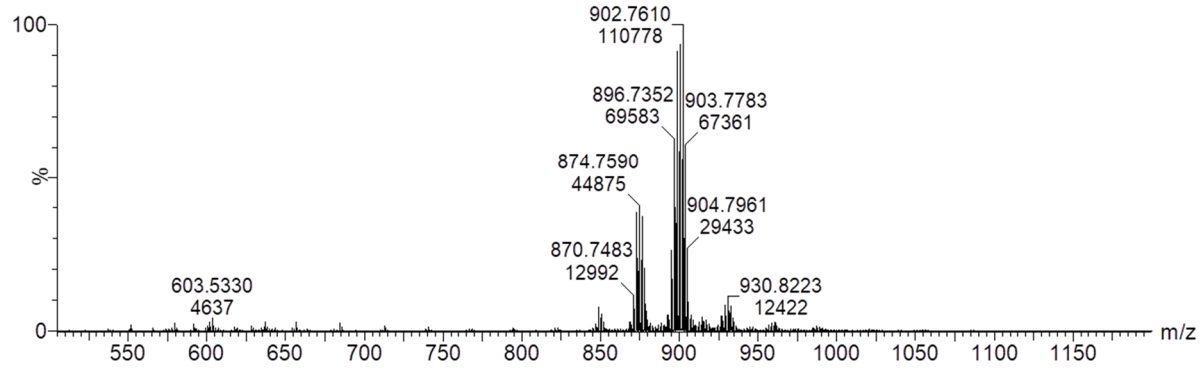

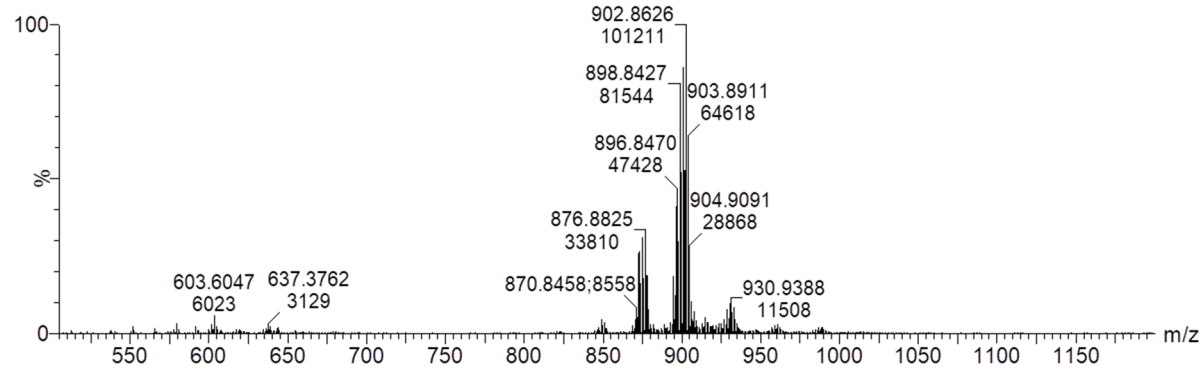

- **Milk butters (three different brands):**

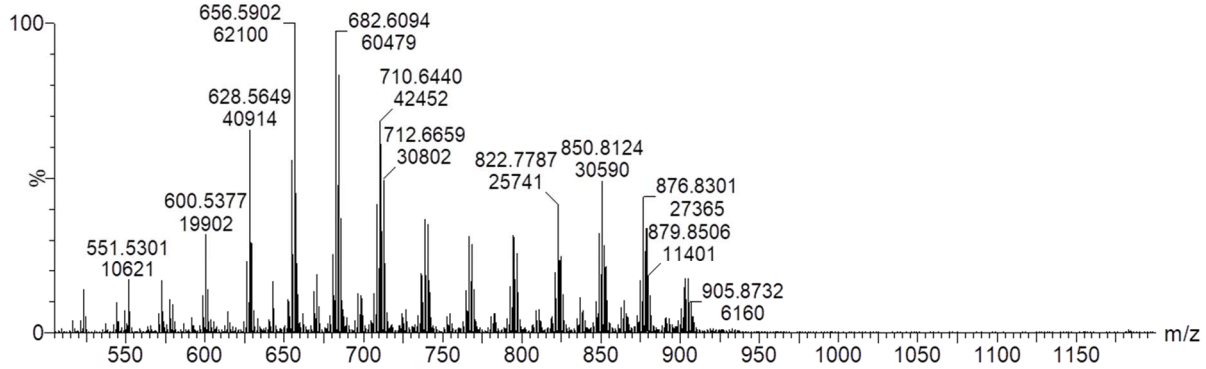

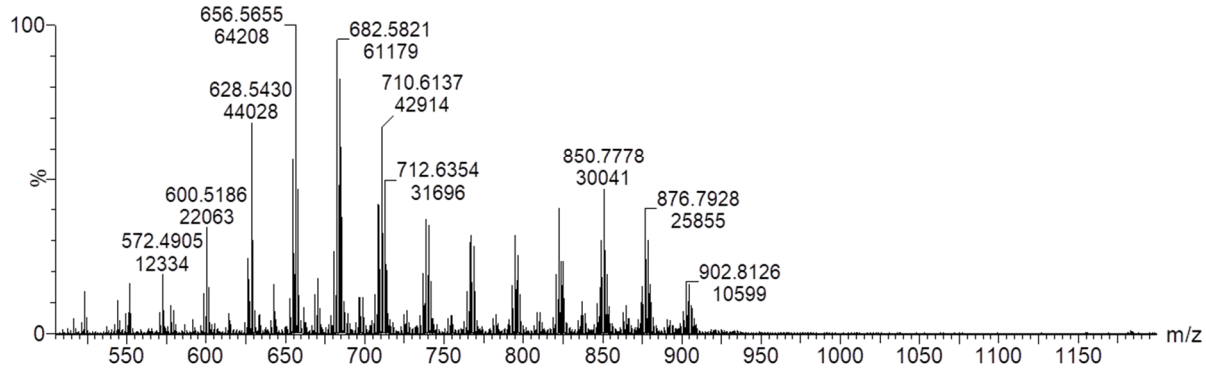

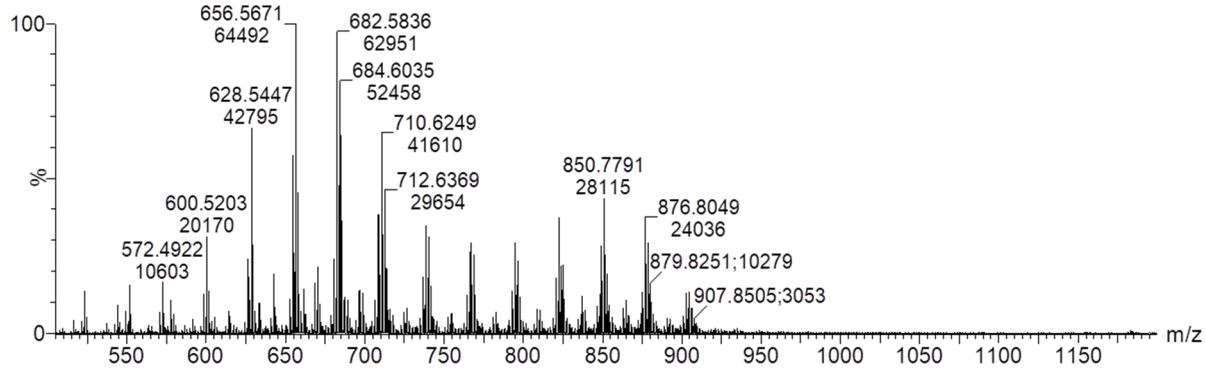

- **Extra virgin olive oils (three different brands):**

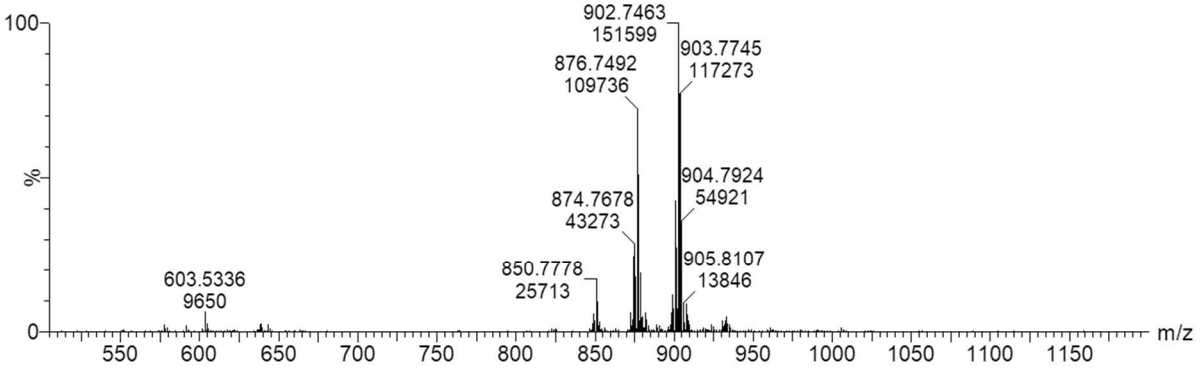

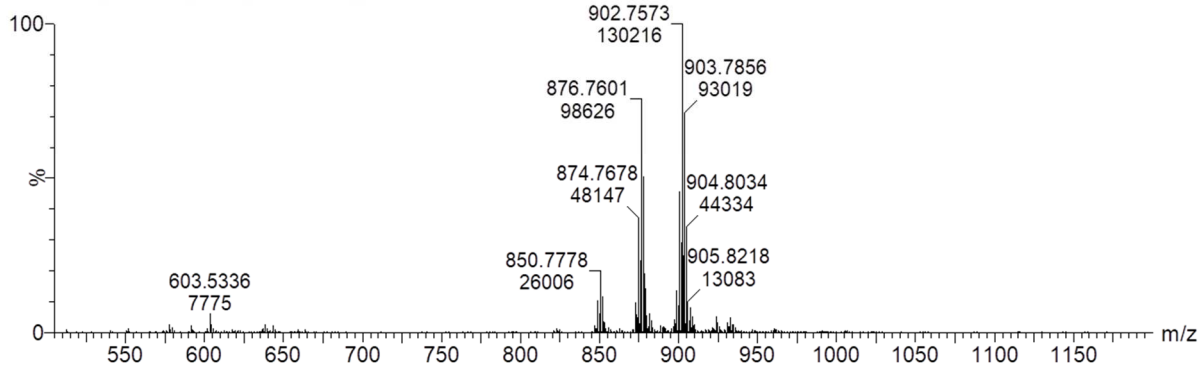

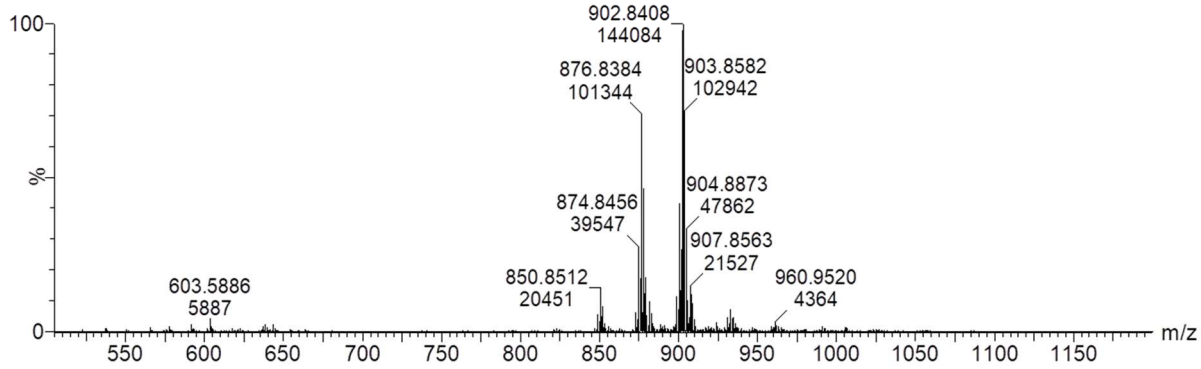

- **Margarine (three different brands):**

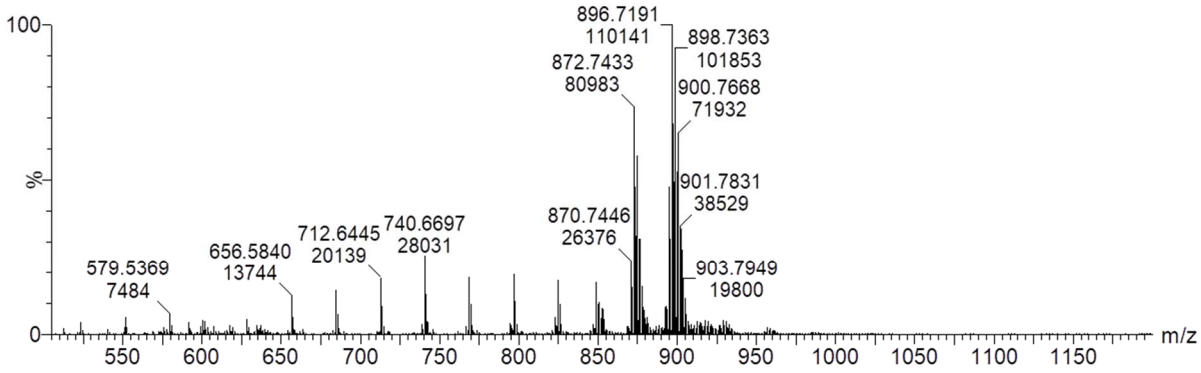

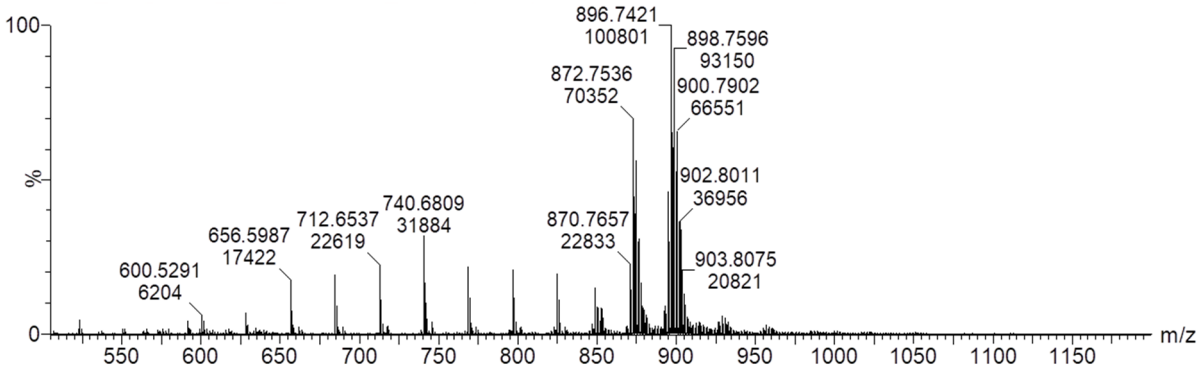

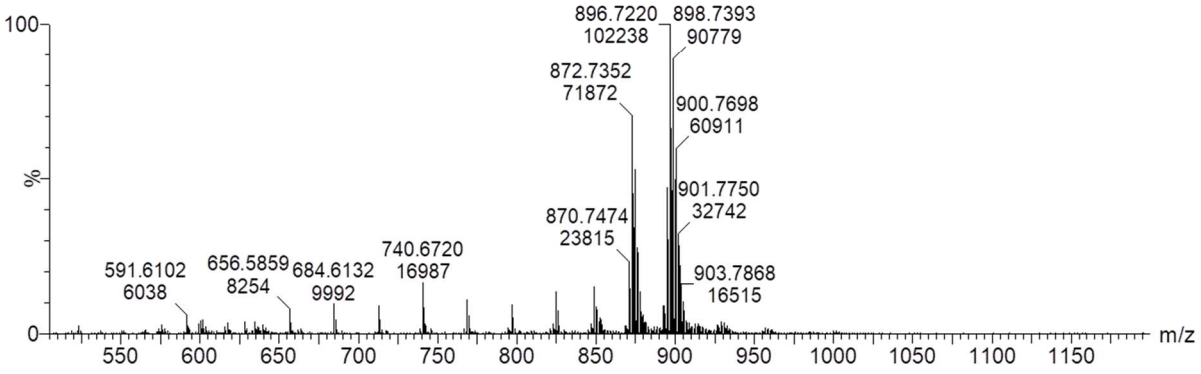

- **Coconut oil (two different brands):**

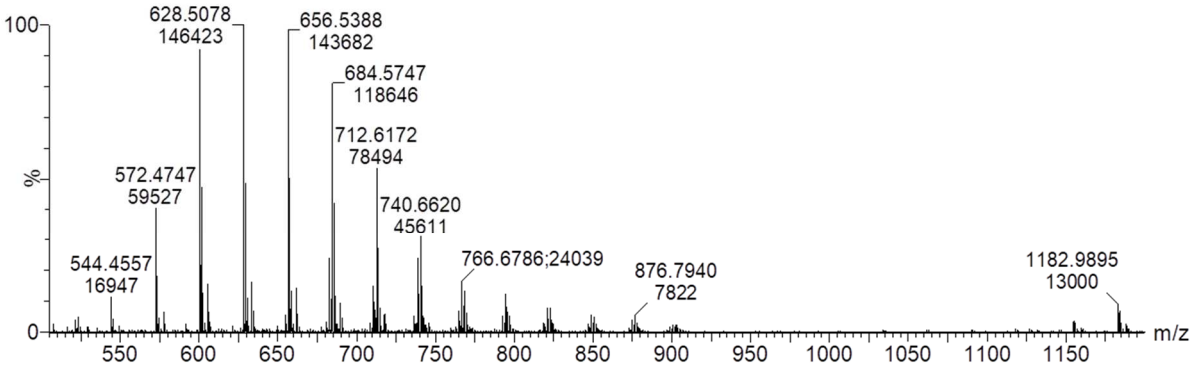

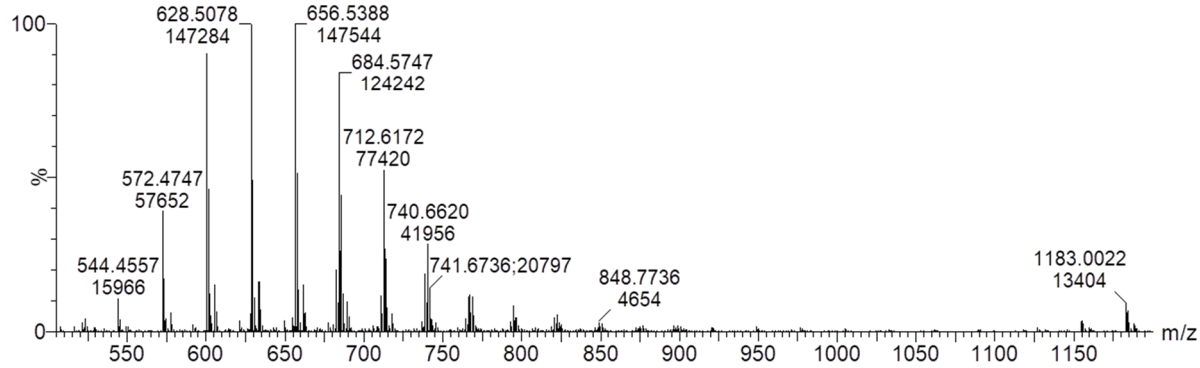

- **Beef tall:**

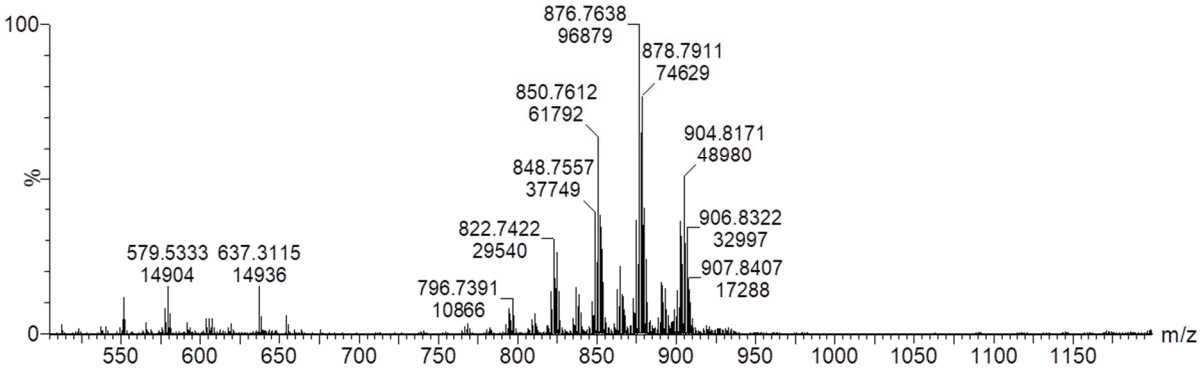

- **Lard:**

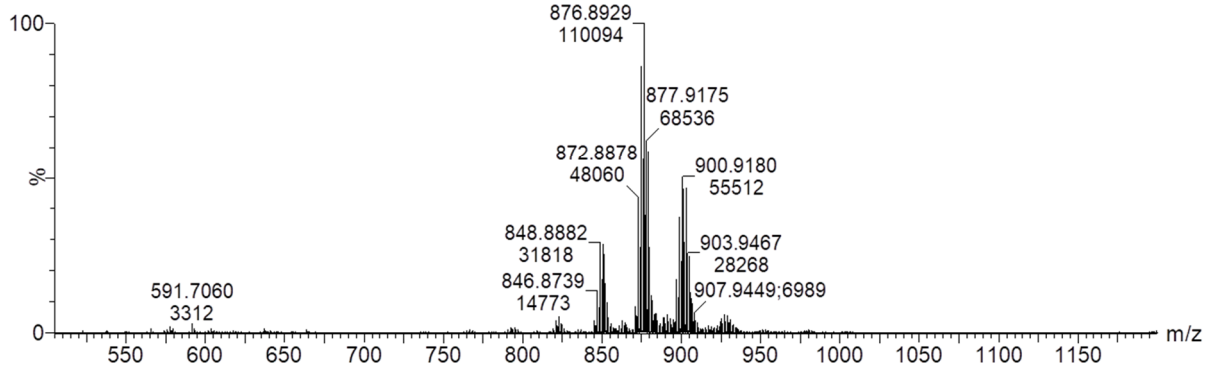
876.8929
110094
877.9175
68536
872.8878
48060
900.9180
55512
848.8882
31818
903.9467
28268
846.8739
14773
907.9449;6989
591.7060
3312
100
%
0
550
600
650
700
750
800
850
900
950
1000
1050
1100
1150
m/z

3) Principal component analysis results:

- **Dendrogram:**

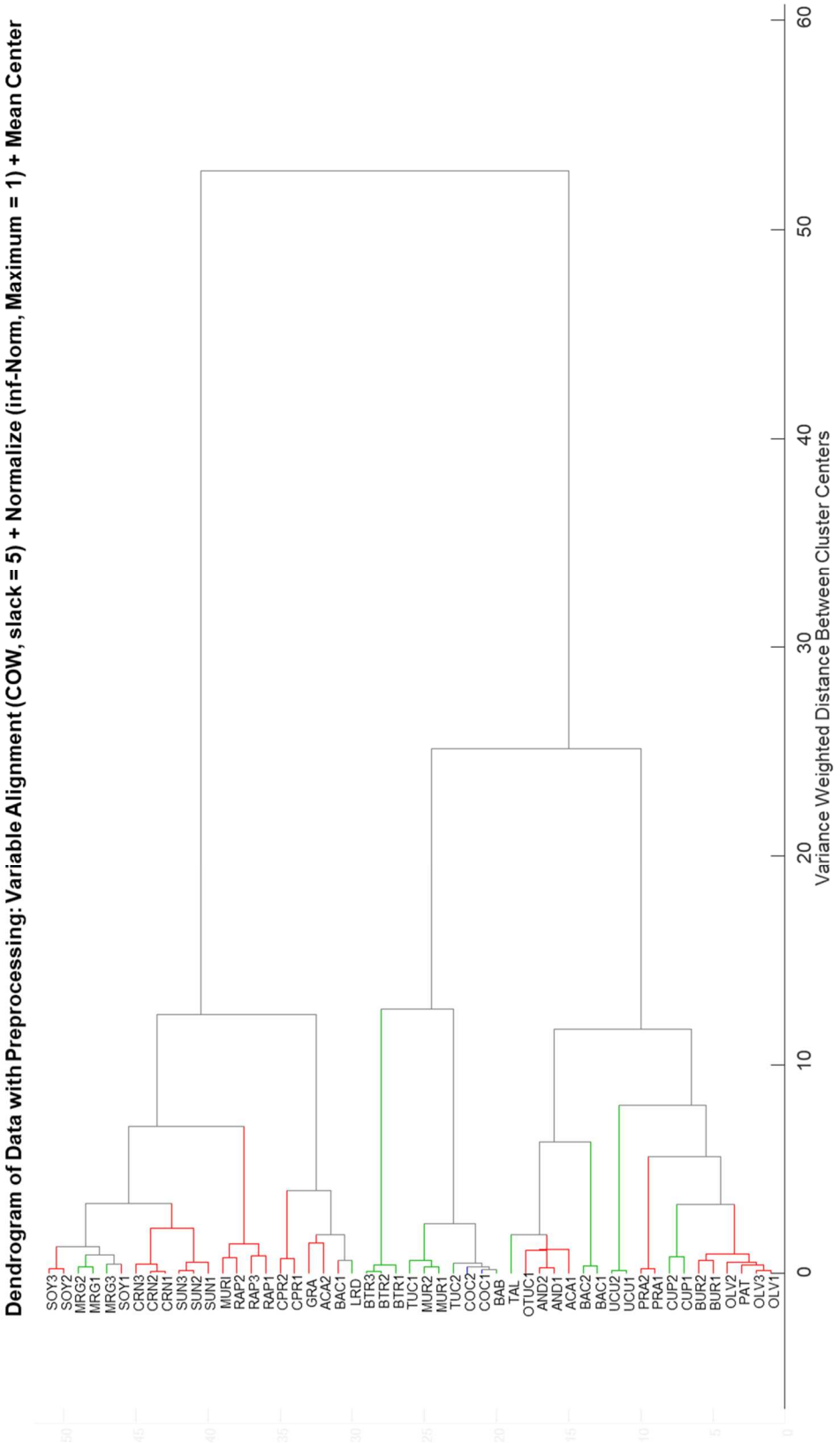

- **Loadings plot:**

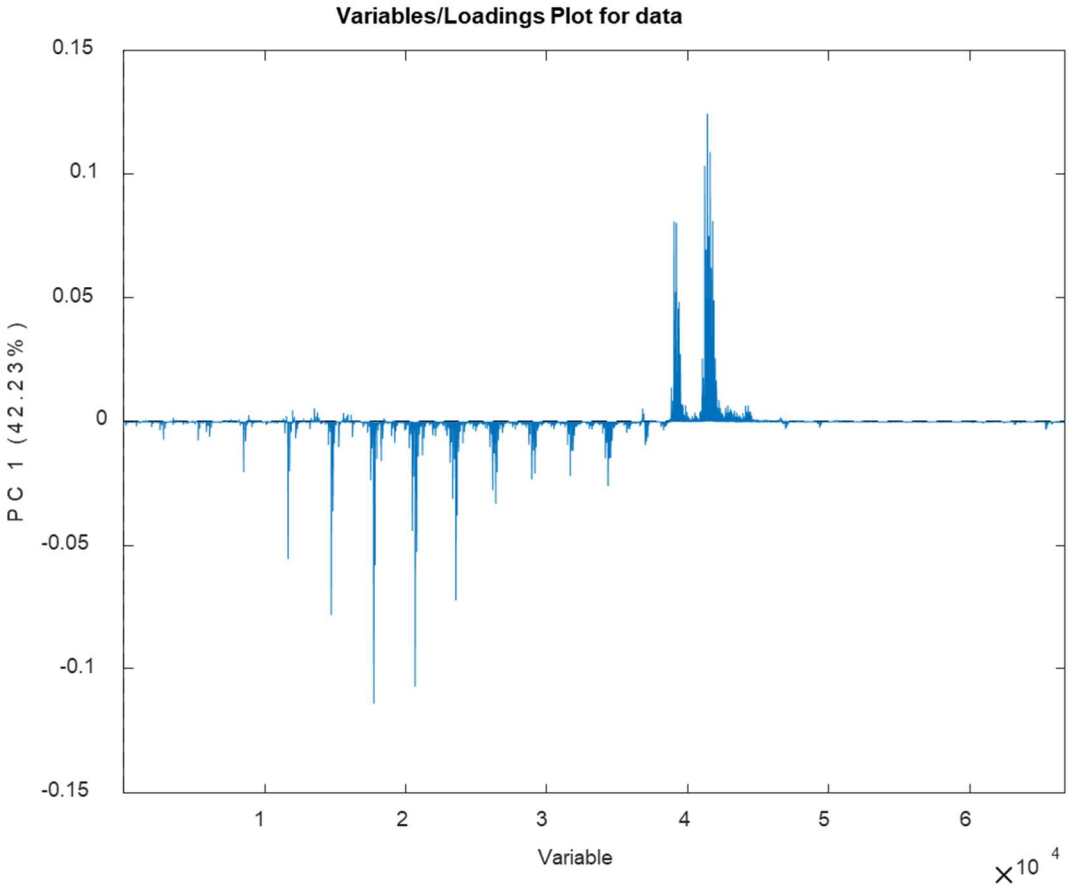

CAPÍTULO 3. DISCUSSÃO

Neste capítulo, serão discutidos os principais resultados obtidos nos quatro diferentes artigos que compuseram esta tese, assim como a motivação para o desenvolvimento dessas pesquisas e as principais contribuições para o tema.

No primeiro artigo *"Wood Chemotaxonomy via ESI-MS profiles of phytochemical markers: The challenging case of African versus Brazilian Mahogany woods"* foi aplicado um método por ESI-QTOF para a diferenciação de metabólitos secundários do mogno brasileiro (MB) e do mogno africano (MA). O método é rápido, simples e "verde": utiliza menos de 2 mL de solvente e 5 minutos em média de análise por amostra.

Este trabalho foi motivado pelo fato que o mogno brasileiro (*Swietenia macrophylla*) é uma das espécies de madeira mais preciosas da Amazônia brasileira, e devido as suas qualidades estéticas e de durabilidade, durante os anos 1990, e até os dias atuais, madeireiras internacionais removeram ilegalmente milhões de metros cúbicos de mogno nativo da floresta amazônica, sendo essa uma das principais causas do desmatamento da Amazônia.

Para impedir a exploração insustentável do mogno brasileiro, e sua consequente extinção, em 2002, esta espécie foi incluída no Apêndice II da Convenção sobre Comércio Internacional de Espécies Ameaçadas (CITES), que estabeleceu uma estrita regulamentação do comércio internacional de espécies nativas do Brasil e em processo de extinção. Além disso, em 2003, o governo brasileiro criou a Lei 4.722, que proíbe o corte de árvores de mogno em todo o país, mesmo em áreas com desmatamento autorizado pelo Instituto Brasileiro do Meio Ambiente e dos Recursos Naturais Renováveis (IBAMA). Embora muitas medidas tenham sido estabelecidas para combater a exploração e a comercialização ilegal de madeira, há uma falta de mecanismos práticos para identificar a origem da madeira e seus produtos. Para isso que, em 2002, o programa de certificação florestal brasileiro (CERFLOR) foi criado e foi desenvolvido pelo Instituto Nacional de Metrologia, Qualidade e Tecnologia (INMETRO), organização governamental ligada ao Ministério do Desenvolvimento, Indústria e Comércio Exterior (MDIC).

Com o objetivo de diminuir o impacto causado pela devastação insustentável da Amazônia, algumas iniciativas começaram a ser tomadas nas últimas décadas.

Uma delas foi a introdução da *Khaya ivorensis* em solo brasileiro, também conhecido como mogno africano. Esta espécie ocorre naturalmente na costa oeste do continente Africano e tem sido usada para o reflorestamento da Amazônia brasileira devido à sua madeira de alta qualidade e sua alta resistência a pragas como a "broca" *Hypsiphyla grandella*, que é a principal praga do mogno brasileiro. Atualmente, estima-se que há um milhão de árvores de mogno africano plantadas no Brasil e pelo menos 400 produtores estão investindo nesta cultura.

Tanto o mogno brasileiro quanto o africano pertencem à família *Meliaceae*, mas a gêneros e espécies diferentes. A diferenciação em campo de ambas as espécies não é uma tarefa fácil, devido à semelhança visual entre ambas, faltando assim ferramentas que atestem a origem da madeira e sirvam de prova legal em casos de suspeita de exploração ilegal, fazendo-se, assim, necessário o desenvolvimento de metodologias analíticas para este propósito.

O objetivo deste artigo foi desenvolver e aplicar uma metodologia de análise rápida e simples, que seja capaz de diferenciar de forma inequívoca o mogno brasileiro nativo e o mogno africano, que vem sido utilizado em regiões de reflorestamento. Uma vez que este método baseado na diferenciação quimiotaxonômica entre ambas as espécies seja estabelecido, espera-se que ele possa vir a servir de ferramenta para a certificação do mogno local do Brasil e mogno utilizado para reflorestamento, inibindo ou contribuindo para impedir a exploração ilegal da *S. macrophylla* na Amazônia.

As amostras de mogno Africano certificado (*K. ivorensis*) foram doados pela Empresa Brasileira de Pesquisa Agropecuária (EMBRAPA - Amazônia Oriental). O Mogno Africano é proveniente da cidade de Belém no Estado do Pará. Já as amostras certificadas mogno brasileiro (*S. macrophylla*) foram provenientes de partes de móveis antigos e foram doados por uma serraria local, uma vez que atualmente não é permitida a extração de árvores de mogno brasileiras nativas no Brasil.

Os extratos metanólicos das amostras de madeira foram preparados *in situ* antes da análise; para o mogno brasileiro, as amostras foram coletadas aleatoriamente a partir das partes móveis e misturados para a preparação e extração das amostras. Para o mogno Africano, as amostras foram coletadas ao longo de todo o raio da seção transversal do tronco da árvore, em pontos de amostragem espaçados por 3 cm de distância um do outro. Os compostos orgânicos presentes nos extratos

metanólicos das madeiras de mogno brasileiro e africano foram investigados utilizando espectrometria de massas de alta e ultra alta resolução.

Sabe-se que as madeiras são principalmente formadas de carboidratos, tais como a celulose, a hemicelulose e as ligninas. [73] Baseando-se nessas classes de compostos, uma composição química muito precisa não pode ser definida para cada espécie de uma dada madeira, porque estas composições dos compostos majoritários variam de acordo com vários parâmetros tais como a parte da árvore, tipo de madeiram origem geográfica e também com as condições ambientais. [74] Uma análise química mais detalhada das madeiras é conseguida através da análise dos compostos minoritários presentes nos "extrativos" da madeira e permite a avaliação quimiotaxonômica das espécies, que é justamente a classificação baseada nos constituintes químicos. Os extrativos são, portanto, uma fração minoritária da madeira (entre 4-10%) que pode ser extraída com água ou solventes orgânicos de diferentes polaridades. Esta fração é composta basicamente de compostos de massa molecular relativamente baixa, geralmente metabólitos secundários característicos de cada espécie.

Da análise em modo de íons positivos, ESI(+), foi possível observar diferenças bastante notáveis nos espectros de massas para o MA e para o MB. O MB apresenta uma série de íons bastante intensos na faixa de *m/z* de 700 a 900. Nenhum íon significativamente intenso nessa mesma faixa de *m/z* pôde ser observado para o espectro obtido para o extrato do MA. Este fato inicialmente indica que, mesmo que ambas as madeiras de mogno sejam muito similares via comparação visual, por pertencerem a gêneros e espécies diferentes, elas apresentam um perfil de metabólitos secundários completamente distintos, o que é de fato esperado. Isso mostra que esta metodologia pode ser bastante promissora para a diferenciação inequívoca entre essas duas espécies.

É esperado que os metabólitos secundários identificados como possíveis biomarcadores de ambas espécies de mogno formem misturas complexas contendo diversas classes de compostos, que podem incluir flavonoides, terpenos, fenóis,

[73] O. Theander, Fundamentals of Thermochemical Biomass Conversion Cellulose, Hemicellulose and Extractives, **1985**, p. 35 - 60.
[74] R.C. Pettersen, The Chemical Composition of Wood. The Chemistry of Solid Wood, **1984**, May 5, 57-126.

alcaloides, esteróis, ceras, gorduras, taninos, carotenóides, polifenóis e limonóides.[75,76]

Os principais íons detectados nas duas espécies de madeira e apresentados também foram caracterizados por MS/MS, e suas massas exatas também foram confirmadas com a técnica auxiliar de FT-ICR-MS, já que devido à complexidade das amostras, o espectrômetro de massas QTOF utilizado não apresentava resolução e exatidão de *m/z* suficiente para uma atribuição de fórmula molecular inequívoca para os metabólitos detectados.

A mesma abordagem foi realizada para as análises em modo de aquisição de íons negativos, ESI(-), porém ao contrário dos resultados observados em ESI(+), os espectros de massas para os mognos de diferentes espécies são mais similares entre si do que no modo positivo. Há um íon de *m/z* 451 que se mostra ser mais característico do mogno brasileiro, que de fato foi detectado como pico base dos espectros de todas as amostras de mogno brasileiro e não foi detectado na amostra de mogno africano.

Em ESI(-) é esperado que sejam detectados compostos com grupos polares facilmente desprotonáveis em suas estruturas. Baseando-se nas classes mais comuns de substâncias que podem ser encontradas em extrativos de madeiras, pode-se esperar que sejam detectadas substâncias tais como ácidos orgânicos e polifenóis. De fato, alguns polifenóis puderam ser identificados com erro de massa inferior a 2 ppm. O íon de *m/z* 451 foi dentificado como cinchonain (isômero IA ou IB). O cinchonain também já foi reportado em outras espécies, tais como *Phyllocladus trichomanoides*, [77] *Rhizoma Smilacis glabrae*,[78] e na *Trichilia catiguá*.[79] Pela primeira vez, essa molécula foi detectada na espécie de *S. macrophylla*, sendo um potencial biomarcador característico do mogno brasileiro quando analisado em modo negativo.

Foram majoritariamente identificados por suas fórmulas moleculares polifenóis como epi/catequina, a partir das análises dos extrativos do mogno africano em modo

---

[75] Gottlieb, O.R., Phytochemicals: Differentiation and Function. *Phytochemistry*, **1990**, 29, 1715.
[76] J. E. Poulton, 1981. The Biochemistry of Plants. Secondary Plant Products (Conn, E E, ed.), p 667 Academic Press, Vol 7. New York
[77] L.Y. Foo, Phenylpropanoid derivatives of catechin, epicatechin and phylloflavan from Phyllocladus trichomanoides. *Phytochemistry,* **1987**, 26. 2825.
[78] S. D. Chen, C. J. Lu , R. Z. Zao, Qualitative and quantitative analysis of Rhizoma Smilacis glabrae by ultra high performance liquid chromatography coupled with LTQ OrbitrapXL hybrid mass spectrometry. *Molecules*, **2014**, 19, 10427.
[79] F. L. Beltrame, E. R. Filho, F. A. P. Barros, D. A. G. Cortez, Q. B. Cass, A validated higher-performance liquid chromatography method for quantification of cinchonain Ib in bark and phytopharmaceuticals of Trichilia catigua used as Catuaba, *Journal of Chromatography A,* **2006,** 1119, 257.

negativo. Um aspecto interessante dos espectros em ESI(-) é que se observa uma série de íons que podem ser atribuídos a polímeros de catequina (ou epicatequina, já que não é possível realizar a diferenciação isomérica nessa análise) através de seus íons $[M - H]^-$, ou seja, dímeros (*m/z* 577), trímeros (*m/z* 865) e tetrâmeros (*m/z* 1153), que são flavonoides conhecidos como proantocianidinas. Esta série também foi detectada nos extrativos do mogno brasileiro quando analisado em ESI(-).

Todos os conjuntos de dados obtidos tanto em modo positivo quanto negativo de íons para os extrativos das espécies de mogno africano de brasileiro mostram que, através de conjuntos característicos de limonóides e polifenóis, é possível distinguir quimicamente e, portanto, inequivocamente ambas as espécies de madeira. A abordagem quimiotaxonômica demonstrada aqui somente pôde ser alcançada através da técnica de espectrometria de massas aplicada neste trabalho.

Em seguida, o segundo artigo apresentado nesta tese foi o intitulado "*Two-point normalization using internal and external standards for a traceable determination of $\delta^{13}C$ values of fatty acid methyl esters by gas chromatography/combustion/isotope ratio mass spectrometry*". Neste trabalho, apresentou-se o desenvolvimento de um método analítico através da técnica GC-IRMS para a determinação rastreável do valor isotópico de carbono ($\delta^{13}C$) dos ésteres metílicos de ácidos graxos (*fatty acid methyl esters* - FAMEs) de amostras de óleo de pinhão manso (de diferentes origens geográficas) com um diferencial de utilizar dois padrões para a correção de possíveis desvios provenientes de fracionamento isotópico que podem ocorrer durante a conversão do óleo vegetal em FAME, ou durante a análise em si.

A motivação desse trabalho foi a importância da determinação exata e rastreável dos valores isotópicos de FAMEs, que se destacam como um grupo importante de moléculas para muitas áreas, uma vez que a análise desta classe de compostos é geralmente empregada na caracterização de alimentos, em sistemas biológicos, em esferas ambientais como sedimentos, e atualmente também na área dos biocombustíveis. Principalmente com a consolidação do biodiesel como um dos biocombustíveis mais utilizados atualmente, várias espécies oleaginosas têm sido alvo de desenvolvimentos e melhorias genéticas para garantir a melhor qualidade, rendimento e performance em motores. [80] Além disso, dependendo da fonte de

[80] P. S. Nigam, A. Singh, Production of liquid biofuels from renewable resources. *Progress in energy and combustion science*, **2011**, 37(1), 52.

matéria prima empregada para a produção do biodiesel, sua sustentabilidade pode ser fortemente questionada. Sendo assim, a IRMS pode ser usada para determinar as assinaturas isotópicas de diferentes fontes de matérias-primas empregadas para produção do biodiesel.

Como exemplo, tem-se a *Jatropha curcas*, mais conhecida como pinhão manso, que é considerada uma das oleaginosas mais promissoras para a produção de biodiesel devido a diversas características que tornam seu biodiesel bastante adequado ao uso em larga escala. [81] Com isso, esse artigo pretendeu avaliar o perfil isotópico de carbono em diferentes amostras de pinhão-manso produzidas no Brasil, uma vez que não havia dados sobre este parâmetro reportado na literatura.

Como explicado em detalhes no item 1.3.2 desta tese, na técnica de IRMS, as amostras (ou compostos específicos) são convertidas em um gás através de processos de oxidação e/ou redução (dependendo do elemento de interesse) em uma interface com o sistema de introdução de amostra (seja um cromatógrafo a gás, a líquido ou um analisador elementar) e comparado a um gás de referência cujo valor isotópico é determinado através da utilização de padrões aceitos internacionalmente e rastreáveis a escala internacional. Para isso, os materiais de referência certificados (MRC) são utilizados para atribuir um valor isotópico ao gás de referência, assim como para normalizar os valores isotópicos brutos determinados nas amostras. O grande problema é que os MRC aceitos internacionalmente para medições isotópicas são sólidos não voláteis ou materiais viscosos, e por isso eles são exclusivamente compatíveis com analisadores elementares. Então, equipamentos de IRMS que tenham apenas a técnica de GC como sistema de introdução de amostras não tem como determinar o valor isotópico do gás de referência usando os MRC internacionalmente aceitos. E, por consequência, os valores isotópicos determinados através da técnica não tem rastreabilidade e, muitas vezes, são inexatos. Então, neste caso, métodos de normalização dos dados brutos determinados por GC-IRMS são altamente recomendados, utilizando padrões secundários de trabalho de alta pureza, com propriedades físicas e químicas semelhantes aos analitos de interesse, mesma faixa de valores isotópicos, cujos valores isotópicos tenham sido devidamente determinados através da técnica de EA-IRMS e rastreáveis à escala internacional.

[81] M. Y. Koh, T. I. M. Ghazi, A review of biodiesel production from *Jatropha curcas* L. oil. *Renewable and Sustainable Energy Reviews*, **2011**, 15(5), 2240.

Sendo assim, o objetivo geral deste artigo foi desenvolver uma metodologia para determinar a assinatura isotópica $^{13}C/^{12}C$ de óleos de *J. curcas* de diferentes origens geográficas do Brasil, bem como a dos FAMEs correspondentes das amostras de biodiesel obtidas de cada um dos óleos. Para avaliar a exatidão das medições isotópicas, pesquisaram-se as fontes de fracionamento isotópico em todas as etapas de obtenção das amostras, desde a extração de óleo até as análises em si por GC-IRMS. Para isso, utilizaram-se padrões internos e externos para corrigir o fracionamento isotópico que ocorre durante a transesterificação da amostra e durante a análise cromatográfica. Ao todo 9 amostras de *J. curcas* foram analisadas neste capítulo. Algumas delas foram recebidas como sementes e outras já como óleos extraídos. Apenas uma das amostras não teve a sua origem garantida, identificada como “desconhecida”.

As extrações de óleo das sementes de *J. Curcas* forneceram bons resultados, obtendo-se de 32,1 a 43,7% (m/m) de rendimento, que são os valores esperados para essas sementes oleaginosas. Também se realizou a extração das sementes em triplicata para verificar se poderiam haver variações do $\delta^{13}C$ devido a não homogeneidade das amostras ou devido a alguma fonte de fracionamento isotópico durante a extração de óleo. Para avaliar isso, mediram-se os valores de $\delta^{13}C$ globais de todas as triplicatas de extração de óleo da amostra 813 (selecionada aleatoriamente) por EA-IRMS. Os valores médios foram completamente equivalentes, sendo o desvio padrão dos valores $\delta^{13}C$ para cada repetição de extração equivalente ao desvio padrão da medição da técnica para uma mesma amostra (0,04 *versus* 0,03 mUr). Assim, as replicatas de extração de óleo podem ser agrupadas em apenas uma, uma vez que não foi detectada falta de homogeneidade ou qualquer fracionamento isotópico na etapa de obtenção do óleo.

Os valores de $\delta^{13}C$ dos óleos de *J. curcas* de diferentes origens geográficas do Brasil foram, então, determinados pela técnica de EA-IRMS. Os valores obtidos para diferentes amostras foram muito próximos entre si para todas as amostras, variando de -29,90 a -28,50 mUr, com o valor médio de -28,97 ± 0,43 mUr (n = 9 amostras). Os resultados para a assinatura isotópica de $\delta^{13}C$ para a *J. curcas* estão de acordo com os valores esperados para plantas de metabolismo C3, tais como a canola, palma,

soja e oliva, que se encontram na faixa de cerca de -31 a -29 mUr, conforme já descrito na literatura. [82]

A etapa seguinte consistiu na otimização do método de transesterificação do óleo de *J. curcas*. O método de transesterificação otimizado neste trabalho permitiu obter mais de 95% de conversão do óleo em ésteres totais. Todas as amostras puderam ser derivatizadas simultaneamente em banho ultrassônico com aquecimento, o que é importante para garantir condições de repetibilidade durante a derivatização das amostras e assim minimizar fontes de fracionamento isotópico. Outro aspecto importante desse preparo de amostra foi a adição do padrão de éster metílico C22:0 no início da reação, juntamente com o óleo *J. curcas* e os reagentes de derivatização, o que significa que o padrão foi submetido ao princípio do tratamento idêntico (*Identical Treatment* – IT) durante o curso reacional e pode ser usado para corrigir ou minimizar algum fracionamento isotópico oriundo desse processo. Após a transesterificação das amostras, o padrão de éster metílico C19:0 foi usado como padrão externo, para corrigir somente variações instrumentais ou fracionamento isotópico durante o curso das análises por GC-IRMS.

O material de referência (MR) de FAME C18:0 (produzido pela *Indiana University, Bloomington*, IN, EUA) é adequado para a calibração do gás de referência, uma vez que é um FAME presente nas amostras de estudo e porque possui um valor isotópico na faixa de valores esperados para os valores isotópicos dos FAMEs da *J. curcas*. Já os padrões analíticos de FAMEs C22:0 e C19:0 foram utilizados como padrões internos e externos, como já mencionado: o primeiro para a corrigir as fontes de desvio que vem da transesterificação; e o segundo para corrigir os desvios da exclusivamente da própria análise GC-IRMS. Seus valores de $\delta^{13}C$ de referência foram determinados com a técnica de EA-IRMS, sendo rastreáveis à escala internacional através do padrão primário internacionalmente aceito, o MRC NBS22, produzido pelo IAEA (*International Atomic Energy Agency*) em parceria com o NIST (*National Institute of Standards and Technology*). Esses valores foram usados como

[82] A) F. Angerosa , O. Bréas , S. Contento , C. Guillou , F. Reniero , E. Sada. Application of stable isotope ratio analysis to the characterization on the geographical origin of olive oils. J. *Agric. Food Chem*, **1999**, 47, 1013; B) J. E. Spangenberg, S. A. Macko, J. Hunziker, Characterization of olive oil by carbon isotope analysis of individual fatty acids: Implications for authentication. *J. Agric. Food Chem.*, **1998**, 46, 4179; C) F. Angerosa, L.Camera, S. Cumitini, G. Gleixner, F. Reniero, Carbon stable isotopes and olive oil adulteration with pomace oil. *J. Agric. Food Chem.*, **1997**, 45, 3044; D) A. Royer, C. Gerard, N. Naulet, M. Lees, G. J Martin. Stable isotope characterization of olive oils. I - Compositional and carbon-13 profiles of fatty acids. *J. A. O. C. S.*, **1999**, 76, 357.

valores "verdadeiros" para normalizar os valores brutos de $\delta^{13}C$ dos FAMEs de *J.curcas* usando o método de normalização de dois pontos.

Juntamente com a estratégia de normalização dos dados brutos utilizando padrões internos e externos, a resolução cromatográfica é outro aspecto muito importante da análise para garantir exatidão e precisão dos resultados. Comparando as resoluções cromatográficas das técnicas GC acoplada a MS convencional e de GC-IRMS, a resolução desta última tende a ser pior, devido a um processo de difusão longitudinal na interface de combustão, resultando em picos cromatográficos mais alargados e assimétricos. Portanto, para ser acoplada ao IRMS, é necessária uma resolução cromatográfica melhorada, já que os analitos ao eluir da coluna entrarão no reator de combustão e sofrerão difusão longitudinal por gradiente de concentração inerente deste processo. Duas colunas foram testadas, uma CP-WAX e uma DB-23, no entanto, esta última forneceu melhores resultados em termos de formato de pico cromatográfico e resolução.

Foram elaboradas cartas controle dos valores isotópicos brutos dos FAMEs C18:0 e C22:0 injetados entre amostras para verificar a resposta instrumental do equipamento. De fato, observa-se um desvio considerável dos valores de referência (superior ao desvio padrão esperado para uma medição de GC-IRMS, que é de aproximadamente ± 0,20 mUr). Este comportamento aponta que os resultados brutos das amostras certamente devem ser submetidos à normalização para garantir a exatidão dos valores medidos. Outro fato notável é que esses dois padrões não apresentaram o mesmo comportamento: o $\delta^{13}C$ de C18:0 apresentou, em média, uma tendência positiva (-22,99 mUr *versus* o valor de referência de -23,24 mUr) enquanto o C22:0 teve uma tendência negativa (-27,31 mUr em relação ao valor de referência medido por EA- IRMS de -27,09 mUr). Portanto, pelo menos dois padrões devem ser implementados para a normalização dos dados para evitar a introdução de erros sistemáticos nas medições. Entretanto, a diferença encontrada para estes dois padrões é relativamente baixa, o que mostra que as variações instrumentais não são tão graves, mas que precisam ser verificadas, principalmente em sequências longas de injeção.

Observando-se também os dados brutos para os FAME C19:0 e C22:0, usados como padrões interno e externo, analisados juntamente com as amostras de *J. curcas*, pode-se notar que todos os valores do C22:0 apresentaram uma tendência positiva e

sofrem variações mais acentuadas, enquanto o C19:0 tem um comportamento diferente: seus valores permanecem estáveis por mais tempo e tendem a tornar-se mais negativos com o número de análises. Portanto, podem ser recomendados pequenos períodos de oxidação do reator de combustão para minimizar esse efeito. A conclusão mais importante, porém, sobre as tendências mostradas nas cartas controle elaboradas, é que a preparação da amostra tem uma contribuição mais pronunciada para a falta de exatidão dos resultados, podendo levar a erros sistemáticos, como observado com o erro positivo para o padrão C22:0.

Admitindo-se que os FAMEs da *J. curcas* estão sendo submetidos aos mesmos processos físico-químicos dos padrões C19:0 e C22:0, tanto nas etapas de derivatização, quanto nas análises de GC-IRMS, e que estão seguindo o princípio do tratamento idêntico, os valores de $\delta^{13}C$ medidos de ambos os padrões foram utilizados para corrigir os valores brutos de $\delta^{13}C$ para todos os FAMEs das amostras de *J. curcas*. Os valores isotópicos médios variaram entre -28,29 e -30,82 mUr, sendo o C18:2 o ácido graxo com o valor isotópico mais negativo para todas as amostras. Os valores isotópicos médios globais para todas as amostras e cadeias de ácidos graxos foram de -29,51 ± 1,03 mUr, o que está de acordo com o valor médio para amostras do óleo de *J. curcas* determinado por EA-IRMS, -28,97 ± 0,43 mUr, indicando a exatidão dos resultados.

Todos os dados apresentados neste trabalho mostraram que procedimentos de garantia de qualidade devem ser utilizados para garantir a exatidão dos resultados de valores isotópicos, mesmo para procedimentos de derivatização mais simples, como transesterificações; e também para amostras simples como óleos vegetais puros. A reação de transesterificação é a principal fonte de fracionamento isotópico e resultados com erros sistemáticos podem ser obtidos. A medição em si também pode levar a erros sistemáticos e aleatórios. Ambos os efeitos podem ser eliminados - ou pelo menos minimizados - usando padrões internos e externos adequados para a normalização de dados brutos, seguindo o princípio de tratamento idêntico como descrito neste trabalho.

O terceiro artigo apresentado nesta tese, intitulado *"Microalgae biomass characterization using ion mobility-mass spectrometry"* teve como objetivo principal aplicar a técnica de mobilidade iônica acoplada à espectrometria de massas de alta resolução para a caracterização de diferentes biomassas de alga. Para isso, duas

abordagens foram utilizadas: a primeira delas foi a infusão direta dos extratos das algas diretamente na fonte ESI do equipamento de mobilidade iônica, e a segunda abordagem tratou-se de um método de metabolômica, utilizando a cromatografia líquida de ultra performance (UPLC – *ultra performance liquid chromatography*) acoplada a IMS utilizando o método de aquisição por *data independent analysis* (DIA) - MS^E - com o objetivo de realizar uma identificação abrangente dos lipídios, através de softwares para tratamento de dados de ciências ômicas.

A motivação deste trabalho foi a crescente pesquisa sobre a produção de algas para a produção de biocombustíveis. Inicialmente, os biocombustíveis feitos a partir de algas estavam enquadrados como de segunda geração, porém quando ficou evidente que as algas eram capazes de fornecer rendimentos bem melhores do que outros processos com outras biomassas e através de meios de produção teoricamente mais simples, as algas foram enquadradas em uma nova categoria. Elas têm sido alvo de pesquisas massivas para uma produção mais eficiente de vários biocombustíveis.[83] Uma vantagem bastante interessante da utilização de algas como fonte de biomassa, é que elas podem ser cultivadas em águas residuais como o esgoto e águas salinas, atuando simultaneamente como fontes biorremediadoras. [84]

Atualmente já existem estudos e aplicações de algas para a produção diversos biocombustíveis. [85, 86,87,88] Dentre eles, o biodiesel é o biocombustível mais promissor a ser produzido através de algas, visto que algumas algas oleaginosas chegam a ter de 30 – 60% (m/m) de triacilgliceróis em base seca, sendo sintetizados para acumulação lipídica em seus cloroplastos. [89,90] Para obter melhores rendimentos na produção de lipídios precursores de biodiesel, como os triacilgliceróis, as espécies de microalgas são avaliadas em diferentes meios de cultivos, contendo diferentes nutrientes e condições físico-químicas como pH e temperatura. Esses parâmetros têm

---

[83] S. A. Scott, M. P Davey, J. S. Dennis, I. Horst, C. J. Howe, D.J Lea-Smith, A. G. Smith, Biodiesel from algae: challenges and prospects, *Current Opinion in Biotechnology*, **2010**, 21 (3), 277 - 286.
[84] D.C. Kligerman, E. J. Bouwer. Prospects for biodiesel production from algae-based wastewater treatment in Brazil: A review. *Renewable and Sustainable Energy Reviews,* **2015**, 52, 1834 – 1846.
[85] O. Kruse, B. Hankamer. Microalgal hydrogen production. *Current Trends in Biotechnology*, **2010**, 21, 238 – 243.
[86] Yang J, Xian M, Su S, et al. Enhancing Production of Bio-Isoprene Using Hybrid MVA Pathway and Isoprene Synthase in E. coli. Williams, *PLoS ONE,* **2012**, 7(4), e33509.
[87] R. P. John, G.S. Anisha, K. M. Nampoothiri, A. Pandey, Micro and macroalgal biomass: A renewable source for bioethanol, *Bioresource Technology*, **2011**, 102(1), 186-193.
[88] L. L. Beer, E. S Boyd, J. W Peters, M. C. Posewitz, Engineering algae for biohydrogen and biofuel production, *Current Opinion in Biotechnology,* **2009**, 20, 264 – 271.
[89] T. M. Mata, A. A. Martins, N. S. Caetano, Microalgae for biodiesel production and other applications: A review. *Renewable and Sustainable Energy Reviews*, **2010**, 14(1), 217 – 232.
[90] Y. Chisti. Biodiesel from microalgae beats bioethanol. *Trends in Biotechnology*, **2008**, 26 (3), 126-131.

uma forte influência na composição da biomassa, já que as algas tendem a adaptar seu metabolismo às condições de crescimento relacionadas ao seu meio de cultivo. [91]

A caracterização da composição química das algas é uma etapa fundamental para garantir que sejam dadas as melhores aplicações biotecnológicas para elas, seja para a produção de biocombustíveis, biogás, para a biorremediação ou até mesmo para a área de alimentos nutracêuticos. Para isso, técnicas multidimensionais de espectrometria de massas podem ser bastante adequadas, visto que a biomassa proveniente de algas é extremamente complexa em termos de classes de compostos químicos. Desta forma, a técnica de IM-MS pode ser uma ferramenta analítica bastante poderosa para a caracterização de classes de compostos em amostras de biomassa de alga, tais como os lipídios precursores de biodiesel. Além da separação com base nas m/z dos íons formados na fonte, a mobilidade iônica separa os íons com relação à estrutura tridimensional (CCS – *collision cross section*), carga e diferentes interações do tipo íon-dipolo com o gás de mobilidade. Estudos prévios já demonstraram a excelente performance da técnica para a caracterização de misturas complexas, [92] bem como para o aumento da seletividade de análises de lipidômica e metabolômica. [93]

A biomassa de alga é uma mistura complexa de diversos metabólitos. [94] Este trabalho focou somente na parte lipídica, já que o foco do trabalho foi a aplicação de algas para a produção de biodiesel. Para ser adequada para a produção de biodiesel a biomassa de alga deve possuir em especial uma alta concentração de lipídios transesterificáveis precursores de FAMEs, que são principalmente os TAGs. Diversos estudos têm sido conduzidos com o objetivo de produzir algas com o maior teor possível de TAGs, para fornecer um maior rendimento na produção de biodiesel. [95] Entretanto, essa não é a única aplicação: algas com um alto teor de compostos

---

[91] E. J. Kerkhoven, K. R Pomraning, S. E. Baker, J. Nielsen, Regulation of amino-acid metabolism controls flux to lipid accumulation in Yarrowia lipolytica. *npj Systems Biology and Applications*, **2016**, 2, 16005

[92] S. J. Valentine, M. Kulchania, C. A. S. Barnes, D. E. Clemmer, Multidimensional separations of complex peptide mixtures: a combined high-performance liquid chromatography/ion mobility/time-of-flight mass spectrometry approach, *International Journal of Mass Spectrometry*, **2001**, 212, 97-109.

[93] G. Paglia, G. Astarita, Metabolomics and lipidomics using traveling-wave ion mobility mass spectrometry. *Nature Protocols*, **2017**, 12, 797 – 813.

[94] F. Collard, J. Blin, A review on pyrolysis of biomass constituents: Mechanisms and composition of the products obtained from the conversion of cellulose, hemicelluloses and lignin, *Renewable and Sustainable Energy Reviews*, 2014, 38, 594 - 608.

[95] Q. Hu, M. Sommerfeld, E. Jarvis, M. Ghirardi, M. Posewitz, M. Seibert, A. Darzins, Microalgal triacylglycerols as feedstocks for biofuel production: perspectives and advances. *The Plant Journal*, **2008**, 54, 621 – 639.

nitrogenados, por exemplo, podem ser direcionadas para aplicações em biorremediação, enquanto que algas ricas em ácidos graxos poli-insaturados podem ser adequadas para serem aplicadas na área de alimentos nutraceuticos. [96] Para determinar a melhor aplicação para a alga, as biorrefinarias de alga devem dispor de uma ferramenta robusta para a análise dessas biomassas. Ao todo nesse trabalho, dezesseis biomassas de algas foram analisadas, incluindo diferentes espécies, tempos e meios de cultura.

A primeira abordagem explorada foi a análise por infusão direta dos extratos das algas analisadas. Diferentes perfis foram observados nos espectros, o que mostra que a composição da biomassa de alga é alterada em função da forma de cultivo e que essas alterações são facilmente detectadas através dessa análise. Entretanto, entender quais classes de compostos aumentam ou diminuem de concentração em função dos parâmetros de crescimento das algas é fundamental para a otimização das condições de produção.

Os espectros de massas para cada alga foram avaliados estatisticamente, através de quimiometria, utilizando a análise de componentes principais (PCA). Observou-se que o agrupamento das amostras se dá principalmente pelo gênero da alga, indicando que esse deva ser a principal variável a ser considerada em um estudo para a prospecção de algas para determinada aplicação biotecnológica. Uma vez definidas as melhores cepas de determinadas gêneros e espécies, as condições de meio de cultura devem ser estudadas. Além disso, esta abordagem pode ser bastante interessante para a comparação com amostras de referência, ou seja, algas que já se mostraram adequadas para determinada aplicação, ou que o perfil lipídico já tenha sido caracterizado. É uma abordagem relativamente simples e rápida, e fornece uma boa resposta para uma avaliação inicial de um dado conjunto de amostras.

Da mesma forma, os extratos de algas também foram avaliados adicionando-se mais uma dimensão aos dados de MS, correspondente à separação por mobilidade iônica. Nesta análise, as soluções dos extratos de algas são diretamente infundidas na fonte ESI, e os lipídios e metabólitos ionizados serão direcionados para a cela de mobilidade, onde serão separados de acordo com suas estruturas tridimensionais, cargas e interações com o gás de mobilidade. Em estudos metabolômicos, essa nova

[96] S. P. Slocombe, Q. Zhang, M. Ross, A. Anderson, N. J. Thomas, A. Lapresa, C. Rad-Menéndez, C. N. Campbell, Kenneth D. Black, Michele S. Stanley & John G. Day. Unlocking nature's treasure-chest: screening for oleaginous algae. *Nature Scientific Reports,* **2015**, 9844. 1-17

dimensão dos dados é bastante útil, pois espécies não resolvidas cromatograficamente, ou que caiam na mesma faixa de *m/z* no caso da infusão direta, podem ser separadas pela IMS, o que aumenta a capacidade de detecção da técnica. Em misturas complexas, diferentes classes de compostos se distribuem na forma de tendências, ou seja, regiões de "*drift time versus m/z"* características para cada classe.

De fato, observou-se nos espectros tridimensionais de *"drift time versus m/z"* que existem classes de compostos que se separam através de tendências distintas de *drift time*, mesmo em uma mesma faixa de *m/z*. A visualização das diferenças dos perfis de cada alga fica, então, mais evidente. Essa abordagem também é bastante interessante para um "*screening*" do perfil lipídico da amostra. Por exemplo, para a investigação do teor de TAG em um extrato lipídico, visto que essa classe de compostos apresentará além de determinada faixa de *m/z* (que, no entanto pode estar sobreposta a diversos outros metabótitos, o que torna difícil a sua diferenciação), uma tendência de *drift times* característicos, para uma dada condição experimental. Portanto, pode-se oferecer uma resposta rápida para tomadas de decisão em estudos de cultura de algas, ou até mesmo para interromper/avançar com processos em biorrefinarias de produção de alga.

Realizar a caracterização abrangente dos diferentes componentes das amostras de forma manual, através dos espectros de MS/MS obtidos por infusão direta dos extratos é uma tarefa laboriosa e que consome muito tempo, devido à enorme complexidade das amostras, que apresentam diversas classes de lipídios, além de outros metabólitos. Para isso, a técnica de UPLC-HDMS^E foi empregada. O método de MS^E é método de aquisição de espectros de MS e MS/MS de forma automatizada, em que o analisador opera tanto em modo de baixa energia, quanto de alta energia para promover a dissociação induzida por colisão de íons, assim resultando também em espectros de fragmentos produtos alinhados com o do íon precursor. Nesta técnica, o termo HD vem de "*high definition*", pois neste caso a técnica de aquisição por MS^E é também acoplada à mobilidade iônica. Com isso, além dos dados de massa exata para os íons precursores e fragmentos, também são obtidos dados de CCS para o íon precursor, através da calibração utilizando substâncias cujo CCS é conhecido, aumentando, assim a "definição" dos dados. No caso desse trabalho, os valores de CCS foram calibrados utilizando uma solução de poli-d-alanina, cujos oligômeros monocarregados já tem valores de CCS

determinados. Cada corrida cromatográfica, juntamente com os espectros de MS e IMS associados a ela, foi importada no software Progenesis QI, que através da comparação com banco de dados LIPIDMAPS, HMDB e um banco de dados de CCS provido pela Waters, realiza a identificação de forma automatizada dos dados, realizando a comparação experimental/teórica da massa exata dos precursores e fragmentos, padrão isotópico, perfil de fragmentação e CCS.

Das 16 amostras analisadas, todas na mesma condição, coletivamente foram identificados 1251 diferentes compostos. Desses, 210 foram identificados somente como lipídios. Dentre esses compostos, 30 deles também foram identificados pelos seus CCS, admitindo-se uma variação experimental/teórica menor que 4%. O número de compostos identificados pelo CCS é menor, pois o banco de dados utilizados não é amplo como o LIPIDMAPS ou o HMDB. A partir das abundâncias de cada lipídio identificado por amostra, várias interpretações podem ser realizadas. Adicionalmente, os CCS dos TAGs também foram investigados usando outro banco de dados externo ao Progenesis QI, o LipidCCS, e os resultados experimentais ficaram bem próximos dos valores de CCS daquela base de dados.

Foi possível avaliar a distribuição das abundâncias de classes de lipídios por amostra, a partir das abundâncias para cada íon identificado em cada amostra. Pode-se ressaltar que as amostras TG3, TG4 e DUDEF_CHL3 foram as que apresentaram a maior abundância de TAGs, o que poderia indicar que nesse conjunto de amostras analisadas, elas poderiam fornecer melhores rendimentos para a produção de biodiesel.

Outra abordagem que pode auxiliar na comparação do perfil de lipídios das amostras de algas é a comparação dos espectros de *drift time x m/z* dois a dois, através do software HDMS Compare (Waters). Nessa abordagem, os espectros de mobilidade iônica são sobrepostos, e com isso pode-se destacar quais classes de compostos são mais abundantes em cada amostra, gerando um mapa em que cada amostra é marcada com uma cor. Foi realizada a comparação dos espectros das amostras TG3 com uma mistura de vários óleos vegetais comerciais. Pôde-se observar a tendência dos TAGs da amostra está sobreposta à dos TAGs da mistura de óleos vegetais. Comparando outras amostras cuja abundância dos TAGs é baixa, não se observa a sobreposição destas tendências, o que os resultados convergem com os resultados obtidos através da análise de lipidômica.

Por fim, o quarto e último artigo que compôs esta tese foi intitulado como *"Compendium on Amazon oils composition. Part I - Triacylglycerols characterization and comparison with commercial trivial vegetable oils and fats*", e teve como objetivo principal realizar a caracterização detalhada da composição de óleos e manteigas obtidas através de espécies oleaginosas nativa da floresta Amazônica Brasileira. O compêndio da composição de óleos Amazônicos é um projeto audacioso, que visou otimizar e aplicar diferentes metodologias analíticas utilizando a MS como técnica central para identificar com maior nível de detalhamento a composição dessas amostras. O artigo apresentado nesta tese, relata apenas a primeira parte desse compêndio, em que somente a composição majoritária dos óleos foi explorada.

Do ponto de vista motivacional, a realização de um compendio sobre a composição dos óleos Amazônicos se deu porque as matérias primas ligadas à biodiversidade amazônica têm recebido cada vez mais atenção de diversas indústrias, como por exemplo de cosméticos, farmacêutica e alimentícia, uma vez que os óleos de suas espécies nativas têm mostrado um potencial benéfico para a saúde humana. Além disso, a produção de óleos a partir de frutos oriundos da biodiversidade da Amazônia é considerada uma prática sustentável. Considerando que esses óleos são extraídos de sementes, amêndoas e polpa dos frutos dessa árvores, garante-se a proteção e manutenção dessas espécies nativas, uma vez que, incentivando o uso do fruto dessas espécie, agrega-se valor a ele e inibe-se o extrativismo (muitas vezes ilegal) da madeira, minimizando-se os riscos de que determinada espécie nativa entre em extinção. Além disso, existem vários estudos na literatura sobre a composição de espécies vegetais da Amazônia, bem como muitas crenças populares sobre suas propriedades benéficas. Por isso, este compêndio está sendo elaborado para elucidar mais detalhadamente a composição desses óleos, o que pode ajudar a garantir sua autenticidade e qualidade, e também corroborar o entendimento de suas propriedades, através da identificação de compostos bioativos.

Ao todo, foram analisadas quinze espécies diferentes, e quando possível, pelo menos duas amostras de cada tipo de óleo ou manteiga foram analisadas. Todas as amostras possuem rastreabilidade de produção e certificado de autenticidade, o que dá embasamento para os resultados obtidos. Inicialmente, foi realizado um levantamento bibliográfico das principais propriedades e composição já descritas na literatura para as espécies (não somente para os óleos). Essa pesquisa servirá como

base para associar propriedades com a composição dos óleos e manteigas estudados.

A caracterização dos compostos majoritários foi realizada através de duas metodologias: a clássica de transesterificação dos óleos utilizando BF_3-metanol, com formação dos FAMEs seguida da análise e quantificação através da técnica de GC-MS, e a análise dos triacilgliceróis intactos, através da infusão direta de uma solução dos óleos em metanol com NH_4HCO_3 10 $mmol \cdot L^{-1}$ para a indução da formação de adutos com o íon amônio. Tanto o perfil de TAGs quanto sua identificação através de seus espectros de MS/MS, foram realizados em um equipamento do tipo QTOF, equipado com fonte ESI em modo de íons positivos, ESI(+)-QTOF. Os espectros de íons produtos oriundos da fragmentação por CID para cada íon de TAG detectado nas amostras foram comparados com a base de dados LIPIDMAPS.

Com a análise dos FAMEs por GC-MS foi possível obter um resultado dos perfis de distribuição de ácidos graxos para cada amostra, que diferem de fato de acordo com a espécie analisada. Ressalta-se a presença de ácidos graxos saturados de cadeia mais curta nas amostras de manteiga (tucumã, murumuru, uccuba e babaçu), bem como o alto teor de ácido oleico (C18:1) nas amostras de açaí, buriti, patauá e óleo de polpa de tucumã. Isso é um aspecto interessante, pois é sabido que a ingestão de gorduras monoinsaturadas traz benefícios à saúde humana. Também foram reportados os teores de gorduras saturadas, monoinsaturadas e poli-insaturadas, visto que esses valores são de grande importância principalmente para a indústria de alimentos.

Além do perfil de ácidos graxos, realizou-se a caracterização dos íons dos TAGs mais abundantes, bem como a dos íons de TAG com intensidades relativas inferiores a 0,1%. Como exemplo, tem-se a análise do óleo de pracaxi. Através da análise de MS/MS foi possível caracterizar 76 diferentes TAGs. Entretanto, como a identificação manual de todos os TAGs através da comparação dos espectros de MS/MS com o banco de dados LIPID MAPS é uma tarefa laboriosa, optou-se por caracterizar detalhadamente somente os íons correspondentes aos dez TAGs mais abundantes, já que eles descrevem de 70 a 98% da abundância total de todos TAGs detectados nos óleos e manteigas estudados. Ressalta-se a grande ocorrência de isômeros: no mínimo 2 TAGs com diferentes distribuições de radicais acila, porém resultando em uma mesma fórmula elementar, que foram detectados em cada íon

fragmentado. Entretanto, para alguns íons de algumas amostras até dez TAGs isoméricos diferentes foram caracterizados a partir de seus fragmentos característicos. Os espectros de ESI(+)-QTOF, bem como a identificação dos dez íons mais abundantes foram apresentados para cada amostra. Observou-se que algumas amostras apresentam perfil espectral bastante semelhante, como é o caso das manteigas de babaçu, murumuru e tucumã, ou para as amostras de óleo de patauá e buriti. Isso mostra que quando uma variedade grande de espécies é considerada, dificilmente é possível afirmar que cada amostra apresente um *fingerprint* único e exclusivo. Para diferenciar essas amostras, faz-se, então, necessário o emprego de outras técnicas analíticas, focadas na análise de outras classes de compostos que não os TAGs.

Os espectros de ESI(+)-QTOF das amostras Amazônicas também foram comparadas com amostras de óleos e gorduras comerciais e mais comumente usadas como óleo de soja, milho, girassol, canola, côco, manteiga de leite de vaca, margarina, azeite de oliva extra virgem, sebo bovino e banha de porco de uso culinário. A partir da análise de componentes principais (PCA), foi possível observar a formação de 3 grupos principais: manteigas compostas principalmente de ácidos graxos de cadeia curta saturada (babaçu, tucuma, murumuru, ucuuba, óleo de côco e manteiga de leite de vaca); óleos com maior abundância de ácido oleico (açaí, andiroba, patauá, buriti e azeite de oliva); e óleos com maior quantidade de ácido linoleico (soja, milho, girassol, canola e murici); algumas manteigas desconectadas, como bacuri e cupuaçu, com composições mais próximas dos óleos que de outras manteigas, bem como alguns óleos com composições intermediárias entre o grupo dos oleicos e dos linoleicos, como a graviola, bacaca e castanha do pará. As amostras de sebo bovino, banha de porco e margarina, também se agruparam mais com outros óleos do que com manteigas. Essa análise serviu principalmente para “posicionar” comparativamente as amostras Amazônicas frente a amostras mais conhecidas e amplamente empregadas, o que pode ampliar ou corroborar novas aplicações e formas de consumo.

CAPÍTULO 4. CONCLUSÕES E PERSPECTIVAS FUTURAS

No primeiro artigo desta tese, mostrou-se que a metodologia por ESI-MS por infusão direta do extrato metanólico, obtido de forma simples e rápida a partir de um pequeno pedaço de madeira, possibilita de diferenciar amostras de mogno brasileiro nativo e de mogno africano, usado para reflorestamento de áreas devastadas. Através da caracterização de conjuntos específicos de marcadores fitoquímicos para cada espécie, é possível auxiliar na investigação forense da exploração ilegal de mogno brasileiro, para assegurar que somente haja a exploração legal para fins comerciais do mogno Africano em áreas permitidas no Brasil.

Como pontos inéditos deste trabalho, destacam-se principalmente a identificação de cinchonain no extrativo de *S. macrophylla*, bem como a caracterização do mogno Africano que foi plantado no Brasil, e não de seu local nativo no continente africano, que mostra que seus metabólitos secundários são realmente fatores mais característicos de sua espécie, do que de seu local de origem.

Como perspectivas futuras, pretende-se extrapolar a metodologia para outras espécies de árvores nativas e em extinção, com o objetivo de criar um banco de dados químico para essas espécies, que futuramente pode ser usado em estudos de exploração ilegal de madeiras em solo brasileiro.

Já no segundo artigo, descreveu-se a otimização de uma metodologia simples para a determinação rastreável e exata dos valores de $\delta^{13}C$ de ésteres metílicos de ácidos graxos, utilizando amostras de biodiesel de *J. curcas* como prova-de-conceito para o método desenvolvido. Foi observado que a reação de transesterificação do óleo utilizando o método clássico com BF_3 – metanol, agitação e aquecimento em banho ultrassônico causam fracionamento isotópico e resultam em valores inexatos, tendendo a ser positivamente tendenciosos em cerca de 2 mUr, o que de fato foi observado para o padrão de FAME C22:0 adicionado no começo da reação. Devido a este fato, os dados brutos de valores isotópicos para os FAMEs da *J. curcas* foram normalizados usando os valores medidos pela técnica de GC-IRMS e os valores de referência (obtidos por EA-IRMS) para o padrões secundários de trabalho C22:0 e C19:0, que atuam como padrão interno e externo, respectivamente: o primeiro para corrigir ou minimizar qualquer fracionamento isotópico devido ao processo de derivatização; o segundo para corrigir exclusivamente qualquer erro aleatório na

resposta instrumental do sistema de GC-IRMS. Desta forma, resultados mais exatos puderam ser obtidos, sendo o valor médio global para todos os ácidos graxos de todas as amostras de *J. curcas* avaliadas de $\delta^{13}C_{VPDB}$ = - 29,51 ± 1,03 mUr, enquanto o valor obtido com EA-IRMS foi de -28,97 ± 0,43 mUr, uma assinatura típica de plantas de metabolismo C3.

Esse artigo também demonstra que ferramentas de garantia de qualidade devem ser aplicadas para determinações exatas e rastreáveis dos valores isotópicos, especialmente nas análises de GC-IRMS, já que os padrões internacionalmente aceitos para a normalização da escala internacional não são compatíveis com a técnica de cromatografia gasosa. Isso também demonstra que a falta de materiais de referência de isótopos estáveis adequados pode ser parcialmente resolvida usando padrões secundários de trabalho com os valores de referência devidamente determinados pela EA-IRMS e rastreáveis à escala internacional, aplicando métodos de normalização adequados e obedecendo ao princípio do tratamento idêntico para a amostra e o padrão de referência.

Já no terceiro artigo que compôs esta tese, foi demonstrado que a técnica de mobilidade iônica acoplada à espectrometria de massas permite a obtenção de um perfil rápido de extratos de algas, já que a nova dimensão da mobilidade iônica ajuda a visualização das classes lipídicas. A variabilidade dos lipídios nas algas é incrivelmente alta e sensível aos parâmetros de cultivo, porém a classificação estatística entre as amostras apontou que o principal parâmetro que influencia a composição dos extratos é o gênero e espécie da alga. A comparação, tanto estatística ou dois a dois dos espectros das amostras pode ser muito útil, principalmente se uma alga de referência for conhecida.

Entretanto, através da infusão direta dos extratos, realizar a identificação abrangente de todos os íons das amostras é laboriosa. O alto grau de complexidade da amostra requer uma metodologia mais poderosa. Para isso, a técnica UPLC-HDMS^E foi usada para caracterizar inequivocamente cerca 200 lipídios com base em parâmetros muito intrínsecos dos íons detectados (massa precisa, padrão de fragmentação e CCS). Certamente, as metodologias otimizadas e aplicadas neste trabalho podem ser aplicadas em biorefinarias de produção de algas, para prever se algumas algas específicas serão viáveis para a produção de biodiesel ou para outras aplicações em biotecnologia.

Por fim, no quarto e último artigo que compôs esta tese foi abordada a caracterização detalhada da composição óleos e manteigas provenientes de quinze espécies oleaginosas amazônicas, tanto com relação ao perfil de ácidos graxos, quanto ao dos TAGs intactos. Até onde se tem conhecimento, esse estudo é o mais abrangente, com o maior número de amostras e com maior nível de detalhamento com relação à composição majoritária para essas amostras já realizado. Foram detectados diversos isômeros de TAGs para o mesmo íon precursor, o que demonstra que a complexidade destas amostras. Além disso, as amostras Amazônicas também foram comparadas com óleos e manteigas comerciais e cujo uso é mais trivial, com o objetivo de posicionar as oleaginosas da Amazônia frente a amostras mais conhecidas, visando ampliar ou corroborar novas aplicações e formas de consumo.

As perspectivas futuras para este trabalho, já em andamento, são a caracterização dos compostos minoritários polares e dos componentes voláteis, também empregando técnicas de MS como ferramentas principais. Esses resultados, irão compor a parte II e III deste compêndio. Espera-se que, contribuindo com a geração de mais literatura a cerca da composição detalhada de óleos e manteigas amazônicas, mais aplicações sejam dadas a eles, fornecendo mais estratégias para a garantia da autenticidade e qualidade, além de poder se estar auxiliando o entendimento sobre suas propriedades através da identificação de compostos bioativos. Tudo isso, para cada vez mais incentivar a produção sustentável e uso adequado dos recursos da floresta Amazônica.

As várias aplicações da espectrometria de massas desta tese mostraram o quanto esta técnica apresenta potencial para auxiliar na proteção de espécies nativas brasileiras, tanto para a área de certificação e controle de exploração de espécies ameaçadas, quanto para a ampliação de conhecimento acerca da nossa biodiversidade, além de poder auxiliar pesquisas que busquem uso adequado e sustentável dos recursos naturais do planeta.

CAPÍTULO 5. REFERÊNCIAS BIBLIOGRÁFICAS

A. Royer, C. Gerard, N. Naulet, M. Lees, G. J Martin. Stable isotope characterization of olive oils. I - Compositional and carbon-13 profiles of fatty acids. *J. A. O. C. S.*, **1999**, 76, 357.

D.C. Kligerman, E. J. Bouwer. Prospects for biodiesel production from algae-based wastewater treatment in Brazil: A review. *Renewable and Sustainable Energy Reviews,* **2015**, 52, 1834 – 1846.

E. J. Kerkhoven, K. R Pomraning, S. E. Baker, J. Nielsen, Regulation of amino-acid metabolism controls flux to lipid accumulation in Yarrowia lipolytica. *npj Systems Biology and Applications*, **2016**, 2, 16005

F. Angerosa , O. Bréas , S. Contento , C. Guillou , F. Reniero , E. Sada. Application of stable isotope ratio analysis to the characterization on the geographical origin of olive oils. J. *Agric. Food Chem*, **1999**, 47, 1013.

F. Angerosa, L.Camera, S. Cumitini, G. Gleixner, F. Reniero, Carbon stable isotopes and olive oil adulteration with pomace oil. *J. Agric. Food Chem.*, **1997**, 45, 3044.

F. Collard, J. Blin, A review on pyrolysis of biomass constituents: Mechanisms and composition of the products obtained from the conversion of cellulose, hemicelluloses and lignin, *Renewable and Sustainable Energy Reviews*, 2014, 38, 594 - 608.

F. L. Beltrame, E. R. Filho, F. A. P. Barros, D. A. G. Cortez, Q. B. Cass, A validated higher-performance liquid chromatography method for quantification of cinchonain Ib in bark and phytopharmaceuticals of Trichilia catigua used as Catuaba, *Journal of Chromatography A,* **2006,** 1119, 257.

G. Paglia, G. Astarita, Metabolomics and lipidomics using traveling-wave ion mobility mass spectrometry. *Nature Protocols*, **2017**, 12, 797 – 813.

Gottlieb, O.R., Phytochemicals: Differentiation and Function. *Phytochemistry*, **1990**, 29, 1715.

J. E. Poulton, 1981. The Biochemistry of Plants. Secondary Plant Products (Conn, E E, ed.), p 667 Academic Press, Vol 7. New York

J. E. Spangenberg, S. A. Macko, J. Hunziker, Characterization of olive oil by carbon isotope analysis of individual fatty acids: Implications for authentication. *J. Agric. Food Chem.*, **1998**, 46, 4179.

L. L. Beer, E. S Boyd, J. W Peters, M. C. Posewitz, Engineering algae for biohydrogen and biofuel production, *Current Opinion in Biotechnology,* **2009**, 20, 264 – 271.

L.Y. Foo, Phenylpropanoid derivatives of catechin, epicatechin and phylloflavan from Phyllocladus trichomanoides. *Phytochemistry,* **1987**, 26. 2825.

M. Y. Koh, T. I. M. Ghazi, A review of biodiesel production from *Jatropha curcas* L. oil. *Renewable and Sustainable Energy Reviews*, **2011**, 15(5), 2240.

O. Kruse, B. Hankamer. Microalgal hydrogen production. *Current Trends in Biotechnology*, **2010**, 21, 238 – 243.

O. Theander, Fundamentals of Thermochemical Biomass Conversion Cellulose, Hemicellulose and Extractives, **1985**, p. 35 - 60.

P. S. Nigam, A. Singh, Production of liquid biofuels from renewable resources. *Progress in energy and combustion science*, **2011**, 37(1), 52.

Q. Hu, M. Sommerfeld, E. Jarvis, M. Ghirardi, M. Posewitz, M. Seibert, A. Darzins, Microalgal triacylglycerols as feedstocks for biofuel production: perspectives and advances. *The Plant Journal*, **2008**, 54, 621 – 639.

R. P. John, G.S. Anisha, K. M. Nampoothiri, A. Pandey, Micro and macroalgal biomass: A renewable source for bioethanol, *Bioresource Technology*, **2011**, 102(1), 186-193.

R.C. Pettersen, The Chemical Composition of Wood. The Chemistry of Solid Wood, **1984**, May 5, 57-126.

S. A. Scott, M. P Davey, J. S. Dennis, I. Horst, C. J. Howe, D.J Lea-Smith, A. G. Smith, Biodiesel from algae: challenges and prospects, *Current Opinion in Biotechnology*, **2010**, 21 (3), 277 - 286.

S. D. Chen, C. J. Lu , R. Z. Zao, Qualitative and quantitative analysis of Rhizoma Smilacis glabrae by ultra high performance liquid chromatography coupled with LTQ OrbitrapXL hybrid mass spectrometry. *Molecules*, **2014**, 19, 10427.

S. J. Valentine, M. Kulchania, C. A. S. Barnes, D. E. Clemmer, Multidimensional separations of complex peptide mixtures: a combined high-performance liquid chromatography/ion mobility/time-of-flight mass spectrometry approach, *International Journal of Mass Spectrometry*, **2001**, 212, 97-109.

S. P. Slocombe, Q. Zhang, M. Ross, A. Anderson, N. J. Thomas, A. Lapresa, C. Rad-Menéndez, C. N. Campbell, Kenneth D. Black, Michele S. Stanley & John G. Day. Unlocking nature's treasure-chest: screening for oleaginous algae. *Nature Scientific Reports,* **2015**, 9844. 1-17

T. M. Mata, A. A. Martins, N. S. Caetano, Microalgae for biodiesel production and other applications: A review. *Renewable and Sustainable Energy Reviews*, **2010**, 14(1), 217 – 232.

Y. Chisti. Biodiesel from microalgae beats bioethanol. *Trends in Biotechnology*, **2008**, 26 (3), 126-131.

Yang J, Xian M, Su S, et al. Enhancing Production of Bio-Isoprene Using Hybrid MVA Pathway and Isoprene Synthase in E. coli. Williams, *PLoS ONE,* **2012**, 7(4), e33509.

ANEXOS

DECLARAÇÃO

As cópias dos documentos de minha autoria ou de minha coautoria, já publicados ou submetidos para publicação em revistas científicas ou anais de congressos sujeitos a arbitragem, que constam da minha Tese de Doutorado, intitulada "*Uso da espectrometria de massas para a caracterização de produtos ligados à biodiversidade, química verde e sustentabilidade*" não infringem os dispositivos da Lei nº 9.610/98, nem o direito autoral de qualquer editora.

Campinas, 06 de dezembro de 2018

Maíra F P Lima

Maíra Fasciotti Pinto Lima
R.G. nº 11423446-1

Marcos Nogueira Eberlin
RG nº 11662030-4

Ministério do Meio Ambiente
CONSELHO DE GESTÃO DO PATRIMÔNIO GENÉTICO

SISTEMA NACIONAL DE GESTÃO DO PATRIMÔNIO GENÉTICO E DO CONHECIMENTO TRADICIONAL ASSOCIADO

Comprovante de Cadastro de Acesso

Cadastro nº AB27DCD

A atividade de acesso ao Patrimônio Genético, nos termos abaixo resumida, foi cadastrada no SisGen, em atendimento ao previsto na Lei nº 13.123/2015 e seus regulamentos.

Número do cadastro:	**AB27DCD**
Usuário:	**INMETRO**
CPF/CNPJ:	**00.662.270/0001-68**
Objeto do Acesso:	**Patrimônio Genético**
Finalidade do Acesso:	**Pesquisa**

Espécie
Euterpe Oleracae
Carapas guianensis
Orbignya Oleifera Arecaceae
Oenocarpus distichus Arecaceae
Platonia insignis Clusiaceae
Mauritia venifera
Betholetia Excelsa H. B. K.
Theobroma grandiflorum
Annona Muricata Annonaceae
Byrsonima Crassifolia
Astrocarium murumuru
Oenocarpus bataua Arecaceae
Pentaclethra Filamentosa

Astrocaryum vulgare Aricaceae

Virola Sebifera

Swietenia macrophylla Meliaceae

Jatropha curcas

Título da Atividade:	**Uso da espectometria de massas para a caracterização de produtos ligados a biodiversidade, química verde e sustentabilidade**

Equipe

Maíra Fasciotti Pinto Lima	**INMETRO**
Simone Carvalho Chiapetta	**Instituto Nacional de Tecnologia**
Thays Vieira da Costa Monteiro	**INMETRO**
Michael Murgu	**Waters Corporation**
Werickson Fortunato de Carvalho Rocha	**INMETRO**
Luiz Roberto Moraes	**Amazon Oil**
Marcos Nogueira Eberlin	**UNICAMP**
Alessandra Sussulini	**UNICAMP**
Valnei Smarçaro da Cunha	**INMETRO**
Alexandre de Andrade Ferreira	**Cenpes/Petrobras**
Elaine Cristina Cabral Polcelli	**UNICAMP**

Parceiras Nacionais

01.263.896/0004-07 / Instituto Nacional de Tecnologia - INT

46.068.425/0001-33 / Universidade Estadual de Campinas

07.928.840/0001-68 / ROMERA IND. E COM. DE PERFUME EIRELI - ME

00.158.141/0001-37 / WATERS TECHNOLOGIES DO BRASIL LTDA.

33.000.167/0819-42 / CENPES/PETROBRAS

Data do Cadastro:	**23/10/2018 17:07:10**
Situação do Cadastro:	**Concluído**

Conselho de Gestão do Patrimônio Genético

Situação cadastral conforme consulta ao SisGen em **16:25** de **24/10/2018**.

SISTEMA NACIONAL DE GESTÃO DO PATRIMÔNIO GENÉTICO E DO CONHECIMENTO TRADICIONAL ASSOCIADO - **SISGEN**